A matter of delivery: nanocarriers and the engineering of protective immunity in tuberculosis vaccination

Szachniewicz, M.M.

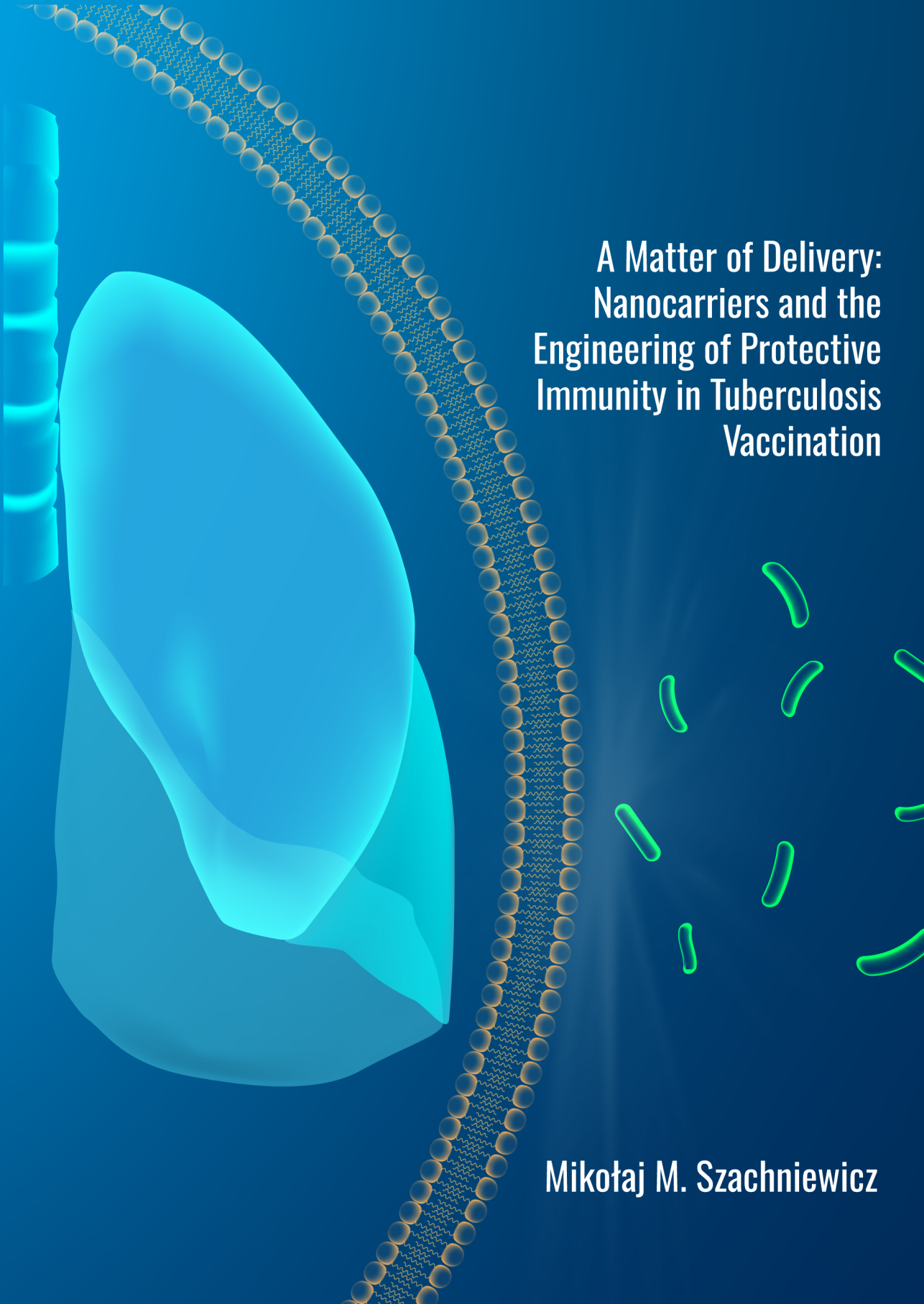

A Matter of Delivery: Nanocarriers and the Engineering of Protective Immunity in Tuberculosis Vaccination

Mikołaj M. Szachniewicz

Stellingen
behorende bij het proefschrift getiteld

A MATTER OF DELIVERY: NANOCARRIERS AND THE ENGINEERING OF PROTECTIVE IMMUNITY IN TUBERCULOSIS VACCINATION

1. The immunostimulatory effects of cationic lipids are shaped not only by their surface charge but also by their molecular structure, which modulates nanoparticle properties and immune cell interactions.

   Adapted from Chapter 2, this thesis.

2. Nanoparticle-based delivery systems modulate antigen processing and immune activation, acting as active immunological components rather than passive carriers.

   Adapted from Chapter 3, this thesis.

3. The abundance of IFNγ-producing or polyfunctional T-cells does not reliably predict protection against *Mycobacterium tuberculosis,* highlighting limitations of conventional immune readouts.

   Adapted from Chapter 4, this thesis.

4. Antigen immunogenicity is not solely intrinsic but can be significantly enhanced through formulation and delivery strategies.

   Adapted from Chapter 5, this thesis.

5. The absence of robust immune correlates of protection remains a major obstacle to rational TB vaccine design.

Adapted from Wang, J., et al. *npj Vaccines* (2024).

6. Protective immunity against TB is multifactorial and unlikely to be attributed to a single cellular or molecular correlate.

Adapted from Brighenti, S., Joosten, S. A. *Journal of internal medicine* (2018).

7. Correlates of TB vaccine efficacy may lie in underexplored areas such as tissue localization, unconventional T-cell responses, and host-intrinsic factors beyond standard cytokine-based profiling.

Adapted from Nemes, E., et al. *Frontiers in immunology* (2020).

8. Integrating human-relevant *in vitro* models early in vaccine development can enhance the predictive value of preclinical screening.

Adapted from Bowley, T. Y., et al. *Frontiers in Immunology* (2025).

9. The COVID-19 pandemic demonstrated that rapid vaccine development is feasible, but equitable distribution, strategic preparedness, and global coordination remain critical barriers to achieving population-wide protection.

Adapted from Agampodi, S., et al. *Expert Review of Vaccines* (2024).

10. Even the most effective vaccine cannot succeed if public trust is eroded by misinformation and vaccine hesitancy.

A MATTER OF DELIVERY: NANOCARRIERS AND THE ENGINEERING OF PROTECTIVE IMMUNITY IN TUBERCULOSIS VACCINATION

Mikołaj Mieczysław Szachniewicz

A Matter of Delivery: Nanocarriers and the Engineering of Protective Immunity in Tuberculosis Vaccination
PhD Thesis, Leiden University Medical Center, The Netherlands
by Mikołaj M. Szachniewicz

Cover Design & Artwork: © Mikołaj M. Szachniewicz, 2026
Layout by: Mikołaj M. Szachniewicz
Printed by: PrintSupport4U
ISBN: 978-94-93289-99-4

The conducted research was supported by the Dutch Research Council (NWO) Domain Applied and Engineering Sciences grant, project number: 15240.

A MATTER OF DELIVERY: NANOCARRIERS AND THE ENGINEERING OF PROTECTIVE IMMUNITY IN TUBERCULOSIS VACCINATION

Proefschrift

ter verkrijging van

de graad van doctor aan de Universiteit Leiden,

op gezag van rector magnificus prof.dr. S. de Rijcke,

volgens besluit van het college voor promoties

te verdedigen op woensdag 4 februari 2026

klokke 10:00 uur

door

Mikołaj Mieczysław Szachniewicz

geboren te Łódź, Polen

in 1992

Promotores:

Prof. dr. T.H.M. Ottenhoff

Prof. dr. J.A. Bouwstra (Leiden Academic Centre for Drug Research)

Leden promotiecommissie:

Prof. dr. S.H. van der Burg

Prof. dr. A.H. Meijer (Institute of Biology Leiden)

Prof. dr. M. Barz (Leiden Academic Centre for Drug Research)

Dr. S.A. Joosten

Dr. K. van der Maaden

The conducted research was supported by the Dutch Research Council (NWO) Domain Applied and Engineering Sciences grant, project number: 15240.

TABLE OF CONTENTS

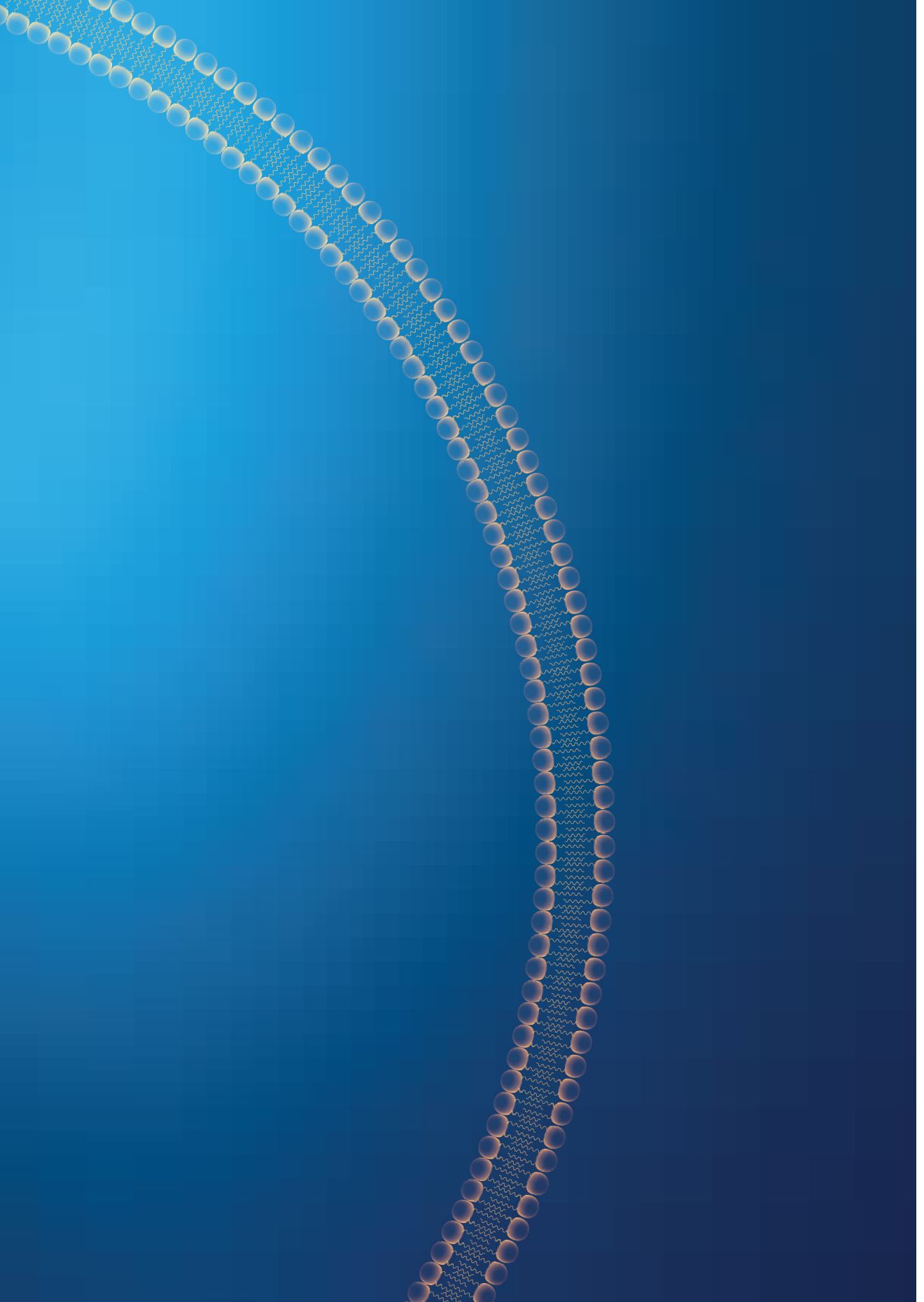

CHAPTER 1

General introduction and thesis outline

1. TUBERCULOSIS – AN OVERVIEW

Tuberculosis (TB) is a contagious airborne disease that is both preventable and curable in modern times. Evidence of human TB infection dates back to the Neolithic era, around 9,000 years ago.[1] The causative agent, *Mycobacterium tuberculosis* (Mtb), has co-evolved with humans for many millennia. It is theorized that Mtb accompanied humans for 6 to 70 thousand years,[2] allowing it to emerge as a sophisticated pathogen capable of surviving in its host for years without symptoms. Currently, the World Health Organization (WHO) estimates that about a quarter of the global population is latently infected with Mtb, with 5-10 % of these individuals likely to develop active TB.[3]

In 2023, TB likely regained its position as the world's leading cause of death from a single infectious agent, after being surpassed by COVID-19 for three years, and caused nearly twice as many deaths as HIV/AIDS.[4] It also significantly contributed to deaths related to antimicrobial resistance. An estimated 10.8 million people, including 1.3 million children, contracted TB that year, with eight countries: India, Indonesia, China, the Philippines, Pakistan, Nigeria, Bangladesh, and the Democratic Republic of the Congo, accounting for over two-thirds of the global total.[4] COVID-19 disruptions between 2020 and 2023 led to a 4.6 % increase in the TB incidence rate, reversing nearly two decades of annual declines of about 2 %, and resulted in nearly 700,000 additional TB deaths.[4]

Global efforts have made significant strides in combating TB, saving an estimated 79 million lives since 2000. In 2023, 8.2 million people were newly diagnosed with TB, the highest number since WHO monitoring began in 1995. Despite these efforts, there remains a substantial gap between the estimated number of TB cases and those diagnosed, with approximately 2.7 million people undiagnosed or unreported in 2023.[4]

Several new modalities are now in the pipeline to alleviate the TB burden. As of January 2024, the Tuberculosis Vaccine Initiative (TBVI) reports 16 prophylactic TB vaccines and one therapeutic vaccine in clinical trials.[5] Additionally, WHO notes that 28 drugs for TB treatment are in clinical trials, including 18 new compounds, two with

accelerated approval, one recently approved by the US FDA, and seven repurposed drugs. There are also at least 29 trials and studies evaluating drug regimens and delivery models for TB preventive treatment.[6]

2. VACCINES

A vaccine is a biological preparation that enhances immunity against a specific pathogen. The primary goal of vaccination is to protect those at risk, including children, the elderly, immunocompromised individuals, people with chronic diseases, and those in disease-endemic areas. Vaccines against infectious diseases contain an agent resembling a disease-causing microorganism, made from weakened or killed forms of the pathogen, its toxins, or components such as nucleic acids or proteins. This agent stimulates the immune system of the host to recognize, destroy, and "remember" the pathogen for future defense. They are widely recognized as the most effective and cost-efficient means of combating infectious diseases. Their success in eradicating smallpox and rinderpest underscores their efficacy.[7] Various types of vaccines are in use and research.

Since the discovery of the smallpox vaccine in 1798, numerous vaccines have become available. According to the WHO, vaccines can currently prevent 25 life-threatening infectious diseases, helping people of all ages live longer, healthier lives.[8] Immunization prevents 3.5 to 5 million deaths annually, [9] and more vaccines against 16 infectious diseases are in development.[8]

3. SIMPLIFIED MECHANISM OF ACTION OF VACCINES

Regardless of the type, all vaccines operate through a common general mechanism: they introduce antigens into the body to train the immune system to recognize and respond to a specific pathogen (e.g., *Mtb*) or disease state (e.g., cancer). These antigens can take various forms, that instructs host cells to produce antigenic proteins.[10]

The primary goal of vaccination is to deliver these antigens to specialized immune cells known as antigen-presenting cells (APCs), such as dendritic cells (DCs), which play a central role in initiating adaptive immune responses. Depending on the form of the antigen, APCs process it via different intracellular pathways. Protein

and peptide antigens are typically degraded into smaller fragments called epitopes. These epitopes are then loaded onto specialized surface receptors known as major histocompatibility complexes (MHCs),[11] which come in two forms:

- **MHC Class I**: presents antigens to $CD8^+$ cytotoxic T cells.
- **MHC Class II**: presents antigens to $CD4^+$ helper T cells.

In humans, MHC molecules are referred to as human leukocyte antigens (HLAs).[11]

To effectively initiate an immune response, vaccines must also include components that stimulate APC activation. These are known as adjuvants and may consist of compounds derived from microbes or synthetic molecules designed to mimic such compounds. The activation of APCs is crucial, as it ensures effective antigen processing and presentation to T and B lymphocytes.[11]

Once activated, APCs migrate from the site of antigen encounter (typically the site of vaccine injection) to the nearest draining lymph nodes via the lymphatic system. In the lymph nodes, they present antigens to naïve T cells and B cells, facilitating the initiation of the adaptive immune response. This interaction not only triggers the production of disease-specific effector immune cells but also establishes immunological memory, which enables a faster and more robust immune response upon subsequent exposure to the pathogen or disease antigen.[11]

The process of antigen presentation involves three essential signals:

1. **Signal 1** – Antigen Recognition: APCs present processed epitopes on MHC molecules to the T-cell receptor (TCR) on naïve T cells (MHC I to $CD8^+$ T cells; MHC II to $CD4^+$ T cells).
2. **Signal 2** – Co-stimulatory Activation: APCs express co-stimulatory molecules (e.g., CD80, CD86) that interact with receptors on T cells (e.g., CD28), providing the necessary secondary activation signal.
3. **Signal 3** – Cytokine Signaling: APCs secrete cytokines that further direct T-cell differentiation and functional polarization (e.g., toward Th1, Th2, or cytotoxic responses).[12]

Following successful antigen presentation, T and B cells undergo activation, clonal expansion, and differentiation into effector and memory cells. This leads to the

generation of memory T cells and memory B cells, which are central to long-term immunity. Upon future encounters with the pathogen or cancer antigen, these memory cells enable the immune system to mount a rapid and effective response.[11]

This coordinated process of antigen delivery, immune activation, and memory formation is the fundamental goal of all prophylactic and therapeutic vaccines.[10]

4. SOLE LICENSED TB VACCINE – BCG

Despite the success of traditional vaccines, effective vaccines for several infectious diseases, including TB, remain elusive. The only available TB vaccine, *Mycobacterium bovis* bacille Calmette–Guérin (BCG), has been in use since 1921 and is recommended at birth in over 180 countries.[13] Unfortunately, BCG provides inconsistent and often insufficient protection, ranging from 0 to 80 %,[14] particularly against the transmissive pulmonary form of TB in adolescents and adults.[15–17] It is more effective in preventing disseminated and meningeal TB in children.[18,19] This protection is thought to be partly mediated by BCG-induced trained immunity, which enhances the nonspecific responsiveness of innate immune cells and may contribute to broader early-life protection.[20,21]

The variable efficacy of the BCG vaccine against adult pulmonary TB is likely influenced by several factors.[22] BCG's effectiveness may wane with age, though evidence varies widely across studies.[23–25] BCG may be less effective in endemic areas due to exposure to environmental non-tuberculous mycobacteria (NTM), especially in tropical regions where BCG efficacy is inversely related to NTM prevalence.[26,27] Exposure to NTM may theoretically elicit immune responses that nullify BCG benefits in certain populations.[22] Differences in BCG vaccine preparations and genetic variability of different strains have also been proposed as factors,[28] though there is insufficient evidence to support this hypothesis.[29–32] Finally, host factors, including sociological factors, genetics, and environmental exposures, likely contribute to variable BCG efficacy.[33–36]

5. TB VACCINE CANDIDATES

This inadequacy of the BCG vaccine has prompted the development of new vaccine candidates, with 17 currently in various stages of clinical trials. These candidates employ various innovative vaccine technologies, including viral vector platforms, subunit (protein-based) vaccines, inactivated, and live-attenuated strains, to

hopefully offer more robust and consistent protection against TB across different demographic groups. A selection of vaccine candidates in a preclinical phase of development was summarized in Table 1, while vaccines that are in clinical trials were described in Table 2.

Table 1. TB vaccine candidates in a preclinical phase of development that are listed by the Working Group on New TB Vaccines (WGNV),[37] part of the Stop TB Partnership and Tuberculosis Vaccine Initiative (TBVI)[5] grouped by the type of vaccine technology as of June 2025.

Vaccine	Description	Additional information
	Mycobacterial – live attenuated	
MtbDsigH Tulane University and Texas Biomedical Research Institute	Mtb clinical isolate CDC1551 lacking SigH gene (RNA polymerase σ-H factor) regulating stress-response resulting in poor scavenging of ROS.[38,39] In macaques, it induced strong central memory $CD4^+$ and $CD8^+$ responses and induced protection in lethal Mtb challenge.[38]	- Prevention of Mtb infection or sustained infection - Prevention of TB disease - Adolescents, adults, children, and infants - Mucosal administration - Non-human primate models
AY035 Anyong Dingye Biotechnology Ltd.	Recombinant BCG-Japan over-expressing *M. bovis* allele of phoP-phoR displaying enhanced immunogenicity and protection in C57BL/6 mice and guinea pigs.[40]	- Prevention of Mtb infection or sustained infection - Prevention of TB disease - Adolescents, adults -Intramuscular administration - Guinea pigs and mice models

BCG::ESAT6-PE25SS James Cook University	Recombinant BCG-Danish constructed by fusing gene esxA to the general secretion signal for the mycobacterial type VII secretion pathway protein PE25. It secretes full-length ESAT-6 via the ESX-5 secretion system. In mice, it induced immune responses and protection against a clinical Mtb isolate Beijing 17919.[41]	- Prevention of TB disease - Immunotherapy/shortening TB treatment and prevention of TB recurrence - Adolescents, adults, children, and infants - Mucosal administration - Mice and rabbit models
Mycobacterium microti ATCC 35782 Institut Pasteur Paris	ATCC 35872 vole isolate lacking a specific RD1^{mic} region encoding the ESX-1 type VII secretion system. Shown to be completely inoffensive in highly susceptible SCID mice surpassing BCG and as effective in protection against Mtb as BCG in guinea pigs.[42]	- Prevention of TB disease - Elderly and people living with HIV - Intradermal administration - Guinea pigs and mice models
BCG::ESX-1Mmar Institut Pasteur Paris	Recombinant BCG Pasteur 1173P2 transformed with pRD1-2F9 and pESX-1 (*M. marinum*) cosmids expressing ESX-1 type VII secretion system. It displayed robust immunogenicity and superior protection relative to the parental BCG against Mtb H37Rv and hypervirulent HN878 and M2.[43]	- Prevention of TB disease - Prevention of Mtb infection or sustained infection, and prevention of TB recurrence - Adolescents, adults, children, and infants - Intradermal administration - Guinea pigs and mice models

BCGΔBCG1419c Centro de Investigación y Asistencia en Tecnología y diseño del Estado de Jalisco, A.C. (CIATEJ)	Recombinant BCG Pasteur ATCC 35734, lacking antibiotic-resistance markers and the BCG1419c gene (encoding cyclic di-GMP phosphor-diesterase), has been demonstrated to induce better protection against TB-induced lung pathology during the chronic stages of infection compared to BCG and improved immune responses profile.[44,45]	- Prevention of TB disease - Prevention of Mtb infection or sustained infection - Adolescents, adults, children, infants, people living with HIV, with/ without Mtb infection - Subcutaneous administration - Guinea pigs and mice models
BCG w/MK-2206 Institut Pasteur de Tunis (IPT)	Immunization with BCG Pasteur strain 1173P2 followed 24 hours later by administration of anti-cancer Akt inhibitor, MK-2206 shown to induce enhanced protection of BCG in Mtb aerosol-challenged mice and guinea pigs.[46]	- Prevention of Mtb infection or sustained infection - Prevention of TB disease - Adolescents, adults, children, and infants - Subcutaneous/intradermal administration - Guinea pigs and mice models
BCG-ZMP1 University of Zürich	Recombinant BCG-Danish lacking zmp1 gene encoding a zinc metalloprotease linked to inhibition of phagolysosome maturation by preventing inflammasome activation.	- Prevention of Mtb infection or sustained infection - Prevention of TB disease - Adolescents, adults, children, and infants

	It showed enhanced immunogenicity *in vitro* and *in vivo*.[47]	- Subcutaneous administration - Guinea pigs, mice, and cattle models
Subunit – protein-based		
CysVac2/Advax University of Sydney	Fusion protein antigen comprising Ag85B and CysD formulated with Advax adjuvant, a particulate polysaccharide delta-inulin adjuvant containing CpG. It induced IL-17-dependent protection against aerosol Mtb infection in C57BL/6 mice.[48]	- Prevention of Mtb infection or sustained infection - Prevention of TB disease - Adolescents and adults - Mucosal administration - Mice models
Spore-FP1 St George's University of London	Inactivated *Bacillus subtilis* spores coated with the FP1 fusion protein comprising Ag85B, Acr/HspX, and the N-terminal domain of HBHA antigen, and formulated with Poly(I:C). Intended as a mucosal boost vaccine in BCG-immunised hosts. Shown to be highly protective in guinea pigs but failed to improve protection in non-human primates.[49]	- Prevention of Mtb infection or sustained infection - Prevention of TB disease - Adolescents, adults, children, and people with Mtb infection - Mucosal administration - Guinea pigs, mice, and non-human primates models

Spray Dried ID93+GLA-SE Access to Advanced Health Institute (AAHI)	Fusion protein antigen comprising Rv3619, Rv1813, Rv3620, and Rv2608 (ID93), formulated with GLA-SE adjuvants, a squalene emulsion containing gluco-pyranosyl lipid A (GLA) (Toll-like receptor 4 agonist).[50]	- Prevention of TB disease - Prevention of Mtb infection or sustained infection - Adolescents, adults, elderly - Mucosal administration - Mice models
	Vector vaccine	
BCG, ChadOx/ MVA 5Ag University of Oxford	A replication-deficient recombinant chimpanzee adenovirus expressing four antigens from the mycobacterium Esx-5a system (PPE15, PE8, EsxI, EsxJ) and Ag85A. It enhanced BCG efficacy in mice and showed promise in non-human primates.[51]	- Prevention of Mtb infection or sustained infection - Prevention of TB disease - Adolescents and adults - Mucosal/intramuscular administration. - Mice and non-human primates models
Lm::Mtb9Ag University of California (UCLA)	A live attenuated *Listeria monocytogenes* vector (Lm ΔactA ΔinlB prfA) with two major virulence gene deletions and a mutation that enhances T-cell immunity, expressing nine Mtb protein antigens: Mpt64, TB10.4, ESAT-6, CFP10, Ag85B, EsxN, PPE68, EspA, and TB8.4. It demonstrated efficacy	- Prevention of TB disease - Prevention of Mtb infection or sustained infection, prevention of TB recurrence - Adolescents, adults, elderly, and people without Mtb infection

	against Mtb aerosol challenge in BALB/c, C57BL/6 mice, and guinea pigs.[52]	- Subcutaneous administration - Guinea pigs, mice, and non-human primate models

Table 2. TB vaccine candidates in a clinical phase of development grouped by the phase of clinical trial as of June 2025.[53]

Vaccine	Description	Additional information
	Phase 1	
AdHu5Ag85A Vector vaccine McMaster University, CanSino Biologics	A recombinant type 5 human adenovirus vector encoding Ag85A antigen. Mucosal but not intramuscular administration induced polyfunctional airway tissue-resident $CD4^+$ and $CD8^+$ T-cells in humans after a single dose. It was demonstrated to be safe and well tolerated.[54]	- Prevention of Mtb infection or sustained infection - Prevention of TB disease - Adolescents and adults - Mucosal/intramuscular administration - NCT02337270 - Completed in September 2021
BNT164(a1, b1) mRNA vaccine BioNTech SE	Two multi-antigen RNA vaccine candidates formulated with lipid nanoparticles.[55]	- Prevention of TB disease - Adolescents and adults - Intramuscular administration - NCT05537038 - NCT05547464 - Ongoing

H107e/CAF10b Subunit protein-based vaccine Statens Serum Institut	Fusion protein construct consisting of 8 non-BCG-cross-reactive antigens (PPE68, ESAT-6, EspI, EspC, EspA, MPT64, MPT70, and MPT83) in a cationic liposomal formulation containing DDA, monomycoloyl glycerol (MMG) and CpG. It was shown to induced protection when co-administrated with BCG-Danish in mice, and induced robust Th1/Th17 responses in Cyno-molgus macaques.[56–58]	- Prevention of TB disease - Adolescents, adults, infants, People living with HIV, with/without Mtb infection - Intramuscular administration - NCT06050356 - Ongoing
TB/FLU-05E Vector vaccine Smorodintsev Research Institute of Influenza	A recombinant attenuated influenza vector (Flu/THSP) expressing a truncated NS1 protein and Mtb antigens TB10.4 and HspX proteins. In BCG-prime with mucosal TB/FLU-05E boost regimen protected mice and guinea pigs from Mtb better than BCG alone.[59,60]	- Prevention of Mtb infection or sustained infection - Prevention of TB recurrence - Adolescents, adults, and children - Intranasal administration - NCT05945498 - Completed in September 2023

Phase 2a		
AEC/BC02 Subunit protein-based vaccine Anhui Zhifei Longcom Biopharmaceutical Co., Ltd.	Mixture of Ag85B with ESAT-6-CFP10 fusion protein and adjuvant BC02 comprising CpG and aluminum hydroxide. In mice showed protective immune responses but failed to control TB in guinea pigs.[61] In a therapeutic approach combined with isoniazid and rifapentine lowered CFUs better than antibiotics alone.[62]	- Prevention of TB disease - Adults, elderly, and people with Mtb infection - Intramuscular administration - NCT05284812 - Ongoing
ChAdOx1.85A + MVA85A Vector vaccine University of Oxford	Prime with simian adenovirus ChAdOx1.85A expressing Ag85A followed by boost with vaccinia virus Ankara MVA85A expressing Ag85A. In mice, BCG boosted with ChAdOx1.85A and then boosted with MVA85A improved BCG efficacy.[63] In humans, in phase 1 induced strong cellular and humoral responses.[64]	- Prevention of TB disease - Prevention of Mtb infection or sustained infection and prevention of TB recurrence - Adolescents, adults, children, and infants - Intramuscular administration - NCT03681860 - Completed in May 2021
ID93+GLA-SE (QTP101) Subunit protein-based vaccine Quratis, NIAID/NIH	Fusion protein antigen comprising Rv3619, Rv1813, Rv3620, and Rv2608 (ID93), formulated with GLA-SE adjuvants, a squalene emulsion containing gluco-pyranosyl lipid A (GLA) (Toll-like receptor	- Prevention of TB disease - Prevention of Mtb infection or sustained infection and Prevention of TB recurrence - Adolescents and adults

	4 agonist).[50] In BCG-vaccinated healthy adults, vaccine induced antigen-specific cellular and humoral immune res-ponses.[65]	- Intramuscular administration - NCT03806686 - Completed in June 2020
	Phase 2b	
BCG (Revaccination) Live attenuated vaccine Bill & Melinda Gates Medical Research Institute	Revaccination with AJVaccines' BCG SSI (Danish 1331) of QuantiFERON-TB Gold Plus (QFT)-negative individuals. In the phase 2b trial, BCG revaccination reduced the rate of sustained QFT conversion with an efficacy of 45.4 % in a high transmission setting.[66]	- Prevention of Mtb infection or sustained infection - Adolescents and children - Intradermal administration - NCT04152161 - Ongoing
DAR-901 Inactivated vaccine Dartmouth, St. Louis University	Whole-cell booster of BCG, comprising of non-tuberculous *Mycobacterium obuense* grown by broth fermentation of SRL 172 strain and heat-inactivated.[67] In phase 1 trial, it induced vaccine-specific Th1 polyfunctional effector memory immune responses.[68] In phase 2b, it did not prevent initial or persistent IGRA conversion. However, vaccin-ated IGRA converters showed	- Prevention of TB disease - Adolescents, adults, and people living with HIV - Intradermal administration - NCT02712424 - Completed in February 2020

	enhanced responses to ESAT-6.[69] It may be later tested for prevention of TB instead of Mtb infection.	
RUTI® Inactivated vaccine Archivel Farma, S.L	RUTI is a preparation comprising detoxified cellular H37Rv Mtb nanofragments formulated in liposomes (size 100 nm).[70] In mice, it inhibited the growth of BCG Pasteur *ex vivo*.[71] In phase 2 trial, in LTBI ($HIV^{-/+}$) patients pre-treated for 1 month with isoniazid polyantigenic responses were observed.[72]	- Immunotherapy and shortening TB treatment - Improving TB cure rates, prevention of TB disease and recurrence - Adolescents, adults, people with active TB, MDR-TB, and Mtb infection - Subcutaneous administration - NCT04919239 - Ongoing
Phase 3		
BCG (Travel vaccine) Live attenuated vaccine Henry M. Jackson Foundation for the Advancement of Military Medicine	Glutamate BCG Japan (Tokyo 172) administrated as a single dose to adults with no history of prior BCG vaccination or Mtb infection traveling to countries with high TB burden.	- Prevention of Mtb infection or sustained infection - Adults - Intradermal administration - NCT04453293 - Ongoing

GamTBvac Subunit protein-based vaccine Ministry of Health of the Russian Federation	Fusion protein construct comprising Ag85A-ESAT-6-CFP10 fused with dextran-binding domain from *Leuconostoc mesenteroides*. The construct was formulated with adjuvants consisting of dextran covered in CpG. In mice and guinea pigs, it showed robust immunogenicity and protection against H37Rv aerosol and intravenous challenges as an effective BCG booster.[73] In phase 1 trial, it induced robust cellular and humoral vaccine-specific immune responses.[74]	- Prevention of TB disease - Prevention of TB recurrence - Adults - Subcutaneous administration - NCT04975737 - Ongoing
Immuvac (MIP) Inactivated vaccine Cadila Pharmaceuticals, Indian Council of Medical Research	Immuvac is a heat-killed suspension of a non-pathogenic, cultivable atypical *Mycobacterium Indicus Pranii* (MIP) in saline, originally formulated against leprosy. It has been clinically evaluated as a treatment against category II TB, Gram-negative sepsis, non-small cell lung cancer, HIV, muscle-invasive bladder cancer, and COVID-19 with promising results.[75]	- Prevention of TB disease - Adolescents and adults - Intradermal administration - CTRI/2019/01/017026 - Ongoing

M72/AS01E Subunit protein-based vaccine GSK Vaccines, Bill & Melinda Gates Medical Research Institute	Fusion protein M72 comprising of Mtb antigens Mtb32A and Mtb39A formulated with $AS01_E$ adjuvant, which is a liposomal formulation containing MPLA, *Quillaja saponaria* Molina, fraction 21 (QS-21; a triterpene glycoside), and cholesterol. In a phase 2b trial, the vaccine induced 49.7 % protection against TB after 3 years in a TB-endemic population.[76]	- Prevention of TB disease - Adolescents, adults, people living with HIV, people with/without Mtb infection - Intramuscular administration - NCT06062238 - Ongoing
MTBVAC Live attenuated vaccine Biofabri, Bharat Biotech, University of Zaragoza, IAVI, TBVI, HIV Vaccine Trials Network	MTBVAC is an attenuated clinical Mtb strain Mt103 in which phoP and fadD26 virulence genes were deleted. It contains RD1 region absent in BCG, which contains 23 % of the known human T-cell epitopes present in Mtb. In the phase 1b trial, it induced robust polyfunctional Th1 responses in neonates.[77]	- Prevention of TB disease - Adolescents, adults, and infants - Intradermal administration - NCT04975178 (infants up to 7 days of age) - Ongoing
VPM1002 Live attenuated vaccine Serum Institute of India, Vakzine Projekt Management GmbH	BCG vaccine strain which is urease C-deficient, and expresses listeriolysin from *Listeria monocytogenes* (rBCGΔureC:Hly) to improve the immunogenicity and safety. In phase 2 trial, it was safe and immunogenic; however, IFNγ	- Prevention of Mtb infection or sustained infection - Prevention of TB disease and recurrence - Adolescents and adults

production, polyfunctional $CD4^{+}$, and $CD8^{+}$ T-cell responses were inferior compared to BCG in neonates.[78]	- Intradermal administration - CTRI/2019/01/017026 - Ongoing

6. TYPES OF TB VACCINES

Vaccines can be broadly classified into two categories: live (capable of replication) and non-live (incapable of replication). This classification distinguishes vaccines that use attenuated, replicating strains of the relevant pathogen, like the BCG vaccine, from those that consist of only pathogen components, such as antigens in the form of proteins, peptides, or genetic material (DNA or mRNA encoding antigens). These non-live vaccines may deliver these components via micro- or nanoparticles (NPs), or through vector organisms like viruses or bacteria, or they may use inactivated whole organisms.[79]

Another key distinction is between prophylactic and therapeutic vaccines. Prophylactic vaccines are designed to prevent infection, disease onset, or transmission of the pathogen. In contrast, therapeutic vaccines aim to treat existing infections or support standard treatments, such as antibiotics, by enhancing the immune response.[79]

6.1 Live-attenuated Whole-cell Vaccines

Live-attenuated vaccines are engineered to replicate just enough in a healthy individual to generate a strong immune response without causing significant disease symptoms. Crucially, these vaccine strains should not establish a persistent infection in the host and should be naturally cleared by the immune system without the need for medical intervention. Achieving this balance is vital, as it ensures that the pathogen replicates sufficiently to stimulate robust immunity while remaining attenuated enough to avoid causing illness.[79]

However, this technology faces several challenges. The manufacturing process is labor-intensive and requires stringent quality control to ensure consistent efficacy and safety, resulting in higher production costs.[80] Additionally, the use of these vaccines in immunocompromised individuals, particularly in TB-endemic regions

where HIV co-infection is common, poses significant safety risks. [81] Another major limitation is the reliance on cold chain logistics. In regions where TB vaccines are most needed, maintaining refrigeration throughout the distribution process is extremely difficult, compounded by frequent electricity shortages.[82] It is worth noting that cold chain dependency is a common challenge across nearly all vaccines.

Despite these challenges, live-attenuated vaccines offer significant advantages. They can provoke a complex and diverse immune response by presenting a wide range of antigens and pathogen-associated molecular patterns (PAMPs), closely mimicking a natural infection and providing long-lasting protection.[79]

The smallpox vaccine, which used the live cowpox vaccinia virus, is the most notable example of a live-attenuated vaccine. Developed by Edward Jenner in 1796, it was the first vaccine ever created. Its effectiveness and relative safety led to its refinement, mass production in the 20th century, and the implementation of a global vaccination program.[83] This effort culminated in the complete eradication of smallpox, officially declared by the WHO in 1980, making smallpox the only human disease to be eradicated.[84] Other examples of live-attenuated vaccines include those for influenza, measles, mumps, rubella, rotavirus, oral polio, and BCG.[80]

Currently, new live-attenuated whole-cell TB vaccine candidates are being developed as prophylactic vaccines to potentially replace BCG vaccination in neonates. These candidates are also under evaluation as post-exposure vaccines in adults to prevent TB recurrence. Examples of such vaccines currently in the clinical trials are: BCG revaccination and travel programmes, MTBVAC, and VPM1002.

6.2 Inactivated Vaccines

Inactivated vaccines are formulated using pathogens that have been killed or rendered non-infectious through chemical or physical methods, such as heat or radiation. These vaccines cannot replicate or cause disease but retain many structural components of the original pathogen, including key antigens and PAMPs. This allows them, in theory, to elicit a broad immune response targeting multiple antigens.[79]

Pathogens used for vaccine production are cultured and inactivated under strictly controlled and validated conditions to ensure both safety and consistent

immunogenicity. Failure to achieve complete inactivation could leave viable pathogenic remnants, posing a safety risk, though modern manufacturing standards make this highly unlikely.[79]

Since inactivated vaccines cannot replicate in the host, they are considered safer than live-attenuated vaccines and are suitable for use in immunocompromised individuals. However, their inability to replicate also results in weaker and less durable immune responses, typically dominated by humoral (antibody-mediated) immunity. To overcome this limitation, inactivated vaccines often require the addition of adjuvants to enhance immunogenicity and multiple booster doses to establish and maintain protective immunity. Advanced adjuvant systems may also improve the induction of cellular immune responses, but this remains a challenge compared to live vaccines.[79]

The first inactivated vaccines were developed in the late 19th century for diseases such as cholera, plague, and typhoid fever. Today, inactivated vaccines are licensed for the prevention of several diseases, including influenza, polio (Salk vaccine), rabies, hepatitis A, pertussis (as part of acellular pertussis vaccines),[85] and some COVID-19 vaccines (e.g., CoronaVac, BBIBP-CorV).

While inactivated vaccines are not the primary focus of TB vaccine development, several candidates in the pipeline utilize this approach:

- **DAR-901**: Derived from *Mycobacterium obuense*, developed for TB prevention.[69]
- **RUTI®**: A therapeutic vaccine based on detoxified fragments of *Mtb* (H37Rv strain) encapsulated in liposomes, intended to shorten treatment duration and prevent relapse.[71]
- **Immuvac (MIP)**: Based on *Mycobacterium indicus pranii*, explored for both TB prevention and as an immunotherapeutic agent.[75]

6.3 Genetic Vaccines

Genetic vaccines work by delivering genetic material encoding specific antigens into host cells, prompting those cells to produce the target antigens internally. This, in turn, stimulates the immune system to recognize and respond to the pathogen.

The genetic material used in these vaccines is typically either DNA or messenger RNA (mRNA). Delivery can be achieved through various platforms, including gene delivery systems such as NPs or viral vectors.[79]

Genetic vaccines can be classified into three main types:

- **DNA Vaccines**: Utilize plasmid DNA to encode antigens that have to be transcribed to mRNA by the host to produce antigens.
- **mRNA Vaccines**: Use mRNA to directly instruct cells to produce antigens.
- **Viral Vector Vaccines**: Employ modified viruses (usually non-replicating) to deliver genetic material encoding antigens.[86]

While DNA vaccines have been explored in various infectious disease contexts, they are not a significant focus in current TB vaccine development efforts and will not be further discussed here.

In contrast, mRNA vaccines and viral vector vaccines are actively being investigated as innovative platforms for TB vaccines due to their potential to induce robust cellular immunity, which is critical for protection against *Mtb*.

6.3.1 Vector Vaccines

Viral vector vaccines utilize genetically engineered viruses to deliver genetic material encoding specific antigens into host cells. These vectors are modified to be replication-deficient, ensuring they cannot cause disease. Once inside the host cells, the delivered genetic material directs the production of antigens, which stimulate the immune system to mount a response against the target pathogen, not the vector itself. This approach effectively mimics natural infection, promoting robust immune responses.[87]

The selection of viral vectors depends on several critical factors. Pre-existing immunity in the target population is particularly important, as prior exposure to certain viruses, such as common human adenoviruses, can reduce vaccine efficacy by neutralizing the vector before it delivers its genetic payload. Additionally, the type of immune response induced by the vector is a key consideration. For diseases like cancer, HIV, and TB, strong cellular immunity is essential, especially the activation

of cytotoxic $CD8^+$ T cells. Other important factors include the vector's safety profile, particularly for immunocompromised individuals, and the feasibility of large-scale manufacturing and long-term stability of the vaccine.[87]

Adenoviruses are among the most widely used viral vectors. These double-stranded DNA viruses include human adenovirus serotypes 5 (Ad5) and 26 (Ad26), as well as the chimpanzee-derived ChAdOx1 vector. They have been employed in several COVID-19 vaccines, including Oxford–AstraZeneca's ChAdOx1 nCoV-19, Janssen's Ad26.COV2.S, Sputnik V (which uses both Ad26 and Ad5), and Convidecia, developed by CanSino Biologics. Adenovirus vectors are also being explored in TB vaccine candidates, such as AdHu5Ag85A and ChAdOx1.85A combined with MVA85A. These vectors are known for inducing strong cellular and humoral immune responses; however, pre-existing immunity to human adenoviruses remains a significant limitation, potentially reducing vaccine effectiveness.[88]

Modified Vaccinia Ankara (MVA), a highly attenuated poxvirus, is another widely used viral vector. It has an excellent safety profile and is particularly effective at inducing strong $CD4^+$ T-helper cell responses, although its ability to stimulate cytotoxic $CD8^+$ T-cell responses is generally weaker than that of adenoviruses. MVA is used in licensed smallpox and mpox vaccines and has also been incorporated into TB vaccine candidates, such as the heterologous prime-boost strategy using ChAdOx1.85A followed by MVA85A.[89]

Vesicular stomatitis virus (VSV), a negative-strand RNA virus, has been successfully used as the vector in the Ervebo Ebola vaccine (rVSV-ZEBOV), the first approved vaccine for Ebola. VSV-based vectors are highly immunogenic, inducing both strong cellular and humoral immune responses. However, there are some concerns regarding safety, particularly related to potential neurovirulence, which has limited their broader application.[90]

The measles virus, another negative-strand RNA virus, has also been investigated as a vaccine vector for diseases such as HIV, TB, and chikungunya. It shows promise in inducing long-lasting immunity based on preclinical research. However, the widespread global immunity to measles resulting from routine vaccination significantly limits its effectiveness as a vector, as most individuals would rapidly neutralize the vector before it can deliver its genetic material.[91]

Cytomegalovirus (CMV), a large DNA virus, is being explored experimentally as a viral vector, particularly for chronic infections like HIV and TB. CMV has a unique ability to establish long-term antigen expression and induce robust and persistent $CD8^+$ T-cell memory responses. Despite these promising characteristics, no vaccines using CMV as a vector have been approved for human use to date, and research remains at the preclinical stage.[92]

As of June 2025, six viral vector vaccines against infectious diseases have been approved for human use. Four of them target COVID-19: the Oxford–AstraZeneca vaccine (ChAdOx1 nCoV-19 / AZD1222), Janssen's Ad26.COV2.S, Sputnik V (Gam-COVID-Vac), and Convidecia from CanSino Biologics. In addition, two vaccines have been approved for the prevention of Ebola virus infection. Zabdeno/Mvabea, a two-dose regimen using Ad26.ZEBOV and MVA-BN-Filo vectors, has been approved by the European Commission.[93]

Viral vector vaccines have played a critical role in combating global infectious disease threats such as COVID-19 and Ebola. Their ability to induce strong immune responses, particularly cellular immunity, makes them highly valuable platforms for both current and future vaccine development efforts, including TB.

6.3.2 mRNA Vaccines

mRNA vaccines are a class of genetic vaccines that utilize synthetic messenger RNA (mRNA) to direct the production of protein-based antigens within host cells. Once delivered into the cytoplasm, the mRNA is translated by the host cell's ribosomes into the encoded antigen. These antigens are then processed by the cell, initiating a cascade of immune processes leading to the activation of adaptive immunity, including the generation of effector cells and long-lasting immunological memory.[79]

Because mRNA is highly unstable and susceptible to enzymatic degradation, it must be delivered using specialized delivery systems. The most widely used and clinically validated delivery platform is lipid NPs (LNPs), which protect the mRNA and facilitate its uptake by host cells.[94]

Although mRNA vaccine technology has been under investigation for several decades, the first mRNA vaccines were only recently approved during the COVID-19 pandemic, marking a significant milestone in vaccine development. As of 2025, approved mRNA vaccines are available for the prevention of COVID-19 and

respiratory syncytial virus (RSV). However, numerous mRNA vaccine candidates are currently in clinical trials targeting a range of other diseases, including TB, influenza, cytomegalovirus, and various cancers.[95]

Among these candidates are BNT164a1 and BNT164b1, investigational mRNA-based TB vaccines developed by BioNTech SE. Both vaccines employ multi-antigen mRNA sequences formulated with LNPs.[96,97] These candidates are currently being evaluated in a two-part, randomized, placebo-controlled, observer-blind, Phase Ib/IIa clinical trial conducted in South Africa and Mozambique. The trial is designed to assess safety, tolerability, and immunogenicity across up to four different dose levels, with the goal of determining a safe and effective dose for a three-dose vaccination schedule in healthy, BCG-vaccinated adult argue that mRNA vaccines re in a way also subunit vaccine.t volunteers.[55]

6.4 Subunit Vaccines

Subunit vaccines are a class of vaccines that contain only selected, purified components of a pathogen, such as proteins, peptides, polysaccharides, or polysaccharide–protein conjugates, that are specific to the pathogen and capable of eliciting an immune response. These components are chosen for their antigenic properties, meaning they can be recognized by the immune system and trigger an adaptive immune response. While subunit antigens can be directly extracted from cultured pathogens, they are more commonly produced synthetically or through recombinant DNA technology, allowing for precise manufacturing and quality control.[98]

In the context of therapeutic cancer vaccines, subunit vaccines often utilize tumor-specific antigens or neoantigens, which are short peptides or proteins derived from mutations unique to cancer cells. These neoantigens help train cytotoxic $CD8^+$ T cells to recognize and destroy malignant cells while sparing healthy tissue, leveraging the immune system's ability to distinguish "non-self" from "self."[99]

The first subunit vaccine approved for human use was the hepatitis B vaccine, which consists of recombinant hepatitis B surface antigen (HBsAg). Since then, subunit vaccines have become a cornerstone of modern vaccinology, with examples including vaccines against human papillomavirus (HPV), pertussis (acellular pertussis), and pneumococcal disease (using polysaccharide-protein conjugates).[100]

Because subunit vaccines do not contain whole organisms or innate immune stimulatory molecules, they require the addition of adjuvants – immunostimulatory compounds that activate APCs and enhance the magnitude and quality of the immune response. Without appropriate immune activation, subunit vaccines risk eliciting suboptimal responses, such as anergy (non-responsiveness), immune tolerance, or ineffective immune polarization. Additionally, they often require multiple doses or booster shots to achieve durable and protective immunity.[101]

One of the major advantages of subunit vaccines over live-attenuated or inactivated whole-pathogen vaccines is their safety profile. Because they contain no replicating organisms or infectious materials, they pose minimal risk of reversion or infection and are well-suited for immunocompromised populations, such as individuals living with HIV. This is particularly important in regions where both HIV and other infectious diseases like TB are endemic, and safe, effective vaccines are critically needed.[102]

Subunit vaccines can also be rationally designed and tailored to direct the immune response toward specific effector mechanisms (e.g., Th1, Th2, or cytotoxic T-cell responses). They are typically more stable, easier to store and transport, and less expensive to manufacture at scale than many traditional vaccine platforms.[102]

A crucial element in the success of subunit vaccines is formulation, particularly the integration of advanced delivery systems. These platforms are designed to improve antigen stability, target delivery to specific cells (such as DCs), and optimize the kinetics of antigen release. Delivery systems can be biological (e.g., viral vectors or engineered bacteria) or synthetic, with the latter category including polymers, antibodies, liposomes, micelles, and microparticles or NPs. Synthetic, non-replicating systems are generally preferred for subunit vaccine delivery due to their safety and versatility.[102]

Subunit vaccines are a major focus in TB vaccine development, with several candidates in clinical trials. H107e/CAF10b (Statens Serum Institut) contains eight non-BCG-cross-reactive antigens in cationic liposomes with DDA, MMG, and CpG, showing strong Th1/Th17 responses in macaques and protection in mice.[56–58] AEC/BC02 (Anhui Zhifei) combines Ag85B, ESAT-6-CFP10, CpG, and a traditional adjuvant aluminum hydroxide.[61,62] ID93+GLA-SE (Quratis) includes a four-antigen fusion with a TLR4 agonist emulsion and induced immune responses in BCG-vaccinated adults.[65] GamTBvac (Russian Ministry of Health), a fusion of Ag85A, ESAT-6, and CFP10 with

dextran-CpG adjuvant, showed protection in animal models and strong responses in a phase 1 trial.[73,74] M72/AS01E (GSK) combines Mtb32A and Mtb39A with a liposomal MPLA/QS-21 adjuvant, offering 49.7 % protection over three years in a phase 2b trial.[76]

The main topic of this thesis is protein subunit vaccines formulated with NP-based delivery systems, representing a promising strategy to enhance immunogenicity, reduce antigen dose requirements, and improve vaccine outcomes.

7. NP-BASED VACCINES

NPs have become indispensable components in the design and delivery of modern vaccines. Among the most prominent examples are lipid NPs, which played a central role in the success of mRNA-based COVID-19 vaccines such as Comirnaty (Pfizer–BioNTech) and Spikevax (Moderna).[103,104] NPs are typically defined as fine particulate structures with at least one dimension in the nanometer range, most commonly between 1 and 100 nanometers. However, in applied biomedical fields, especially drug and vaccine delivery, functional definitions are more relevant. These definitions consider particles up to approximately 200–250 nanometers as NPs when they exhibit unique behaviors at the biological level, such as enhanced uptake by APCs, that are not observed at larger scales.[105]

In the context of immunization, particles below this size threshold are more efficiently internalized by APCs, including dendritic cells and macrophages. This enhanced uptake is central to their utility in vaccine formulations. Beyond passive transport, NPs offer a range of benefits. Their small size and surface properties enable them to traverse biological barriers and target specific immune cell populations. Some NPs possess intrinsic immunostimulatory properties, allowing them to function as adjuvants in addition to delivery vehicles. Moreover, NPs can co-deliver multiple functional components, such as antigens, molecular adjuvants, targeting ligands, and immunomodulatory agents, within a single structure. This multifunctionality allows for the precise tuning of the immune response, including directing it toward desired T-cell profiles or enhancing mucosal immunity.[102,105]

A major advantage of NP-based vaccine systems is their capacity to reduce the antigen dose required to elicit protective immunity. By enhancing antigen presentation and delivery to key immune cells, NPs often enable significant dose-sparing, which

has cost and scalability benefits. Additionally, they can prolong antigen retention at the injection site, acting as a depot that maintains antigen exposure over time and thereby strengthens the immune response. NPs can also be engineered to control the kinetics of antigen release, enabling burst release, sustained release, or environmentally triggered release (e.g., pH- or enzyme-dependent), further improving immunogenicity and therapeutic precision. Importantly, they protect labile vaccine components such as proteins, peptides, or nucleic acids from degradation during manufacturing, storage, and transport in the body.[102,105]

A wide range of NP types is currently under investigation for vaccine applications. Inorganic NPs, including gold, silica, carbon-based structures, aluminum salts (alum), calcium phosphate, and magnetic NPs, have been studied both for their delivery capacity and as immunostimulatory adjuvants. However, organic NPs are more commonly used due to their superior biocompatibility, flexibility in formulation, and easier regulatory pathways. These include polymeric NPs (e.g., PLGA), liposomes, solid lipid NPs, niosomes, micelles, dendrimers, immunostimulatory complexes (ISCOMs), virus-like particles (VLPs), and nanoemulsions. Each type presents unique physicochemical characteristics and biological behavior, offering distinct advantages for specific vaccine strategies, though also posing formulation challenges.[106]

Several licensed vaccines incorporate NPs as delivery systems or adjuvants. mRNA vaccines such as Comirnaty and Spikevax use lipid NPs to encapsulate and protect their mRNA cargo. mRESVIA, Moderna's RSV vaccine, also uses this technology. Protein subunit vaccines have also benefited from NP technologies. Nuvaxovid (Novavax COVID-19 vaccine) uses Matrix-M, a saponin-based NP adjuvant, in combination with recombinant spike proteins assembled into NPs. Skycovione (SK Bioscience) employs self-assembling protein NPs displaying the receptor-binding domain of SARS-CoV-2, combined with AS03, an oil-in-water emulsion-based adjuvant that enhances immunogenicity.[104]

VLP vaccines represent another well-established NP-based platform. Gardasil and Gardasil 9, both HPV vaccines, use recombinant L1 proteins assembled into VLPs that mimic the structure of the native virus but lack genetic material, offering a high safety profile and strong immunogenicity. Cervarix, another HPV vaccine, incorporates VLPs of HPV types 16 and 18 and uses the AS04 adjuvant, which combines monophosphoryl lipid A (MPLA) with aluminum hydroxide.[107] The herpes

zoster vaccine Shingrix employs the AS01B adjuvant system, which includes MPLA and the saponin QS-21 encapsulated in liposomes. Similarly, the malaria vaccine RTS,S/AS01 (Mosquirix) uses the AS01 liposomal adjuvant system to deliver *Plasmodium falciparum* antigens effectively.[108]

In the field of TB vaccine research, NPs offer particular promise for enhancing subunit vaccine performance. TB antigens are typically weakly immunogenic on their own and require delivery platforms that enhance antigen uptake. NP systems under active investigation in TB vaccine development include LNPs, liposomes, polymeric NPs (PNPs), such as those based on poly(lactic-*co*-glycolic) acid (PLGA), and nanoemulsions (NEs). These platforms are often combined with potent adjuvants to overcome the limitations of traditional BCG vaccination and to develop novel prophylactic or therapeutic TB vaccines.[102]

7.1 LNPs

LNPs are a versatile and biocompatible class of nanocarriers widely used in pharmaceutical and biomedical research. These nanoscale delivery systems are primarily composed of lipids that self-assemble into structures capable of encapsulating a wide variety of therapeutic agents, including nucleic acids, small molecules, and proteins. Their lipophilic nature, combined with the ability to incorporate hydrophilic and amphiphilic compounds, makes LNPs uniquely suited for overcoming biological barriers such as enzymatic degradation and cellular membranes.[106]

The term "lipid nanoparticles" often encompasses a range of different lipid-based NPs such as liposomes, solid LNPs (SLNs), nanostructured lipid carriers (NLCs), lipid NEs, and lipid–polymer hybrid NPs. However, in the context of nucleic acid delivery, especially mRNA vaccines, the term refers specifically to a formulation of ionizable lipid-based NPs with a core–shell structure optimized for delivering nucleic acids into cells.[104]

LNPs have gained increasing attention due to their ability to address critical challenges in drug delivery. Their nanoscale size facilitates transport across biological barriers, including the blood–brain barrier, and enhances uptake by target tissues. LNPs

exhibit high biocompatibility and are generally well-tolerated. In dermatological applications, their composition allows for good skin compatibility and improved penetration through the stratum corneum, the outermost layer of the skin.[104,106,109]

A major milestone in LNP technology was reached in 2018 with the approval of Onpattro (patisiran), the first siRNA-based drug using LNPs as a delivery vehicle. This formulation uses PEGylated ionizable lipids to deliver siRNA targeting transthyretin for the treatment of hereditary transthyretin-mediated amyloidosis. The approval of Onpattro marked a turning point, demonstrating that LNPs could be safely and effectively used in human gene-silencing therapies.[109]

The most prominent breakthrough in LNP technology came with the emergency use authorization and subsequent full approval of mRNA-based COVID-19 vaccines in 2020. Both the Moderna (Spikevax) and Pfizer–BioNTech (Comirnaty) vaccines employ LNPs to encapsulate and protect fragile mRNA strands encoding the SARS-CoV-2 spike protein. These LNPs are specifically designed for intracellular mRNA delivery: they consist of ionizable lipids that are neutrally charged at physiological pH but become positively charged in the acidic environment of the endosome, facilitating endosomal escape and cytoplasmic release of the mRNA payload. These formulations also include helper lipids (such as cholesterol and phospholipids) and PEGylated lipids to stabilize the NPs and extend circulation time. [104] The same LNP technology by BioNTech is utilized in their two multi-antigen mRNA TB vaccine candidates, BNT164a1 and b1, currently in phase 1a/2b clinical trial.

Unlike traditional solid-core NPs, LNPs used in mRNA vaccine formulations are ionizable amorphous liquid-disordered nanostructures, more accurately described as vesicle-like carriers. They do not form solid crystalline cores; rather, they possess a disordered internal phase that encapsulates the nucleic acid.[110]

7.2 Liposomes

Liposomes are spherical, self-assembling nanocarriers composed of one or more lipid bilayers enclosing an aqueous core. These bilayers are typically made from phospholipids, such as phosphatidylcholine, and often incorporate cholesterol to enhance membrane stability and fluidity. The amphiphilic nature of lipids allows the spontaneous formation of bilayers in aqueous environments, with hydrophilic head groups oriented outward and hydrophobic tails facing inward. This unique structure

enables liposomes to encapsulate both hydrophilic compounds (within the aqueous core) and hydrophobic agents (within the lipid bilayer), making them highly versatile drug and vaccine delivery systems.[111]

The physicochemical and biological behavior of liposomes can be finely tuned by altering their size, surface charge, lipid composition, and surface chemistry. For example, surface modifications such as PEGylation (the addition of polyethylene glycol chains) can improve circulation time and reduce immune recognition, while cationic or ionizable lipids can enhance interactions with negatively charged cell membranes and facilitate intracellular delivery. This adaptability has led to extensive use of liposomes across medicine, cosmetics, nutrition, and nanotechnology.[111]

Liposomes are among the earliest developed nanocarriers in pharmaceutical science. They were first described in 1961 by British hematologist Alec Douglas Bangham at the Babraham Institute in Cambridge, who recognized their structural similarity to biological membranes. This discovery sparked widespread research into their potential as both model systems for cell membranes and carriers for therapeutic agents.[112] In 1981, the first human trial of a liposome-encapsulated drug, liposomal cytarabine, was initiated, highlighting the promise of liposomes for improving drug delivery and pharmacokinetics.[113]

The clinical value of liposomes lies in their ability to enhance drug bioavailability, modify pharmacokinetics, reduce systemic toxicity, and enable targeted delivery. This is especially beneficial for potent but toxic chemotherapeutics. The first FDA-approved liposomal drug, Doxil® (pegylated liposomal doxorubicin), was approved in 1995 for the treatment of Kaposi's sarcoma, and later indicated for ovarian and breast cancers. Doxil dramatically improved the safety profile of doxorubicin by reducing cardiotoxicity. In 1997, AmBisome® (liposomal amphotericin B) was approved for systemic fungal infections, offering potent antifungal activity with significantly reduced nephrotoxicity compared to conventional formulations.[109]

Beyond oncology and antifungal therapy, liposomes have gained particular relevance in the field of vaccine delivery. Cationic and ionizable liposomes are of special interest due to their ability to enhance uptake by APCs, such as DCs, and their capacity to act as immunostimulatory adjuvants. Their surface charge, size, lipid composition, and structural rigidity can all be modified to optimize uptake,

biodistribution, and immune activation. Positively charged liposomes, in particular, interact favorably with negatively charged cell membranes and enhance endosomal escape, facilitating intracellular delivery of antigens and nucleic acids.[111]

Liposomes can efficiently encapsulate a wide range of vaccine-related cargo, including peptides, proteins, protein conjugates, and nucleic acids. The ability to co-deliver antigens along with targeting ligands, stimuli-responsive lipids, and adjuvants allows for the design of advanced vaccine formulations tailored to elicit desired immune responses. Their modularity also permits the targeting of specific tissues and the fine-tuning of release kinetics.[111]

A milestone in liposomal vaccine adjuvant technology was achieved with the development of AS01, a liposome-based adjuvant system used in Shingrix®, the recombinant herpes zoster vaccine approved in 2015. AS01B, the specific formulation in Shingrix, combines liposomal MPLA with the saponin QS-21, resulting in robust humoral and cellular immunity and superior efficacy compared to earlier zoster vaccines. In the same year, Mosquirix® (RTS,S/AS01), the first malaria vaccine to receive regulatory approval (via a positive opinion from the European Medicines Agency), also employed the AS01 adjuvant system, marking another significant application of liposomal delivery in infectious disease prevention.[108]

In the TB vaccine pipeline, two candidates utilize liposomal delivery systems. H107e/CAF10b (Statens Serum Institut) employs cationic liposomes formulated with dimethyldioctadecylammonium (DDA), monomycoloyl glycerol (MMG), and CpG.[56–58] M72/AS01E (GSK Vaccines) incorporates the $AS01_E$ adjuvant, a liposomal formulation containing monophosphoryl lipid A (MPLA), *Quillaja saponaria* Molina fraction 21 (QS-21), and cholesterol.[76]

7.3 Polymeric NPs (PNPs)

PNPs are nanoscale carriers composed of natural or synthetic polymers and have emerged as one of the most adaptable and promising platforms for drug and vaccine delivery. Their polymeric composition allows for a high degree of control over key structural features, including size, shape, surface chemistry, and surface charge, making them ideal candidates for targeted and responsive delivery systems. The remarkable chemical versatility of polymers enables the incorporation of a wide range of functional groups, ligands, and responsive moieties, allowing PNPs

to interact selectively with biological environments, trigger cargo release under specific conditions, and localize effectively within tissues or even subcellular compartments.[114,115]

PNPs can encapsulate, incorporate, or adsorb therapeutic agents, including antigens, adjuvants, and small-molecule drugs, within or onto their matrix. This provides protection from enzymatic degradation in physiological fluids and improves the bioavailability of labile compounds. The release of cargo from PNPs can be precisely engineered through modifications to polymer composition and surface properties. Controlled or stimuli-responsive release can be triggered by external factors such as pH changes, temperature, light, magnetic fields, or enzymatic activity, which is especially useful in pathological microenvironments like tumors or infected tissues. Additionally, the surface of PNPs can be functionalized with targeting ligands, such as peptides, antibodies, or carbohydrates, to achieve receptor-mediated uptake by specific cell types.[115]

A wide range of polymers has been investigated for NP fabrication. Natural polymers such as chitosan, alginate, dextran, and gelatin offer biocompatibility and biodegradability, often with intrinsic biological activity. Synthetic polymers, including poly(lactic-co-glycolic acid) (PLGA), polylactic acid (PLA), polycaprolactone (PCL), polyethylene glycol (PEG), and polymethacrylates, provide highly tunable physicochemical properties and are well characterized in terms of safety and degradation. Many of these polymers can be combined into copolymers to further tailor their release kinetics, mechanical strength, and biological interactions.[115]

In the field of vaccinology, PNPs offer multiple advantages. Their structure allows for the co-delivery of antigens and adjuvants, enabling synchronized immune activation. The rigid nature of many PNPs can promote enhanced uptake by antigen-presenting cells (APCs) compared to softer lipid-based systems. Moreover, their ability to sustain antigen release over extended periods enables prolonged immune stimulation, which is particularly beneficial for building strong immunological memory. PNPs can also be engineered to be mucoadhesive, a critical feature for the development of mucosal vaccines, administered via oral, nasal, or pulmonary routes, where residence time at mucosal surfaces significantly impacts vaccine efficacy.[115]

Despite their strong potential, PNP vaccines have not yet achieved regulatory approval for human use. In the TB vaccine pipeline, however, the GamTBvac candidate

incorporates a PNP-based adjuvant composed of a core of diethylaminoethyl (DEAE)-dextran, a polycationic dextran derivative, coated with CpG oligonucleotides.[73] While no PNP vaccines are currently licensed, polymer-based delivery systems are already in clinical use in other therapeutic fields, underscoring their translational promise. Several injectable controlled-release formulations based on PLGA microspheres have been approved and are commercially available. These include Lupron Depot® (approved in 1989), which delivers leuprolide acetate for the treatment of prostate cancer through sustained hormone suppression, and Sandostatin LAR® Depot, used for acromegaly and neuroendocrine tumors. Other examples include Risperdal Consta® for schizophrenia and Bydureon® for type 2 diabetes mellitus. Although these formulations are based on microscale rather than nanoscale carriers, they exemplify the clinical viability of polymer-based systems and underscore the future potential of PNPs in vaccine development.[115]

7.4 Nanoemulsions (NEs)

NEs are colloidal dispersions composed of two immiscible liquids, typically oil and water, stabilized by surfactants and co-surfactants. Characterized by droplet sizes ranging from approximately 20 to 200 nanometers, NEs form translucent or opaque systems with unique physicochemical properties that enhance the delivery of both hydrophobic and hydrophilic therapeutic agents. Depending on the internal and external phases, NEs can be classified into oil-in-water (O/W), water-in-oil (W/O), or multiple emulsions such as W/O/W and O/W/O systems.[106]

The advantages of NEs in drug and vaccine delivery are numerous. Their small size increases surface area and improves absorption, leading to enhanced bioavailability of poorly soluble drugs. NEs also provide protection from enzymatic degradation, enable controlled and stimuli-responsive release, and can be administered via multiple routes, including oral, intravenous, intranasal, pulmonary, ocular, and transdermal. In particular, their ability to protect labile compounds in harsh environments (such as gastric pH or enzymatic conditions) makes them useful for oral formulations. For parenteral applications, NEs act as protective carriers, improving drug stability and targeting efficiency while reducing systemic toxicity.[116]

Polymer- or lipid-stabilized NEs can be further functionalized with ligands, including antibodies, peptides, or small molecules, enabling targeted delivery through

receptor-mediated uptake. Moreover, NEs can be engineered to respond to biological stimuli such as pH, enzymes, or temperature, triggering cargo release in specific tissues or intracellular compartments.[116]

In addition to drug delivery, NEs have demonstrated utility in gene and vaccine delivery. Compared to traditional liposomes, certain NE systems have shown superior gene transfer efficiency, likely due to improved stability and membrane penetration. Photosensitizer-loaded NEs have also been explored for photodynamic therapy, addressing issues such as poor solubility, nonspecific toxicity, and self-aggregation of conventional formulations.[106]

In vaccinology, NEs serve three primary functions: as antigen delivery vehicles, as immune potentiators (adjuvants), and as mucosal delivery platforms. Their nanoscale properties facilitate antigen uptake APCs, promote both humoral and cellular immune responses, and support co-delivery of antigens and immunostimulants. NEs are particularly promising for mucosal vaccines delivered intranasally or sublingually, where they enable efficient absorption and immune activation without the need for needles. Early applications include mucosal vaccines for influenza and HIV, which progressed to clinical trials. Ongoing research continues to explore their use for diseases such as hepatitis B and anthrax. [106]

Two NE-based adjuvants have been approved for human use [106]. MF59®, developed by Chiron (now part of CSL Seqirus), is a squalene-based O/W NE with an average droplet size of approximately 160 nm. It is stabilized with Tween 80 and Span 85 and was the first NE adjuvant to receive regulatory approval, granted in Europe in 1997.[117] MF59 is currently used in seasonal and pandemic influenza vaccines, such as Fluad®.[106] It enhances immune responses by promoting the recruitment of immune cells to the injection site and activating antigen-presenting cells (APCs).

AS03, developed by GlaxoSmithKline (GSK) and approved in Europe in 2009, is another O/W adjuvant with a droplet size around 150 nm. Its formulation includes squalene, DL-α-tocopherol (vitamin E), and polysorbate 80. AS03 is used in vaccines such as Pandemrix®, Arepanrix®, and Skycovione (in South Korea). The combination of squalene and vitamin E induces local inflammation and potent APC activation, with a notable dose-sparing effect.[118]

In the clinical trials, a TB vaccine candidate ID93+GLA-SE (QTP101) (Quratis) utilizes an NE-based adjuvant. The GLA-SE adjuvant is a stable O/W NE composed of squalene and glucopyranosyl lipid A (TLR4 agonist).[50]

8. MOTIVATION AND RATIONALE FOR THE STUDY

Despite global efforts to control TB, the disease remains a leading cause of death from a single infectious agent, particularly in low- and middle-income countries. Although the BCG vaccine offers protection against severe forms of TB in children, its efficacy in preventing pulmonary TB in adults is inconsistent and limited. This has led to an urgent demand for novel, more effective TB vaccines. Among the strategies currently under exploration, subunit vaccines offer several advantages in terms of safety and versatility. However, subunit vaccines are often poorly immunogenic and require delivery and adjuvant systems to enhance their efficacy. NP-based delivery platforms, particularly those using liposomes and biodegradable polymers, are being investigated to address these challenges.

A critical knowledge gap in the field concerns the optimization of NP vaccine delivery systems, particularly regarding the physicochemical properties of the carriers and how these properties influence the immune response. Although liposomes and PLGA-based particles have been studied in various biomedical contexts, their specific immunological impact in TB vaccine applications remains poorly understood. In particular, limited information exists on how different cationic lipids, cholesterol content, or pH-sensitivity affect the functionality of liposomal vaccine formulations. Similarly, the comparative performance of liposomes, PLGA NPs, and hybrid particles combining both systems has not been systematically evaluated in TB models.

The overarching goal of this research was to address these knowledge gaps by systematically developing, optimizing, and evaluating multiple NP-based vaccine platforms carrying a fusion protein antigen (Ag85B-ESAT6-Rv2034, AER) previously shown to confer protection in mouse and guinea pig models. We aimed to:

- Investigate the role of different cationic lipids in liposome formulations to determine whether various cationic lipids affect immunogenicity beyond simply providing a positive charge.
- Study the underexplored area of pH-sensitive liposomes in TB vaccine development: formulation, stability, and immunogenicity.

- Translate these new findings *in vivo* in a biologically relevant mouse model of intranasal TB infection using the established strain H37Rv of Mtb.
- Explore other understudied NP systems in TB vaccine research, such as PLGA NPs, and pH-sensitive lipid-PLGA hybrid NPs, *in vivo* in a side-by-side comparison.
- Explore the effects of alternative routes of vaccine administration, such as intradermal delivery.

Together, these studies aimed to form a comprehensive body of work that elucidates how rational design and engineering of NP-based delivery and adjuvant systems influence immune responses to subunit vaccines. By identifying and validating critical parameters such as lipid composition, pH-sensitivity, hybrid NP architecture, and administration route, this research addresses key challenges in TB vaccine development. These findings offer practical insights for future preclinical and clinical efforts aimed at creating safer, more effective TB vaccines and may also inform vaccine design strategies for other challenging infectious diseases.

9. SCOPE AND OUTLINE OF THE THESIS

This thesis explores the rational design, development, and evaluation of NP-based delivery systems to enhance the efficacy of subunit vaccines against TB. The primary focus is on optimizing physicochemical parameters of liposomal and polymeric NPs to improve antigen delivery, immune activation, and protection in preclinical models.

The scope of the work encompasses both *in vitro* and *in vivo* studies. It begins with investigating how specific lipid components within cationic liposomes affect DC activation and immunogenicity. Subsequent chapters explore pH-sensitive liposomes designed to enhance cytosolic delivery of antigens and their immunological effects both *in vitro* and in a mouse model of TB. This is followed by a direct comparison of three NP platforms – liposomes, PLGA particles, and lipid-PLGA hybrid NPs – to evaluate their performance as vaccine carriers. The final study addresses the effect of vaccine administration route (subcutaneous vs. intradermal) and dose reduction using hybrid NPs, with the goal of improving vaccine practicality and accessibility.

The thesis is structured as follows:

- **Chapter 1**: General introduction and thesis outline.
  Provides background on TB as a global health threat, limitations of current vaccines, and the rationale for subunit and NP-based vaccine strategies.

- **Chapter 2**: Intrinsic immunogenicity of liposomes for tuberculosis vaccines: Effect of cationic lipid and cholesterol.[119]
  Investigates the immunogenic effects of various cationic lipids and cholesterol content in liposome formulations using DCs.

- **Chapter 3**: Cationic pH-sensitive liposomes as tuberculosis subunit vaccine delivery systems: Effect of liposome composition on cellular innate immune responses.[120]
  Focuses on the design and *in vitro* evaluation of pH-responsive liposomes for delivering TB fusion protein antigen.

- **Chapter 4:** Cationic pH-sensitive liposome-based subunit tuberculosis vaccine induces protection in mice challenged with Mycobacterium tuberculosis.[121]
  Assesses immunogenicity and protective efficacy of the liposomal vaccine compared to BCG and antigen-adjuvant mixtures.

- **Chapter 5**: Evaluation of PLGA, lipid-PLGA hybrid nanoparticles, and cationic pH-sensitive liposomes as tuberculosis vaccine delivery systems in a Mycobacterium tuberculosis challenge mouse model – A comparison.[122]
  Compares three NP delivery platforms for their ability to induce immune responses and reduce bacterial burden in mice.

- **Chapter 6**: Intradermal versus subcutaneous immunization: Effects of administration route using a lipid-PLGA hybrid nanoparticle tuberculosis vaccine.[123]
  Explores alternative administration routes and reduced antigen dosing to improve immunogenicity and practical applicability.

- **Chapter 7**: General Discussion and Future Perspectives.
  Summarizes key findings, discusses implications for TB vaccine development, and outlines directions for future research.

10. REFERENCES

1. Hershkovitz, I. *et al.* Detection and Molecular Characterization of 9000-Year-Old Mycobacterium tuberculosis from a Neolithic Settlement in the Eastern Mediterranean. *PLoS One* 3, e3426 (2008).
2. Zein-Eddine, R. *et al.* The paradoxes of Mycobacterium tuberculosis molecular evolution and consequences for the inference of tuberculosis emergence date. *Tuberculosis* 143, 102378 (2023).
3. World Health Organization. Fact sheets - Tuberculosis. https://www.who.int/news-room/fact-sheets/detail/tuberculosis.
4. World Health Organization. *Global Tuberculosis Report 2024*. (2024).
5. Tuberculosis Vaccine Initiative. Pipeline of vaccines - TBVI. https://www.tbvi.eu/what-we-do/pipeline-of-vaccines/.
6. World Health Organization. *Global Tuberculosis Report 2023*. (2023).
7. Woodland, D. L. Vaccine Development. *Viral Immunology* 30, 141 (2017).
8. World Health Organization. Immunization, Vaccines and Biologicals. https://www.who.int/teams/immunization-vaccines-and-biologicals/diseases.
9. World Health Organization. Vaccines and immunization. https://www.who.int/health-topics/vaccines-and-immunization/.
10. Amanna, I. J. & Slifka, M. K. Successful Vaccines. *Current Topics in Microbiology and Immunology* 428, 1–30 (2018).
11. Hangartner, L. *et al.* Vaccination Strategies Against Highly Variable Pathogens. Springer, (2020).
12. Curtsinger, J. M. & Mescher, M. F. Inflammatory cytokines as a third signal for T cell activation. *Current Opinion in Immunology* 22, 333–340 (2010).
13. Zwerling, A. *et al.* The BCG World Atlas: A Database of Global BCG Vaccination Policies and Practices. *PLoS Med* 8, e1001012 (2011).
14. Andersen, P. & Doherty, T. M. The success and failure of BCG — implications for a novel tuberculosis vaccine. *Nature Reviews Microbiology* 3:8, 656–662 (2005).
15. Rodrigues, L. C., *et al.* Protective effect of BCG against tuberculous meningitis and miliary tuberculosis: A meta-analysis. *International Journal of Epidemiology* 22, 1154–1158 (1993).

16. Trunz, B. B. *et al.* Effect of BCG vaccination on childhood tuberculous meningitis and miliary tuberculosis worldwide: a meta-analysis and assessment of cost-effectiveness. *Lancet* 367, 1173–1180 (2006).
17. Fine, P. E. M. Variation in protection by BCG: implications of and for heterologous immunity. *The Lancet* 346, 1339–1345 (1995).
18. Mangtani, P. *et al.* Protection by BCG Vaccine Against Tuberculosis: A Systematic Review of Randomized Controlled Trials. *Clinical Infectious Diseases* 58, 470–480 (2014).
19. Abubakar, I. *et al.* Systematic review and meta-analysis of the current evidence on the duration of protection by bacillus Calmette-Guérin vaccination against tuberculosis. *Health Technology Assessment (Winchester, England)* 17:37 (2013).
20. Covián, C. *et al.* BCG-Induced Cross-Protection and Development of Trained Immunity: Implication for Vaccine Design. *Frontiers in Immunology* 10, 504051 (2019).
21. Chen, J. *et al.* BCG-induced trained immunity: history, mechanisms and potential applications. *Journal of Translational Medicine* 21, 1–9 (2023).
22. Lai, R., Ogunsola, A. F., Rakib, T. & Behar, S. M. Key advances in vaccine development for tuberculosis—success and challenges. *NPJ Vaccines 2023 8:1* 8, 1–10 (2023).
23. Whittaker, E. *et al.* Age-related waning of immune responses to BCG in healthy children supports the need for a booster dose of BCG in TB endemic countries. *Scientific Reports 2018 8:1* 8, 1–10 (2018).
24. Mangtani, P. *et al.* Observational study to estimate the changes in the effectiveness of bacillus Calmette Guerin (BCG) vaccination with time since vaccination for preventing tuberculosis in the UK. *Health Technology Assessment* 21, 1–54 (2017).
25. Abubakar, I. *et al.* Systematic review and meta-analysis of the current evidence on the duration of protection by bacillus Calmette-Guérin vaccination against tuberculosis. *Health Technology Assessment* 17:37 (2013).
26. Rowland, R. *et al.* Non-Tuberculous Mycobacteria Interference with BCG-Current Controversies and Future Directions. *Vaccines* 8:4, 688 (2020).
27. Poyntz, H. C. *et al.* Non-tuberculous mycobacteria have diverse effects on BCG efficacy against Mycobacterium tuberculosis. *Tuberculosis* 94, 226–237 (2014).

28. Behr, M. A. BCG - Different strains, different vaccines? *Lancet Infectious Diseases* 2, 86–92 (2002).
29. Ritz, N., Hanekom, W. A., Robins-Browne, R., Britton, W. J. & Curtis, N. Influence of BCG vaccine strain on the immune response and protection against tuberculosis. *FEMS Microbiology Reviews* 32, 821–841 (2008).
30. Leung, A. S. *et al.* Novel genome polymorphisms in BCG vaccine strains and impact on efficacy. *BMC Genomics* 9, 1–12 (2008).
31. Frankel, H. *et al.* Different effects of BCG strains – A natural experiment evaluating the impact of the Danish and the Russian BCG strains on morbidity and scar formation in Guinea-Bissau. *Vaccine* 34, 4586–4593 (2016).
32. Horwitz, M. A. *et al.* Commonly administered BCG strains including an evolutionarily early strain and evolutionarily late strains of disparate genealogy induce comparable protective immunity against tuberculosis. *Vaccine* 27, 441–445 (2009).
33. Marimani, M. *et al.* The role of epigenetics, bacterial and host factors in progression of Mycobacterium tuberculosis infection. *Tuberculosis (Edinb)* 113, 200–214 (2018).
34. Wilson, M. E. *et al.* Geographic latitude and the efficacy of bacillus Calmette-Guérin vaccine. *Clinical Infectious Diseases* 20, 982–991 (1995).
35. Narayanan, P. R. Influence of sex, age & nontuberculous infection at intake on the efficacy of BCG: re-analysis of 15-year data from a double-blind randomized control trial in South India. *Indian Journal of Medical Research* 123, 119–124 (2006).
36. Dowd, J. B. *et al.* Social determinants and BCG efficacy: a call for a socio-biological approach to TB prevention. *F1000Research* 7, 224 (2018).
37. Stop TB Partnership. TB Vaccine Preclinical Pipeline - Working Group on New TB Vaccines. https://newtbvaccines.org/tb-vaccine-pipeline/preclinical-stage/.
38. Kaushal, D. *et al.* Mucosal vaccination with attenuated Mycobacterium tuberculosis induces strong central memory responses and protects against tuberculosis. *Nature Communications* 6:1, 1–14 (2015).
39. Foreman, T. W. *et al.* Nonpathologic Infection of Macaques by an Attenuated Mycobacterial Vaccine Is Not Reactivated in the Setting of HIV Co-Infection. *American Journal of Pathology* 187, 2811–2820 (2017).

40. Ahn, S. K. *et al.* Recombinant BCG Overexpressing phoP-phoR Confers Enhanced Protection against Tuberculosis. *Molecular Therapy* 26, 2863–2874 (2018).
41. Heijmenberg, I. *et al.* ESX-5-targeted export of ESAT-6 in BCG combines enhanced immunogenicity & efficacy against murine tuberculosis with low virulence and reduced persistence. *Vaccine* 39, 7265–7276 (2021).
42. Orgeur, M. *et al.* Pathogenomic analyses of mycobacterium microti, an esx-1-deleted member of the mycobacterium tuberculosis complex causing disease in various hosts. *Microbial Genomics* 7, 1–18 (2021).
43. Gröschel, M. I. *et al.* Recombinant BCG Expressing ESX-1 of Mycobacterium marinum Combines Low Virulence with Cytosolic Immune Signaling and Improved TB Protection. *Cell Reports* 18, 2752–2765 (2017).
44. Kwon, K. W. *et al.* BCGΔBCG1419c increased memory CD8+ T cell-associated immunogenicity and mitigated pulmonary inflammation compared with BCG in a model of chronic tuberculosis. *Scientific Reports* 12:1, 1–14 (2022).
45. Gunasena, M. *et al.* Evaluation of early innate and adaptive immune responses to the TB vaccine Mycobacterium bovis BCG and vaccine candidate BCGΔBCG1419c. *Scientific Reports* 12:1, 1–16 (2022).
46. Bouzeyen, R. *et al.* Co-Administration of Anticancer Candidate MK-2206 Enhances the Efficacy of BCG Vaccine Against Mycobacterium tuberculosis in Mice and Guinea Pigs. *Frontiers in Immunology* 12, 645962 (2021).
47. Khatri, B. *et al.* BCG Δzmp1 vaccine induces enhanced antigen specific immune responses in cattle. *Vaccine* 32, 779–784 (2014).
48. Counoupas, C. *et al.* Mucosal delivery of a multistage subunit vaccine promotes development of lung-resident memory T cells and affords interleukin-17-dependent protection against pulmonary tuberculosis. *NPJ Vaccines* 5:1, 1–12 (2020).
49. White, A. D. *et al.* Spore-FP1 tuberculosis mucosal vaccine candidate is highly protective in guinea pigs but fails to improve on BCG-conferred protection in non-human primates. *Frontiers in Immunology* 14, 1246826 (2023).
50. Gomez, M. *et al.* Development and Testing of a Spray-Dried Tuberculosis Vaccine Candidate in a Mouse Model. *Frontiers in Pharmacology* 12, 799034 (2022).

51. Stylianou, E. *et al.* A five-antigen Esx-5a fusion delivered as a prime-boost regimen protects against M.tb challenge. *Frontiers in Immunology* 14, 1263457 (2023).
52. Jia, Q., Masleša-Galić, S., Nava, S. & Horwitz, M. A. Listeria-vectored multi-antigenic tuberculosis vaccine protects C57BL/6 and BALB/c mice and guinea pigs against Mycobacterium tuberculosis challenge. *Communications Biology* 5:1, 1–15 (2022).
53. World Health Organization. TB Research Tracker. https://tbtrialtrack.who.int/.
54. Jeyanathan, M. *et al.* Induction of an Immune-Protective T-Cell Reportsertoire With Diverse Genetic Coverage by a Novel Viral-Vectored Tuberculosis Vaccine in Humans. *The Journal of Infectious Diseases* 214, 1996–2005 (2016).
55. ClinicalTrials.gov. Safety and Immune Responses After Vaccination With Two Investigational RNA-based Vaccines Against Tuberculosis in BCG Vaccinated Volunteers. https://www.clinicaltrials.gov/study/NCT05547464.
56. Woodworth, J. S. *et al.* A novel adjuvant formulation induces robust Th1/Th17 memory and mucosal recall responses in Non-Human Primates. *bioRxiv* 2023.02.23.529651 (2023).
57. Woodworth, J. S. *et al.* A Mycobacterium tuberculosis-specific subunit vaccine that provides synergistic immunity upon co-administration with Bacillus Calmette-Guérin. *Nature Communications* 12:1, 1–13 (2021).
58. Dijkman, K. *et al.* A protective, single-visit TB vaccination regimen by co-administration of a subunit vaccine with BCG. *NPJ Vaccines* 8:1, 1–13 (2023).
59. Vasilyev, K. *et al.* Enhancement of the local CD8+ T-cellular immune response to Mycobacterium tuberculosis in BCG-primed mice after intranasal administration of influenza vector vaccine carrying tb10.4 and hspx antigens. *Vaccines (Basel)* 9, 1273 (2021).
60. Sergeeva, M. *et al.* Mucosal Influenza Vector Vaccine Carrying TB10.4 and HspX Antigens Provides Protection against Mycobacterium tuberculosis in Mice and Guinea Pigs. *Vaccines* 9:4, 394 (2021).
61. Chen, L. *et al.* The development and preliminary evaluation of a new Mycobacterium tuberculosis vaccine comprising Ag85b, HspX and CFP-10:ESAT-6 fusion protein with CpG DNA and aluminum hydroxide adjuvants. *FEMS Immunology and Medical Microbiology* 59, 42–52 (2010).

62. Lu, J. *et al.* Therapeutic evaluation of antibiotics combined with recombinant tuberculosis vaccine AEC/BC02 in a guinea pig model of Mycobacterium tuberculosis infection. *Chinese Journal of Microbiology and Immunology* 38, 414–419 (2018).
63. Stylianou, E. *et al.* Improvement of BCG protective efficacy with a novel chimpanzee adenovirus and a modified vaccinia Ankara virus both expressing Ag85A. *Vaccine* 33, 6800–6808 (2015).
64. Wilkie, M. *et al.* A phase I trial evaluating the safety and immunogenicity of a candidate tuberculosis vaccination regimen, ChAdOx1 85A prime – MVA85A boost in healthy UK adults. *Vaccine* 38, 779–789 (2020).
65. Choi, Y. H. *et al.* Safety and Immunogenicity of the ID93 + GLA-SE Tuberculosis Vaccine in BCG-Vaccinated Healthy Adults: A Randomized, Double-Blind, Placebo-Controlled Phase 2 Trial. *Infectious Diseases and Therapy* 12, 1605–1624 (2023).
66. Nemes, E. *et al.* Prevention of M. tuberculosis Infection with H4:IC31 Vaccine or BCG Revaccination. *New England Journal of Medicine* 379, 138–149 (2018).
67. Lahey, T. *et al.* Immunogenicity and Protective Efficacy of the DAR-901 Booster Vaccine in a Murine Model of Tuberculosis. *PLoS One* 11, e0168521 (2016).
68. Masonou, T. *et al.* CD4+ T cell cytokine responses to the DAR-901 booster vaccine in BCG-primed adults: A randomized, placebo-controlled trial. *PLoS One* 14, e0217091 (2019).
69. Munseri, P. *et al.* DAR-901 vaccine for the prevention of infection with Mycobacterium tuberculosis among BCG-immunized adolescents in Tanzania: A randomized controlled, double-blind phase 2b trial. *Vaccine* 38, 7239–7245 (2020).
70. Cardona, P. J. *et al.* Immunotherapy with fragmented Mycobacterium tuberculosis cells increases the effectiveness of chemotherapy against a chronical infection in a murine model of tuberculosis. *Vaccine* 23, 1393–1398 (2005).
71. Prabowo, S. A. *et al.* RUTI vaccination enhances inhibition of mycobacterial growth ex vivo and induces a shift of monocyte phenotype in mice. *Frontiers in Immunology* 10, 440725 (2019).

72. Nell, A. S. *et al.* Safety, Tolerability, and Immunogenicity of the Novel Antituberculous Vaccine RUTI: Randomized, Placebo-Controlled Phase II Clinical Trial in Patients with Latent Tuberculosis Infection. *PLoS One* 9, e89612 (2014).
73. Tkachuk, A. P. *et al.* Multi-subunit BCG booster vaccine GamTBvac: Assessment of immunogenicity and protective efficacy in murine and guinea pig TB models. *PLoS One* 12, e0176784 (2017).
74. Vasina, D. V. *et al.* First-In-Human Trials of GamTBvac, a Recombinant Subunit Tuberculosis Vaccine Candidate: Safety and Immunogenicity Assessment. *Vaccines* 7:4, (2019).
75. Dogra, S., Jain, S., Sharma, A., Chhabra, S. & Narang, T. Mycobacterium indicus pranii (MIP) vaccine: Pharmacology, indication, dosing schedules, administration, and side effects in clinical practice. *Indian Dermatology Online Journal* 14, 753–761 (2023).
76. Tait, D. R. *et al.* Final Analysis of a Trial of M72/AS01 E Vaccine to Prevent Tuberculosis. *New England Journal of Medicine* 381, 2429–2439 (2019).
77. Tameris, M. *et al.* Live-attenuated Mycobacterium tuberculosis vaccine MTBVAC versus BCG in adults and neonates: a randomised controlled, double-blind dose-escalation trial. *Lancet Respiratory Medicine* 7, 757–770 (2019).
78. Cotton, M. F. *et al.* Safety and immunogenicity of VPM1002 versus BCG in South African newborn babies: a randomised, phase 2 non-inferiority double-blind controlled trial. *Lancet Infectious Diseases* 22, 1472–1483 (2022).
79. William Tong, C. Y. Different Types of Vaccines. *Tutorial Topics in Infection for the Combined Infection Training Programme* (2019).
80. Minor, P. D. Live attenuated vaccines: Historical successes and current challenges. *Virology* 479–480, 379–392 (2015).
81. Tang, J. *et al.* Mycobacterium tuberculosis infection and vaccine development. *Tuberculosis* 98, 30–41 (2016).
82. Checkley, A. M. & McShane, H. Tuberculosis vaccines: Progress and challenges. *Trends in Pharmacological Sciences* 32, 601–606 (2011).
83. Verardi, P. H. *et al.* A vaccinia virus renaissance. *Human Vaccines & Immunotherapeutics* 8, 961–970 (2012).
84. Strassburg, M. A. The global eradication of smallpox. *American Journal of Infection Control* 10, 53–59 (1982).

85. Sanders, B., *et al.* Inactivated viral vaccines. *Vaccine Analysis: Strategies, Principles, and Control* 45–80 (2015).
86. Cagigi, A. & Douradinha, B. Have mRNA vaccines sentenced DNA vaccines to death? *Expert Review of Vaccines* 22, 1154–1167 (2023).
87. Ewer, K. J. *et al.* Viral vectors as vaccine platforms: from immunogenicity to impact. *Current Opinion in Immunology* 41, 47–54 (2016).
88. Mendonça, S. A. *et al.* Adenoviral vector vaccine platforms in the SARS-CoV-2 pandemic. *NPJ Vaccines* 6:1, 1–14 (2021).
89. Volz, A. & Sutter, G. Modified Vaccinia Virus Ankara: History, Value in Basic Research, and Current Perspectives for Vaccine Development. *Advances in Virus Research* 97, 187–243 (2017).
90. Suder, E. *et al.* The vesicular stomatitis virus-based Ebola virus vaccine: From concept to clinical trials. *Human Vaccines & Immunotherapeutics* 14, 2107–2113 (2018).
91. Gerke, C. *et al.* Measles-vectored vaccine approaches against viral infections: a focus on Chikungunya. *Expert Review of Vaccines* 18, 393–403 (2019).
92. Zeng, J. *et al.* Exploring the Potential of Cytomegalovirus-Based Vectors: A Review. *Viruses* 15:10, 2043 (2023).
93. Lundstrom, K. Viral Vectors in Gene Therapy: Where Do We Stand in 2023? *Viruses* 15:3, 698 (2023).
94. Hou, X., Zaks, T., Langer, R. & Dong, Y. Lipid nanoparticles for mRNA delivery. *Nature Reviews Materials* 6, 1078–1094 (2021).
95. Matarazzo, L. & Bettencourt, P. J. G. mRNA vaccines: a new opportunity for malaria, tuberculosis and HIV. *Frontiers in Immunology* 14, 1172691 (2023).
96. Larsen, S. E. *et al.* Tuberculosis vaccines update: Is an RNA-based vaccine feasible for tuberculosis? *International Journal of Infectious Diseases* 130, S47–S51 (2023).
97. BioNTech. Safety and Immune Responses After Vaccination With Two Investigational RNA-based Vaccines Against Tuberculosis in BCG Vaccinated Volunteers, Trial ID BNT164-02. https://clinicaltrials.biontech.com/trials/BNT164-02.
98. Ghattas, M. *et al.* Vaccine Technologies and Platforms for Infectious Diseases: Current Progress, Challenges, and Opportunities. *Vaccines* 9:12, 1490 (2021).
99. Lang, F. *et al.* Identification of neoantigens for individualized therapeutic cancer vaccines. *Nature Reviews Drug Discovery* 21:4, 261–282 (2022).

100. Tan, M. & Jiang, X. Recent advancements in combination subunit vaccine development. *Human Vaccines & Immunotherapeutics* 13, 180–185 (2017).
101. Lee, W. & Suresh, M. Vaccine adjuvants to engage the cross-presentation pathway. *Frontiers in Immunology* 13, 940047 (2022).
102. Duong, V. T. *et al.* Towards the development of subunit vaccines against tuberculosis: The key role of adjuvant. *Tuberculosis* 139, 102307 (2023).
103. Anselmo, A. C. *et al.* Nanoparticles in the clinic: An update post COVID-19 vaccines. *Bioengineering & Translational Medicine* 6, e10246 (2021).
104. Tenchov, R. *et al.* Lipid Nanoparticles from Liposomes to mRNA Vaccine Delivery, a Landscape of Research Diversity and Advancement. *ACS Nano* 15, 16982–17015 (2021).
105. Singh, R. & Lillard, J. W. Nanoparticle-based targeted drug delivery. *Experimental and Molecular Pathology* 86, 215–223 (2009).
106. Filipić, B. *et al.* Nanoparticle-Based Adjuvants and Delivery Systems for Modern Vaccines. *Vaccines* 11:7, 1172 (2023).
107. Mohsen, M. O. *et al.* Major findings and recent advances in virus–like particle (VLP)-based vaccines. *Seminars in Immunology* 34, 123–132 (2017).
108. Roman, F. *et al.* Adjuvant system AS01: from mode of action to effective vaccines. *Expert Review of Vaccines* 23, 715–729 (2024).
109. Etter, E. L. *et al.* Delivering more for less: nanosized, minimal-carrier and pharmacoactive drug delivery systems. *Advanced Drug Delivery Reviews* 179, 113994 (2021).
110. Unruh, T. *et al.* Mesoscopic Structure of Lipid Nanoparticle Formulations for mRNA Drug Delivery: Comirnaty and Drug-Free Dispersions. *ACS Nano* 18, 9746–9764 (2024).
111. Schmidt, S. T. *et al.* Liposome-based adjuvants for subunit vaccines: Formulation strategies for subunit antigens and immunostimulators. *Pharmaceutics* 8, 1–22 (2016).
112. Bangham, A. D. & Horne, R. W. Action of saponin on biological cell membranes. *Nature* 196, 952–953 (1962).
113. Salehi, B. *et al.* Liposomal Cytarabine as Cancer Therapy: From Chemistry to Medicine. *Biomolecules* 9:12, 773 (2019).
114. Niculescu, A. G. & Grumezescu, A. M. Polymer-Based Nanosystems—A Versatile Delivery Approach. *Materials* 14:22, 6812 (2021).

115. Beach, M. A. *et al.* Polymeric Nanoparticles for Drug Delivery. *Chemical Reviews* 124, 5505–5616 (2024).
116. Jacob, S. *et al.* Innovations in Nanoemulsion Technology: Enhancing Drug Delivery for Oral, Parenteral, and Ophthalmic Applications. *Pharmaceutics* 16:10, 1333 (2024).
117. O'Hagan, D. T. *et al.* The history of MF59® adjuvant: A phoenix that arose from the ashes. *Expert Review of Vaccines* 12, 13–30 (2013).
118. Morel, S. *et al.* Adjuvant System AS03 containing α-tocopherol modulates innate immune response and leads to improved adaptive immunity. *Vaccine* 29, 2461–2473 (2011).
119. Szachniewicz, M. M. *et al.* Intrinsic immunogenicity of liposomes for tuberculosis vaccines: Effect of cationic lipid and cholesterol. *European Journal of Pharmaceutical Sciences* 195, 106730 (2024).
120. Szachniewicz, M. M. *et al.* Cationic pH-sensitive liposomes as tuberculosis subunit vaccine delivery systems: Effect of liposome composition on cellular innate immune responses. *International Immunopharmacology* 145, 113782 (2025).
121. Szachniewicz, M. M. *et al.* Cationic pH-sensitive liposome-based subunit tuberculosis vaccine induces protection in mice challenged with Mycobacterium tuberculosis. *European Journal of Pharmaceutics and Biopharmaceutics* 203, 114437 (2024).
122. Szachniewicz, M. M. *et al.* Evaluation of PLGA, lipid-PLGA hybrid nanoparticles, and cationic pH-sensitive liposomes as tuberculosis vaccine delivery systems in a Mycobacterium tuberculosis challenge mouse model – A comparison. *International Journal of Pharmaceutics* 666, 124842 (2024).
123. Szachniewicz, M. M. *et al.* Intradermal versus subcutaneous immunization: Effects of administration route using a lipid-PLGA hybrid nanoparticle tuberculosis vaccine. *European Journal of Pharmaceutical Sciences* 205, 106995 (2025).

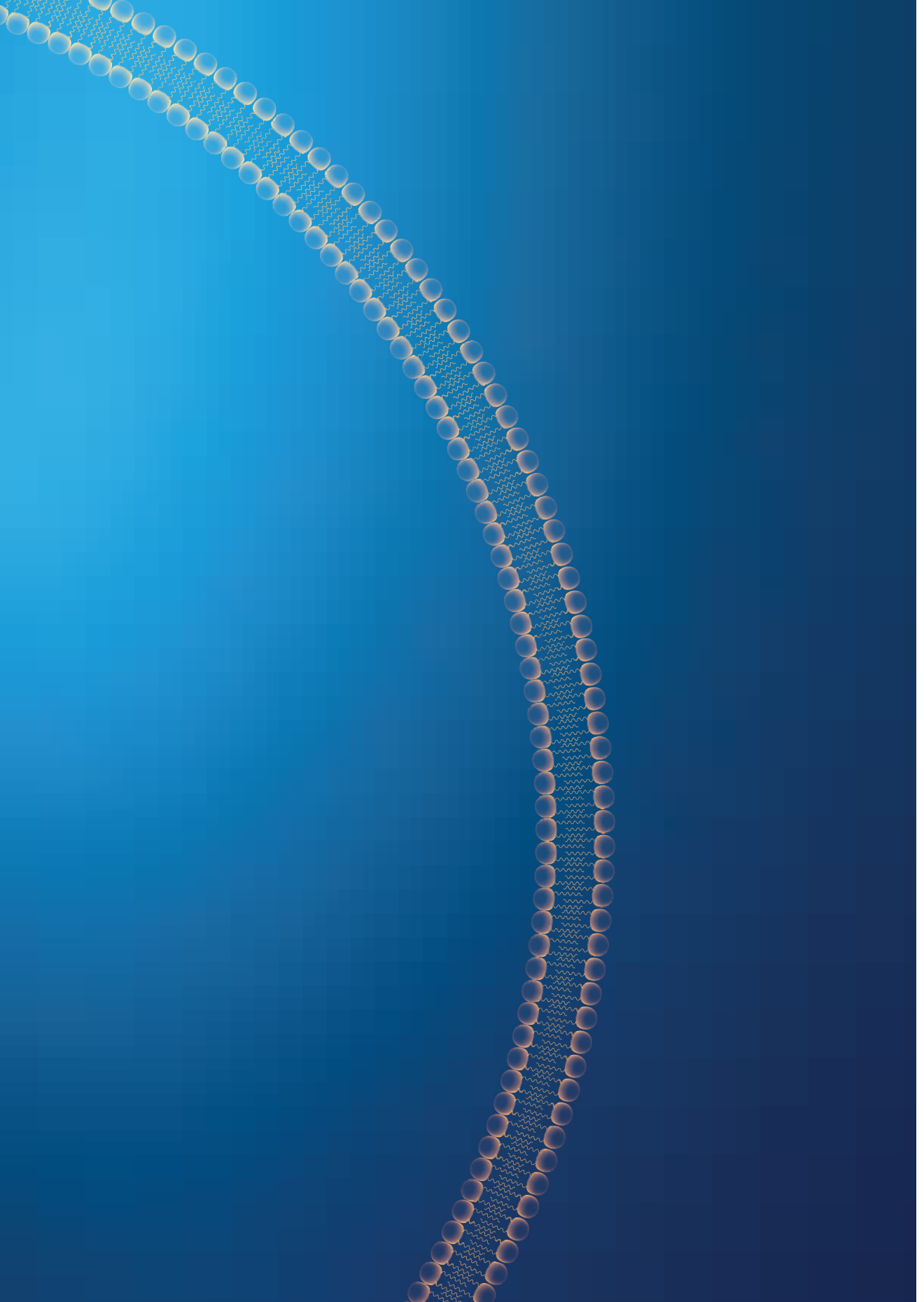

CHAPTER 2

Intrinsic immunogenicity of liposomes for tuberculosis vaccines: effect of cationic lipid and cholesterol

M.M. Szachniewicz, M.A. Neustrup, K.E. van Meijgaarden, W. Jiskoot,
J.A. Bouwstra, M.C. Haks, A. Geluk, T.H.M. Ottenhoff

Adapted from European Journal of Pharmaceutical Sciences, 2024, 195: 106730

ABSTRACT

Tuberculosis (TB) is still among the deadliest infectious diseases, hence there is a pressing need for more effective TB vaccines. Cationic liposome subunit vaccines are excellent vaccine candidates offering effective protection with a better safety profile than live vaccines. In this study, we aim to explore intrinsic adjuvant properties of cationic liposomes to maximize immune activation while minimizing aspecific cytotoxicity. To achieve this, we developed a rational strategy to select liposomal formulation compositions and assessed their physicochemical and immunological properties in *in vitro* models using human monocyte-derived dendritic cells (MDDCs). A broad selection of commercially available cationic compounds was tested to prepare liposomes containing Ag85B-ESAT6-Rv2034 (AER) fusion protein antigen. 1,2-Dioleoyl-*sn*-glycero-3-ethylphosphocholine (EPC)-based liposomes exhibited the most advantageous activation profile in MDDCs as assessed by cell surface activation markers, cellular uptake, antigen-specific T-cell activation, cytokine production, and cellular viability. The addition of cholesterol to 20 mol% improved the performance of the tested formulations compared to those without it; however, when its concentration was doubled there was no further benefit, resulting in reduced cell viability. This study provides new insights into the role of cationic lipids and cholesterol in liposomal subunit vaccines.

1. INTRODUCTION

Tuberculosis (TB) is among the top ten causes of lethality in low-income and lower-middle-income countries with an estimated 3.6 million undiagnosed individuals.[1] Approximately a quarter of the entire human population is (latently) infected with *Mycobacterium tuberculosis* (Mtb), and in 2021, 10.6 million people fell ill, and 1.6 million died from TB.[2] Moreover, the TB burden is aggravated by the increased occurrence of drug-resistant strains. Thus, TB continues to be a global problem that requires improved (early) diagnosis,[3] treatment, and prevention.[2,4] In this study, we aim to advance the knowledge of TB prevention by developing novel vaccine modalities.

Vaccines are commonly recognized as the most effective and inexpensive way of solving the burden of infectious diseases.[5,6] The complete eradication of smallpox and rinderpest, and the more recent success of SARS-CoV2 vaccines, have proven the efficacy of vaccines in disease prevention.[7] Unfortunately, it is difficult to develop effective and safe vaccines against some infectious diseases, including TB. Currently, the only available vaccine against TB is *Mycobacterium bovis* Bacillus Calmette–Guérin (BCG).[8] The BCG vaccine confers variable and often inadequate protection, especially against the pulmonary form in adults, which is accountable for Mtb transmission in adolescents and adults.[9–11] Therefore, there is still an urgent need for improved vaccines against TB.[8] The development of subunit vaccines can contribute to this demand.

Subunit vaccines are based either on synthesized or purified antigens, DNA, or RNA.[12] Being non-live, they are one of the safest vaccine types and as a result can potentially be administrated to a very broad population, including immunocompromised individuals.[13,14] Hence, a subunit vaccine is a logical candidate for a TB vaccine, as the countries with the highest TB rates have a substantial incidence of HIV infection.[2] However, intrinsically subunit vaccines are often insufficiently immunogenic[14–16] as they lack immune-activating constituents, such as pathogen-associated molecular patterns (PAMPs), which are present in traditional (live-attenuated and inactivated) vaccines. Hence, this vaccine type often cannot induce proficient maturation of antigen-presenting cells (APCs), including dendritic cells (DCs). As a result, they fail to induce adequate protective

immunity.[17] Thus, in order to overcome this inherent limitation, the development of subunit vaccine delivery systems is of utmost importance. This study addresses this issue.

Cationic liposomes are excellent subunit vaccine delivery systems that act as particulate adjuvants.[12,18–21] Several liposome-based subunit vaccines have been approved for clinical use.[22–24] Liposomes can protect their antigenic cargo from degradation, and potentially co-deliver antigens with molecular adjuvants and PAMPs such as Toll-like receptor (TLRs) ligands. In addition, such delivery systems facilitate and enhance antigen uptake by APCs allowing a reduction of the required dose of antigens as well as molecular adjuvants to induce the desired immune responses.[12,20,25–28] In particular, cationic liposomes can potently enhance antigen-specific immune responses as they have intrinsic immune-stimulatory properties to induce maturation of DCs and can trigger subsequent $CD4^+$–Th1 and $CD8^+$ T-cell responses.[20,28–32] Therefore, cationic liposomes provide a powerful and versatile platform for vaccination.

The full potential of cationic liposomes as vaccine components has not been fully explored yet. It is known that the physicochemical properties of liposomes, like size and surface charge, affect the immunological outcomes, yet the role of the lipids forming the bilayer is still not fully understood.[20,33–36] Several studies have compared cationic lipids and investigated their effect on immune responses; however, the available data is not conclusive.[20,33–35,37–39] In many of these reports, the evaluated range of cationic lipids was limited. Therefore, it is challenging to draw definitive conclusions in the vaccine field. Moreover, the choice of biological systems, in which these liposomes were tested, varied greatly. Some of those studies used *in vitro* mouse or human models (using primary cells or cell lines) mainly looking at changes in (surface) activation markers of DCs. Others used *in vivo* models and focused on outcomes such as total Ig titers or neutralizing antibody titers. Similarly, the interplay of cationic lipids and liposome components with cholesterol has not been researched thoroughly. It is known that cholesterol can improve uptake of liposomes by APCs and phagocytes; however, the concentration required for this improvement and to what extent the immune response can be improved has not been clearly elucidated.[15,40–44] Therefore, in

this study, we have examined the effect of cholesterol incorporation into various liposomal compositions on the physicochemical properties of liposomes and on various biological outcomes in a systematic way.

The goal of this study was to formulate liposomes with different cationic lipids and cholesterol contents, investigate their effect on the physicochemical properties and assess human immune responses *in vitro*. The best-performing formulations were optimized to achieve the most potent immune stimulation while minimizing cellular toxicity. We compared several commercially available cationic lipids formulated in liposomal formulations containing the designed Mtb antigen AER, a hybrid antigen composed of three Mtb proteins with different functions. Previously, we showed that AER can reduce the bacterial load in HLA-DR3 transgenic mice as well as guinea pigs models of acute TB.[45] The formulations that fulfilled our predefined inclusion criteria were subsequently tested on primary human monocyte-derived DCs (MDDCs), cellular viability, antigen uptake, and cellular activation. The best-performing formulations were selected and optimized to maximize immune activation and minimize cytotoxicity. Since $CD4^+$ Th1 cell responses are an important correlate of immunity and protection against TB, the potential efficacy of the four best-performing vaccine formulations was further determined *in vitro* using the activation of Rv2034 and Ag85B antigen-specific reporter $CD4^+$ T-cell clones/lines.

2. MATERIALS AND METHODS

1.1 Materials

1,2-dioleoyl-3-trimethylammonium-propane chloride salt (DOTAP), 3ß-[N-(N',N'-dimethyl-aminoethane)-carbamoyl]cholesterol hydrochloride (DC-chol), dimethyldioctadecyl-ammonium bromide salt (DDA), 1,2-dioleoyl-*sn*-glycero-3-ethylphosphocholine chloride salt (EPC), N^4-cholesteryl-spermine hydrochloride (GL-67), 1,2-dioleyloxy-3-dimethylamino-propane (DODMA), N1-[2-((1S)-1-[(3-aminopropyl)amino]-4-[di(3-amino-propyl)amino]-butylcarboxamido)ethyl]-3,4-di[oleyloxy]-benzamide (MVL5), 1,2-dioleoyl-*sn*-glycero-3-phosphocholine (DOPC), and 1,2-distearoyl-*sn*-glycero-3-phosphocholine (DSPC) were purchased from Avanti Polar Lipids, Inc. (USA). Cholesterol was obtained from Merck KGaA.(Germany). Recombinant fusion protein AER was produced using the previously described method.[46] Briefly, MTB genes were amplified using polymerase chain reaction (PCR)

from genomic DNA of lab strain H37Rv and cloned using Gateway technology (Invitrogen, USA) in a bacterial expression vector containing an N-terminal hexahistidine (His) tag. Correct insertion of the products was confirmed using sequencing. The recombinant protein was expressed in *Escherichia coli* strain BL21 (DE3) and purified. The quality of the protein in terms of size and purity was evaluated by gel electrophoresis using Coomassie brilliant blue staining and Western blotting using an anti-His antibody (Invitrogen, USA). The endotoxin level in the protein was measured using a ToxinSensor™ Chromogenic Limulus Amebocyte Lysate (LAL) Endotoxin Assay Kit (GenScript, USA). The endotoxin contents were below 50 EU (endotoxin unit) per mg of a protein. Subsequently, AER was tested to exclude non-specific T-cell stimulation and cellular toxicity in the IFNγ release assay. For this assay PBMCs of *in vitro* purified protein derivative (PPD) negative, healthy Dutch donors recruited at the Sanquin Blood Bank, Leiden, the Netherlands were used.

1.2 Preparation of liposomal formulations

The liposomal formulations were prepared using the thin-film hydration method. Lipids were dissolved in chloroform and added to round-bottom flasks. Various cationic lipids and zwitterionic lipids were used, and additionally, cholesterol was added to some formulations (Table 1). The lipids of choice were diluted in chloroform from 25 mg/ml stock solutions. The final total amount of lipids used per formulation was 5 mg (10 mg/ml) in chloroform. The lipid solution was transferred to a round-bottom flask, and the chloroform was evaporated using a rotary evaporator (Buchi rotavapor R210, Switzerland). Subsequently, the lipid film was rehydrated with 1 ml of 100 µg/ml AER in 10 mM phosphate buffer (PB) with 9.8 % sucrose (pH = 7.4) to prepare AER-loaded liposomes. For the preparation of empty liposomes (without AER) and fluorescent-labeled liposomes (also without AER), only the buffer was used for rehydration. After the hydration, the liposomes were downsized using a tip sonicator (Branson Sonifier 250, US). The sonication program consisted of eight cycles, each cycle encompassed 30 s of sonication at a 10 % amplitude followed by a break of 60 s. Samples were submerged in ice during the sonication. Short sonication times at a low amplitude alongside submersion in ice allowed to reduce degradation of lipids. Hereafter, the liposomes were centrifuged (Allegra X-12R, US) at 524 g for 5 min to spin down the metal particles shed by the tip sonicator. To remove the metal-particle pellets, the supernatants containing liposomal formulations were transferred to new tubes, and the pellets were discarded. To avoid that the tip

sonication would degrade the fluorophore, fluorescent-labeled liposomes (without AER) were downsized using a 10 ml extruder (LIPEX extruder, Northern Lipids, Canada). The liposomal formulations were extruded 5-6 times at room temperature, first through carbonate filters with a pore size of 400 nm and then through a 200 nm filter (Nucleopore Millipore, the Netherlands). Hereafter, the liposomes (5 mg/ml lipids) were stored at 4 °C. To assess the impact of tip sonication on biological results we investigated the effect of pre-sonicated and non-sonicated solutions of AER as controls. We also studied the effects of AER-free non-labeled liposomes that were not sonicated but extruded similarly to fluorescent-labeled liposomes.

1.3 Particle size and Zeta-potential determination

The intensity-weighted average hydrodynamic diameter (Z-average size) and polydispersity index (PDI) of the liposomes were determined by dynamic light scattering, and the Zeta-potential was determined by laser Doppler electrophoresis. For the measurements, the formulations were diluted to 0.25 mg/mL lipid in 10 mM PB (pH = 7.4) and added to 1.5 ml VWR Two-Sided Disposable PS Cuvettes (VWR, the Netherlands). Measurements were conducted in technical triplicates with a minimum of ten runs for each measurement at 20 °C using a nano ZS Zetasizer coupled with a 633 nm laser and 173° optics (Malvern Instruments, Worcestershire, UK). The data were analyzed with Zetasizer Software v7.13 (Malvern Instruments).

1.4 Generation of dendritic cells and macrophages from peripheral blood mononuclear cells

Peripheral blood mononuclear cells (PBMCs) were isolated from buffy coats obtained from healthy individuals after written informed consent (Sanquin Blood Bank, The Netherlands). PBMCs were separated from the blood using the Ficoll-based density gradient centrifugation method. Subsequently, $CD14^+$ cells were isolated from the PBMCs using the magnetic cell isolation (MACS) technique with an autoMACS Pro Separator (Miltenyi Biotec BV, the Netherlands). DCs, anti- (M2), and pro-inflammatory (M1) macrophages were generated from these $CD14^+$ cells by incubating them for six days in the presence of cytokines. To generate MDDCs, cells were incubated with 10 ng/ml recombinant human granulocyte-macrophage colony-stimulating factor (GM-CSF; Miltenyi Biotec BV, the Netherlands) and 10 ng/ml recombinant human interleukin 4 (IL-4; Peprotech, USA). M2 macrophages

were differentiated in the presence of 50 ng/ml macrophage colony-stimulating factor (M-CSF; Miltenyi Biotec BV, the Netherlands), and M1 macrophages in the presence of 5 ng/ml GM-CSF (Miltenyi Biotec BV, the Netherlands).[47] All cell types were cultured at 37 °C / 5 % CO_2 in a complete Roswell Park Memorial Institute (RPMI) 1640 medium that was supplemented with 10 % fetal bovine serum (FBS), 100 units/ml penicillin and 100 µg/ml streptomycin, and 2mM GlutaMAX (Gibco, Thermo Fisher Scientific, Belgium). MDDCs were harvested by pipetting the medium, and macrophages were harvested with trypsinization (Trypsin-EDTA 0.05 %, phenol red, Gibco, Thermo Fisher Scientific, Belgium).

1.5 Activation and viability of MDDCs

To assess the potential cellular toxicity and the ability of the empty and AER-containing liposomal formulations to activate MDDCs, the formulations were added to round-bottom 96-well plates (CELLSTAR, Greiner Bio-One GmbH, Germany), seeded with 30,000 MDDCs/well (25 – 250 µg/ml lipids, in 200 µl medium) and incubated for 1 h at 37 ˚C / 5 % CO_2. Hereafter, the cells were washed with a complete RPMI medium to remove the free liposomes and cultured overnight at 37 °C / 5 % CO_2. The following day, the cells were spun down, and the supernatants were collected and stored at -20 ˚C till further use. To stain the cells for flow cytometry, the cells were first washed with FACS buffer (PBS containing 0.1 % bovine serum albumin; Merck, Germany) and incubated for 5 min with 5 % human serum (Sanquin Blood Bank, the Netherlands) in PBS to block non-specific Fc-receptor binding. Next, the cells were washed, and the cell surface markers on the MDDCs were stained for at least 30 min with monoclonal antibodies (CCR7-BB515 (clone 3D12), CD83-PE (clone HB15e), CD40-APC (clone 5C3), CD80-APC-R700 (clone L307.4), HLA-DR-V500 (clone G46-6) from BD Biosciences, Belgium, and CD86-BV421 (clone IT2.2) from BioLegend, the Netherlands) in FACS buffer. Subsequently, the cells were washed and stained with SYTOX AADvanced Dead Cell Stain (Invitrogen, Thermo Fisher Scientific, Belgium) in FACS buffer. Viability was calculated as a percentage of SYTOX AADvanced-negative cell population in relation to all recorded cells. Acquisition of flow cytometry data was performed using a BD FACSLyric Flow Cytometer (BD Biosciences, Belgium). Data were analyzed using FlowJo (version 10.6, FlowJo LLC, BD, USA) software.

1.6 Liposomal uptake study

MDDCs, M1, or M2 macrophages were seeded in round-bottom 96-well plates at a density of 30,000 cells/well. Afterwards, the cells were exposed to 1 % v/v empty fluorescent-labeled liposomes (containing 0.1 mol% of 1,2-dioleoyl-*sn*-glycero-3-phosphoethanolamine-N-(Cyanine 5) (18:2 PE-Cy5) Avanti Polar Lipids, Inc., USA) for 1 h. Hereafter, the cells were washed with FACS buffer 3 times to remove free liposomes. The acquisition of flow cytometry data was performed using a BD FACSLyric Flow Cytometer. Data were analyzed using FlowJo (version 10.6) software.

1.7 T-cell activation

Similarly, heterozygous HLA-DR3$^+$ MDDCs were exposed for 1 hour with liposomal formulations at 5 µg/ml AER and 250 µg/ml lipids in 200 µl of complete RPMI (Gibco, Thermo Fisher Scientific, Bleiswijk, the Netherlands) at 37 ˚C / 5 % CO_2. Cells were washed twice and 2×10^4 pre-pulsed HLA-DR3$^+$ MDDCs were cocultured with either 1×10^5 T-cells from the Rv2034 specific[48] T-cell clone (1B4 recognizing peptide 75-105) or an Ag85B-specific[49] T-cell clone (L10B4 recognizing peptide 56-65) in a 5 ml Falcon tube in a total volume of 400 µl of Iscove's Modified Dulbecco's Medium supplemented with Glutamax, 100 U/ml penicillin, 100 µg/ml streptomycin (Gibco, Thermo Fisher Scientific, Bleiswijk, the Netherlands) and 10 % pooled human serum (Sigma, Merck, Darmstadt, Germany). After 6 hours Brefeldin-A was added (3 µg/ml) (Sigma, Merck, Darmstadt, Germany) and cells were incubated for an additional 16 hours at 37 ˚C / 5 % CO_2. Subsequently, cells were harvested and stained for flow cytometric analysis with the violet live/dead stain (ViViD, Invitrogen, Thermo Fisher Scientific, Bleiswijk, the Netherlands), surface markers CD3-HorizonV500 (UCHT1, BD Horizon, Belgium), CD4-AlexaFluor 700 (RPA-T4, BD Pharmingen, Belgium), CD8-FITC (HIT8a, BioLegend, the Netherlands) and after fixation and permeabilization with fix/perm reagents (Nordic MUbio, Susteren, the Netherlands) for IFN-Y-PerCP-Cy5.5 (4S.B3, Invitrogen, Thermo Fisher Scientific, the Netherlands) and CD154-PE (TRAP1, BD Pharmingen, Belgium).

1.8 Luminex assay

Supernatants from activation and viability experiments were tested in two Bio-Plex panels (Bio-Rad, Veenendaal, the Netherlands) according to the manufacturer's

protocols. In total 16 analytes were measured. The chemokine panel consisted of CXCL9, CXCL11, CCL8, and CCL22. The cytokine panel included CCL11 (Eotaxin), GM-CSF, IFN-α2, IL-1β, IL-1rα, IL-6, CXCL10, CCL2 (MCP-1), CCL3, CCL4, RANTES and TNF-α. Samples were acquired on a Bio-Plex 200 system and analyzed with Bio-Plex manager software version 6.1.

1.9 Statistical analysis

Statistical analyses were performed in GraphPad Prism, version 8.01 (GraphPad Software, Prism, USA). The results were analyzed with the Kruskal-Wallis test followed by an uncorrected Dunn's post-hoc test when comparing non-parametric data sets of three or more groups to the control group, where $P < 0.05$ was considered as statistically significant (*$P < 0.05$, **$P < 0.01$, ***$P < 0.001$, ****$P < 0.0001$). Wilcoxon matched-pairs signed rank test was performed when comparing two non-parametric data groups.

3. RESULTS3.1 Preparation and characterization of cationic liposomal formulations

A schematic overview of the development of our liposomal vaccine formulations is depicted in Figure 1. In the first step, we tested the effect of the selected cationic lipids and cholesterol on the physicochemical properties of liposomes. We excluded formulations that were unstable or formed liposomes with Z-average size above 250 nm and PDI above 0.35 from further testing *in vitro*. Liposomal formulations with the various commercially available positively charged lipids (Figure 2) at physiological pH were prepared. To test the effect of cholesterol (20 mol%), the zwitterionic phospholipid (either DOPC or DSPC) was replaced by cholesterol, while keeping the positively charged molar lipid content constant. The liposomal formulations had an antigen-to-lipid weight ratio of 1:50 and were prepared with the thin-film hydration method followed by tip sonication. The formulations are summarized in Table 1.

Subsequently, all formulations were characterized in terms of their Z-average size, PDIs, and Zeta-potentials. The following selection criteria were included: no visible signs of aggregation or precipitation in the liposomal suspension, Z-average size < 250 nm, PDI < 0.33, and a Zeta-potential between 15 and 40 mV. These inclusion criteria were selected to assure the comparability of tested formulations by

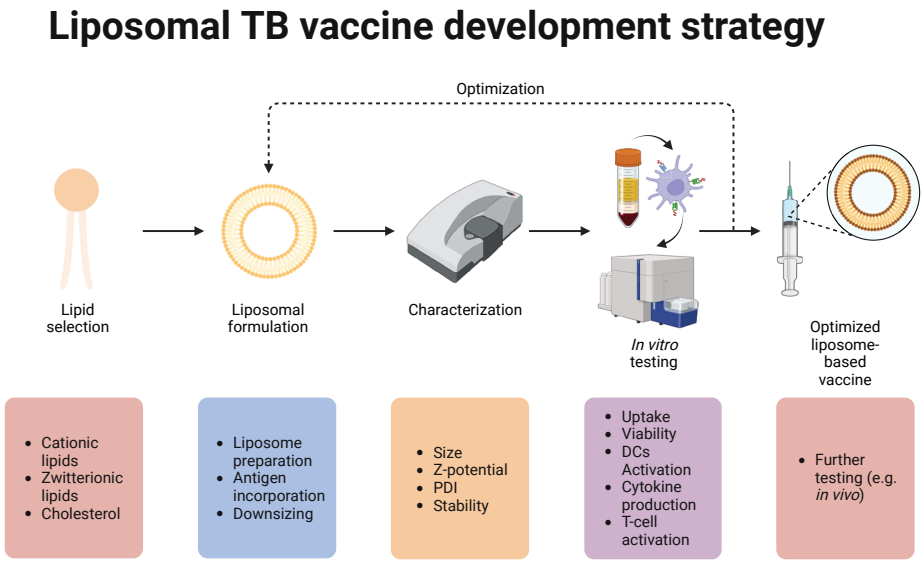

Figure 1. Schematic overview of the strategy used for the development and optimization of liposomal TB vaccines. Created with BioRender.com.

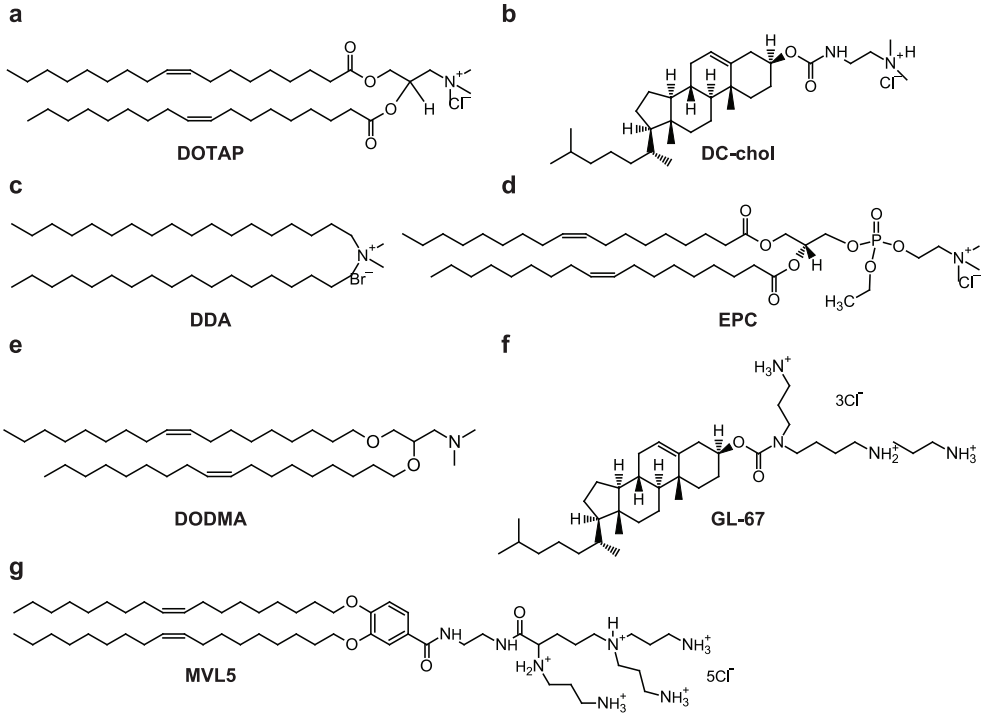

← **Figure 2.** Molecular structures of cationic compounds. a) DOTAP: 1,2-dioleoyl-3-trimethyl-ammonium-propane (chloride salt), b) DC-chol: 3ß-[N-(N',N'-dimethylaminoethane)-carbamoyl]cholesterol hydrochloride, c) DDA: dimethyldioctadecylammonium (bromide salt), d) EPC: 1,2-dioleoyl-*sn*-glycero-3-ethylphosphocholine (chloride salt), e) DODMA: 1,2-dioleyloxy-3-dimethylaminopropane, f) GL-67: N^4-cholesteryl-spermine hydrochloride, and g) MVL5: N1-[2-((1S)-1-[(3-aminopropyl)amino]-4-[di(3-amino-propyl)amino]butyl-carbox-amido)ethyl]-3,4-di[oleyloxy]-benzamide.

Table 1. List of investigated liposomal vaccine formulations.

Cationic lipid	Cholesterol	DOPC/DSPC	Molar lipid ratio
DOTAP	N.A.	DOPC	1:4
DC-chol	N.A.	DOPC	1:4
DDA	N.A.	DOPC	1:4
EPC	N.A.	DOPC	1:4
DOTAP	cholesterol	DOPC	1:1:3
DDA	cholesterol	DOPC	1:1:3
EPC	cholesterol	DOPC	1:1:3
DOTAP	N.A.	DSPC	1:4
DC-chol	N.A.	DSPC	1:4
DDA	N.A.	DSPC	1:4
EPC	N.A.	DSPC	1:4
DOTAP	cholesterol	DSPC	1:1:3
DDA	cholesterol	DSPC	1:1:3
EPC	cholesterol	DSPC	1:1:3
MVL5	N.A.	DSPC	1:4
MVL5	cholesterol	DSPC	1:1:3
GL-67	N.A.	DOPC	1:4
DODMA	N.A.	DOPC	1:4
DODMA	cholesterol	DOPC	1:1:3
GL-67	N.A.	DSPC	1:4
MVL5	cholesterol	DSPC	1:1:3
DODMA	cholesterol	DSPC	1:1:3

Table 2. Physicochemical properties of the selected formulations. The results represent mean ± SD. Number of batches n ≥ 3.

Formulation	Z-average size (nm)	PDI (-)	Zeta-potential (mV)
AER/DOTAP:DOPC	86 ± 1	0.25 ± 0.01	25.5 ± 0.4
AER/DC-chol:DOPC	102 ± 1	0.27 ± 0.01	24.1 ± 0.3
AER/DDA:DOPC	86 ± 1	0.23 ± 0.01	22.0 ± 0.5
AER/EPC:DOPC	92 ± 1	0.26 ± 0.01	26.4 ± 0.6
AER/DOTAP:cholesterol:DOPC	104 ± 6	0.23 ± 0.01	22.5 ± 2.5
AER/DDA:cholesterol:DOPC	106 ± 4	0.23 ± 0.01	27.0 ± 4.1
AER/EPC:cholesterol:DOPC	98 ± 3	0.26 ± 0.01	26.1 ± 4.3
AER/GL-67:DOPC	95 ± 3	0.32 ± 0.05	24.4 ± 0.4
AER/DC-chol:DSPC	121 ± 3	0.26 ± 0.02	20.2 ± 3.6
AER/DODMA:DOPC	182 ± 5	0.23 ± 0.02	16.1 ± 0.3
AER/DODMA:cholesterol:DOPC	230 ± 11	0.22 ± 0.03	17.3 ± 0.4

minimizing the effect of size differences. The physicochemical properties of the formulations that met these criteria are presented in Table 2. The results of the remaining formulations are presented in Table S1.

The physicochemical properties for most of the selected liposomal formulations were very similar with Z-average sizes between 80 and 100 nm, PDIs between 0.22 and 0.26, and Zeta-potentials between +15 and +24 mV. However, four formulations exceeded these ranges: AER/GL-67:DOPC which had a PDI value of 0.32, and AER/DC-chol:DSPC, AER/DODMA:DOPC, and AER/DODMA:cholesterol:DOPC which had Z-average sizes of 121, 182, and 230 nm, respectively. Although the physicochemical properties differed from the other formulations, we included them for further investigation as the liposome suspensions were stable and did not meet the exclusion criteria. The selected formulations remained stable for at least seven months during storage at 4 °C (remeasured after 4 or 7 months, Table S4). All the formulations were used within six weeks after preparation.

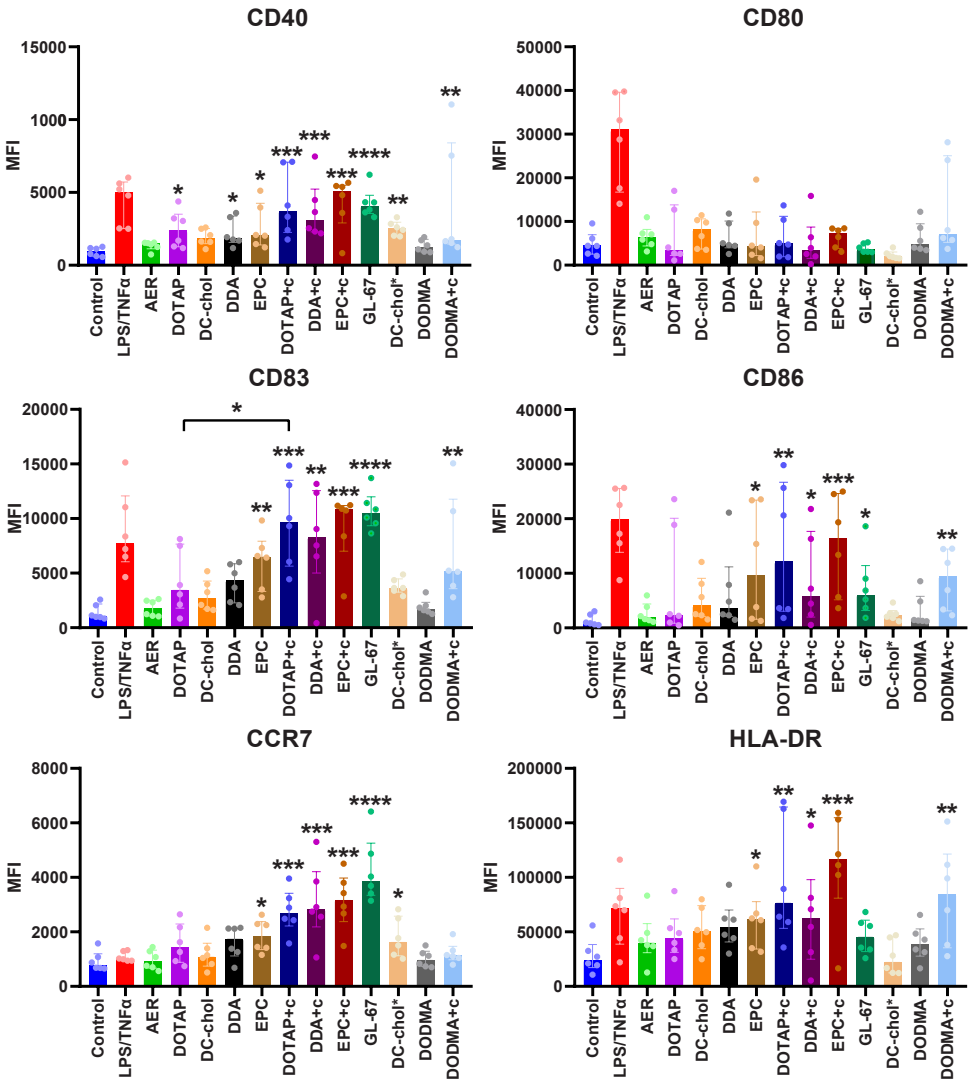

Figure 3. Cell surface activation marker expression levels in MDDCs after stimulation with medium (control), a combination of LPS and TNFα (100 and 5 ng/ml, respectively) as the positive control, unadjuvanted AER (5 µg/ml), and liposomal formulations (5 µg/ml AER, 250 µg/ml liposomes). Median fluorescence intensities related to the expression of indicated activation markers: CD40, CD80, CD83, CD86, CCR7, and HLA-DR. The formulations are compared to the control in the significance testing. Groups in order: Control (medium), LPS/TNFα, AER, DOTAP:DOPC, DC-chol:DOPC, DDA:DOPC, EPC:DOPC, DOTAP:cholesterol:DOPC, DDA:cholesterol:DOPC, EPC:cholesterol:DOPC, GL-67:DOPC, DC-chol:DSPC, DODMA:DOPC, and DODMA:cholesterol:DOPC. The results represent median ± IQR. n = 6 (cell donors).

3.2 Effect of composition of liposomal vaccines on the activation of primary human dendritic cells

The selected liposomal formulations were examined on their ability to induce activation of human MDDCs. To assess DC activation, we measured the expression of cell surface DC activation markers. As shown in Figure 3 and Figure S1 a large variation in expression of activation markers was observed between cells derived from different donors. When compared to the control (medium only), many of the formulations induced a statistically significant upregulation of MDDC surface activation markers e.g., CD40, CD83, and CCR7, evident from both increased median fluorescence intensity values (Figure 3) and histograms (using concatenation displaying the integrated results of all six donors; Figure S1). Interestingly, the highest expression of surface activation markers was observed in response to formulations containing cholesterol, either as a component: AER/DDA:cholesterol:DOPC, AER/DOTAP:cholesterol:DOPC, and AER/EPC:cholesterol:DOPC, or as a structural part of the cationic constituent (GL-67): AER/GL-67:DOPC. The three latter induced similar or higher upregulation compared to the positive control LPS/TNFα. However, the remaining formulations containing cholesterol or its derivatives, AER/DC-chol:DOPC, AER/DC-chol:DSPC, and AER/DODMA:cholesterol:DOPC did not show the same potency to activate MDDCs, which also applied to the formulations without cholesterol: AER/DOTAP:DOPC, AER/DDA:DOPC, AER/EPC:DOPC, and AER/DODMA:DOPC. When comparing formulations containing the same cationic compound with their cognate formulations containing cholesterol, the cholesterol-containing formulations tended to increase the expression of the markers; however, only AER/DOTAP:cholesterol:DOPC induced a statistically significant increase of CD83 compared to AER/DOTAP:DOPC ($p < 0.05$) (Table S2). The most potent formulations were AER/DDA:cholesterol:DOPC, AER/EPC:cholesterol:DOPC, and AER/GL-67:DOPC. None of the formulations induced a statistically significant upregulation of CD80. Unadjuvanted AER did not increase the expression of any of the tested activation markers. The experiment was repeated, and similar results were obtained for batch 2 (Figure S2 and S3). Furthermore, corresponding liposomal formulations without AER were tested and yielded similar results (Figure S4), confirming that the upregulated cell surface expression levels were because of the liposomal constituents and not the loaded antigen.

The DC-chol:DSPC formulations were excluded from the following studies because of suboptimal performance in the MDDC activation study. The effect of the sonication method was also investigated. In the repeated experiment (Figure S3) in the AER control group pre-sonicated AER was used. Comparing the results from the original AER batch (batch 1, Figure S3) and the sonicated batch (batch 2) revealed identical outcomes. Empty liposomal formulations (Figure S4), which were downsized with the extrusion method instead of sonication, demonstrated no impact on MDDC activation. From these findings, we concluded that the sonication method did not have any measurable effects on our results.

In summary, these data indicate that DOPC formed more stable liposomes in these formulations compared to DSPC; the most effective cationic lipids were DDA, EPC, and GL-67. Moreover, the addition of cholesterol seemed to increase the DC activation capacity of cationic liposomes.

3.3 Effect of lipid composition on the uptake, viability, and cytokine production by MDDCs

Empty fluorescently labeled liposomes were used to evaluate the uptake of vaccine formulations by human MDDCs (Figure 4a). The uptake depended on the composition of the formulations. The formulations that induced the highest uptake contained either cholesterol, DOTAP:cholesterol:DOPC and EPC:cholesterol:DOPC, or contained the cationic cholesterol-based derivative GL-67:DOPC. This correlated with the profile of the activation markers (Figure 3). DC-chol:DOPC and DDA:cholesterol:DOPC were not taken up effectively, and neither were DODMA:cholesterol:DOPC liposomes. Therefore, the MDDCs do not take up all formulations equally, demonstrating clear selectivity. Compared to their cholesterol-free counterparts, EPC:cholesterol:DOPC and DOTAP:cholesterol:DOPC liposomes were taken up significantly better than the corresponding liposomes without cholesterol ($p < 0.05$). The full statistical comparison of the formulations is summarized in Table S3.

Liposome uptake was also studied for human macrophages. These were (GM-CSF differentiated) human (pro-inflammatory) M1 macrophages and (M-CSF differentiated) human (anti-inflammatory) M2 macrophages (Figure S5), both of which are APCs and can locally play a role in processing and presenting antigens.

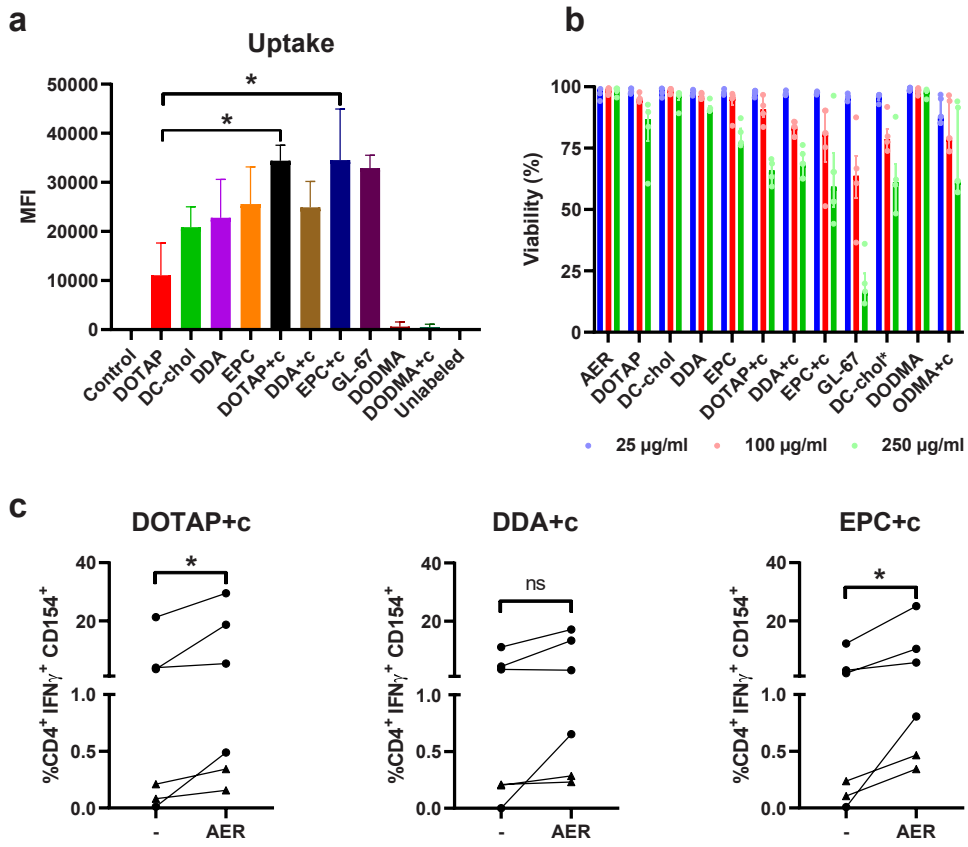

Figure 4. Effect of lipid composition on the uptake of liposomes, the viability of MDDCs, and the T-cell activation. a) Uptake of Cy5-labeled (empty) liposomes in MDDCs, n = 12, b) viability of MDDCs after exposure to AER-containing liposomal formulations, n = 6 (cell donors), c) T-cell activation as a percentage of CD4+ T-cells that produce IFNγ and express CD154. Comparison between empty (-) and AER-loaded (AER) liposomes (5 µg/ml AER, 250 µg/ml liposomes), exposure 1 h. Circles represent the L10B4 clone (Ag85B p56-65) and triangles the 1B4 clone (Rv2034 p75-105). Groups in order: Control (medium), LPS/TNFα, AER, DOTAP:DOPC, DC-chol:DOPC, DDA:DOPC, EPC:DOPC, DOTAP:cholesterol:DOPC, DDA:cholesterol:DOPC, EPC:cholesterol:DOPC, GL-67:DOPC, DC-chol:DSPC, DODMA:DOPC, and DODMA:cholesterol:DOPC. The results in panels a and b represent median ± IQR.

Importantly, macrophages are the predominant habitat of Mtb and thus must be recognized by T-cells for bacterial control.[8] While sharing the same uptake pattern, both M1 and M2 macrophages had a higher liposome uptake than MDDCs, and GL-67:DOPC liposomes were taken up to the highest degree by the M1 and M2 macrophages.

Subsequently, the effect of the antigen-loaded liposomes on the viability of human MDDCs was tested. Each liposomal formulation was tested in three lipid concentrations: 25, 100, and 250 μg/mL with an AER-to-lipid weight ratio of 1:50. The viability of the cells depended substantially on the formulation added (Figure 4b) as at the lowest concentration, none of the formulations reduced cellular viability. At the highest concentrations AER/DOTAP:cholesterol:DOPC, AER/DDA:cholesterol:DOPC, AER/EPC:cholesterol:DOPC caused intermediate cell death (between 25 % and 35 %) while also inducing the highest upregulation of the activation markers and the uptake in MDDCs and M1 and M2 macrophages. The formulations that increased the upregulation of the surface markers to a low degree also had a low impact on cellular viability (>85 % viability). Only the AER/GL-67:DOPC liposomes caused an unacceptable reduction of viability as less than 20 % of cells remained viable at the highest concentration. In general, cellular viability decreased as the concentration of AER and lipid concentration increased.

3.4 Antigen-specific T-cell responses

The three most promising liposomal formulations: AER/DOTAP:cholesterol:DOPC, AER/DDA:cholesterol:DOPC, AER/EPC:cholesterol:DOPC were selected to examine T-cell activation. GL-67-containing liposomes were highly toxic and did not improve the upregulation of surface markers in MDDCs substantially better than the other formulations, therefore we decided that these liposomes were not appropriate for further testing. Two HLA-DR3 restricted AER-specific T-cell clones were exposed to HLA-DR3$^+$ MDDCs from different donors, that had been incubated with the formulations. When MDDCs take up the liposomes, they will process the antigen and present it to T-cell clones that recognize the relevant peptide epitope presented via HLA-DR3.[45] If the MDDCs receive costimulatory signals, they will mature and interact with the T cells, which will upregulate antigen-specific surface markers (CD154) and start producing cytokines (IFNγ) as a result, which can be detected by flow cytometry using intracellular staining (Figure 4c). Two of the AER-loaded formulations: DOTAP:cholesterol:DOPC and EPC:cholesterol:DOPC induced statistically significant increases in T-cell clone activation by an increase of the percentage of IFNγ$^+$ CD154$^+$ double-positive cells compared to the empty liposomes. No statistical difference in the activation

of T-cells was observed between the two AER-containing formulations. However, it has to be noted that variability in expression between different HLA-DR3$^+$ MDDCs donors was considerable.

3.5 Optimization of the best-performing formulations

The best-performing compositions in regard to cellular toxicity, uptake, and stimulatory capacities contained cholesterol and either DDA or EPC. DOTAP liposomes with cholesterol performed equally well, however, in a parallel unpublished work we saw that DOTAP liposomes were intrinsically less immunogenic, hence we did not include them. In the subsequent optimization step, we doubled the molar content of the cationic compound and/or cholesterol compared to formulations discussed above resulting in cationic lipid:cholesterol:DOPC molar ratios of 2:1:2, 1:2:2, and 2:2:1. The Z-average sizes, PDIs, and Zeta-potentials of the formulations are summarized in Table 3. We observed that the new variants of the AER/DDA:cholesterol:DOPC formulation did not meet our above-specified criteria in regard to the physicochemical properties and therefore were excluded from further analysis.

Table 3. Physicochemical properties of optimized formulations. n≥3 (batches).

Formulation	Molar lipid ratio	Z-average size (nm)	PDI (-)	Zeta-potential (mV)
AER/DDA:cholesterol:DOPC*	2:1:2	141 ± 2	0.44 ± 0.01	33.5 ± 1.0
AER/DDA:cholesterol:DOPC*	1:2:2	136 ± 2	0.33 ± 0.01	30.1 ± 1.4
AER/DDA:cholesterol:DOPC*	2:2:1	156 ± 1	0.33 ± 0.01	31.7 ± 1.0
AER/EPC:cholesterol:DOPC	2:1:2	95 ± 6	0.28 ± 0.02	30.9 ± 0.8
AER/EPC:cholesterol:DOPC	1:2:2	109 ± 2	0.28 ± 0.01	31.6 ± 0.4
AER/EPC:cholesterol:DOPC	2:2:1	89 ± 1	0.26 ± 0.01	36.4 ± 3.6

*Visibly aggregated formulation. The sample for the measurement of the Z-average size, PDI and Zeta-potential was taken from the upper part of the solution that was free of visible aggregates.

3.6 Effect of the increased cationic lipid and cholesterol contents on human DC activation, viability, T-cell activation, and cytokine production

The MDDCs were exposed to the best-performing formulation: AER/EPC:cholesterol:DOPC (molar lipid ratio 1:1:3 used in the first series of studies) and its three variations are reported in Table 3. The upregulation of the activation markers was evaluated (Figure 5 and Figure S6, statistical data is shown in Table S5). The initially developed AER/EPC:cholesterol:DOPC 1:1:3 liposomes induced all the evaluated activation markers, except for CD80 (Table S4). The two variations that contained a double amount of EPC induced a more robust activation indicated by increased Median Fluorescence Intensities values, e.g., CD40 and CCR7 (Figure 5a), and histograms shifted towards high-intensity values (Figure S6). At the highest tested concentration (5 μg/ml AER with 250 μg/ml total lipids), both the 2:1:2 and 2:2:1 formulations induced a statistically significant upregulation of CD80 when compared to the control. This was not achieved by any of the liposome formulations in the prior MDDC activation experiments. Interestingly, no difference was observed between 2:1:2 and 2:2:1 variants (that contain the double amount of EPC), and between 1:2:2 and 1:1:3 variants. We observed a decrease in cellular viability for these double-amount formulations, especially for 2:2:1.

The formulation AER/EPC:cholesterol:DOPC 2:1:2 selected as the best upregulator of surface activation markers was tested again for T-cell recognition. Indeed, this formulation showed a significant increase in the percentage of $IFN\gamma^+$ $CD154^+$ double-positive cells when compared to the empty liposomes.

Finally, we measured the levels of cytokines and chemokines with multiplex assays in the supernatants from MDDC cultures exposed to the original formulation of AER/EPC:cholesterol:DOPC and the three variations. We assessed the levels of several cytokines and chemokines (Figure 6) and observed that formulations 2:1:2 and 2:2:1 induced significantly increased levels of CCL3, CCL4, CXCL10, and CCL11, compared to the AER alone and the 1:1:3 and 1:2:2 variants. For CCL2 and CCL22 we observed a (statistically non-significant) trend towards upregulationof the cytokine levels. For IL-12p40, IL-10, IL-1β, and TNFα we did not observe changes in the concentration of detectable cytokines compared to the medium control.

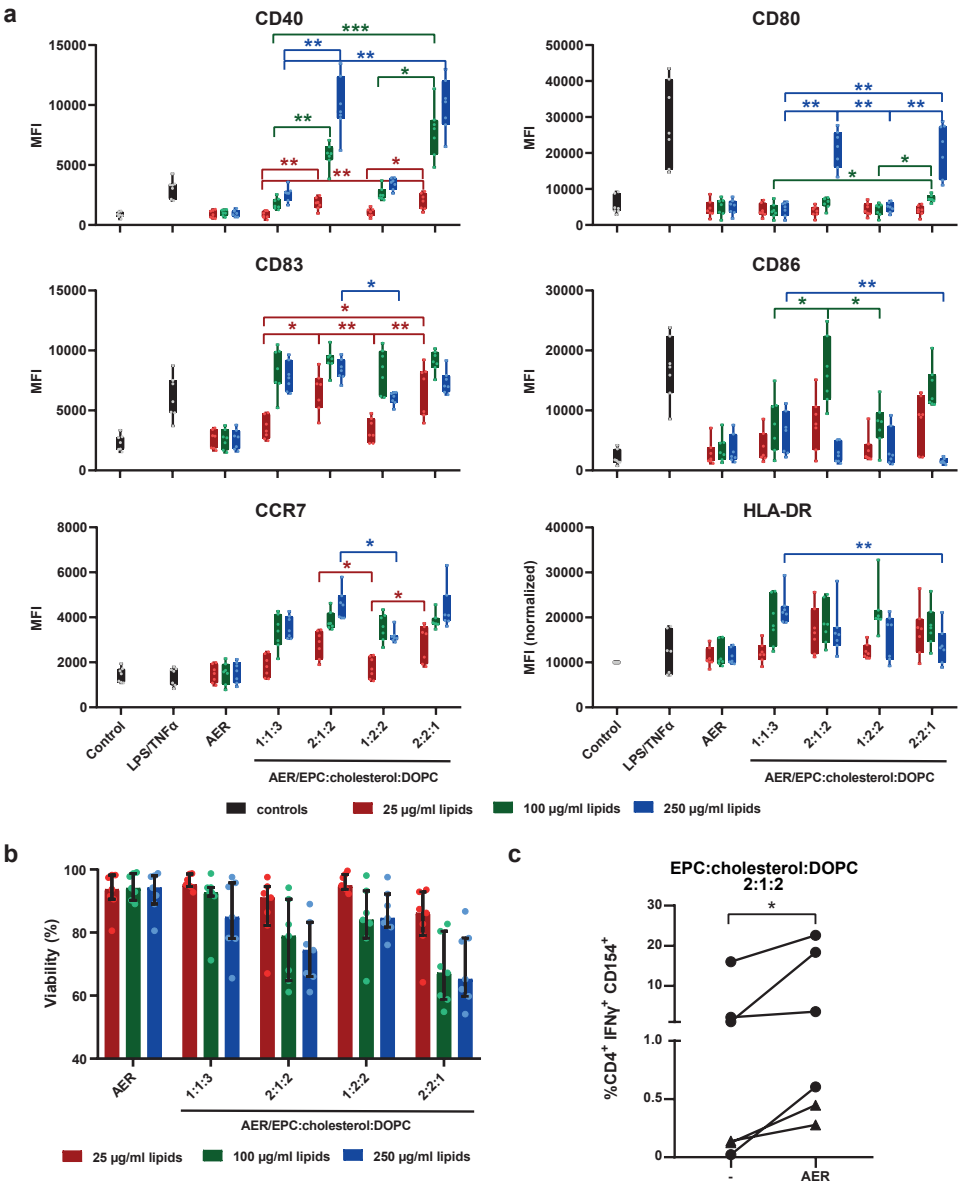

Figure 5. Upregulation of cell surface activation markers and the viability of MDDCs exposed to liposomal formulations containing AER/EPC:cholesterol:DOPC in different molar ratios. a) Median fluorescence intensities related to the expression of indicated activation markers: CD40, CD80, CD83, CD86, CCR7, and HLA-DR, n = 7 (cell donors). b) Viability of MDDCs after 1-h exposure to the liposomal formulations, n = 7 (cell donors). c) T-cell activation as a percentage of $CD4^+$ T-cells that produce IFNγ and express CD154. Circles represent the L10B4 clone (Ag85B p56-65) and triangles the 1B4 clone (Rv2034 p), n = 6 (cell donors). The results represent median ± IQR.

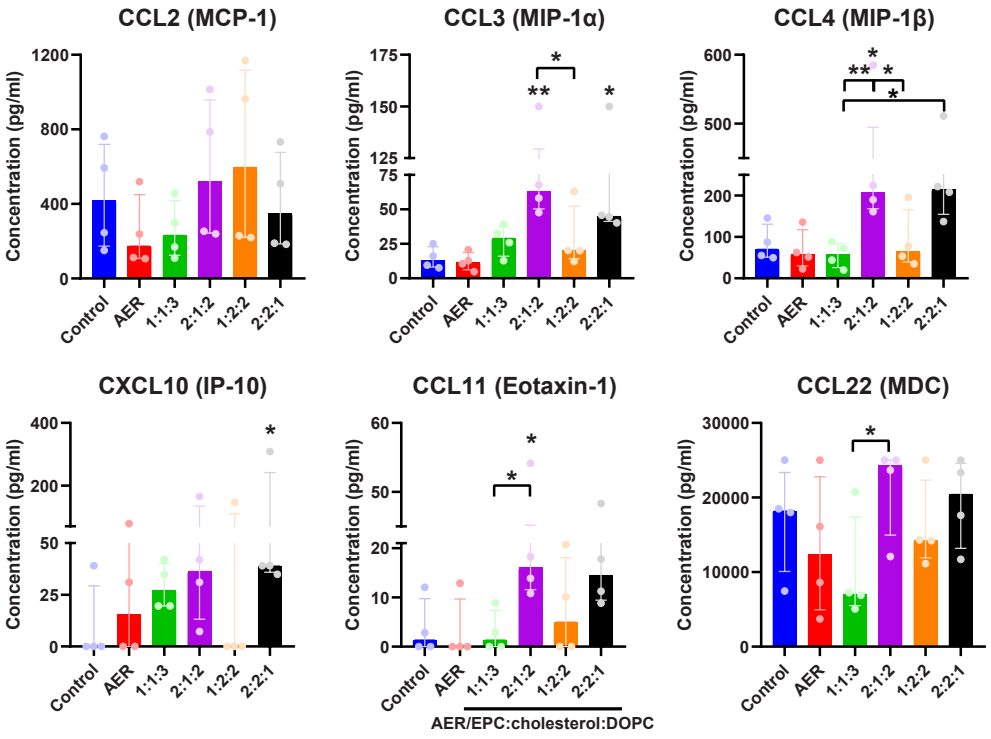

Figure 6. Production of cytokines by MDDCs exposed to liposomal formulations (5 µg/ml AER, 250 µg/ml liposomes, exposure 1 h), n = 4 (cell donors). The results represent median ± IQR.

4. DISCUSSION

Cationic liposomes are not only potent delivery systems for subunit vaccines but also exhibit intrinsic adjuvant properties. In this study, we explored these properties with an extensive list of commercially available cationic lipids and different cholesterol concentrations to evaluate their role in the physicochemical properties of liposomes and immunological outcomes as summarized in Figure 1.

In this way, we aim to fill the gap in publicly available data. We used a rationalized selection of assays that allowed us to perform a head-to-head comparison of multiple liposomes to identify the optimal formulation based on human in vitro immune responses.

4.1 The selection of lipids and stability of liposomes

The selected cationic lipids differ substantially in terms of their chemical structures, which can affect the stability of liposomes and, consequently, the interaction between the liposomes and APCs. We observed that the mean size of liposomes prepared with DODMA is larger compared to the other formulations, and this is likely because of its head group structure, which is smaller compared to quaternary ammonium cations. Liposomes prepared with MVL-5 and GL-67 were large and unstable in the presence of the AER. Their massive cationic head groups might interact with the antigen and cause aggregation, resulting in unstable suspensions.

The choice of lipids affects the stability, size, and PDI of the liposomes. We observed that liposomes that consisted of unsaturated lipids, e.g., AER/DOTAP:DOPC and AER/EPC:DOPC, were smaller than AER/DOTAP:DSPC and AER/EPC:DSPC liposomes that consisted of a mix of unsaturated and saturated lipids. Liposomes containing DDA, which is a saturated lipid, or cholesterol-based compounds like DC-chol and GL-67 should be stable. As expected, DC-chol formed stable liposomes when formulated with DOPC and DSPC. Surprisingly, AER/GL-67:DSPC and AER/DDA:DSPC formulations did not, this could be ascribed to the addition of the antigen.

4.2 The choice of lipid and consequent immunological response

The formulations that fulfilled our predefined selection criteria for further immunological evaluation were tested in several biological assays. We observed that liposomes containing cholesterol were taken up more efficiently by human MDDCs and also induced a higher expression of activation markers, but also increased cellular toxicity, which did not lead to massive cell death, compared to liposomes without cholesterol. This is likely because of the liquid-ordered organization of the bilayer of liposomes, which is more rigid than a liquid-disordered phase in liposomes without cholesterol.[50–53] This finding is in line with reports that more rigid liposomes with higher cholesterol content are more efficiently taken up by DCs[15] and macrophages.[43,54,55]

When focusing on the cationic lipids, formulations containing DOTAP, DDA, EPC, and GL-67 induced the highest upregulation of surface activation markers. This

might be a consequence of the higher uptake by MDDCs. We observed that liposomes containing DDA, EPC, and GL-67 tended to be more toxic as they reduced the viability of MDDCs more than those with DOTAP and DC-chol. Induction of cell death and activation of MDDCs can be mechanistically linked: apoptotic vesicles from dying cells can interact with TLRs on viable DCs, which can lead to cross-priming and induction of $CD8^+$ T-cells *in vivo*.[56,57] The liposomal formulation with the cation GL-67 reduced the viability pronouncedly, even at lower concentrations. This is most probably caused by the induction of necrosis by the primary amines in GL-67[58,59] It has been reported that liposomes containing cholesterol and eDPPC (ethyl dipalmitoylphosphatidylcholine), are taken up by APCs to a higher degree than liposomal formulations with both cholesterol and DDA or DC-chol.[15] This may suggest that cationic compounds having ethyl phosphocholine head groups, such as eDPPC and EPC, increased liposomal uptake. Vangasseri and colleagues reported that EPC-containing liposomes were superior in stimulating bone marrow-derived DCs (namely in upregulation of the surface expression of CD80) compared to liposomes containing other compounds e.g., DOTAP.[60] Based on these results, we selected three formulations for further evaluation: DOTAP:cholesterol:DOPC, DDA:cholesterol:DOPC and EPC:cholesterol:DOPC.

To gain more insights into the immunomodulatory capacity of these formulations, we used human T -cell activation assays, a step not commonly reported in adjuvant/delivery literature. The specific interaction of the liposome-treated DCs and T-cells is essential to protective immunity against TB. We observed that all AER-loaded liposomes induced a higher activation of two different antigen-specific T-cell clones compared to the empty liposomes. This indicates that the AER-containing liposomal formulations were not only efficiently taken up by MDDCs, but were processed and their epitopes presented to activate the T-cell clones. DOTAP:cholesterol:DOPC and EPC:cholesterol:DOPC induced a statistically significant increase of antigen-specific T-cell activation compared to the empty counterparts, demonstrating clear antigen specificity. This was, however, not observed for DDA:cholesterol:DOPC, suggesting that this formulation was not as effective in delivering the antigen and activating MDDCs as the DOTAP- and EPC-based liposomes.

To further improve the quality of the immune response, we selected the cationic lipids DDA and EPC formulations and doubled the cationic lipid and/or cholesterol content. Because of the unfavorable physicochemical properties of the DDA

formulation when increasing the cationic or cholesterol levels, we focused on the EPC formulations. Liposomes that contained a double amount of EPC, but not double cholesterol induced an increased upregulation of surface activation markers CD40 and CD80. This is in line with the literature showing that increasing the content of the cationic compound leads to stronger DC maturation[25] and increased IgG titers *in vivo*.[20] Similar to the initial set of formulations, the liposome variants that upregulated DCs activation markers induced also more cell death. Doubling the cholesterol content did not affect surface marker expression, however, there was reduced viability when a higher cholesterol content variant was used. We speculate that once a more rigid liquid-ordered organization occurs at 2:1:2 liposomal composition a further increase of cholesterol provides no additional beneficial effect. Therefore, we decided to only test the 2:1:2 liposome in the T-cell activation assay. We observed a statistically significant increase of CD154 and IFNγ double positive T-cells when MDDCs were pre-treated with AER-containing liposome compared to the empty one. This indicates that increased EPC content did not negatively affect the ability of the liposome to activate T-cells and it is likely to induce effective antigen presentation to T-cells *in vivo*.

Lastly, the capacity of the AER-containing liposomes to induce cytokine production in MDDCs was assessed and we observed increased cytokine production for a few cytokines, especially CCL3 (MIP-1α), CCL4 (MIP-1β), CXCL10 (IP-10), and CCL11 (Eotaxin-1). CCL3 and CCL4 have been shown to actively chemoattract $CD8^+$ T-cells,[61] modulate the interactions between T-cells and APCs in the draining lymph nodes after immunization, and enhance memory T-cell responses.[62–64] CXCL10 is reported as a specific chemoattractant for effector T-cells[65] and is thought to be directly involved in the generation of antigen-specific $CD8^+$ T-cell responses after vaccination.[66] Moreover, it is a marker of trained immunity, mediating the inhibition of mycobacterial growth in human macrophages.[67] Therefore, this may indicate that liposomes containing 40 mol% EPC favor a microenvironment that is beneficial for TB vaccination, as both $CD4^+$ and $CD8^+$ T-cell responses are important to prevent TB.[8] CCL11 is an eosinophil-specific chemoattractant.[68] We observed a small increase in the CCL2 (MCP-1) production, which promotes the trafficking of effector cells including monocytes, memory T-cells, and natural killer cells from the circulation across the endothelium,[69] and CCL22 (MDC). Expression of CCL22 induces cellular contacts of DCs with regulatory T-cells through the CCR4 receptor[70] and inhibits the

T-cell activation capacities of DCs by decreasing the expression of HLA molecules and CD80.[71] Expression of CCL22 may therefore reduce T-cell activation *in vivo*. We did not detect any production of IL-12, IFNα, which concurs with previous reports that cationic liposomes without molecular adjuvants do not induce IL-12 production in DCs.[72] The lack of these cytokines combined with the low production of pro-inflammatory cytokines (CCL3, CCL4, CXCL10) indicates that cationic liposomal formulations require additional adjuvants e.g., TLR agonists, to achieve robust immune responses *in vivo*.

5. CONCLUSIONS

TB is still among the leading causes of death and it has been the deadliest infectious disease worldwide for decades. Therefore, additional measures that can control and combat this disease are highly needed. This study presents a strategy to compare, optimize, and select cationic liposomal compositions formulated with the multivalent Mtb antigen AER, based on a rational pipeline of in vitro testing and down-selecting using human cells, as a prelude further pre-clinical investigations, thus reducing animal experimentation. The best-performing formulation was comprised of an AER-containing formulation containing the lipids EPC:cholesterol:DOPC in a molar ratio of 2:1:2, as assessed by an increase in cell surface activation markers, cellular uptake, antigen-specific T-cell activation, cytokine production, and cellular viability. Moreover, the addition of cholesterol improved the performance of the formulations. The liposomal TB vaccine development strategy described in this paper can be used to elucidate which molecular adjuvants should be incorporated in the liposomal formulations before evaluating the effect of the composition in animal models and can be extended to other pathogens besides Mtb.

ABBREVIATIONS

AER, Ag85B-ESAT6-Rv2034 antigen; APC, antigen-presenting cell; BCG, *Mycobacterium bovis* Bacillus Calmette–Guérin; CCL, chemokine (C-C motif) ligand; CCR7, C-C chemokine receptor type 7; CD, cluster of differentiation; CXCL, chemokine (C-X-C motif) ligand; DC, dendritic cell; DC-cholesterol, 3ß-[N-(N',N'-dimethylaminoethane)-carbamoyl]cholesterol; DDA, dimethyl-dioctadecylammonium bromide; DODMA, 1,2-dioleyloxy-3-dimethylaminopropane; DOPC, 1,2-dioleoyl-*sn*-glycero-3-phosphocholine;

DOTAP, 1,2-dioleoyl-3-trimethylammonium-propane; DSPC, 1,2-distearoyl-*sn*-glycero-3-phosphocholine; EPC, 1,2-dioleoyl-*sn*-glycero-3-ethylphosphocholine; FBS, fetal bovine serum; GL-67, N4-cholesteryl-spermine; GM-CSF, granulocyte-macrophage colony-stimulating factor; HLA, human leukocyte antigen; IFN, interferon; Ig, immunoglobulin, IL, interleukin; IQR, interquartile range; MACS, magnetic cell isolation; M-CSF, macrophage colony-stimulating factor; MDDC, monocyte-derived dendritic cell; Mtb, *Mycobacterium tuberculosis*; MVL5, N1-[2-((1S)-1-[(3-aminopropyl)amino]-4-[di(3-amino-propyl)amino]butylcarboxamido) ethyl]-3,4-di[oleyloxy]-benzamide; PAMP, pathogen-associated molecular pattern; PBMC, peripheral blood mononuclear cell; PDI, polydispersity index; SA, stearylamine; TB, tuberculosis; Th1, type 1 helper T-cell, TLR, Toll-like receptor; TNF, tumor necrosis factor.

APPENDICES

Supplementary materials

DECLARATION OF COMPETING INTEREST

The authors declare no conflict of interest.

DATA AVAILABILITY

Data will be made available on request.

ACKNOWLEDGMENTS

In memoriam professor Wim Jiskoot. We would like to recognize and appreciate his involvement and contribution to the research presented in this work. Also, we would like to acknowledge Kees L.M.C. Franken for the preparation of the recombinant antigen used in this study. This work was supported by the Dutch Research Council (NWO) Domain Applied and Engineering Sciences grant, project number: 15240.

CREDIT AUTHOR CONTRIBUTION STATEMENT

M.M. Szachniewicz: Conceptualization, Methodology, Formal Analysis, Investigation, Writing – Original Draft. **M.A. Neustrup**: Conceptualization, Methodology, Formal Analysis, Investigation, Writing – Original Draft. **K.E. van Meijgaarden**: Conceptualization, Methodology, Formal Analysis, Investigation, Writing – Review & Editing, Supervision. **W. Jiskoot**: Conceptualization, Supervision. **J.A. Bouwstra**:

Conceptualization, Writing – Review & Editing, Project Administration, Funding Acquisition, Supervision. **M.C. Haks**: Conceptualization, Supervision. **A. Geluk**: Conceptualization, Writing – Review & Editing, Project Administration, Funding Acquisition, Supervision. **T.H.M. Ottenhoff**: Conceptualization, Writing – Review & Editing, Project Administration, Funding Acquisition, Supervision.

REFERENCES

1. World Health Organization. The top 10 causes of death. https://www.who.int/news-room/fact-sheets/detail/the-top-10-causes-of-death (2020).
2. World Health Organization. *Global Tuberculosis Report 2022*. (2022).
3. Pierneef, L. *et al.* Host biomarker-based quantitative rapid tests for detection and treatment monitoring of tuberculosis and COVID-19. *iScience* 26, 105873 (2023).
4. World Health Organization. UN General Assembly adopts Declaration of the first-ever United Nations High Level Meeting on TB. *World Health Organization* (2018).
5. Pollard, A. J. & Bijker, E. M. A guide to vaccinology: from basic principles to new developments. *Nature Reviews Immunology* 21:2, 83–100 (2020).
6. Rémy, V. *et al.* Vaccination: the cornerstone of an efficient healthcare system. *Journal of Market Access & Health Policy* 3, 27041 (2015).
7. Woodland, D. L. Vaccine Development. *Viral Immunology* 30, 141 (2017).
8. Ottenhoff, T. H. M. & Kaufmann, S. H. E. Vaccines against Tuberculosis: Where Are We and Where Do We Need to Go? *PLoS Pathogens* 8, e1002607 (2012).
9. Rodrigues, L. C. *et al.* Protective effect of bcg against tuberculous meningitis and miliary tuberculosis: A meta-analysis. *International Journal of Epidemiology* 22, 1154–1158 (1993).
10. Trunz, B. B. *et al.* Effect of BCG vaccination on childhood tuberculous meningitis and miliary tuberculosis worldwide: a meta-analysis and assessment of cost-effectiveness. *Lancet* 367, 1173–1180 (2006).
11. Fine, P. E. M. Variation in protection by BCG: implications of and for heterologous immunity. *The Lancet* 346, 1339–1345 (1995).
12. Christensen, D. *et al.* Cationic liposomes as vaccine adjuvants. *Expert Review of Vaccines* 10, 513–521 (2011).
13. Moyle, P. M. & Toth, I. Modern Subunit Vaccines: Development, Components, and Research Opportunities. *ChemMedChem* 8, 360–376 (2013).

14. O'Hagan, D. T. *et al.* Recent developments in adjuvants for vaccines against infectious diseases. *Biomolecular Engineering* 18:3, 69–85 (2001).
15. Barnier-Quer, C. *et al.* W. Adjuvant effect of cationic liposomes for subunit influenza vaccine: Influence of antigen loading method, cholesterol and immune modulators. *Pharmaceutics* 5, 392–410 (2013).
16. Schmidt, S. T. *et al.* Liposome-based adjuvants for subunit vaccines: Formulation strategies for subunit antigens and immunostimulators. *Pharmaceutics* 8, 1–22 (2016).
17. Moser, M. & Leo, O. Key concepts in immunology. *Vaccine* 28:3, C2–C13 (2010).
18. Latif, N. & Bachhawat, B. K. The effect of surface charges of liposomes in immunopotentiation. *Bioscience Reports* 4, 99–107 (1984).
19. Yan, W. *et al.* Mechanism of adjuvant activity of cationic liposome: Phosphorylation of a MAP kinase, ERK and induction of chemokines. *Molecular Immunology* 44, 3672–3681 (2007).
20. Barnier Quer, C. *et al.* Cationic liposomes as adjuvants for influenza hemagglutinin: More than charge alone. *European Journal of Pharmaceutics and Biopharmaceutics* 81, 294–302 (2012).
21. Liu, X. *et al.* A novel liposome adjuvant DPC mediates Mycobacterium tuberculosis subunit vaccine well to induce cell-mediated immunity and high protective efficacy in mice. *Vaccine* 34, 1370–1378 (2016).
22. Khademi, F. *et al.* Potential of cationic liposomes as adjuvants/delivery systems for tuberculosis subunit vaccines. *Reviews of Physiology, Biochemistry and Pharmacology* 175, 47–69 (2018).
23. Tretiakova, D. S. & Vodovozova, E. L. Liposomes as Adjuvants and Vaccine Delivery Systems. *Biochemistry (Moscow), Supplement Series A: Membrane and Cell Biology* 16:1, 1–20 (2022).
24. Luwi, N. E. M. *et al.* Liposomes as immunological adjuvants and delivery systems in the development of tuberculosis vaccine: A review. *Asian Pacific Journal of Tropical Medicine* 15:1, 7–16 (2022).
25. Ma, Y. *et al.* The role of surface charge density in cationic liposome-promoted dendritic cell maturation and vaccine-induced immune responses. *Nanoscale* 3, 2307–2314 (2011).
26. Marasini, N. *et al.* Liposomes as a Vaccine Delivery System. *Micro- and Nanotechnology in Vaccine Development,* 221–239 (2017).

27. Heuts, J. *et al.* Cationic Liposomes: A Flexible Vaccine Delivery System for Physicochemically Diverse Antigenic Peptides. *Pharmacological Research* 35, 1–9 (2018).
28. Varypataki, E. M. *et al.* Cationic Liposomes Loaded with a Synthetic Long Peptide and Poly(I:C): a Defined Adjuvanted Vaccine for Induction of Antigen-Specific T Cell Cytotoxicity. *AAPS Journal* 17, 216–226 (2015).
29. Du, G. *et al.* Intradermal vaccination with hollow microneedles: A comparative study of various protein antigen and adjuvant encapsulated nanoparticles. *Journal of Controlled Release* 266, 109–118 (2017).
30. Nakanishi, T. *et al.* Positively charged liposome functions as an efficient immunoadjuvant in inducing cell-mediated immune response to soluble proteins. *Journal of Controlled Release* 61, 233–240 (1999).
31. Brgles, M. *et al.* Liposome fusogenicity and entrapment efficiency of antigen determine the Th1/Th2 bias of antigen-specific immune response. *Vaccine* 27, 5435–5442 (2009).
32. Henriksen-Lacey, M. *et al.* Liposomes based on dimethyldioctadecylammonium promote a depot effect and enhance immunogenicity of soluble antigen. *Journal of Controlled Release* 142, 180–186 (2010).
33. Rosenkrands, I. *et al.* Cationic liposomes containing mycobacterial lipids: A new powerful Th1 adjuvant system. *Infection and Immunity* 73, 5817–5826 (2005).
34. Even-Or, O. *et al.* A new intranasal influenza vaccine based on a novel polycationic lipid-ceramide carbamoyl-spermine (CCS). II. Studies in mice and ferrets and mechanism of adjuvanticity. *Vaccine* 29, 2474–2486 (2011).
35. Soema, P. C. *et al.* Predicting the influence of liposomal lipid composition on liposome size, zeta potential and liposome-induced dendritic cell maturation using a design of experiments approach. *European Journal of Pharmaceutics and Biopharmaceutics* 94, 427–435 (2015).
36. Benne, N. *et al.* Orchestrating immune responses: How size, shape and rigidity affect the immunogenicity of particulate vaccines. *Journal of Controlled Release* 234, 124–134 (2016).
37. Guy, B. *et al.* Design, characterization and preclinical efficacy of a cationic lipid adjuvant for influenza split vaccine. *Vaccine* 19, 1794–1805 (2001).

38. Jiao, X. Modulation of cellular immune response against hepatitis C virus nonstructural protein 3 by cationic liposome encapsulated DNA immunization. *Hepatology* 37, 452–460 (2003).
39. Chen, W. *et al.* A simple but effective cancer vaccine consisting of an antigen and a cationic lipid. *Cancer Immunology, Immunotherapy* 57, 517–530 (2008).
40. Bakouche, O. & Gerlier, D. Enhancement of immunogenicity of tumour virus antigen by liposomes: the effect of lipid composition. *Immunology* 58, 507–13 (1986).
41. Batenjany, M. M. *et al.* The effect of cholesterol in a liposomal Muc1 vaccine. *Biochimica Et Biophysica Acta-Biomembranes* 1514, 280–290 (2001).
42. Ishida, T. *et al.* Effect of cholesterol content in activation of the classical versus the alternative pathway of rat complement system induced by hydrogenated egg phosphatidylcholine-based liposomes. *International Journal of Pharmaceutics* 224, 69–79 (2001).
43. Kaur, R. *et al.* Effect of incorporating cholesterol into DDA:TDB liposomal adjuvants on bilayer properties, biodistribution, and immune responses. *Molecular Pharmaceutics* 11, 197–207 (2014).
44. Aramaki, K. *et al.* Charge boosting effect of cholesterol on cationic liposomes. *Colloids and Surfaces A: Physicochemical and Engineering Aspects* 506, 732–738 (2016).
45. Commandeur, S. *et al.* The in vivo expressed Mycobacterium tuberculosis (IVE-TB) antigen Rv2034 induces $CD4^+$ T-cells that protect against pulmonary infection in HLA-DR transgenic mice and guinea pigs. *Vaccine* 32, 3580–3588 (2014).
46. Franken, K. L. M. C. *et al.* Purification of His-Tagged Proteins by Immobilized Chelate Affinity Chromatography: The Benefits from the Use of Organic Solvent. *Protein Expression and Purification* 18, 95–99 (2000).
47. Verreck, F. A. W. *et al.* Phenotypic and functional profiling of human proinflammatory type-1 and anti-inflammatory type-2 macrophages in response to microbial antigens and IFN-γ- and CD40L-mediated costimulation. *Journal of Leukocyte Biology* 79, 285–293 (2006).
48. Commandeur, S. *et al.* Clonal Analysis of the T-Cell Response to In Vivo Expressed Mycobacterium tuberculosis Protein Rv2034, Using a CD154 Expression Based T-Cell Cloning Method. *PLoS One* 9, e99203 (2014).

49. Geluk, A. *et al.* A DR17-restricted T cell epitope from a secreted Mycobacterium tuberculosis antigen only binds to DR17 molecules at neutral pH. *European Journal of Immunology* 27, 842–847 (1997).
50. Benne, N. *et al.* Atomic force microscopy measurements of anionic liposomes reveal the effect of liposomal rigidity on antigen-specific regulatory T cell responses. *Journal of Controlled Release* 318, 246–255 (2020).
51. Martinez-Seara, H., *et al.* Cholesterol Induces Specific Spatial and Orientational Order in Cholesterol/Phospholipid Membranes. *PloS one*, 5(6), e11162 (2010).
52. Krause, M. R. & Regen, S. L. The structural role of cholesterol in cell membranes: From condensed bilayers to lipid rafts. *Accounts of Chemical Research* 47, 3512–3521 (2014).
53. Takechi-Haraya, Y. *et al.* Atomic Force Microscopic Analysis of the Effect of Lipid Composition on Liposome Membrane Rigidity. *Langmuir* 32, 6074–6082 (2016).
54. Christensen, D. *et al.* A cationic vaccine adjuvant based on a saturated quaternary ammonium lipid have different in vivo distribution kinetics and display a distinct CD4 T cell-inducing capacity compared to its unsaturated analog. *Journal of Controlled Release* 160, 468–476 (2012).
55. Takano, S. *et al.* Physicochemical properties of liposomes affecting apoptosis induced by cationic liposomes in macrophages. *Pharmacological Research* 20, 962–968 (2003).
56. Winau, F. *et al.* Apoptotic vesicles crossprime CD8 T cells and protect against tuberculosis. *Immunity* 24, 105–117 (2006).
57. Caruso, S. & Poon, I. K. H. Apoptotic cell-derived extracellular vesicles: More than just debris. *Frontiers in Immunology* 9, 1486 (2018).
58. Mayhew, E. *et al.* Toxicity of non-drug-containing liposomes for cultured human cells. *Exp Cell Res* 171, 195–202 (1987).
59. Arisaka, M. *et al.* Involvement of protein kinase Cδ in induction of apoptosis by cationic liposomes in macrophage-like RAW264.7 cells. *FEBS Letters* 584, 1016–1020 (2010).
60. Vangasseri, D. P. *et al.* Immunostimulation of dendritic cells by cationic liposomes. *Molecular Membrane Biology* 23, 385–395 (2006).
61. Honey, K. CCL3 and CCL4 actively recruit CD8+ T cells. *Nature Reviews Immunology* 6, 427 (2006).

62. Castellino, F. *et al.* Chemokines enhance immunity by guiding naive CD8+ T cells to sites of CD4+ T cell-dendritic cell interaction. *Nature* 440, 890–895 (2006).
63. Hugues, S. *et al.* Dynamic imaging of chemokine-dependent CD8+ T cell help for CD8+ T cell responses. *Nature Immunology* 8, 921–930 (2007).
64. Askew, D. *et al.* Transient Surface CCR5 Expression by Naive CD8 + T Cells within Inflamed Lymph Nodes Is Dependent on High Endothelial Venule Interaction and Augments Th Cell–Dependent Memory Response. *The Journal of Immunology* 196, 3653–3664 (2016).
65. Khan, I. A. *et al.* IP-10 is critical for effector T cell trafficking and host survival in Toxoplasma gondii infection. *Immunity* 12, 483–494 (2000).
66. Majumder, S. *et al.* CXCL10 Is Critical for the Generation of Protective CD8 T Cell Response Induced by Antigen Pulsed CpG-ODN Activated Dendritic Cells. *PLoS One* 7, e48727 (2012).
67. Joosten, S. A. *et al.* Mycobacterial growth inhibition is associated with trained innate immunity. *Journal of Clinical Investigation* 128, 1837–1851 (2018).
68. Lacy, P. Eosinophil Cytokines in Allergy. *Cytokine Effector Functions in Tissues,* 173–218 (2017).
69. Deshmane, S. L. *et al.* Monocyte chemoattractant protein-1 (MCP-1): An overview. *Journal of Interferon and Cytokine Research* 29:6, 313–325 (2009).
70. Rapp, M. *et al.* CCL22 controls immunity by promoting regulatory T cell communication with dendritic cells in lymph nodes. *Journal of Experimental Medicine* 216, 1170–1181 (2019).
71. Kühnemuth, B. *et al.* CCL22 impedes T cell activation capacities of dendritic cells by reducing membrane expression of MHC molecules and CD80. *The Journal of Immunology* 198, (2017).
72. Varypataki, E. M. *et al.* Cationic Liposomes Loaded with a Synthetic Long Peptide and Poly(I:C): a Defined Adjuvanted Vaccine for Induction of Antigen-Specific T Cell Cytotoxicity. *AAPS Journal* 17, 216–226 (2015).

SUPPLEMENTARY MATERIALS

Supplementary Table S1. Physicochemical properties of the formulations that did not meet the inclusion criteria. The listed formulations had visible aggregation. The results represent mean ± SD.

Formulation	Z-average size (nm)	PDI (-)	Z-potential (mV)
AER/DOTAP:DSPC	>1000 (± 85)	0.84 ± 0.60	23.4 ± 1.8
AER/DDA:DSPC	>1000 (± 644)	1.00 ± 0.01	21.2 ± 0.5
AER/EPC:DSPC	402 ± 20	0.87 ± 0.10	18.2 ± 0.2
AER/DOTAP:chol:DSPC	215 ± 5	0.37 ± 0.01	33.6 ± 0.4
AER/DDA:chol:DSPC	143 ± 4	0.23 ± 0.03	32.0 ± 0.3
AER/EPC:chol:DSPC	741 ± 24	0.63 ± 0.01	30.3 ± 0.8
AER/GL-67:DSPC	>1000 (± 525)	0.27 ± 0.08	10.4 ± 5.4
AER/MVL5:DOPC	>1000 (± 980)	0.23 ± 0.11	6.7 ± 0.8
AER/MVL5:chol:DOPC	>1000 (± 655)	0.74 ± 0.40	0.7 ± 0.6
AER/MVL5:chol:DSPC	>1000 (± 1268)	1.00 ± 0.01	4.1 ± 0.1
AER/DODMA:chol:DSPC	258 ± 16	0.65 ± 0.31	10.9 ± 0.3

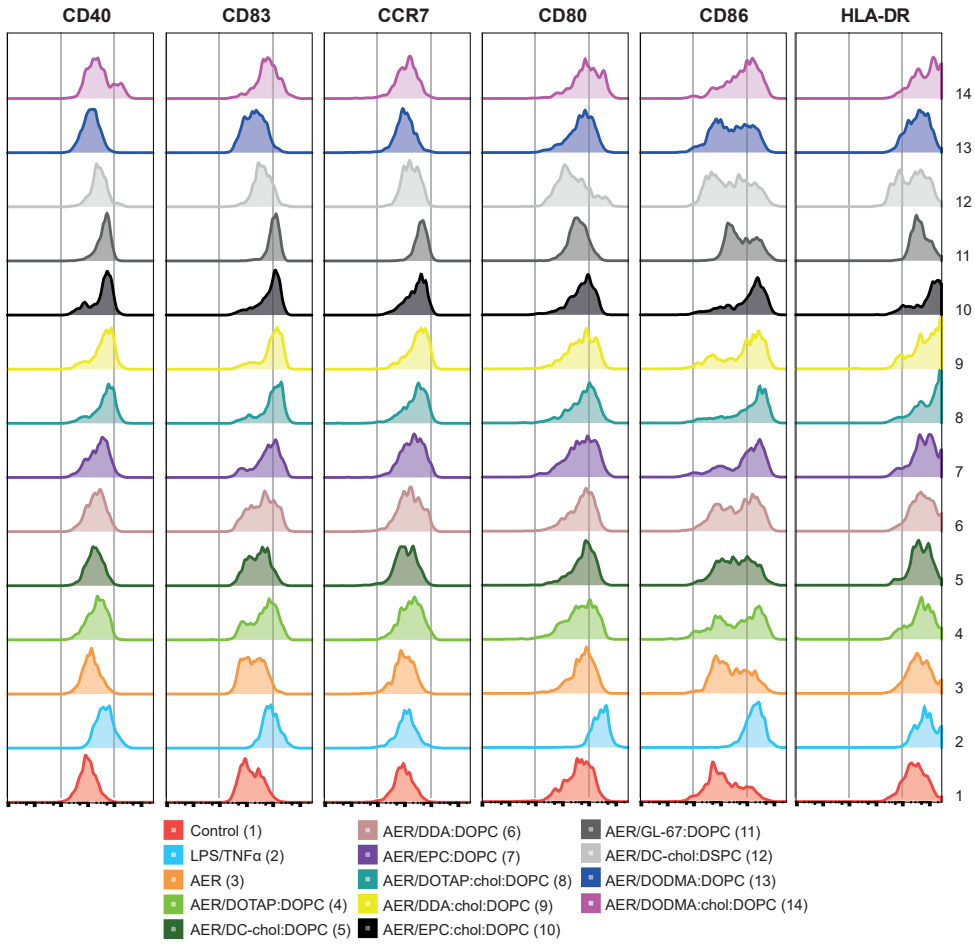

Supplementary Figure S1. Upregulation of surface activation markers in MDDCs (GM-CSF/IL-4 differentiated) after stimulation with medium (negative control), a combination of LPS/TNFα (100 and 5 ng/ml, respectively), AER (5 µg/ml) and liposomal formulations (5 µg/ml AER, 250 µg/ml liposomes, exposure 1 h). The upregulation of the surface activation markers is presented as concatenated flow cytometry data of all donors, n = 6.

Supplementary Table S2. Statistical comparisons between different groups as measured by Kruskal-Wallis and Uncorrected Dunn's test (Figure 2a). Medium (negative control), a combination of LPS/TNFα (100 and 5 ng/ml, respectively), AER (5 µg/ml) and liposomal formulations (5 µg/ml AER, 250 µg/ml liposomes, exposure 1 h) ns $p > 0.05$, * $p < 0.05$, ** $p < 0.01$, *** $p < 0.001$, **** $p < 0.0001$.

Uncorrected Dunn's test	Significance					
	CD40	CD80	CD83	CD86	CCR7	HLA-DR
Control vs. LPS/TNFα	****	**	***	****	ns	*
Control vs. AER	ns	ns	ns	ns	ns	ns
Control vs. AER/DOTAP:DOPC	*	ns	ns	ns	ns	ns
Control vs. AER/DC-chol:DOPC	ns	ns	ns	ns	ns	ns
Control vs. AER/DDA:DOPC	*	ns	ns	ns	ns	ns
Control vs. AER/EPC:DOPC	*	ns	**	*	*	*
Control vs. AER/DOTAP:chol:DOPC	***	ns	***	**	***	**
Control vs. AER/DDA:chol:DOPC	***	ns	**	*	***	*
Control vs. AER/EPC:chol:DOPC	***	ns	***	***	***	***
Control vs. AER/GL-67:DOPC	****	ns	****	*	****	ns
Control vs. AER/DC-chol:DSPC	**	ns	ns	ns	*	ns
Control vs. AER/DODMA:DOPC	ns	ns	ns	ns	ns	ns
Control vs. AER/DODMA:chol:DOPC	**	ns	**	**	ns	**
LPS/TNFα vs. AER	***	*	***	**	ns	ns
LPS/TNFα vs. AER/DOTAP:DOPC	ns	**	ns	*	ns	ns
LPS/TNFα vs. AER/DC-chol:DOPC	*	*	*	*	ns	ns
LPS/TNFα vs. AER/DDA:DOPC	*	*	ns	*	ns	ns
LPS/TNFα vs. AER/EPC:DOPC	ns	**	ns	ns	ns	ns
LPS/TNFα vs. AER/DOTAP:chol:DOPC	ns	**	ns	ns	**	ns
LPS/TNFα vs. AER/DDA:chol:DOPC	ns	***	ns	ns	**	ns
LPS/TNFα vs. AER/EPC:chol:DOPC	ns	*	ns	ns	**	ns
LPS/TNFα vs. AER/GL-67:DOPC	ns	***	ns	ns	***	ns
LPS/TNFα vs. AER/DC-chol:DSPC	ns	****	ns	**	ns	*
LPS/TNFα vs. AER/DODMA:DOPC	***	**	**	**	ns	ns
LPS/TNFα vs. AER/DODMA:chol:DOPC	ns	ns	ns	ns	ns	ns
AER vs. AER/DOTAP:DOPC	ns	ns	ns	ns	ns	ns
AER vs. AER/DC-chol:DOPC	ns	ns	ns	ns	ns	ns
AER vs. AER/DDA:DOPC	ns	ns	ns	ns	ns	ns
AER vs. AER/EPC:DOPC	ns	ns	*	ns	*	ns

Uncorrected Dunn's test	Significance					
	CD40	CD80	CD83	CD86	CCR7	HLA-DR
AER vs. AER/DOTAP:chol:DOPC	**	ns	***	*	**	ns
AER vs. AER/DDA:chol:DOPC	**	ns	**	ns	**	ns
AER vs. AER/EPC:chol:DOPC	**	ns	***	**	***	*
AER vs. AER/GL-67:DOPC	***	ns	****	ns	****	ns
AER vs. AER/DC-chol:DSPC	*	**	ns	ns	ns	ns
AER vs. AER/DODMA:DOPC	ns	ns	ns	ns	ns	ns
AER vs. AER/DODMA:chol:DOPC	ns	ns	**	ns	ns	ns
AER/DOTAP:DOPC vs. AER/DC-chol:DOPC	ns	ns	ns	ns	ns	ns
AER/DOTAP:DOPC vs. AER/DDA:DOPC	ns	ns	ns	ns	ns	ns
AER/DOTAP:DOPC vs. AER/EPC:DOPC	ns	ns	ns	ns	ns	ns
AER/DOTAP:DOPC vs. AER/DOTAP:chol:DOPC	ns	ns	*	ns	ns	ns
AER/DOTAP:DOPC vs. AER/DDA:chol:DOPC	ns	ns	ns	ns	ns	ns
AER/DOTAP:DOPC vs. AER/EPC:chol:DOPC	ns	ns	*	*	*	*
AER/DOTAP:DOPC vs. AER/GL-67:DOPC	ns	ns	**	ns	**	ns
AER/DOTAP:DOPC vs. AER/DC-chol:DSPC	ns	ns	ns	ns	ns	ns
AER/DOTAP:DOPC vs. AER/DODMA:DOPC	ns	ns	ns	ns	ns	ns
AER/DOTAP:DOPC vs. AER/DODMA:chol:DOPC	ns	ns	ns	ns	ns	ns
AER/DC-chol:DOPC vs. AER/DDA:DOPC	ns	ns	ns	ns	ns	ns
AER/DC-chol:DOPC vs. AER/EPC:DOPC	ns	ns	ns	ns	ns	ns
AER/DC-chol:DOPC vs. AER/DOTAP:chol:DOPC	ns	ns	**	ns	**	ns
AER/DC-chol:DOPC vs. AER/DDA:chol:DOPC	ns	ns	*	ns	**	ns
AER/DC-chol:DOPC vs. AER/EPC:chol:DOPC	ns	ns	**	ns	**	ns
AER/DC-chol:DOPC vs. AER/GL-67:DOPC	*	ns	**	ns	***	ns
AER/DC-chol:DOPC vs. AER/DC-chol:DSPC	ns	**	ns	ns	ns	ns
AER/DC-chol:DOPC vs. AER/DODMA:DOPC	ns	ns	ns	ns	ns	ns
AER/DC-chol:DOPC vs. AER/DODMA:chol:DOPC	ns	ns	ns	ns	ns	ns
AER/DDA:DOPC vs. AER/EPC:DOPC	ns	ns	ns	ns	ns	ns
AER/DDA:DOPC vs. AER/DOTAP:chol:DOPC	ns	ns	*	ns	ns	ns
AER/DDA:DOPC vs. AER/DDA:chol:DOPC	ns	ns	ns	ns	ns	ns
AER/DDA:DOPC vs. AER/EPC:chol:DOPC	ns	ns	ns	ns	*	ns
AER/DDA:DOPC vs. AER/GL-67:DOPC	*	ns	*	ns	**	ns
AER/DDA:DOPC vs. AER/DC-chol:DSPC	ns	*	ns	ns	ns	ns
AER/DDA:DOPC vs. AER/DODMA:DOPC	ns	ns	ns	ns	ns	ns
AER/DDA:DOPC vs. AER/DODMA:chol:DOPC	ns	ns	ns	ns	ns	ns

Uncorrected Dunn's test	Significance					
	CD40	CD80	CD83	CD86	CCR7	HLA-DR
AER/EPC:DOPC vs. AER/DOTAP:chol:DOPC	ns	ns	ns	ns	ns	ns
AER/EPC:DOPC vs. AER/DDA:chol:DOPC	ns	ns	ns	ns	ns	ns
AER/EPC:DOPC vs. AER/EPC:chol:DOPC	ns	ns	ns	ns	ns	ns
AER/EPC:DOPC vs. AER/GL-67:DOPC	ns	ns	ns	ns	*	ns
AER/EPC:DOPC vs. AER/DC-chol:DSPC	ns	ns	ns	ns	ns	*
AER/EPC:DOPC vs. AER/DODMA:DOPC	ns	ns	*	ns	ns	ns
AER/EPC:DOPC vs. AER/DODMA:chol:DOPC	ns	ns	ns	ns	ns	ns
AER/DOTAP:chol:DOPC vs. AER/DDA:chol:DOPC	ns	ns	ns	ns	ns	ns
AER/DOTAP:chol:DOPC vs. AER/EPC:chol:DOPC	ns	ns	ns	ns	ns	ns
AER/DOTAP:chol:DOPC vs. AER/GL-67:DOPC	ns	ns	ns	ns	ns	ns
AER/DOTAP:chol:DOPC vs. AER/DC-chol:DSPC	ns	ns	*	*	ns	**
AER/DOTAP:chol:DOPC vs. AER/DODMA:DOPC	**	ns	***	*	**	*
AER/DOTAP:chol:DOPC vs. AER/DODMA:chol:DOPC	ns	ns	ns	ns	*	ns
AER/DDA:chol:DOPC vs. AER/EPC:chol:DOPC	ns	ns	ns	ns	ns	ns
AER/DDA:chol:DOPC vs. AER/GL-67:DOPC	ns	ns	ns	ns	ns	ns
AER/DDA:chol:DOPC vs. AER/DC-chol:DSPC	ns	ns	ns	ns	ns	*
AER/DDA:chol:DOPC vs. AER/DODMA:DOPC	**	ns	**	ns	**	ns
AER/DDA:chol:DOPC vs. AER/DODMA:chol:DOPC	ns	ns	ns	ns	*	ns
AER/EPC:chol:DOPC vs. AER/GL-67:DOPC	ns	ns	ns	ns	ns	*
AER/EPC:chol:DOPC vs. AER/DC-chol:DSPC	ns	*	*	*	ns	***
AER/EPC:chol:DOPC vs. AER/DODMA:DOPC	**	ns	***	**	**	*
AER/EPC:chol:DOPC vs. AER/DODMA:chol:DOPC	ns	ns	ns	ns	**	ns
AER/GL-67:DOPC vs. AER/DC-chol:DSPC	ns	ns	*	ns	*	ns
AER/GL-67:DOPC vs. AER/DODMA:DOPC	***	ns	****	ns	****	ns
AER/GL-67:DOPC vs. AER/DODMA:chol:DOPC	ns	ns	ns	ns	***	ns
AER/DC-chol:DSPC vs. AER/DODMA:DOPC	*	*	ns	ns	ns	ns
AER/DC-chol:DSPC vs. AER/DODMA:chol:DOPC	ns	**	ns	ns	ns	**
AER/DODMA:DOPC vs. AER/DODMA:chol:DOPC	ns	ns	*	ns	ns	ns

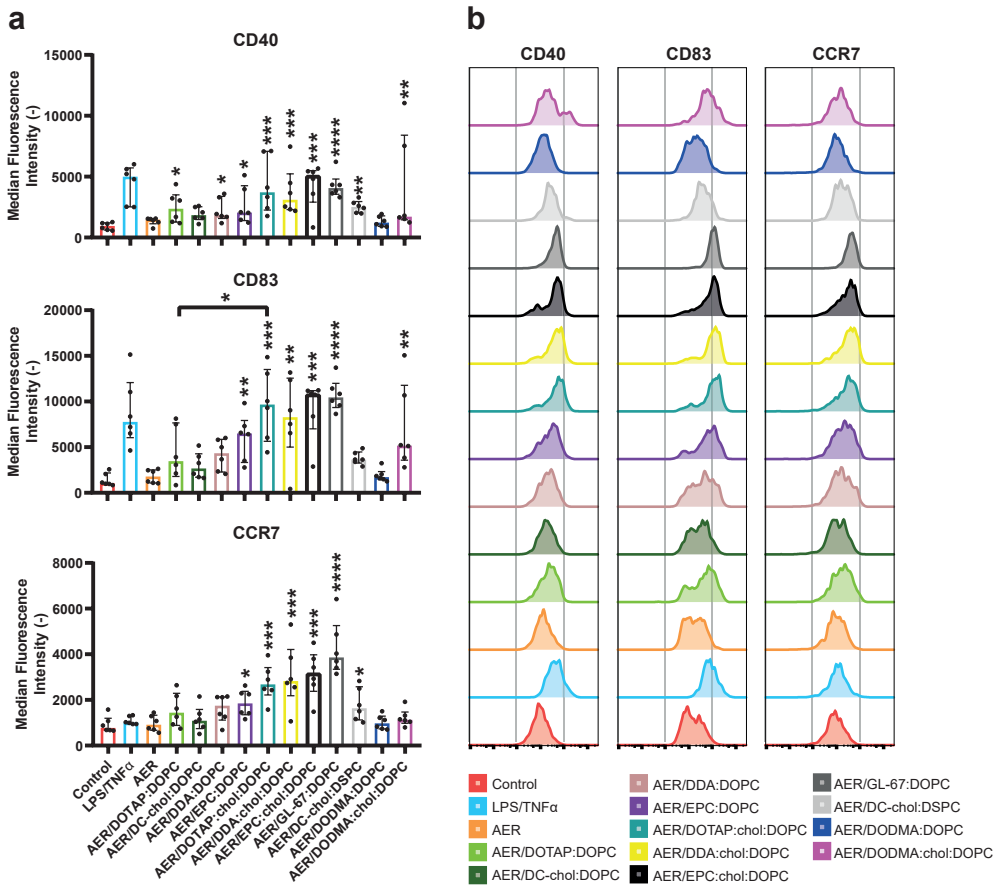

Supplementary Figure S2. Upregulation of surface activation markers in MDDCs in the second experiment with selected liposomal formulations. A) Median fluorescence intensities related to expression of indicated (selected) activation markers: CD40, CD83 and CCR7. B) Upregulation of the surface activation markers as concatenated flow cytometry data of all donors, n = 7. The statistical significance was measured by the Kruskal-Wallis and Uncorrected Dunn's test, and the formulations were compared to the control.

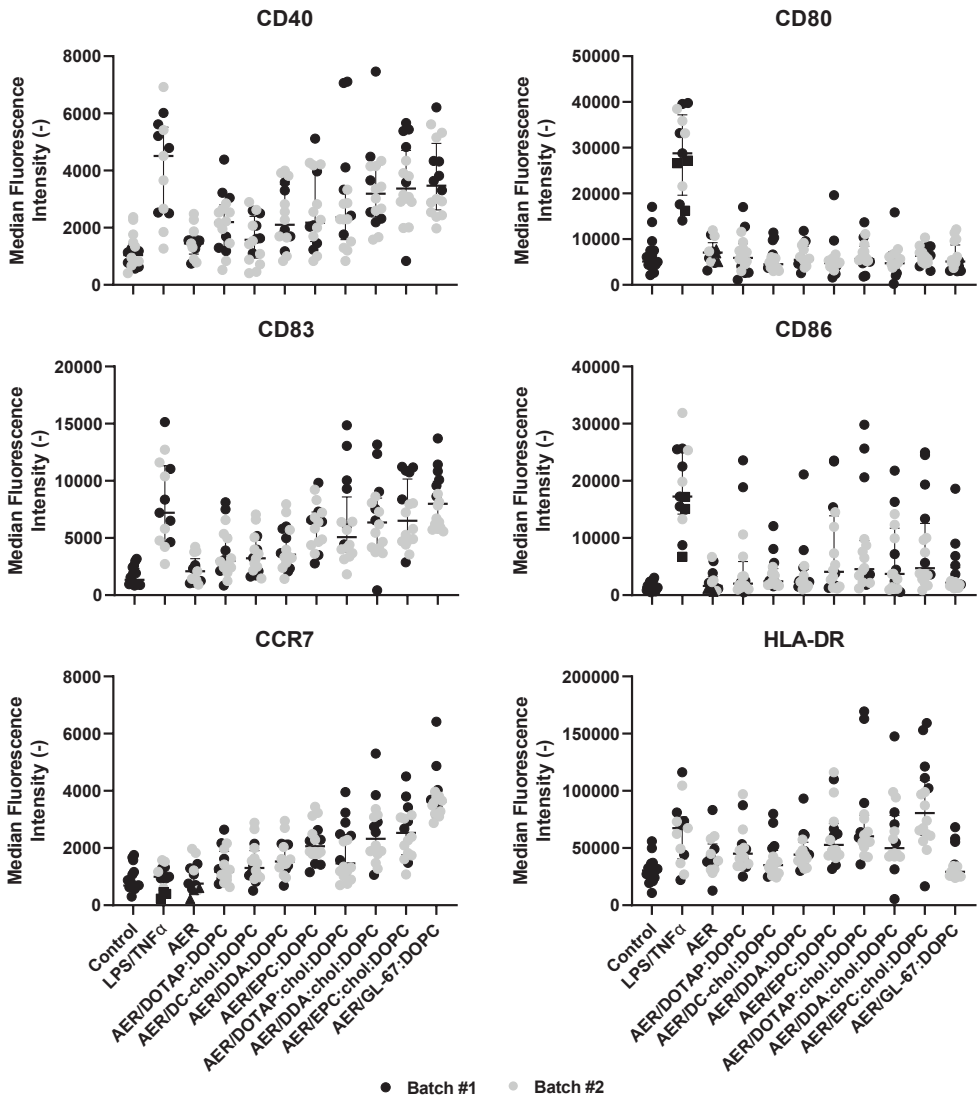

Supplementary Figure S3. Upregulation of surface activation markers in two experiments using MDDCs (the black dots are from the first experiment reported in the main manuscript, and the grey dots are the repeat of this experiment). Median fluorescence intensities related to the expression of the indicated activation markers. The statistical significance is not shown.

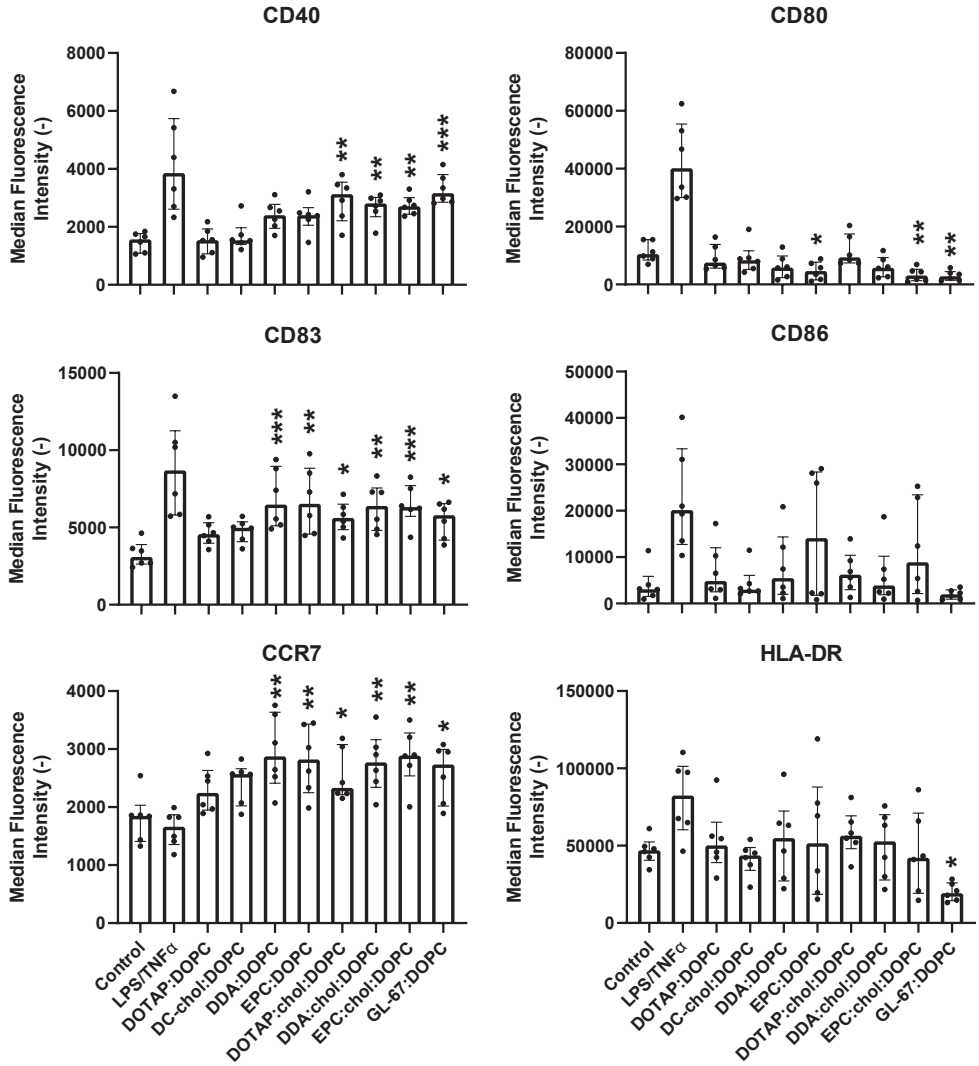

Supplementary Figure S4. Upregulation of surface activation markers in MDDCs after stimulation with empty (antigen-free) liposomal formulations. Median fluorescence intensities related to the expression of indicated activation markers, n = 5. The statistical significance was measured by Kruskal-Wallis and Uncorrected Dunn's test, and the formulations were compared to the control.

Supplementary Table S3. Statistical comparisons between different groups (uptake) as measured by Kruskal-Wallis and Uncorrected Dunn's test (Figure 3a). ns $p > 0.05$, * $p < 0.05$, ** $p < 0.01$, *** $p < 0.001$, **** $p < 0.0001$.

Uncorrected Dunn's test	p-value
Control vs. DOTAP:DOPC	***
Control vs. DC-chol:DOPC	****
Control vs. DDA:DOPC	****
Control vs. EPC:DOPC	****
Control vs. DOTAP:chol:DOPC	****
Control vs. DDA:chol:DOPC	****
Control vs. EPC:chol:DOPC	****
Control vs. GL-67:DOPC	****
Control vs. DODMA:DOPC	ns
Control vs. DODMA:chol:DOPC	ns
Control vs. Unlabeled liposomes	ns
DOTAP:DOPC vs. DC-chol:DOPC	ns
DOTAP:DOPC vs. DDA:DOPC	ns
DOTAP:DOPC vs. EPC:DOPC	ns
DOTAP:DOPC vs. DOTAP:chol:DOPC	*
DOTAP:DOPC vs. DDA:chol:DOPC	ns
DOTAP:DOPC vs. EPC:chol:DOPC	*
DOTAP:DOPC vs. GL-67:DOPC	ns
DOTAP:DOPC vs. DODMA:DOPC	*
DOTAP:DOPC vs. DODMA:chol:DOPC	*
DOTAP:DOPC vs. Unlabeled liposomes	***
DC-chol:DOPC vs. DDA:DOPC	ns
DC-chol:DOPC vs. EPC:DOPC	ns
DC-chol:DOPC vs. DOTAP:chol:DOPC	ns
DC-chol:DOPC vs. DDA:chol:DOPC	ns
DC-chol:DOPC vs. EPC:chol:DOPC	ns
DC-chol:DOPC vs. GL-67:DOPC	ns
DC-chol:DOPC vs. DODMA:DOPC	**
DC-chol:DOPC vs. DODMA:chol:DOPC	**
DC-chol:DOPC vs. Unlabeled liposomes	****
DDA:DOPC vs. EPC:DOPC	ns
DDA:DOPC vs. DOTAP:chol:DOPC	ns
DDA:DOPC vs. DDA:chol:DOPC	ns

Uncorrected Dunn's test	p-value
DDA:DOPC vs. EPC:chol:DOPC	ns
DDA:DOPC vs. GL-67:DOPC	ns
DDA:DOPC vs. DODMA:DOPC	***
DDA:DOPC vs. DODMA:chol:DOPC	***
DDA:DOPC vs. Unlabeled liposomes	****
EPC:DOPC vs. DOTAP:chol:DOPC	ns
EPC:DOPC vs. DDA:chol:DOPC	ns
EPC:DOPC vs. EPC:chol:DOPC	ns
EPC:DOPC vs. GL-67:DOPC	ns
EPC:DOPC vs. DODMA:DOPC	***
EPC:DOPC vs. DODMA:chol:DOPC	***
EPC:DOPC vs. Unlabeled liposomes	****
DOTAP:chol:DOPC vs. DDA:chol:DOPC	ns
DOTAP:chol:DOPC vs. EPC:chol:DOPC	ns
DOTAP:chol:DOPC vs. GL-67:DOPC	ns
DOTAP:chol:DOPC vs. DODMA:DOPC	****
DOTAP:chol:DOPC vs. DODMA:chol:DOPC	****
DOTAP:chol:DOPC vs. Unlabeled liposomes	****
DDA:chol:DOPC vs. EPC:chol:DOPC	ns
DDA:chol:DOPC vs. GL-67:DOPC	ns
DDA:chol:DOPC vs. DODMA:DOPC	***
DDA:chol:DOPC vs. DODMA:chol:DOPC	***
DDA:chol:DOPC vs. Unlabeled liposomes	****
EPC:chol:DOPC vs. GL-67:DOPC	ns
EPC:chol:DOPC vs. DODMA:DOPC	****
EPC:chol:DOPC vs. DODMA:chol:DOPC	****
EPC:chol:DOPC vs. Unlabeled liposomes	****
GL-67:DOPC vs. DODMA:DOPC	****
GL-67:DOPC vs. DODMA:chol:DOPC	****
GL-67:DOPC vs. Unlabeled liposomes	****
DODMA:DOPC vs. DODMA:chol:DOPC	ns
DODMA:DOPC vs. Unlabeled liposomes	ns
DODMA:chol:DOPC vs. Unlabeled liposomes	ns

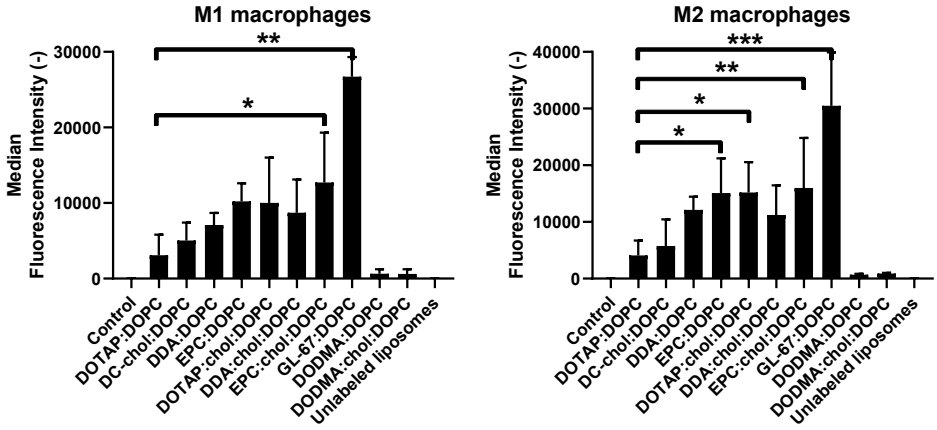

Supplementary Figure S5. Uptake in monocyte-derived macrophages of pro-inflammatory M1 (GM-CSF differentiated) and anti-inflammatory M2 (M-CSF differentiated) macrophages. The statistical significance was measured by the Kruskal-Wallis and Uncorrected Dunn's test, and the formulations were compared to the DOTAP:DOPC formulation.

Supplementary Table S4. Physicochemical properties of selected formulations after preparation and 4 or 7 months after. n = 1 (batches)

DOPC:DOTAP/AER			
Time (months)	**PDI**	**Z-average size (nm)**	**Z-potential (mV)**
0	0.15 ± 0.01	128.1 ± 0.6	30.8 ± 0.5
7	0.16 ± 0.01	129.7 ± 0.5	30.5 ± 0.6
DOPC-DOTAP (empty)			
Time (months)	**PDI**	**Z-average size (nm)**	**Z-potential (mV)**
0	0.12 ± 0.02	157.8 ± 0.5	33.4 ± 0.4
7	0.14 ± 0.01	156.9 ± 0.3	30.2 ± 0.3
DOPC -DC-Chol/AER			
Time (months)	**PDI**	**Z-average size (nm)**	**Z-potential (mV)**
0	0.26 ± 0.01	90.5 ± 0.1	29.2 ± 0.5
4	0.28 ± 0.01	97.8 ± 1.0	30.4 ± 0.3

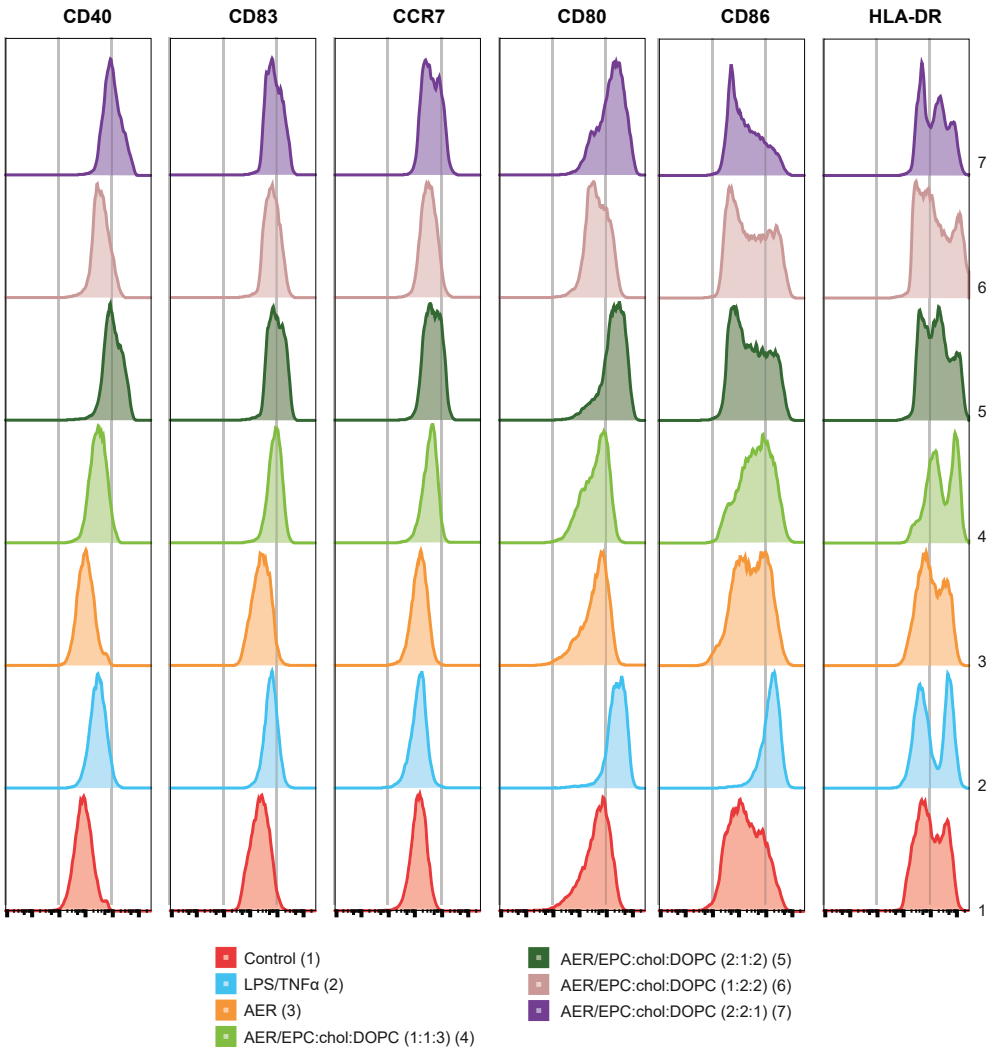

Supplementary Figure S6. Upregulation of surface activation markers in MDDCs after stimulation with medium (control), LPS/TNFα cocktail (100 and 5 ng/ml, respectively), AER (5 µg/ml) and liposomal formulations (5 µg/ml AER, 250 µg/ml liposomes, exposure 1 hour). Upregulation of the surface activation markers is presented as concatenated flow cytometry data of all donors, n = 7.

Supplementary Table S5. Statistical comparisons between different groups as measured by Kruskal-Wallis and Uncorrected Dunn's test (Figure 4a). ns $p > 0.05$, * $p < 0.05$, ** $p < 0.01$, *** $p < 0.001$, **** $p < 0.0001$.

Uncorrected Dunn's test	Significance					
0.5 µg/ml AER / 25 µg/ml lipids	**CD40**	**CD80**	**CD83**	**CD86**	**CCR7**	**HLA-DR**
Control vs. LPS/TNFα	****	*	***	****	ns	ns
Control vs. AER	ns	ns	ns	ns	ns	ns
Control vs. AER/EPC:chol:DOPC 1:1:3	ns	ns	ns	ns	ns	ns
Control vs. AER/EPC:chol:DOPC 2:1:2	**	ns	****	**	**	***
Control vs. AER/EPC:chol:DOPC 1:2:2	ns	ns	ns	ns	ns	*
Control vs. AER/EPC:chol:DOPC 2:2:1	**	ns	****	**	**	***
LPS/TNFα vs. AER	***	**	**	***	ns	ns
LPS/TNFα vs. AER/EPC:chol:DOPC 1:1:3	****	***	*	**	ns	ns
LPS/TNFα vs. AER/EPC:chol:DOPC 2:1:2	ns	***	ns	ns	***	*
LPS/TNFα vs. AER/EPC:chol:DOPC 1:2:2	**	**	*	**	ns	ns
LPS/TNFα vs. AER/EPC:chol:DOPC 2:2:1	ns	***	ns	ns	***	ns
AER vs. AER/EPC:chol:DOPC 1:1:3	ns	ns	ns	ns	ns	ns
AER vs. AER/EPC:chol:DOPC 2:1:2	*	ns	***	*	**	*
AER vs. AER/EPC:chol:DOPC 1:2:2	ns	ns	ns	ns	ns	ns
AER vs. AER/EPC:chol:DOPC 2:2:1	**	ns	***	*	**	*
AER/EPC:chol:DOPC 1:1:3 vs. AER/EPC:chol:DOPC 2:1:2	**	ns	*	ns	ns	ns
AER/EPC:chol:DOPC 1:1:3 vs. AER/EPC:chol:DOPC 1:2:2	ns	ns	ns	ns	ns	ns
AER/EPC:chol:DOPC 1:1:3 vs. AER/EPC:chol:DOPC 2:2:1	**	ns	*	ns	ns	ns
AER/EPC:chol:DOPC 2:1:2 vs. AER/EPC:chol:DOPC 1:2:2	ns	ns	**	ns	*	ns
AER/EPC:chol:DOPC 2:1:2 vs. AER/EPC:chol:DOPC 2:2:1	ns	ns	ns	ns	ns	ns
AER/EPC:chol:DOPC 1:2:2 vs. AER/EPC:chol:DOPC 2:2:1	*	ns	**	ns	*	ns

Uncorrected Dunn's test	Significance					
2 µg/ml AER / 100 µg/ml lipids	**CD40**	**CD80**	**CD83**	**CD86**	**CCR7**	**HLA-DR**
Control vs. LPS/TNFα	**	**	ns	****	ns	ns
Control vs. AER	ns	ns	ns	ns	ns	ns
Control vs. AER/EPC:chol:DOPC 1:1:3	ns	ns	***	ns	**	**
Control vs. AER/EPC:chol:DOPC 2:1:2	****	ns	****	****	***	**
Control vs. AER/EPC:chol:DOPC 1:2:2	**	ns	***	ns	**	****
Control vs. AER/EPC:chol:DOPC 2:2:1	****	ns	***	***	***	**
LPS/TNFα vs. AER	**	***	ns	***	ns	ns
LPS/TNFα vs. AER/EPC:chol:DOPC 1:1:3	ns	****	ns	*	**	*
LPS/TNFα vs. AER/EPC:chol:DOPC 2:1:2	ns	*	*	ns	***	*

Uncorrected Dunn's test	Significance					
2 µg/ml AER / 100 µg/ml lipids	CD40	CD80	CD83	CD86	CCR7	HLA-DR
LPS/TNFα vs. AER/EPC:chol:DOPC 1:2:2	ns	****	ns	*	**	**
LPS/TNFα vs. AER/EPC:chol:DOPC 2:2:1	*	ns	*	ns	***	*
AER vs. AER/EPC:chol:DOPC 1:1:3	ns	ns	**	ns	**	*
AER vs. AER/EPC:chol:DOPC 2:1:2	****	ns	***	***	***	*
AER vs. AER/EPC:chol:DOPC 1:2:2	*	ns	***	ns	**	**
AER vs. AER/EPC:chol:DOPC 2:2:1	****	ns	***	**	***	*
AER/EPC:chol:DOPC 1:1:3 vs. AER/EPC:chol:DOPC 2:1:2	**	ns	ns	*	ns	ns
AER/EPC:chol:DOPC 1:1:3 vs. AER/EPC:chol:DOPC 1:2:2	ns	ns	ns	ns	ns	ns
AER/EPC:chol:DOPC 1:1:3 vs. AER/EPC:chol:DOPC 2:2:1	***	*	ns	ns	ns	ns
AER/EPC:chol:DOPC 2:1:2 vs. AER/EPC:chol:DOPC 1:2:2	ns	ns	ns	*	ns	ns
AER/EPC:chol:DOPC 2:1:2 vs. AER/EPC:chol:DOPC 2:2:1	ns	ns	ns	ns	ns	ns
AER/EPC:chol:DOPC 1:2:2 vs. AER/EPC:chol:DOPC 2:2:1	*	*	ns	ns	ns	ns

Uncorrected Dunn's test	Significance					
5 µg/ml AER / 250 µg/ml lipids	CD40	CD80	CD83	CD86	CCR7	HLA-DR
Control vs. LPS/TNFα	*	***	*	***	ns	ns
Control vs. AER	ns	ns	ns	ns	ns	ns
Control vs. AER/EPC:chol:DOPC 1:1:3	ns	ns	****	*	**	****
Control vs. AER/EPC:chol:DOPC 2:1:2	****	**	****	ns	****	**
Control vs. AER/EPC:chol:DOPC 1:2:2	**	ns	*	ns	*	*
Control vs. AER/EPC:chol:DOPC 2:2:1	****	**	***	ns	***	ns
LPS/TNFα vs. AER	*	***	*	**	ns	ns
LPS/TNFα vs. AER/EPC:chol:DOPC 1:1:3	ns	***	ns	ns	**	***
LPS/TNFα vs. AER/EPC:chol:DOPC 2:1:2	*	ns	*	**	****	ns
LPS/TNFα vs. AER/EPC:chol:DOPC 1:2:2	ns	***	ns	**	*	ns
LPS/TNFα vs. AER/EPC:chol:DOPC 2:2:1	*	ns	ns	****	****	ns
AER vs. AER/EPC:chol:DOPC 1:1:3	ns	ns	***	ns	**	***
AER vs. AER/EPC:chol:DOPC 2:1:2	****	**	****	ns	****	ns
AER vs. AER/EPC:chol:DOPC 1:2:2	**	ns	ns	ns	ns	ns
AER vs. AER/EPC:chol:DOPC 2:2:1	****	**	**	ns	***	ns
AER/EPC:chol:DOPC 1:1:3 vs. AER/EPC:chol:DOPC 2:1:2	**	**	ns	ns	ns	ns
AER/EPC:chol:DOPC 1:1:3 vs. AER/EPC:chol:DOPC 1:2:2	ns	ns	ns	ns	ns	ns
AER/EPC:chol:DOPC 1:1:3 vs. AER/EPC:chol:DOPC 2:2:1	**	**	ns	**	ns	**
AER/EPC:chol:DOPC 2:1:2 vs. AER/EPC:chol:DOPC 1:2:2	ns	**	*	ns	*	ns
AER/EPC:chol:DOPC 2:1:2 vs. AER/EPC:chol:DOPC 2:2:1	ns	ns	ns	ns	ns	ns
AER/EPC:chol:DOPC 1:2:2 vs. AER/EPC:chol:DOPC 2:2:1	ns	**	ns	ns	ns	ns

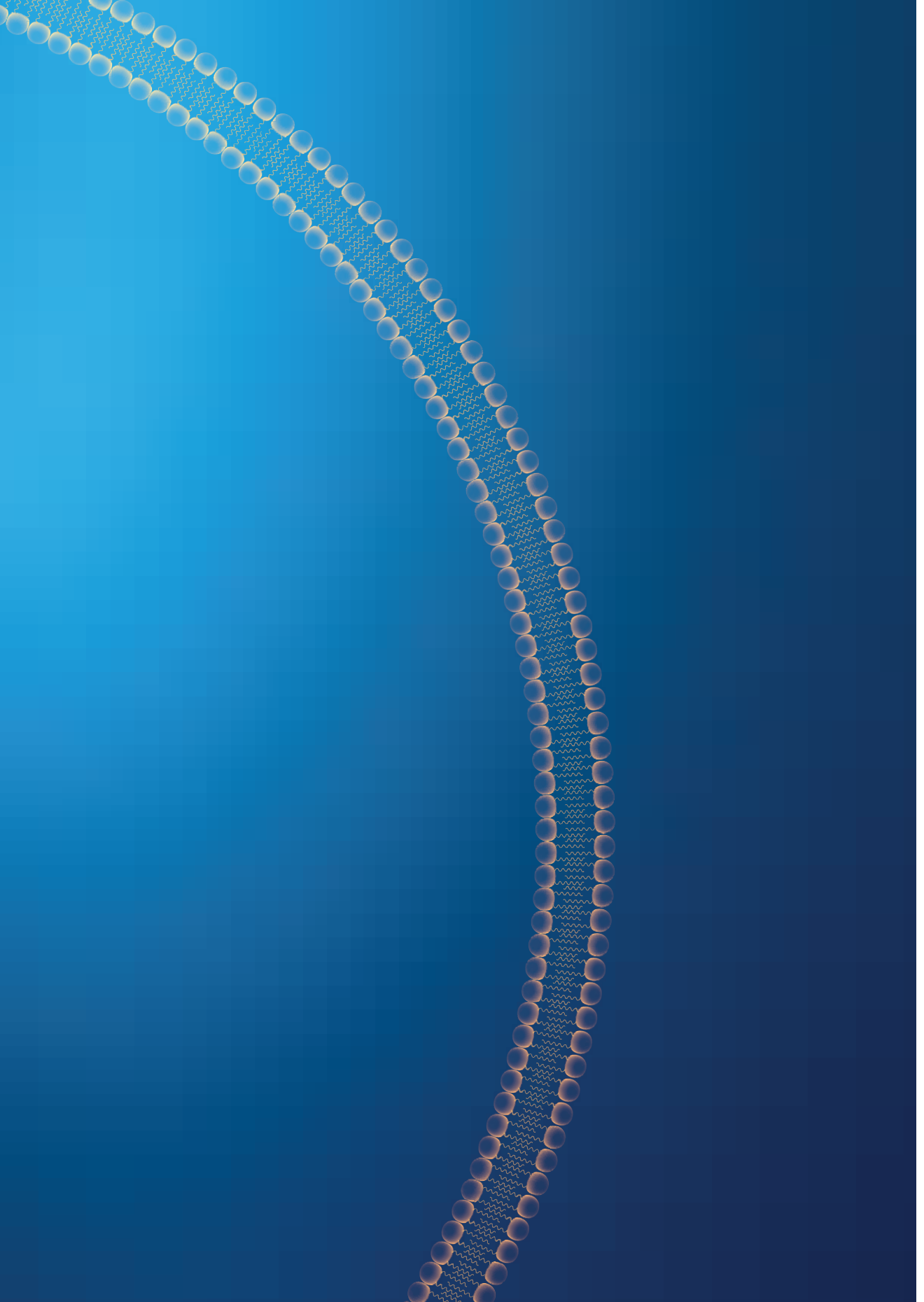

CHAPTER 3

Cationic pH-sensitive liposomes as tuberculosis subunit vaccine delivery systems: effect of liposome composition on cellular innate immune responses

M.M. Szachniewicz, K.E. van Meijgaarden, E. Kavrik, Kees L.M.C. Franken, W. Jiskoot, J.A. Bouwstra, M.C. Haks, A. Geluk, T.H.M. Ottenhoff

Adapted from International Immunopharmacology, 2025, 145: 113782

ABSTRACT

Tuberculosis (TB) is a major global health problem, and the development of effective and safe vaccines is urgently needed. $CD8^+$ T-cells play an important role alongside $CD4^+$ T-cells in the protective immune response against TB. pH-sensitive liposomes are hypothesized to boost $CD8^+$ T-cell responses by promoting class I presentation through a mechanism involving pH-dependent endosomal escape and the cytosolic transfer of antigens. The aim of the study was to explore the potential of pH-sensitive liposomes as a novel delivery system for a multi-stage protein subunit vaccine against TB in primary human cells. The liposomes were formulated with the fusion antigen Ag85b-ESAT6-Rv2034 (AER), which was previously shown to be effective in reducing bacterial load in the lungs HLA-DR3 transgenic mice and guinea pigs. The liposomes were assessed *in vitro* for cellular uptake, cell viability, upregulation of cell surface activation markers, induction of cytokine production using human monocyte-derived dendritic cells (MDDCs), and activation of human antigen-specific T-cells. Liposome DOPC:DOPE:DOBAQ:EPC (3:5:2:4 molar ratio) was effectively taken up, induced several cell surface activation markers, and production of CCL3, CCL4, and TNFα in MDDCs. It also induced upregulation of CD154 and IFNγ in T-cell clones in an antigen-specific manner. Thus, cationic pH-sensitive liposome-based TB vaccines have been demonstrated to be capable of inducing robust protective Mtb-specific immune responses, positioning them as promising candidates for effective TB vaccination.

1. INTRODUCTION

TB is among the leading deadliest infectious diseases worldwide. Until the COVID-19 pandemic at the end of 2019, TB was the number one killing pathogen for the last decades. It is estimated that a quarter of the human population is latently infected with *Mycobacterium tuberculosis* (Mtb), the causative agent of TB. In 2022 1.3 million people died because of it.[1] Unfortunately, the only licensed and available TB vaccine – *Mycobacterium Bovis* Bacillus Calmette-Guérin (BCG) – offers limited protection in adults especially those living in areas of the world where TB is endemic.[2–4] Therefore, there is an urgent need for new TB vaccines.[5]

Liposomes are self-assembled nanovesicles composed of lipids that form a bilayer that surrounds an aqueous core. Liposomes can exhibit many different physicochemical as well as biological properties depending on the lipid composition, size, charge, and surface chemistry.[6-10] One of the subclasses of liposomes is represented by pH-sensitive liposomes. Those liposomes typically respond to a change in the pH in the microenvironment by changing the molecular organization of the bilayer upon acidification. This phenomenon is utilized to deliver their cargo into the cytosol of the cell by avoiding endosomal degradation.[11–15]

Liposomes are often made pH-sensitive by the inclusion of phosphatidylethanolamine (PE) as well as by addition of weakly acidic amphiphiles – i.e. cholesteryl hemisuccinate (CHEMS) or N-(4-carboxybenzyl)-N,N-dimethyl-2,3-bis(oleoyloxy)propan-1-aminium (DOBAQ). PE lipids have a cone-shaped molecular structure that favours the formation of the inverted hexagonal phase instead of stable bilayers, which is why additional amphiphilic lipids are required to stabilize bilayers.[16–22] When exposed to an acidic environment such as inside endosomes, pH-sensitive liposomes undergo destabilization because at lower pH carboxylic groups of the amphiphilic lipids are protonated and therefore are unable to effectively stabilize the bilayer. The unstable lipid phase has a high affinity for other lipids, including those that are present in cellular membranes. Destabilized liposomes fuse with the endosomal membrane such that their cargo is released into the cytosol.[11,15,23–25]

Another mechanism employed by pH-sensitive liposomes is the so-called proton-sponge effect. After liposomes are taken up by the cell through endosome-mediated endocytosis, the endosome fuses with lysosomes, which induces acidification of the

late endosome. Functional groups that can bind free protons (i.e., amines) present on the surface of the liposomes can interfere with this process by capturing the protons and thus preventing the decrease in pH. This prevents liposomal degradation by inhibiting proteolytic and lipase enzymes released by the fusion with lysosomes. Furthermore, osmotic pressure inside the endosome will also increase due to the influx of counter ions (e.g., chloride anions) and subsequently water. This may lead to the rupture of the endosome and the release of its content.[12,26–29]

The unique property of the pH-sensitive liposomes to escape rapid endosomal/lysosomal degradation has potential benefits for vaccination.[30] Other types of liposomes typically remain inside the endosome and undergo degradation.[31,32] Delivered antigens (peptides or proteins) are rapidly degraded and presented mainly via the MHC-II pathway. As a consequence, this would lead to effective $CD4^+$ T-cell responses.[31,32] In contrast, pH-sensitive liposomes due to endosomal escape are capable of protecting antigens from rapid degradation and instead release the antigens into the cytosol. Inside the cytosol, these antigens can be processed by proteasomes instead and presented via the MHC-I pathway, leading to $CD8^+$ T-cell responses.[31,33–35] Such a shift in the balance between the $CD4^+$ and $CD8^+$ T-cell responses can have a potentially significant impact on the type of immune response induced by the vaccine.[36] In the research presented in this paper, we explored the potential of pH-sensitive liposomes for tuberculosis (TB) vaccination.

We investigated the potential of pH-sensitive liposomes as a novel delivery system of a previously designed multi-stage protein subunit vaccine against TB. Mtb is an intracellular pathogen. Such pathogens are specifically eliminated by $CD4^+$ and $CD8^+$ cytotoxic T-cells as well as natural killer cells. It can be hypothesized that if pH-sensitive liposomes further boost $CD8^+$ T-cell responses, it would have an advantage in TB vaccination. The liposomes were formulated with the Mtb fusion antigen AER, which was shown to be effective as a preventive vaccine in HLA-DR3 transgenic mice and guinea pig models.[37] Several stable formulations were developed and we validated their pH-sensitive properties. The liposomes were tested in several *in vitro* assays: cellular uptake by antigen-presenting cells (APCs): human primary MDDCs, and macrophages type 1 and type 2; cellular viability, upregulation of cell surface activation markers, induction of cytokine production, and activation of antigen-specific T-cell clones/lines as assessed by IFNγ secretion and CD154 expression.

2. MATERIALS AND METHODS

2.1 Materials

1,2-dioleoyl-*sn*-glycero-3-phosphocholine (DOPC), 1,2-dioleoyl-3-trimethylammonium-propane chloride salt (DOTAP), 1,2-dioleoyl-sn-glycero-3-ethylphosphocholine chloride salt (EPC), N-(4-carboxybenzyl)-N,N-dimethyl-2,3-bis(oleoyloxy)propan-1-aminium (DOBAQ), cholesteryl hemisuccinate (CHEMS), 1,2-dioleoyl-sn-glycero-3-phosphoethanolamine (DOPE), and 1,2-dioleoyl-sn-glycero-3-phosphoethanolamine-N-(Cyanine 5) (18:2 PE-Cy5) were obtained from Avanti Polar Lipids, Inc. (Alabaster, AL, USA). Cholesterol was purchased from Merck KGaA, (Darmstadt, Germany). The chemical structures of unlabeled lipids are shown in Figure S1. Recombinant fusion protein AER was prepared as described previously.[38] AER is a 519-amino acid protein with a molecular mass of 56 kDa, an isoelectric point (pI) of 5.60, and an aliphatic index of 73.64. In short, genes derived from Mtb (lab strain H37Rv) were amplified using polymerase chain reaction (PCR) from genomic DNA and cloned using Gateway technology (Invitrogen, ThermoFisher Scientific, Bleiswijk, Netherlands) in bacteria containing an N-terminal hexa-histidine (His) tag. Successful insertion of the products was confirmed using sequencing. Subsequently, AER was expressed in *Escherichia coli* strain BL21 (DE3) and purified. The quality of the antigen (size and purity) was assessed by gel electrophoresis using Coomassie brilliant blue staining and Western blotting using an anti-His antibody (Invitrogen, ThermoFisher Scientific, Bleiswijk, Netherlands). Endotoxin contamination in the protein was quantified using a ToxinSensor Chromogenic Limulus Amebocyte Lysate (LAL) Endotoxin Assay Kit (GenScript, Piscataway, NJ, USA). The endotoxin contents were below 50 endotoxin units per 1 mg of the protein. Subsequently, the antigen was evaluated to exclude non-specific T-cell activation and cellular toxicity using IFNγ release assay. In this assay PBMCs of *in vitro* purified protein derivative (PPD) negative, healthy Dutch donors recruited at the Sanquin Blood Bank, Leiden, the Netherlands were used.

2.2 Preparation of liposomes

The liposomes were prepared using the thin-film hydration method as described previously.[39] Appropriate lipids were pre-dissolved in chloroform. The lipids were diluted in chloroform from 25 mg/ml stock solutions. The final total amount of lipids

used per batch was 10 mg (10 mg/ml) in chloroform. The lipid solution was added to a round-bottom flask, and the chloroform was removed using a rotary evaporator (Buchi rotavapor R210, Buchi, Breda, Netherlands). To prepare AER-containing liposomes, the lipid film was rehydrated using 1 ml of 200 µg/ml AER (or 200 µg/ml DQ ovalbumin, Invitrogen, ThermoFisher Scientific, Bleiswijk, Netherlands) in 10 mM phosphate buffer (PB) with 9.8 % sucrose (pH = 7.4). For the preparation of empty liposomes (without AER) and liposomes labeled with 0.1 % 18:2 PE-Cy5 (also without AER), 10 mM PB with 9.8 % sucrose was used for rehydration. After rehydration, the liposomes were downsized by using a tip sonicator (Branson sonifier 250, Branson Ultrasonics, Danbury, UK). The sonication program comprised of eight cycles, 30 s per cycle of sonication at a 10 % amplitude followed by a break of 60 s. The samples were submerged in ice during sonication, which together with short cycles and low amplitude allowed to reduce lipid degradation. After this, the liposomes were spun down (Allegra X-12R, Beckman Coulter, Brea CA, USA) at 1500 RPM for 5 min to remove the metal particles shed by the tip sonicator. To discard the pellet, the liposomal suspensions were transferred to new tubes, and the metal pellets were discarded. To avoid fluorophore degradation by the sonication, fluorescently labeled liposomes were downsized using a 10 ml extruder (LIPEX extruder, Northern Lipids, Evonik, Canada). The liposomal formulations were extruded five times at room temperature. Firstly, through a 400 nm carbonate filter and secondly through a 200 nm filter (Nucleopore Millipore, Amsterdam, Netherlands). The liposomes (5 mg/ml lipids assuming no lipid loss) were stored at 4 °C.

2.3 Particle size and Zeta-potential measurements

The intensity-weighted average hydrodynamic diameter (Z-average size) and polydispersity index (PDI) of the formulations were quantified by dynamic light scattering, and the Zeta-potential was measured with laser Doppler electrophoresis as described previously.[39] The liposomes were diluted to 0.25 mg/ml lipid in 10 mM PB (pH = 7.4) and added to 1.5 ml VWR Two-Sided Disposable PS Cuvettes (VWR, Amsterdam, Netherlands). Measurements were carried out in triplicates with a minimum of ten runs per measurement at 20 °C using a nano ZS zetasizer coupled with a 633 nm laser and 173° optics (Malvern Instruments, Worcestershire, UK). The data were evaluated with Zetasizer Software v7.13 (Malvern Instruments).

2.4 Preparation of dendritic cells and macrophages from peripheral blood mononuclear cells

Buffy coats obtained from healthy donors after written informed consent (Sanquin Blood Bank, Amsterdam, Netherlands) were used to isolate peripheral blood mononuclear cells (PBMCs) as described previously.[39] PBMCs were obtained from buffy coats using the Ficoll-based density gradient centrifugation method. $CD14^+$ cells were isolated using the magnetic cell isolation (MACS) method with an autoMACS Pro Separator (Miltenyi Biotec BV, Leiden, Netherlands). MDDCs, M2, and M1 macrophages were prepared from $CD14^+$ cells by culturing them for six days in the presence of cytokines. To prepare MDDCs, cells were cultured with 10 ng/ml recombinant human granulocyte-macrophage colony-stimulating factor (GM-CSF; Miltenyi Biotec BV, Leiden, Netherlands) and 10 ng/ml recombinant human interleukin 4 (IL-4; Peprotech, Rocky Hill, NJ, USA). M2 macrophages were generated using 50 ng/ml of macrophage colony-stimulating factor (M-CSF; Miltenyi Biotec BV, Leiden, Netherlands), and M1 macrophages were obtained by using 5 ng/ml GM-CSF (Miltenyi Biotec BV, Leiden, Netherlands) (Verreck et al., 2006). All cell types were incubated at 37 °C / 5 % CO2 in Roswell Park Memorial Institute (RPMI) 1640 medium supplemented with 10 % fetal bovine serum (FBS), 100 units/ml penicillin, and 100 µg/ml streptomycin, and 2mM GlutaMAX (Gibco, Thermo Fisher Scientific, Bleiswijk, Netherlands). MDDCs were harvested by pipetting the medium, and macrophages were harvested with trypsinization (Trypsin-EDTA 0.05 %, phenol red, Gibco, Thermo Fisher Scientific, Bleiswijk, Netherlands).

2.5 LysoSensor acidification assay

To quantify the acidification of acidic cellular compartments LysoSensor green (DND-189 dye) was used (Thermo Fisher Scientific, Bleiswijk, Netherlands). Briefly, MDDCs (30,000 cells/well) in round-bottom 96-well plates (CELLSTAR, Greiner Bio-One GmbH, Frickenhausen, Germany) were treated with empty liposomes (250 µg/ml lipids, in 200 µl medium) and incubated for 2.5 h at 37 ˚C / 5 % CO_2. Subsequently, cells were washed with a medium. 10 µM chloroquine (Sigma-Aldrich, Zwijndrecht, the Netherlands) was used as a control and it was added after washing. Afterwards, cells were incubated overnight at 37 ˚C / 5 % CO_2. The following day the LysoSensor (1 µM in 200 µl medium) dye was added to the cells and incubated for 30 min

at 37 ˚C / 5 % CO_2. Measurement of flow cytometry data was carried out using a BD FACSLyric Flow Cytometer (BD Biosciences, Erembodegem, Belgium). Data were analyzed using FlowJo (version 10.6, FlowJo LLC, BD, USA) software.

2.6 DQ-OVA antigen processing assay

To evaluate antigen processing, MDDCs (30,000 cells/well) in round-bottom 96-well plates (CELLSTAR, Greiner Bio-One GmbH, Germany) were treated with either 5 µg/ml DQ™-Ovalbumin (DQ-OVA, Invitrogen, ThermoFisher Scientific, Bleiswijk, Netherlands) or liposomes containing 5 µg/ml DQ-OVA and 250 µg/ml lipids (assuming no lipid loss during extrusion) in a total volume of 200 µL medium. Cells were incubated at 37 °C with 5 % CO_2 for 1 hour. The DQ fluorophore concentration in each liposomal formulation was quantified by measuring fluorescence intensity (excitation at 490 nm, emission at 520 nm) using an Infinite M1000 microplate reader (Tecan Austria GmbH, Grodig, Austria). To standardize fluorophore concentrations, samples were diluted to match the fluorescence intensity of the DOPC:DOPE (3:5:2:4) formulation. Lipid concentration was kept consistent across all samples by adjusting with buffer and corresponding unloaded liposomal formulations. DQ-OVA, a fluorogenic substrate labeled with BODIPY dyes, exhibits fluorescence quenching that is relieved upon protease-mediated hydrolysis, resulting in the production of brightly fluorescent dye-labeled peptides. Flow cytometry data were collected using a BD FACSLyric Flow Cytometer (BD Biosciences, Erembodegem, Belgium) and analyzed with FlowJo software (version 10.6, FlowJo LLC, Ashland, OR, USA).

2.7 Activation and viability of MDDCs

Cellular viability and adjuvant properties of empty and AER-containing liposomes were evaluated using MDDCs as described previously [39]. The liposome suspensions were added in round-bottom 96-well plates (CELLSTAR, Greiner Bio-One GmbH, Frickenhausen, Germany), seeded with 30,000 MDDCs/well (25 – 250 µg/ml lipids, in 200 µl medium), and incubated for 1 h at 37 ˚C / 5 % CO_2. Afterward, the cells were washed with a complete RPMI medium to remove free liposomes and cultured overnight at 37 °C / 5 % CO_2. The next day, the cells were centrifuged, and the supernatants were harvested and kept at -20 ˚C till further use. For flow cytometry analysis, the cells were first washed with FACS buffer (PBS containing 0.1 % bovine serum albumin; Merck, Amsterdam, Netherlands) and incubated for 5 min with 5 % human serum (Sanquin Blood Bank, Amsterdam, Netherlands) in PBS to block

non-specific Fc-receptor binding. Subsequently, the cells were washed, and the cell surface markers on the MDDCs were stained with monoclonal antibodies for 30 min. We used antibodies CCR7-BB515 (clone 3D12), CD83-PE (clone HB15e), CD40-APC (clone 5C3), CD80-APC-R700 (clone L307.4), HLA-DR-V500 (clone G46-6) from BD Biosciences, Belgium, and CD86-BV421 (clone IT2.2) from BioLegend, Amsterdam, Netherlands, all diluted 1:200 in FACS buffer. Subsequently, the cells were washed and stained with SYTOX AADvanced Dead Cell Stain (Invitrogen, Thermo Fisher Scientific, Bleiswijk, Netherlands) diluted 1:2000 in FACS buffer. Viability was calculated as a percentage of SYTOX AADvanced -negative cell population in relation to all recorded cells. Acquisition of flow cytometry data was performed using a BD FACSLyric Flow Cytometer (BD Biosciences, Erembodegem, Belgium). Data were analyzed using FlowJo (version 10.6, FlowJo LLC, Ashland, OR, USA) software.

2.8 Liposomal uptake study

To evaluate cellular uptake of liposomes, MDDCs, M1, or M2 macrophages were seeded in round-bottom 96-well plates with 30,000 cells/well as described previously.[39] Afterwards, the cells were exposed to 1 % v/v empty fluorescent-labeled liposomes (containing 0.1 mol% of 1,2-dioleoyl-sn-glycero-3-phosphoethanolamine-N-(Cyanine 5) (18:2 PE-Cy5) Avanti Polar Lipids, Inc., Alabaster, AL, USA) for 1 h. Subsequently, the cells were washed with FACS buffer 3 times to remove free liposomes. The acquisition of flow cytometry data was performed using a BD FACSLyric Flow Cytometer. Data were analyzed using FlowJo (version 10.6) software.

2.9 T-cell activation

HLA-DR3$^+$, heterozygous MDDCs were exposed with liposomes for 1 h (5 µg/ml AER and 250 µg/ml lipids) in 200 µl RPMI (Gibco, Thermo Fisher Scientific, Bleiswijk, the Netherlands) + 10 % FBS (Hyclone, Cytiva, Medemblik, The Netherlands) as described previously.[39] Cells were washed twice and 2x10^4 liposome-treated HLA-DR3$^+$ MDDCs were cocultured with either 1x10^5 Rv2034-specific[40] T-cells (1B4 clone recognizing peptide 75-105) or Ag85B-specific[41] T-cells (L10B4 clone recognizing peptide 56-65) in a 5 ml Falcon tube in a total volume of 400 µl IMDM supplemented with Glutamax, 100 U/ml penicillin, 100 µg/ml streptomycin (Gibco, Thermo Fisher Scientific, Bleiswijk, the Netherlands) and 10 % pooled human serum (Sigma, Merck, Darmstadt, Germany). After 6 h Brefeldin-A was added (3 µg/ml) (Sigma, Merck, Darmstadt, Germany) and cells were incubated for additional 16 h. Subsequently,

cells were harvested and stained for flow cytometric analysis with the violet live/dead stain (ViViD, Invitrogen, Thermo Fisher Scientific, Bleiswijk, Netherlands), surface markers CD3-HorizonV500 (UCHT1, BD Horizon, Erembodegem, Belgium), CD4-AlexaFluor 700 (RPA-T4, BD Pharmingen, Belgium), CD8-FITC (HIT8a, BioLegend, Amsterdam, Netherlands) and after fixation and permeabilization with fix/perm reagents (Nordic MUbio, Susteren, the Netherlands) for IFN-Y-PerCP-Cy5.5 (4S.B3, Invitrogen, Thermo Fisher Scientific, Bleiswijk, Netherlands) and CD154-PE (TRAP1, BD Pharmingen, Erembodegem, Belgium).

2.10 IL-12p40 and IL-10 enzyme-linked immunosorbent assay (ELISA)

Production of IL-12p40 and IL-10 by MDDCs exposed to liposomal formulations was tested using supernatants from activation and viability experiments. Biolegend's ELISA MAX Standard Set (London, UK) was used to carry out ELISA assays for human IL-12/IL-23 (p40) and human IL-10. All supernatants were tested in duplicates following the manufacturer's instructions. The assays were performed using Microlon high binding 96-well plates (Greiner Bio-One International, Alphen aan den Rijn, Netherlands), and the absorbance of the samples was measured using a Spectramax i3x spectrometer (Molecular Devices, San Jose, CA, USA).

2.11 Luminex assay

Supernatants were tested in two Bio-Plex panels (Bio-Rad, Veenendaal, the Netherlands) according to the manufacturer's protocols. In total 16 analytes were measured. The chemokine panel consisted of CXCL9, CXCL11, CCL8, and CCL22. The cytokine panel included CCL11 (Eotaxin), GM-CSF, IFN-α2, IL-1β, IL-1rα, IL-6, CXCL10, CCL2(MCP-1), CCL3, CCL4, RANTES and TNF-α. Samples were acquired on a Bio-Plex 200 system and analyzed with Bio-Plex manager software version 6.1.

2.12 Statistical analysis

Statistical analyses were performed in GraphPad Prism, version 8.01 (GraphPad Software, Prism, San Diego, CA, USA). The results were analyzed with the Kruskal-Wallis test followed by an uncorrected Dunn's post-hoc test when comparing non-parametric data sets of three or more groups to the control group, where $P < 0.05$ was considered as statistically significant (*$P < 0.05$, **$P < 0.01$, ***$P < 0.001$, ****$P < 0.0001$). Wilcoxon matched-pairs signed rank test was performed when comparing two non-parametric data groups.

3. RESULTS

3.1 Preparation of pH-sensitive liposomes

pH-sensitive liposomes were prepared using the thin film hydration method. Initially, the liposomes were prepared empty (without the addition of AER protein). In total 11 different formulations were prepared, which can be divided into two types depending on the amphiphilic lipid used: DOBAQ-containing liposomes and CHEMS-containing liposomes. Moreover, in some of the formulations DOPE was incorporated as an additional pH-sensitive component that displays fusogenic properties at a pH lower than the physiological pH. DOTAP was used as a cationic lipid to introduce a positive charge and DOPC was used as a bilayer-forming zwitterionic lipid. The chemical structures of the used lipids are depicted in Figure S1. Liposomes had to meet arbitrarily set physicochemical selection criteria for further investigations: liposomes should form stable suspensions without visible aggregation and precipitation, Z-average hydrodynamic diameter should be below 200 nm, polydispersity index (PDI) below 0.3, and Zeta-potential between approximately +20 and +30 mV.

The physicochemical characteristics of all prepared liposomes are presented in Table 1. DOPE is a lipid that does not form stable bilayers and needs to be stabilized with other lipids to form stable liposomes. None of the formulations with DOPE but without DOPC met the size criterium: DOPE:DOBAQ:DOTAP 3:2:2 and 3:2:1, and DOPE:CHEMS:DOTAP 3:2:2 and 3:2:1 (Table 1). Additionally, the Zeta-potential of DOPE:DOBAQ:DOTAP 3:2:1 was too low, probably because it contained too little DOTAP. DOPE:CHEMS:DOTAP 3:2:1, and DOPC:DOPE:CHEMS:DOTAP 7:3:2:2 did not meet the Zeta-potential criterium. Their negative Zeta-potential could be caused by the high content of CHEMS which is negatively charged at physiological pH. To circumvent stability issues, we increased the content of DOPC to stabilize liposomes, increased the DOTAP content, and/or decreased the CHEMS content to increase Zeta-potential. All of the selected formulations (that met the selection criteria) had comparable characteristics: hydrodynamic Z-average diameter between 140 and 180 nm, PDI between 0.13 and 0.30, and Zeta-potential between 19 and 26 mV.

Table 1. Physicochemical properties of the selected formulations. The results represent mean ± SD. The number of batches n ≥ 3. Failed batches (marked with *) were prepared once, and SD represents the deviation of 3 measurements.

Formulation	Z-average size (nm)	PDI (-)	Zeta-potential (mV)
DOBAQ:DOTAP (1:1)	144 ± 4	0.30 ± 0.02	22.0 ± 0.2
DOPE:DOBAQ:DOTAP (3:2:2)*	>1000 ± 290	0.26 ± 0.05	13.0 ± 0.7
DOPE:DOBAQ:DOTAP (3:2:1)*	>1000 ± 50	0.69 ± 0.20	6.8 ± 0.5
DOPC:DOPE:DOBAQ:DOTAP (7:3:2:2)	143 ± 5	0.13 ± 0.01	19.6 ± 0.4
CHEMS:DOTAP (1:1)	144 ± 3	0.15 ± 0.02	26.5 ± 0.7
DOPE:CHEMS:DOTAP (3:2:2)*	260 ± 19	0.11 ± 0.10	16.1 ± 1.3
DOPE:CHEMS:DOTAP (3:2:1)*	218 ± 6	0.21 ± 0.10	-23.2 ± 0.4
DOPC:DOPE:CHEMS:DOTAP (7:3:2:2)*	159 ± 2	0.12 ± 0.02	-9.6 ± 2.6
DOPC:DOPE:CHEMS:DOTAP (9:3:2:4)	138 ± 2	0.15 ± 0.03	19.2 ± 0.8
DOPC:DOPE:DOBAQ:DOTAP (3:5:2:4)	185 ± 3	0.15 ± 0.02	19.4 ± 0.6
DOPC:DOPE:CHEMS:DOTAP (5:5:2:6)	167 ± 3	0.13 ± 0.04	21.8 ± 1.2
DOPC:cholesterol:DOTAP (3:1:1)	104 ± 6	0.23 ± 0.01	22.5 ± 2.5

3.2. Evaluation of pH-sensitive properties of prepared formulations

The selected liposomes were evaluated in various biological assays to assess their pH-sensitive properties in primary human MDDCs. To assess the pH-sensitive behavior of these formulations, the liposomes were loaded with self-quenched ovalbumin (DQ-OVA) which is used here as a reporter of antigen processing. DQ-OVA in its native form is dimly fluorescent. However, upon degradation self-quenching of the fluorophore is diminished and DQ-OVA becomes brightly fluorescent. The change of this fluorescence can be quantified with flow cytometry. While classical liposomes and their cargo are degraded inside endosomes, pH-sensitive liposomes can protect themselves and therefore protect their cargo from degradation by escaping endosomes. As a control liposome formulation, we used DOPC:cholesterol:DOTAP 3:1:1. We selected this formulation because it is a non-pH-sensitive formulation that contains a comparable amount of DOTAP as the pH-sensitive liposomes. Also, we included cholesterol to account for possible effects of CHEMS used in some of the pH-sensitive liposomes that are associated with its cholesterol-like structure. The results of this assay are depicted in Figure 1a. Free DQ-OVA is freely processed

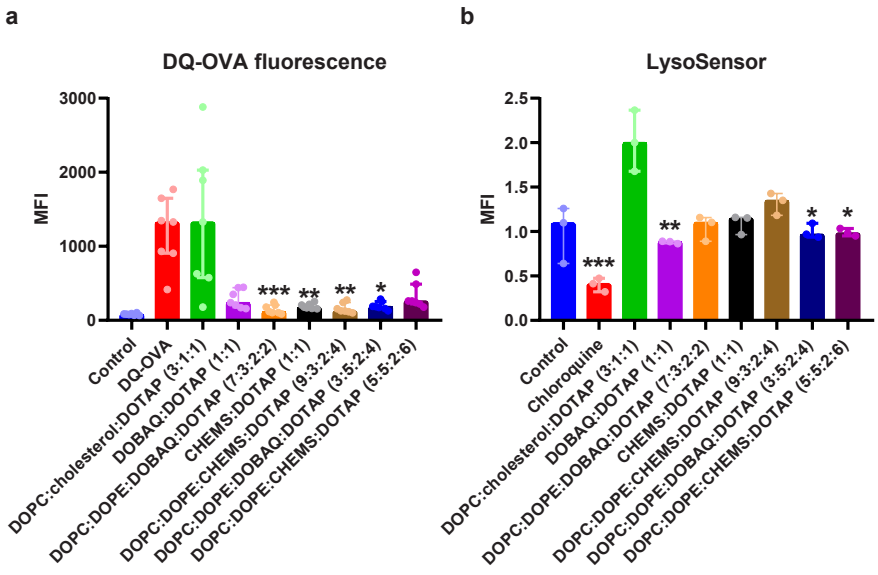

Figure 1. Evaluation of pH-sensitive properties of empty liposomal formulations in human monocyte-derived dendritic cells. (a) Endosomal protein degradation assessed using the DQ™-OVA reporter after 1-hour incubation at 5 µg/ml DQ-OVA (in solution or liposomes) and 250 µg/ml lipids (assuming no lipid loss). Lipid ratios are given as molar ratios. Median fluorescence intensities (MFIs) reflect DQ-OVA intensities, with comparisons made to DOPC:cholesterol:DOTAP (3:1:1). n=7 donors. (b) Cellular acidification measured by the LysoSensor assay. Cells were stimulated for 2.5 hours with liposomes, followed by a 30-minute incubation with LysoSensor the next day. MFIs, normalized to control for donor variability, indicate the reporter intensities. n=3 donors. All results are shown as median ± IQR. Statistical analysis was performed using the Kruskal-Wallis test with uncorrected Dunn's post-hoc test; significance was set at $P < 0.05$ (*$P < 0.05$, **$P < 0.01$, ***$P < 0.001$, ****$P < 0.0001$).

by the MDDCs which is indicated by high fluorescence values. In comparison, the fluorescence of all the selected pH-sensitive liposomes is much lower and in the case of four pH-sensitive formulations, the decrease of fluorescence values was statistically significant in comparison to DOPC:cholesterol:DOTAP 3:1:1. The pH-sensitive properties were also studied with the LysoSensor assay (Figure 1b). LysoSensor assay indicates a decrease in pH inside acidic organelles like lysosomes by an increase in fluorescence intensity of the fluorescent assay reporter. Similarly, the increase in pH is indicated by the decrease in fluorescence. As mentioned, a property of pH-sensitive liposomes is their capability to interfere with the acidification of lysosomes. In this assay, all formulations displayed a pH-buffering effect, which is indicated by the fluorescence that is at the level of the medium control, whereas the control

formulation (DOPC:cholesterol:DOTAP 3:1:1) does not display these properties and this resulted in an increase of the signal. This corresponds to a decrease in pH inside the acidic organelles of MDDCs. To validate the performance of this assay, we used chloroquine which is known to cause an increase in pH within the cells.[42–44] As expected, we observed a significant reduction of the reporter signal in cells treated with chloroquine, which corresponds to increased pH with respect to the medium control. Thus, we demonstrated that the prepared formulations display important properties of pH-sensitive liposomes in the context of vaccination: protection of the antigen from degradation, and disruption of acidification inside endosomes. Non-pH-sensitive liposomes did not display such properties.

3.3 Assessment of uptake, expression of surface activation markers, and viability

The uptake of pH-sensitive formulations was assessed with fluorescently labeled liposomes using MDDCs, M1 (pro-inflammatory), and M2 (anti-inflammatory) macrophages (Figure 2a), which all are antigen-presenting cells (APCs). An increase in median fluorescence intensity is associated with higher uptake of a formulation. The results obtained with MDDCs and both types of macrophages were very comparable. Formulations DOBAQ:DOTAP (1:1), DOPC:DOPE:DOBAQ:DOTAP (7:3:2:2), and DOPC:DOPE:CHEMS:DOTAP (9:3:2:4) were poorly taken up by all tested APCs. Formulation CHEMS:DOTAP (1:1) was moderately taken up, whereas DOPC:DOPE:CHEMS:DOTAP (5:5:2:6) was taken up more by macrophages than MDDCs, although still less effectively than control cationic liposomal formulation (DOPC:chol:DOTAP 3:1:1). The most efficient uptake of pH-sensitive formulation was observed using DOPC:DOPE:DOBAQ:DOTAP (3:5:2:4). It showed the highest uptake in all APCs. All formulations were more taken up by M1 macrophages compared to the other APCs, as indicated by higher median fluorescence values.

Furthermore, the ability of the pH-sensitive liposomal formulations to activate MDDCs was also tested. Most of the tested pH-sensitive formulations were unable to induce measurable activation of MDDCs, as indicated by the lack of increase of activation marker expression in comparison to the medium-only control (Figure 2b, Supplementary Figure S2 and S4). Only DOBAQ:DOTAP (1:1) induced upregulation of activation markers that was significantly different from the negative control condition and as high as or higher than the positive control condition. All cell surface markers except CD80 were upregulated by the DOBAQ:DOTAP (1:1) formulation.

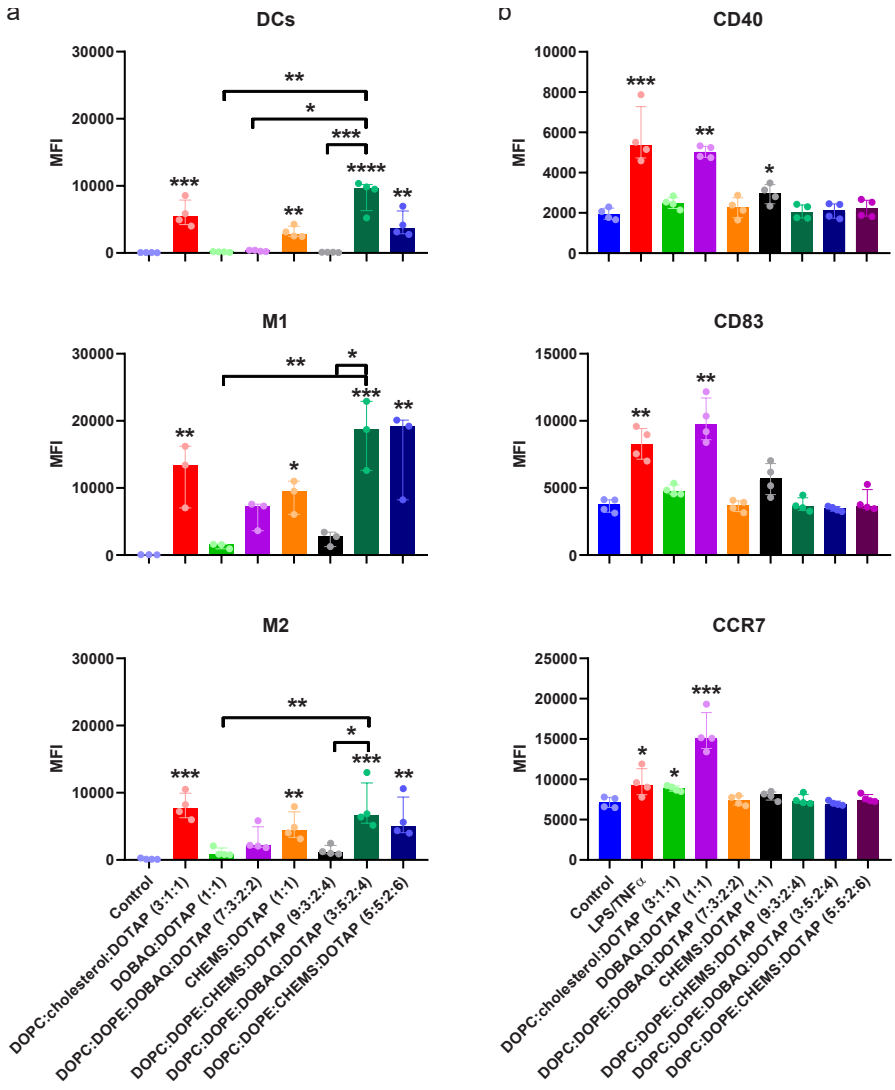

Figure 2. Influence of lipid composition on the uptake of empty liposomes and expression of cell surface activation markers in human monocyte-derived dendritic cells (DCs) and macrophages (M1 and M2). (a) Uptake of Cy5-labeled empty liposomes. Cells were incubated with 1 % v/v liposomes for 1 hour, followed by washing. Median fluorescence intensity (MFI) reflects Cy5 uptake in DCs (n=4), M1 macrophages (n=3), and M2 macrophages (n=4 donors). (b) Expression of activation markers CD40, CD83, and CCR7, shown as MFI. Cells were incubated with 250 µg/ml liposomes (assuming no lipid loss) for 1 hour (n=4 donors). Formulations were compared to a medium-only control unless otherwise specified. Results are presented as median ± interquartile range. Statistical analysis was conducted using the Kruskal-Wallis test with uncorrected Dunn's post-hoc test, with significance at $P < 0.05$ (*$P < 0.05$, **$P < 0.01$, ***$P < 0.001$, ****$P < 0.0001$).

Additionally, the viability of MDDCs after exposure to the pH-sensitive liposomes was quantified (Supplementary Figure S3). In general, pH-sensitive liposomes did not affect the viability of MDDCs. The percentages of viable cells were consistently very similar to those of negative controls, which indicates very low cytotoxicity. Only DOBAQ:DOTAP (1:1) and CHEMS:DOTAP (1:1) formulations caused some decrease in viable cells that was statistically different from the control. However, the observed decrease in MDDCs viability was small. Production of IL-12p40 and IL-10 was quantified with ELISA assays. There was no difference in the cytokine concentrations in supernatants from activation experiments compared to the medium-only controls.

3.4 Optimization of pH-sensitive liposomes

To develop pH-sensitive formulations that are suitable for subunit vaccines, further optimization was necessary. An effective liposomal vaccine delivery system needs to be taken up efficiently and induce APC activation. None of the pH-sensitive formulations we developed met both of these criteria. To further optimize the liposomes we selected DOPC:DOPE:DOBAQ:DOTAP (3:5:2:4) as the starting point, because the formulation was most efficiently taken up in APCs, did not decrease the viability of MDDCs, and its pH-sensitive properties were excellent. The goal of this optimization was to improve adjuvanticity. For this reason, we replaced DOTAP with EPC (we knew from our unpublished work that it induces more activation in APCs), and we decided to incorporate cholesterol (which can improve the immunogenicity of liposomes without a need to change other components).[45–49] We prepared liposomes with 4 different compositions, including the originally selected one. We kept the ratio of DOPE to DOBAQ constant in all formulations, and we incorporated cholesterol at either 20 or 40 mol%. The composition of these liposomes and their physicochemical properties are presented in Table 3. We incorporated AER antigen

Table 3. Physicochemical properties of AER-containing optimized formulations. n≥3 (batches).

Formulation	Z-average size (nm)	PDI (-)	Zeta-potential (mV)
AER/DOPC:DOPE:DOBAQ:DOTAP (3:5:2:4)	160 ± 24	0.18 ± 0.06	20.8 ± 1.7
AER/DOPC:DOPE:DOBAQ:EPC (3:5:2:4)	125 ± 1	0.27 ± 0.01	19.3 ± 1.1
AER/DOPE:DOBAQ:cholesterol:EPC (10:4:11:3)	111 ± 1	0.25 ± 0.01	20.5 ± 0.3
AER/DOPE:DOBAQ:cholesterol:EPC (5:2:3:4)	124 ± 2	0.26 ± 0.01	15.9 ± 0.9

at this stage, so the batches could be directly used for T-cell activation assay. Subsequently, the selected pH-sensitive formulation and 3 new compositions were tested in MDDCs to evaluate if the ability to activate APCs was improved. The results are presented in Figure 3. All of the new formulations induced more activation in comparison to the original formulation but only AER/DOPC:DOPE:DOBAQ:EPC

(3:5:2:4) significantly outperformed the original formulation AER/DOPC:DOPE:DOBAQ:DOTAP (3:5:2:4). A statistically significant increase of expression of surface activation markers was observed for CD40, CD83, and CCR7. In the case of remaining markers, DOPC:DOPE:DOBAQ:EPC (3:5:2:4) induced upregulation of CD86 and HLA-DR that was significantly higher than the control but there was no statistical difference between the optimized and original formulations. CD80 was not upregulated by any of the formulations. Two optimized formulations that contained cholesterol (AER/DOPE:DOBAQ:cholesterol:EPC 10:4:11:3 and AER/DOPE:DOBAQ:cholesterol:EPC 5:2:3:4) induced less activation in comparison to the formulation that did not contain it (AER/DOPC:DOPE:DOBAQ:EPC 3:5:2:4).

The viability of the MDDCs after exposure to the formulations was quantified. All liposomes caused moderate cell death at higher concentrations (5 μg/ml AER, 250 μg/ml lipids) as indicated by viability percentage (Figure 4). On average, the newly developed formulations induced more cell death than the original formulation. Liposomes AER/DOPE:DOBAQ:cholesterol:EPC (10:4:11:3) and AER/DOPE:DOBAQ:cholesterol:EPC (5:2:3:4) tended to be more toxic than AER/DOPC:DOPE:DOBAQ:EPC (3:5:2:4) as the difference in viability observed at already 2 μg/ml AER.

In addition to the expression of activation markers and viability, we quantified cytokines and chemokines produced by MDDCs. Cytokines and chemokines induce immune responses in other cell types and allow the recruitment of certain immune cells. This can modify the induced immune responses and affect T-cell activation. We observed an increase in the production of several cytokines and chemokines (Figure 5). Formulation AER/DOPC:DOPE:DOBAQ:EPC (3:5:2:4) significantly upregulated production of 3 out of 16 cytokines measured:CCL3 (MIP1α), CCL4 (MIP1β), and TNFα. We also observed an increase in CCL2 (MCP1) and IL-1Ra production, but this was not statistically significant. The original formulation containing DOTAP, and two

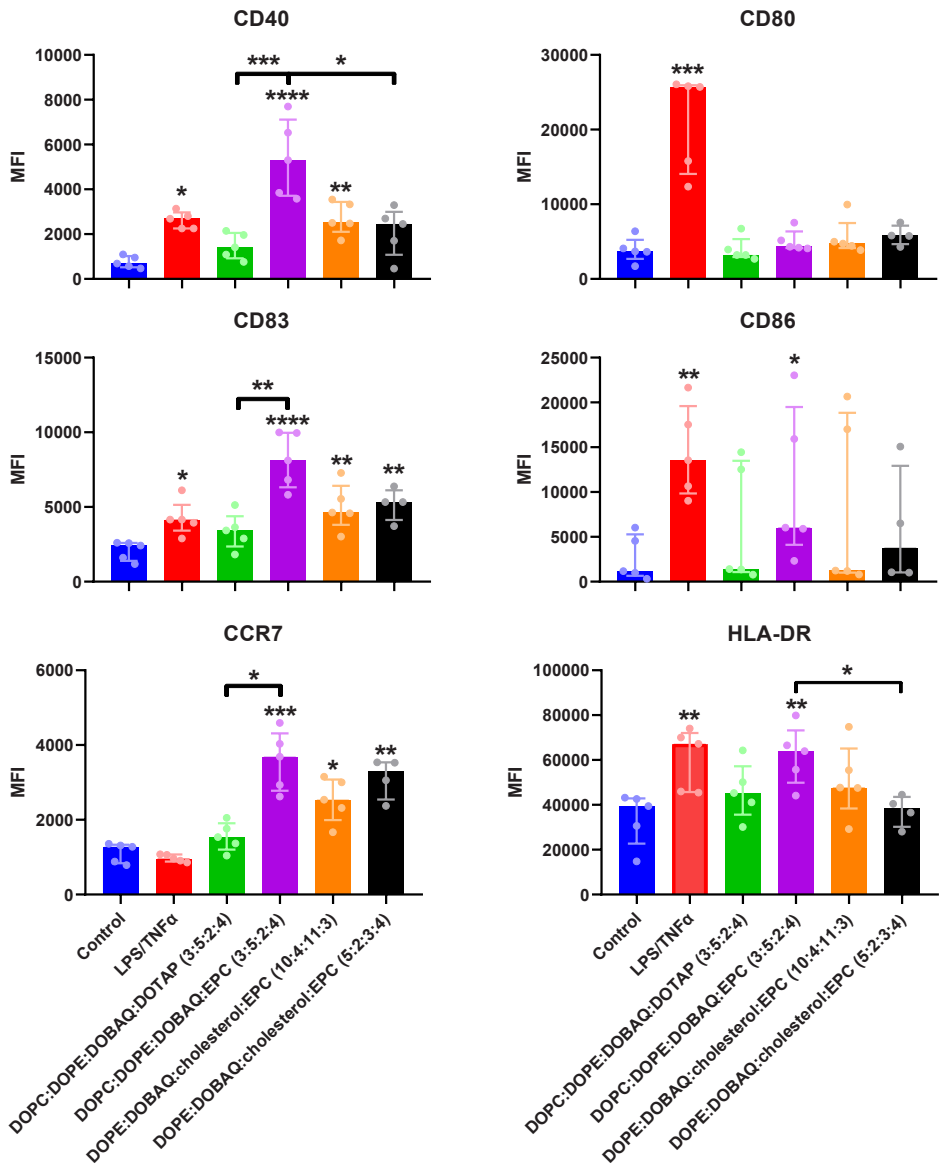

Figure 3. Upregulation of surface activation markers and viability of human monocyte-derived dendritic cells (DCs) following exposure to liposomal formulations loaded with Ag85B-ESAT6-RV2034 antigen for 1 hour. Cells were incubated with formulations containing 5 µg/ml antigen and 250 µg/ml lipids, with lipid ratios specified as molar ratios. Median fluorescence intensities (MFI) indicate expression of activation markers CD40, CD80, CD83, CD86, CCR7, and HLA-DR (n=5 donors). Unless otherwise indicated, formulations were compared to a medium-only control. Results are shown as median ± interquartile range. Statistical significance was determined using the Kruskal-Wallis test with uncorrected Dunn's post-hoc test, with thresholds set at $P < 0.05$ (*$P < 0.05$, **$P < 0.01$, ***$P < 0.001$, ****$P < 0.0001$).

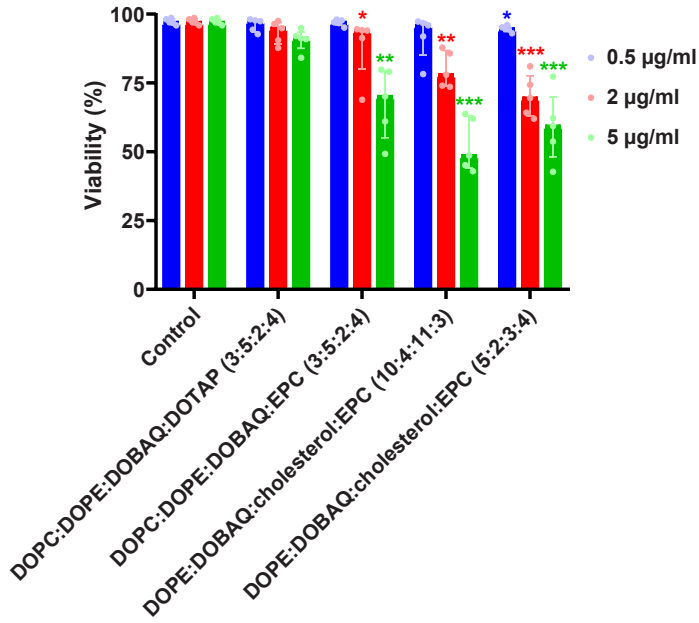

Figure 4. Viability of human monocyte-derived dendritic cells following 1-hour incubation with AER-loaded liposomal formulations. Viability was calculated as the percentage of SYTOX AADvanced-negative cells relative to the total cell population. Antigen concentrations are specified in the figure legend, with lipid concentrations at 50-fold higher than the antigen. Lipid ratios are provided as molar ratios, n=5 donors. Results are shown as median ± interquartile range. Statistical analysis was performed using the Kruskal-Wallis test with uncorrected Dunn's post-hoc test, with significance thresholds at $P < 0.05$ (*$P < 0.05$, **$P < 0.01$, ***$P < 0.001$, ****$P < 0.0001$). Each formulation was compared to a medium-only control within its respective concentration group.

other formulations containing cholesterol did not induce significant upregulations of any of the cytokines. There was also no significant increase in IL-12p40 and IL-10 production as assessed by ELISA assays.

Lastly, the performance of the optimized pH-sensitive liposomes was tested in a T-cell activation study. We selected for this experiment formulation AER/DOPC:DOPE:DOBAQ:EPC (3:5:2:4) because it induced superior upregulation of activation markers (Figure 3) and caused little cell death. To evaluate the ability to induce activation of antigen-specific $CD4^+$ T-cell clones, we compared liposomes containing the antigen with empty formulations (Figure 6). We used a $CD4^+$ T-cell clone *in vitro* assay to demonstrate the ability of delivery systems to specifically activate T-cells. Furthermore, $CD4^+$ T-cells are crucial to efficiently control the

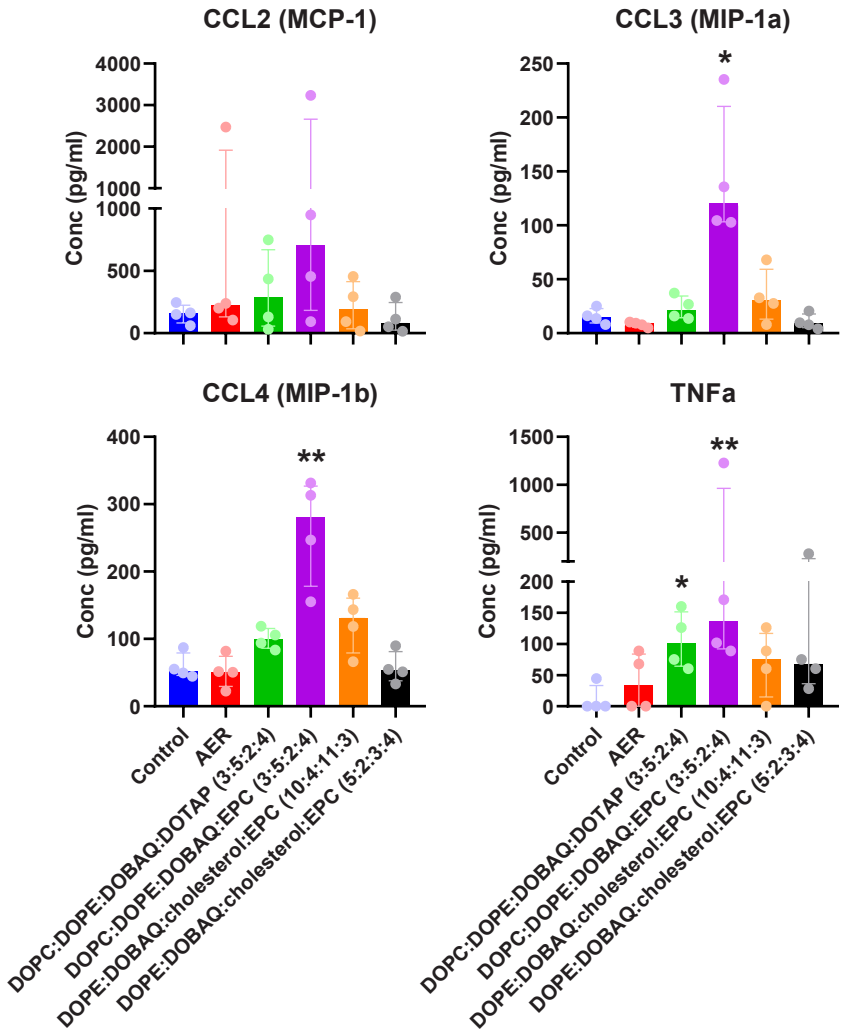

Figure 5. Cytokine production by human monocyte-derived dendritic cells after incubation with liposomal formulations. Cells were exposed to formulations containing 5 µg/ml antigen and 250 µg/ml liposomes for 1 hour (n=4 donors). Formulations were compared to a medium-only control. Results are presented as median ± interquartile range. Statistical significance was assessed using the Kruskal-Wallis test with uncorrected Dunn's post-hoc test, with thresholds at $P < 0.05$ (*$P < 0.05$, **$P < 0.01$, ***$P < 0.001$, ****$P < 0.0001$).

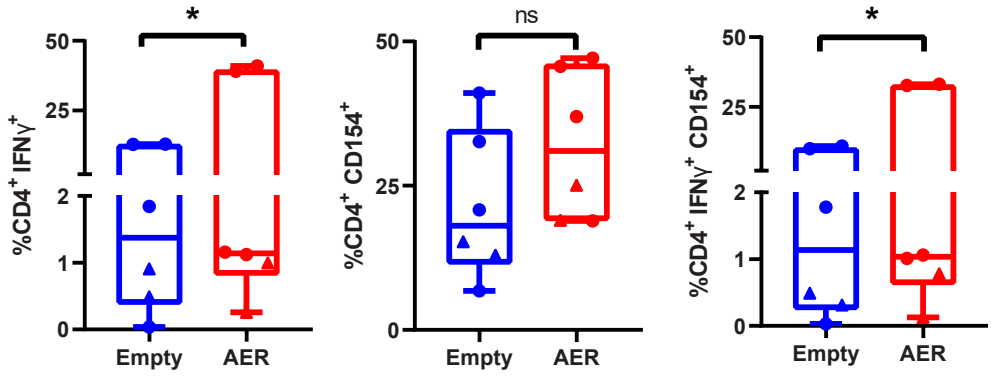

Figure 6. T-cell activation as indicated by the percentage of $CD4^+$ T-cells secreting IFNγ, expressing CD154, or co-expressing IFNγ and CD154 following exposure to empty (without AER antigen) or AER-loaded DOPC:DOPE:DOBAQ liposomes (molar ratio 3:5:2:4) at 5 µg/ml lipids for 1 hour. Circles represent $CD4^+$ T-cell clone L10B4 (specific for Mtb antigen Ag85B peptide 56-65), and triangles represent $CD4^+$ T-cell clone 1B4 (specific for Rv2034 peptide 75-105), with n=6 donors (HLA-$DR3^+$ heterozygous monocyte-derived dendritic cells). Graphs show median ± interquartile range. Statistical comparisons were made using the Wilcoxon matched-pairs signed rank test, with significance thresholds at $P < 0.05$ (*$P < 0.05$, **$P < 0.01$, ***$P < 0.001$, ****$P < 0.0001$).

intracellular pathogen Mtb.[50–52] We observed that antigen-containing liposomes induced significantly higher activation of $CD4^+$ T-cells as indicated by the percentage of cells expressing intracellular IFNγ and $IFN\gamma^+CD154^+$ but not $CD154^+$ alone.

In conclusion, optimized liposome DOPC:DOPE:DOBAQ:EPC (3:5:2:4) overcame the limitations of the previous formulation. It induced significantly higher expression of cell surface activation markers CD40, CD83, and CCR7 compared to the original liposome. The viability of MDDCs after exposure to the liposome decreased when higher concentrations were used. Secretion of cytokines CCL3 (MIP1α), CCL4 (MIP1β), and TNFα was elevated compared to the medium control. HLA-DR3 MDDCs after exposure to DOPC:DOPE:DOBAQ:EPC (3:5:2:4) induced significantly higher activation of antigen-specific $CD4^+$ T-cell clones.

4. DISCUSSION

pH-sensitive liposomes are widely investigated in medical applications such as chemotherapy, immunotherapy, diagnostics, and intracellular drug delivery.[17,53,54] Their unique properties allow for pH-specific release of the delivered cargo, making them an attractive delivery system. In vaccine research, pH-sensitive liposomes are promising for cytosolic delivery and improving $CD8^+$ T-cell responses.

$CD8^+$ T-cells are essential for controlling long-term Mtb infection, both through direct bacterial control and by supporting $CD4^+$ T-cell responses. Inducing Mtb-specific $CD8^+$ T-cells could enhance protective immunity.[5,55,56] Evidence from adoptive transfer,[57] antibody depletion,[58–60] and knockout studies[61–63] demonstrated the necessity of $CD8^+$ T-cells in infection control. Their depletion increased bacterial replication during latency.[64] Additionally, Mtb-specific $CD8^+$ T cell lines can lyse infected macrophages and restrict Mtb growth.[65,66] In animal models, including macaques[67–72] and cattle,[73,74] $CD8^+$ T-cells were vital to Mtb immunity. In humans, $CD8^+$ T-cell function decreased in active TB, both systemically[75] and at infection sites,[76] with a higher antigen burden linked to dysfunction.[77–79] Distinct $CD8^+$ T-cell phenotypes between TB and LTBI subjects,[77,80] especially Mtb-specific $CCR7^-$ $CD45RA^+$ cells, were associated with Mtb control.[81] This evidence underscores $CD8^+$ T-cells as key players in host immunity against Mtb.

$CD8^+$ T-cell responses can be induced by APCs via several pathways including cross-presentation through MHC-class Ia, Ib, and II molecules. Cross-presentation occurs through the cytosolic processing of antigens by proteasomes.[82,83] Protein antigens are typically processed in the endosome compartment, which favors MHC class II antigen presentation that leads to the induction of $CD4^+$ T-cell responses.[31,32] pH-sensitive liposomes can facilitate class I presentation by pH-dependent endosomal escape and delivery of the antigen to the cytosol.

Existing literature on pH-sensitive liposomes shows a significant focus on their application in cancer chemotherapy, immunotherapy, and cancer vaccines, with limited research in the field of vaccines against infectious diseases.[11,17,23,84–86] In the field of TB, three studies are reported in literature where liposomes DOTAP:DOPE (1:1), and/or (egg) PC:DOTAP:DOPE (2:1:1) were used to deliver heat shock 65 plasmid DNA antigen for TB vaccination.[87–89] However, the pH-sensitive properties of these

formulations were not assessed in these studies, and these formulations were not presented as pH-sensitive. Probably these formulations exhibit pH-sensitive properties based on DOPE content.

Delivery of protein-based antigens by pH-sensitive liposomes for vaccination against infectious diseases has not been extensively studied to date. Hence, we wanted to explore this topic for TB vaccination. Several formulations of liposomes that should exhibit such properties due to the incorporation of amphiphilic (CHEMS and DOBAQ) and/or fusogenic (DOPE) lipids were prepared. All pre-selected formulations had similar physicochemical properties (Z-average size, PDI, and Zeta-potential), but varied in their immunological effect. It is unlikely that the observed differences *in vitro* can be attributable to those properties.

Efficient uptake and activation in APCs are crucial for the performance of vaccine delivery systems. We evaluated uptake and activation using MDDCs and macrophage models. DOPC:DOPE:DOBAQ:DOTAP (3:5:2:4) was the most efficiently taken up in MDDCs, M1, and M2 MDMFs, while other formulations were poorly taken up. The majority of the tested formulations failed to upregulate the markers except for DOBAQ:DOTAP (1:1), which induced upregulations in all markers except for CD80. This observation can be explained by the high content of positively charged DOTAP, which is known to cause the activation of DCs.[49,90–93] CHEMS:DOTAP (1:1) liposomal formulation was not efficient probably because CHEMS in contrast to DOBAQ is negatively charged at neutral pH. Therefore, the choice of amphiphilic lipids greatly affected the uptake and activation of MDDCs *in vitro*.

We chose the DOPC:DOPE:DOBAQ:DOTAP (3:5:2:4) formulation based on its efficient uptake and pH-sensitive properties, but it did not effectively activate MDDCs. To improve its immunological effect, we substituted DOTAP with EPC, which we found to be a more potent immune activator in our previous work.[39]

Re-evaluation of MDDCs activation using new formulations showed that DOPC:DOPE:DOBAQ:EPC (3:5:2:4) induced the strongest activation, upregulating all markers except CD80 significantly more than the original formulation. This supports our findings that EPC is a more potent immune activator than DOTAP.[39] Surprisingly, cholesterol-containing formulations were less effective in activating MDDCs, contrary to our previous findings, and other publications[45–49] which showed that cholesterol-containing liposomes show an increased uptake by APCs and subsequently such

liposomes are more effective in activating immune cells. However, in a study by Nakano et al., cholesterol was shown to negatively affect the adjuvanticity of liposomes containing various PE lipids, leading to reduced antigen-specific IgG and preventing IgE production.[94] This suggests that cholesterol in PE-containing liposomes may have a negative effect on APC activation, leading to diminished adaptive immune responses *in vivo*, which might not occur in PE-free liposomes.

Cytokines and chemokine production is crucial for the effective induction of immunity. DOPC:DOPE:DOBAQ:EPC (3:5:2:4) showed the most upregulation in the production of cytokines and chemokines, including CCL3, CCL4, CCL2, IL-1Ra, and TNFα. CCL3 is a chemokine that induces Th1 responses.[95,96] It is essential for the maturation, activation, and migration of DCs to draining lymph nodes. CCL3 depletion results in reduced IFNγ expression by antigen-specific T-cells as well as increased levels of IL-10.[97] Both CCL3 and CCL4 drive Th1 responses[98] by efficient chemoattraction of Th1 cells (but not Th2 cells) in a concentration-dependent manner.[99] They also attract recently activated T-cells[100] and $CD8^+$ T-cells.[101–104] It has been reported that TNFα influences maturation, and recruitment of DCs and activation of T-cells.[105] It has also been demonstrated that TNFα exhibits adjuvant-like properties against viral infections in various models.[106–108] The microenvironment created by the expression of these cytokines can be beneficial for driving protection against Mtb.[109]

MDDCs exposed to AER-containing DOPC:DOPE:DOBAQ:EPC (3:5:2:4) were able to significantly activate two T-cell lines, indicated by increased expression of $IFN\gamma^+$ and $CD154^+$ $IFN\gamma^+$ but not $CD154^+$ alone T-cells whereas the MDDCs exposed to the empty liposome did not induce IFNγ-producing $CD4^+$ $CD154^+$ T-cells. Thus pH-sensitive liposomes and specifically DOPC:DOPE:DOBAQ:EPC (3:5:2:4) formulation are capable of inducing maturation of human MDDCs and enabling these DCs to take up, process, and present two different epitopes to antigen-specific T-cells and induce their activation.

In studies using C57Bl/6 mice, we demonstrated that a DOPC:DOPE:DOBAQ (3:5:2:4)-based TB vaccine, administered subcutaneously with CpG oligonucleotide ODN1826 and monophosphoryl lipid A as molecular adjuvants and AER as the antigen, effectively protected mice against intranasal H37Rv Mtb infection. This was supported by reduced bacterial burdens in the spleen and lungs of infected mice.[110,111] The vaccine elicited robust immune responses, including polyfunctional $CD4^+$

and $CD8^+$ T-cell activation, which are crucial for Mtb control as discussed above. Additionally, after restimulation of splenocytes with AER, we observed activation of B-cell populations, marked by CD69 expression, along with high antigen-specific antibody titers. These findings underscore the vaccine's effectiveness and suggest its potential as a novel TB vaccine. Overall, this study provides valuable insights into the use of pH-sensitive liposomes as carriers for subunit vaccines against TB.

5. CONCLUSIONS

pH-sensitive liposomes are promising for vaccines, as they deliver antigens into the cytosol, bypassing endosomal degradation, and enhance cross-presentation—key for fighting intracellular pathogens like Mtb. This study explores the application of pH-sensitive liposomes for vaccination against TB. We employed a strategy of optimizing liposomal compositions formulated with the Mtb-derived antigen AER using human primary cells for pre-clinical research. We demonstrated the pH-sensitive properties of these formulations and evaluated their immunostimulatory capacities on human cells, including DCs, M1, and M2. The best-performing formulation was DOPC:DOPE:DOBAQ:EPC in a 3:5:2:4 molar ratio. Further research is needed to evaluate the efficacy of this formulation *in vivo* and to incorporate molecular adjuvants to optimize cytokine production induced by these liposomes.

ABBREVIATIONS

AER, Ag85B-ESAT6-Rv2034 antigen; APC, antigen-presenting cell; BCG, *Mycobacterium bovis* Bacillus Calmette–Guérin; CCL, chemokine (C-C motif) ligand; CCR7, C-C chemokine receptor type 7; CD, cluster of differentiation; CHEMS, cholesteryl hemisuccinate, CXCL, chemokine (C-X-C motif) ligand; DC, dendritic cell; DOBAQ, N-(4-carboxybenzyl)-N,N-dimethyl-2,3-bis(oleoyloxy)propan-1-aminium; DOPC, 1,2-dioleoyl-*sn*-glycero-3-phosphocholine; DOPE, 1,2-dioleoyl-sn-glycero-3-phosphoethanolamine; DOTAP, 1,2-dioleoyl-3-trimethylammonium-propane; EPC, 1,2-dioleoyl-*sn*-glycero-3-ethylphosphocholine; FBS, fetal bovine serum; GM-CSF, granulocyte-macrophage colony-stimulating factor; HLA, human leukocyte antigen; IFN, interferon; Ig, immunoglobulin, IL, interleukin; IQR, interquartile range; MACS, magnetic cell isolation; M-CSF, macrophage colony-stimulating factor; LAL, limulus amebocyte lysate; MDDC, monocyte-derived dendritic cell; MHC, major histocompatibility complex; Mtb, *Mycobacterium tuberculosis*; PAMP, pathogen-associated molecular pattern; PBMC, peripheral blood mononuclear cell; PCR,

polymerase chain reaction; PDI, polydispersity index; PE, phosphatidylethanolamine; PE-Cy5, 1,2-dioleoyl-*sn*-glycero-3-phosphoethanolamine-N-(Cyanine 5); PPD, protein purified derivative; TB, tuberculosis; Th1, type 1 helper T-cell; TLR, Toll-like receptor; TNF, tumor necrosis factor.

APPENDICES

Supplementary materials

ACKNOWLEDGMENTS

In memoriam professor Wim Jiskoot.

CREDIT AUTHOR STATEMENT

M.M. Szachniewicz: Conceptualization, Methodology, Formal Analysis, Investigation, Writing – Original Draft. **K.E. van Meijgaarden**: Conceptualization, Methodology, Formal Analysis, Investigation, Writing – Review & Editing, Supervision. **E. Kavrik**: Methodology, Formal Analysis, Investigation. **K.L.M.C. Franken**: Methodology, Investigation, Resources. **W. Jiskoot**: Conceptualization, Supervision. **J.A. Bouwstra**: Conceptualization, Writing – Review & Editing, Project Administration, Funding Acquisition, Supervision. **M.C. Haks**: Conceptualization, Supervision. **A. Geluk**: Conceptualization, Writing – Review & Editing, Project Administration, Funding Acquisition, Supervision. **T.H.M. Ottenhoff**: Conceptualization, Writing – Review & Editing, Project Administration, Funding Acquisition, Supervision.

FUNDING

This work was supported by the Dutch Research Council (NWO) Domain Applied and Engineering Sciences grant, project number: 15240

REFERENCES

1. World Health Organization. *Global Tuberculosis Report 2023*. (2023).
2. Fine, P. E. M. Variation in protection by BCG: implications of and for heterologous immunity. *The Lancet* 346, 1339–1345 (1995).
3. Rodrigues, L. C. *et al.* Protective effect of BCG against tuberculous meningitis and miliary tuberculosis: A meta-analysis. *International Journal of Epidemiology* 22, 1154–1158 (1993).
4. Trunz, B. B. *et al.* Effect of BCG vaccination on childhood tuberculous meningitis and miliary tuberculosis worldwide: a meta-analysis and assessment of cost-effectiveness. *Lancet* 367, 1173–1180 (2006).
5. Ottenhoff, T. H. M. & Kaufmann, S. H. E. Vaccines against Tuberculosis: Where Are We and Where Do We Need to Go? *PLoS Pathogens* 8, e1002607 (2012).
6. Inglut, C. T. *et al.* Immunological and Toxicological Considerations for the Design of Liposomes. *Nanomaterials* 10.2: 190 (2020).
7. Akbarzadeh, A. *et al.* Liposome: Classification, preparation, and applications. *Nanoscale Research Letters* 8, 1–9 (2013).
8. Torchilin, V. P. Recent advances with liposomes as pharmaceutical carriers. *Nature Reviews Drug Discovery 2005 4:2* 4, 145–160 (2005).
9. Shah, S. *et al.* Liposomes: Advancements and innovation in the manufacturing process. *Advanced Drug Delivery Reviews* 154–155, 102–122 (2020).
10. Bozzuto, G. & Molinari, A. Liposomes as nanomedical devices. *International Journal of Nanomedicine* 10, 975 (2015).
11. Karanth, H. & Murthy, R. S. R. pH-Sensitive liposomes-principle and application in cancer therapy. *Journal of Pharmacy and Pharmacology* 59, 469–483 (2007).
12. Momekova, D. *et al.* Long-Circulating, pH-Sensitive Liposomes. *Methods in Molecular Biology* 1522, 209–226 (2017).
13. Zhuo, S. *et al.* pH-Sensitive Biomaterials for Drug Delivery. *Molecules* 25, (2020).
14. Mu, Y. *et al.* Advances in pH-responsive drug delivery systems. *OpenNano* 5, 100031 (2021).
15. Balamurali, V. *et al.* pH Sensitive Drug Delivery Systems: A Review. *American Journal of Drug Discovery and Development* 1, 24–48 (2010).

16. Hamai, C. *et al.* Effect of Average Phospholipid Curvature on Supported Bilayer Formation on Glass by Vesicle Fusion. *Biophysical Journal* 90, 1241–1248 (2006).
17. Paliwal, S. R. *et al.* A review of mechanistic insight and application of pH-sensitive liposomes in drug delivery. *Drug delivery* 22:3, 231-242 (2015).
18. Connor, J. *et al.* pH-sensitive liposomes: acid-induced liposome fusion. *Proceedings of the National Academy of Sciences* 81, 1715–1718 (1984).
19. Siegel, D. P. & Epand, R. M. The mechanism of lamellar-to-inverted hexagonal phase transitions in phosphatidylethanolamine: implications for membrane fusion mechanisms. *Biophysical Journal* 73, 3089 (1997).
20. Lai, M. Z. *et al.* Effects of replacement of the hydroxyl group of cholesterol and tocopherol on the thermotropic behavior of phospholipid membranes. *Biochemistry* 24, 1646–1653 (1985).
21. Seddon, J. M. *et al.* Calorimetric studies of the gel-fluid (L beta-L alpha) and lamellar-inverted hexagonal (L alpha-HII) phase transitions in dialkyl- and diacylphosphatidylethanolamines. *Biochemistry* 22, 1280–1289 (1983).
22. Torchilin, V. P. *et al.* pH-Sensitive Liposomes. *Journal of Liposome Research* 3:2, 201-255 (1993).
23. Liu, X. & Huang, G. Formation strategies, mechanism of intracellular delivery and potential clinical applications of pH-sensitive liposomes. *Asian Journal of Pharmaceutical Sciences* 8, 319–328 (2013).
24. Moitra, P. *et al.* New pH-responsive gemini lipid derived co-liposomes for efficacious doxorubicin delivery to drug resistant cancer cells. *Chemical Communications* 53, 8184–8187 (2017).
25. Balazs, D. A. & Godbey, WT. Liposomes for use in gene delivery. *Journal of Drug Delivery* 2011, 1–12 (2011).
26. Yang, S. & May, S. Release of cationic polymer-DNA complexes from the endosome: A theoretical investigation of the proton sponge hypothesis. *Journal of Chemical Physics* 129, 185105 (2008).
27. Agirre, M. *et al.* Low Molecular Weight Chitosan (LMWC)-based Polyplexes for pDNA Delivery: From Bench to Bedside. *Polymers* 6:6, 1727-1755 (2014).
28. Dehshahri, A. *et al.* Gene transfer efficiency of high primary amine content, hydrophobic, alkyl-oligoamine derivatives of polyethylenimine. *Biomaterials* 30, 4187–4194 (2009).

29. Shigeta, K. *et al.* Novel histidine-conjugated galactosylated cationic liposomes for efficient hepatocyte-selective gene transfer in human hepatoma HepG2 cells. *Journal of Controlled Release* 118, 262–270 (2007).
30. Chang, J. S. *et al.* Development of Th1-mediated CD8+ effector T cells by vaccination with epitope peptides encapsulated in pH-sensitive liposomes. *Vaccine* 19, 3608–3614 (2001).
31. Fehres, C. M. *et al.* Understanding the biology of antigen cross-presentation for the design of vaccines against cancer. *Frontiers in Immunology* 5, 149 (2014).
32. Andersen, B. M. & Ohlfest, J. R. Increasing the efficacy of tumor cell vaccines by enhancing cross priming. *Cancer Letters* 325, 155–164 (2012).
33. Bungener, L. *et al.* Virosome-mediated delivery of protein antigens to dendritic cells. *Vaccine* 20, 2287–2295 (2002).
34. Bungener, L. *et al.* Virosome-mediated delivery of protein antigens in vivo: efficient induction of class I MHC-restricted cytotoxic T lymphocyte activity. *Vaccine* 23, 1232–1241 (2005).
35. Melero, I. *et al.* Therapeutic vaccines for cancer: an overview of clinical trials. *Nature Reviews Clinical Oncology* 11:9, 509–524 (2014).
36. Wang, C. *et al.* Self-adjuvanted nanovaccine for cancer immunotherapy: Role of lysosomal rupture-induced ROS in MHC class I antigen presentation. *Biomaterials* 79, 88–100 (2016).
37. Commandeur, S. *et al.* The in vivo expressed Mycobacterium tuberculosis (IVE-TB) antigen Rv2034 induces CD4+ T-cells that protect against pulmonary infection in HLA-DR transgenic mice and guinea pigs. *Vaccine* 32, 3580–3588 (2014).
38. Franken, K. L. M. C. *et al.* Purification of His-Tagged Proteins by Immobilized Chelate Affinity Chromatography: The Benefits from the Use of Organic Solvent. *Protein Expression and Purification* 18, 95–99 (2000).
39. Szachniewicz, M. M. *et al.* Intrinsic immunogenicity of liposomes for tuberculosis vaccines: Effect of cationic lipid and cholesterol. *European Journal of Pharmaceutical Sciences* 195, 106730 (2024).
40. Commandeur, S. *et al.* Clonal Analysis of the T-Cell Response to In Vivo Expressed Mycobacterium tuberculosis Protein Rv2034, Using a CD154 Expression Based T-Cell Cloning Method. *PLoS One* 9, e99203 (2014).

41. Geluk, A. *et al.* A DR17-restricted T cell epitope from a secreted Mycobacterium tuberculosis antigen only binds to DR17 molecules at neutral pH. *European Journal of Immunology* 27, 842–847 (1997).
42. Pascolo, S. Time to use a dose of Chloroquine as an adjuvant to anti-cancer chemotherapies. *European Journal of Pharmacology* 771, 139–144 (2016).
43. Savarino, A. *et al.* Effects of chloroquine on viral infections: an old drug against today's diseases. *Lancet Infectious Diseases* 3, 722–727 (2003).
44. Zou, L. *et al.* Hydroxychloroquine and chloroquine: a potential and controversial treatment for COVID-19. *Archives of Pharmacological Research* 43, 765–772 (2020).
45. Barnier-Quer, C. *et al.* Adjuvant effect of cationic liposomes for subunit influenza vaccine: Influence of antigen loading method, cholesterol and immune modulators. *Pharmaceutics* 5, 392–410 (2013).
46. Benne, N. *et al.* Atomic force microscopy measurements of anionic liposomes reveal the effect of liposomal rigidity on antigen-specific regulatory T cell responses. *Journal of Controlled Release* 318, 246–255 (2020).
47. Aramaki, K. *et al.* Charge boosting effect of cholesterol on cationic liposomes. *Colloids and Surfaces A: Physicochemical and Engineering Aspects* 506, 732–738 (2016).
48. Kaur, R. *et al.* Effect of incorporating cholesterol into DDA:TDB liposomal adjuvants on bilayer properties, biodistribution, and immune responses. *Molecular Pharmaceutics* 11, 197–207 (2014).
49. Henriksen-Lacey, M. *et al.* Comparison of the depot effect and immunogenicity of liposomes based on dimethyldioctadecylammonium (DDA), 3β-[N-(N',N'-dimethylaminoethane)carbomyl] cholesterol (DC-Chol), and 1,2-dioleoyl-3-trimethylammonium propane (DOTAP): Prolonged liposome retention mediates stronger Th1 responses. *Molecular Pharmaceutics* 8, 153–161 (2011).
50. Leveton, C. *et al.* T-cell-mediated protection of mice against virulent Mycobacterium tuberculosis. *Infection and Immunity* 57, 390–395 (1989).
51. Flory, C. M. *et al.* Effects of in vivo T lymphocyte subset depletion on mycobacterial infections in mice. *Journal of Leukocyte Biology* 51, 225–229 (1992).
52. Müller, I. *et al.* Impaired resistance to Mycobacterium tuberculosis infection after selective in vivo depletion of L3T4+ and Lyt-2+ T cells. *Infection and Immunity* 55, 2037–2041 (1987).

53. Slepushkin, V. A. *et al.* Sterically stabilized pH-sensitive liposomes. Intracellular delivery of aqueous contents and prolonged circulation in vivo. *Journal of Biological Chemistry* 272, 2382–2388 (1997).
54. Zamani, P. *et al.* MPL nano-liposomal vaccine containing P5 HER2/neu-derived peptide pulsed PADRE as an effective vaccine in a mice TUBO model of breast cancer. *Journal of Controlled Release* 303, 223–236 (2019).
55. Boom, W. H. New TB vaccines: is there a requirement for CD8+ T cells? *Journal of Clinical Investigation* 117, 2092–2094 (2007).
56. Behar, S. M. *et al.* Next generation: tuberculosis vaccines that elicit protective CD8+ T cells. *Expert Review of Vaccines* 6, 441–456 (2007).
57. Orme, I. M. The kinetics of emergence and loss of mediator T lymphocytes acquired in response to infection with Mycobacterium tuberculosis. *The Journal of Immunology* 138, 293–298 (1987).
58. Mogues, T. *et al.* The Relative Importance of T Cell Subsets in Immunity and Immunopathology of Airborne Mycobacterium tuberculosis Infection in Mice. *Journal of Experimental Medicine* 193, 271–280 (2001).
59. North, R. J. & Jung, Y. J. Immunity to Tuberculosis. *Annual Review of Immunology* 22:1, 599–623 (2004).
60. Woodworth, J. S. *et al.* Mycobacterium tuberculosis-Specific CD8+ T Cells Require Perforin to Kill Target Cells and Provide Protection In Vivo. *The Journal of Immunology* 181, 8595–8603 (2008).
61. Behar, S. M. *et al.* Susceptibility of Mice Deficient in CD1D or TAP1 to Infection with Mycobacterium tuberculosis. *Journal of Experimental Medicine* 189, 1973–1980 (1999).
62. Flynn, J. L. *et al.* Major histocompatibility complex class I-restricted T cells are required for resistance to Mycobacterium tuberculosis infection. *Proceedings of the National Academy of Sciences* 89, 12013–12017 (1992).
63. Sousa, A. O. *et al.* Relative contributions of distinct MHC class I-dependent cell populations in protection to tuberculosis infection in mice. *Proceedings of the National Academy of Sciences* 97, 4204–4208 (2000).
64. Van Pinxteren, L. A. H. *et al.* Control of latent Mycobacterium tuberculosis infection is dependent on CD8 T cells. *European Journal of Immunology* 30, 3689–3698 (2000).

65. Tan, J. S. *et al.* Human alveolar T lymphocyte responses to Mycobacterium tuberculosis antigens: role for CD4+ and CD8+ cytotoxic T cells and relative resistance of alveolar macrophages to lysis. *The Journal of Immunology* 159, 290–297 (1997).
66. Turner, J. & Dockrell, H. M. Stimulation of human peripheral blood mononuclear cells with live Mycobacterium bovis BCG activates cytolytic CD8+ T cells in vitro. *Immunology* 87, 339–342 (1996).
67. Lin, P. L. & Flynn, J. A. L. CD8 T cells and Mycobacterium tuberculosis infection. *Seminars in Immunopathology* 37, 239–249 (2015).
68. Silver, R. F. *et al.* Diversity of human and macaque airway immune cells at baseline and during tuberculosis infection. *American Journal of Respiratory Cell and Molecular Biology* 55, 899–906 (2016).
69. Gideon, H. P. *et al.* Variability in Tuberculosis Granuloma T Cell Responses Exists, but a Balance of Pro- and Anti-inflammatory Cytokines Is Associated with Sterilization. *PLoS Pathogens* 11, e1004603 (2015).
70. Lin, P. L. *et al.* CD4 T Cell Depletion Exacerbates Acute Mycobacterium tuberculosis While Reactivation of Latent Infection Is Dependent on Severity of Tissue Depletion in Cynomolgus Macaques. *AIDS Research and Human Retroviruses* 28, 1693–1702 (2012).
71. Lin, P. L. *et al.* Early events in Mycobacterium tuberculosis infection in cynomolgus macaques. *Infection and Immunity* 74, 3790–3803 (2006).
72. Lin, P. L. *et al.* Quantitative comparison of active and latent tuberculosis in the cynomolgus macaque model. *Infection and Immunity* 77, 4631–4642 (2009).
73. Villarreal-Ramos, B. *et al.* Investigation of the role of CD8+ T cells in bovine tuberculosis in vivo. *Infection and Immunity* 71, 4297–4303 (2003).
74. Palmer, M. V. *et al.* Lesion development and immunohistochemical changes in granulomas from cattle experimentally infected with Mycobacterium bovis. *Veterinary Pathology* 44, 863–874 (2007).
75. Smith, S. M. *et al.* Human CD8+ T cells specific for Mycobacterium tuberculosis secreted antigens in tuberculosis patients and healthy BCG-vaccinated controls in the Gambia. *Infection and Immunity* 68, 7144–7148 (2000).
76. Andersson, J. *et al.* Impaired expression of perforin and granulysin in CD8+ T cells at the site of infection in human chronic pulmonary tuberculosis. *Infection and Immunity* 75, 5210–5222 (2007).

77. Day, C. L. *et al.* Functional Capacity of Mycobacterium tuberculosis-Specific T Cell Responses in Humans Is Associated with Mycobacterial Load. *The Journal of Immunology* 187, 2222–2232 (2011).
78. Lancioni, C. *et al.* CD8+ T Cells Provide an Immunologic Signature of Tuberculosis in Young Children. *American Journal of Respiratory and Critical Care Medicine* 185:2, 206-212 (2012).
79. Lewinsohn, D. A. *et al.* Mycobacterium tuberculosis–specific CD8+ T Cells Preferentially Recognize Heavily Infected Cells. *American Journal of Respiratory and Critical Care Medicine* 168:11, 1346–1352 (2012).
80. Rozot, V. *et al.* Mycobacterium tuberculosis-specific CD8+ T cells are functionally and phenotypically different between latent infection and active disease. *European Journal of Immunology* 43, 1568–1577 (2013).
81. Bruns, H. *et al.* Anti-TNF immunotherapy reduces CD8+ T cell–mediated antimicrobial activity against Mycobacterium tuberculosis in humans. *Journal of Clinical Investigation* 119, 1167–1177 (2009).
82. Winau, F. *et al.* Apoptotic vesicles crossprime CD8 T cells and protect against tuberculosis. *Immunity* 24, 105–117 (2006).
83. Lin, M. & Ottenhoff, T. Host-Pathogen Interactions in Latent Mycobacterium tuberculosis Infection: Identification of New Targets for Tuberculosis Intervention. *Endocrine, Metabolic & Immune Disorders-Drug Targets* 8, 15–29 (2008).
84. Abri Aghdam, M. *et al.* Recent advances on thermosensitive and pH-sensitive liposomes employed in controlled release. *Journal of Controlled Release* 315, 1–22 (2019).
85. Ferreira, D. D. S. *et al.* pH-sensitive liposomes for drug delivery in cancer treatment. *Therapeutic Delivery* 4, 1099–1123 (2013).
86. Gupta, M, *et al.* pH-sensitive liposomes. *Liposomal Delivery Systems: Advances and Challenges* 1, 74–86 (2015).
87. Gaziola De La Torre, L. *et al.* The synergy between structural stability and DNA-binding controls the antibody production in EPC/DOTAP/DOPE liposomes and DOTAP/DOPE lipoplexes. *Colloids and Surfaces B: Biointerfaces* 73, 175–184 (2009).
88. Rosada, R. S. *et al.* Protection against tuberculosis by a single intranasal administration of DNA-hsp65 vaccine complexed with cationic liposomes. *BMC Immunology* 9, 1–13 (2008).

89. De Paula Rigoletto, T. *et al.* Effects of extrusion, lipid concentration and purity on physico-chemical and biological properties of cationic liposomes for gene vaccine applications. *Journal of microencapsulation* 29:8, 759–769 (2012).
90. Vasievich, E. A. *et al.* Trp2 peptide vaccine adjuvanted with (R)-DOTAP inhibits tumor growth in an advanced melanoma model. *Molecular Pharmaceutics* 9, 261–268 (2012).
91. Riehl, M. *et al.* Combining R-DOTAP and a particulate antigen delivery platform to trigger dendritic cell activation: Formulation development and in-vitro interaction studies. *International Journal of Pharmaceutics* 532, 37–46 (2017).
92. Yan, W. *et al.* Mechanism of adjuvant activity of cationic liposome: Phosphorylation of a MAP kinase, ERK and induction of chemokines. *Molecular Immunology* 44, 3672–3681 (2007).
93. Vangasseri, D. P. *et al.* Immunostimulation of dendritic cells by cationic liposomes. *Molecular Membrane Biology* 23, 385–395 (2006).
94. Nakano, Y. *et al.* Cholesterol Inclusion in Liposomes Affects Induction of Antigen-Specific IgG and IgE Antibody Production in Mice by a Surface-Linked Liposomal Antigen. *Bioconjugate Chemistry* 13, 744–749 (2002).
95. Annunziato, F. *et al.* Limited expression of R5-tropic HIV-1 in CCR5-positive type 1–polarized T cells explained by their ability to produce RANTES, MIP-1α, and MIP-1β. *Blood* 95, 1167–1174 (2000).
96. Canque, B. *et al.* Macrophage inflammatory protein-1alpha is induced by human immunodeficiency virus infection of monocyte-derived macrophages. *Blood* 87, 2011–2019 (1996).
97. Trifilo, M. J. & Lane, T. E. The CC chemokine ligand 3 regulates CD11c+CD11b+CD8α− dendritic cell maturation and activation following viral infection of the central nervous system: implications for a role in T cell activation. *Virology* 327, 8–15 (2004).
98. Nath, A. *et al.* Macrophage inflammatory protein (MIP)1α and MIP1β differentially regulate release of inflammatory cytokines and generation of tumoricidal monocytes in malignancy. *Cancer Immunology, Immunotherapy* 55, 1534–1541 (2006).
99. Siveke, J. T. & Hamann, A. Cutting edge: T helper 1 and T helper 2 cells respond differentially to chemokines. *The Journal of Immunology* 160:2, 550-554 (1998).

100. Sallusto, F. *et al.* Chemokines and chemokine receptors in T-cell priming and Th1/Th2-mediated responses. *Immunol Today* 19, 568–574 (1998).
101. Honey, K. CCL3 and CCL4 actively recruit CD8+ T cells. *Nature Reviews Immunology* 6, 427 (2006).
102. Castellino, F. *et al.* Chemokines enhance immunity by guiding naive CD8+ T cells to sites of CD4+ T cell-dendritic cell interaction. *Nature* 440, 890–895 (2006).
103. Wang, A. *et al.* CCL3 and CCL4 secretion by T regulatory cells attracts CD4+ and CD8+ T cells (P1077). *The Journal of Immunology* 190, 121.10-121.10 (2013).
104. Sektioglu, I. M. *et al.* Basophils promote tumor rejection via chemotaxis and infiltration of CD8+ T cells. *Cancer Research*`77, 291–302 (2017).
105. Calzascia, T. *et al.* TNF-α is critical for antitumor but not antiviral T cell immunity in mice. *Journal of Clinical Investigation* 117, 3833–3845 (2007).
106. Brunner, C. *et al.* Enhanced Dendritic Cell Maturation by TNF-α or Cytidine-Phosphate-Guanosine DNA Drives T Cell Activation In Vitro and Therapeutic Anti-Tumor Immune Responses In Vivo. *The Journal of Immunology* 165, 6278–6286 (2000).
107. Chen, Z. *et al.* Enhanced HER-2/neu-specific antitumor immunity by cotransduction of mouse dendritic cells with two genes encoding HER-2/neu and alpha tumor necrosis factor. *Cancer Gene Therapy* 9:9, 778–786 (2002).
108. Nimal, S. *et al.* Enhancement of immune responses to an HIV gp120 DNA vaccine by fusion to TNF alpha cDNA. *Vaccine* 24, 3298–3308 (2006).
109. Salgame, P. Host innate and Th1 responses and the bacterial factors that control Mycobacterium tuberculosis infection. *Current Opinion in Immunology* 17, 374–380 (2005).
110. Szachniewicz, M. M. *et al.* Evaluation of PLGA, lipid-PLGA hybrid nanoparticles, and cationic pH-sensitive liposomes as tuberculosis vaccine delivery systems in a Mycobacterium tuberculosis challenge mouse model – A comparison. *International Journal of Pharmaceutics* 666, 124842 (2024).
111. Szachniewicz, M. M. *et al.* Cationic pH-sensitive liposome-based subunit tuberculosis vaccine induces protection in mice challenged with Mycobacterium tuberculosis. *European Journal of Pharmaceutics and Biopharmaceutics* 203, 114437 (2024).

SUPPLEMENTARY MATERIALS

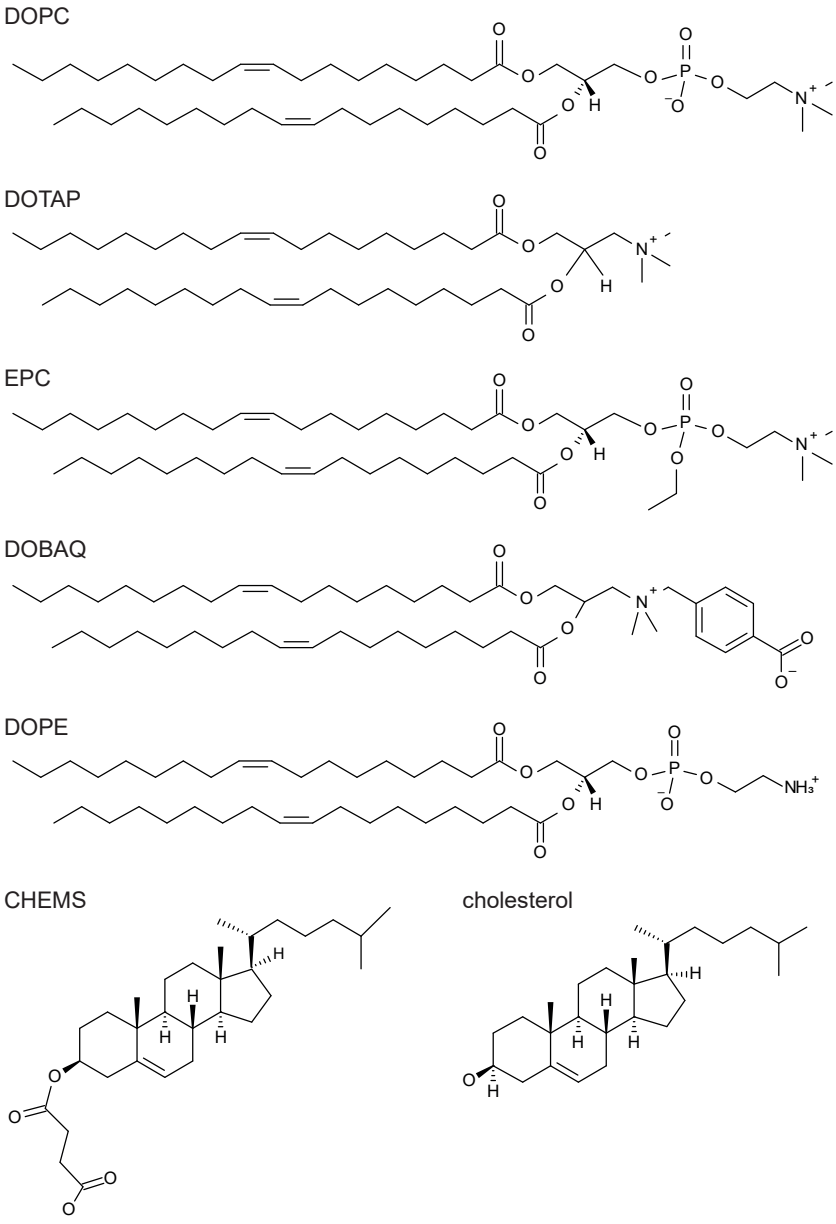

Supplementary Figure S1. Chemical structures of lipids used in production of pH-sensitive liposomes.

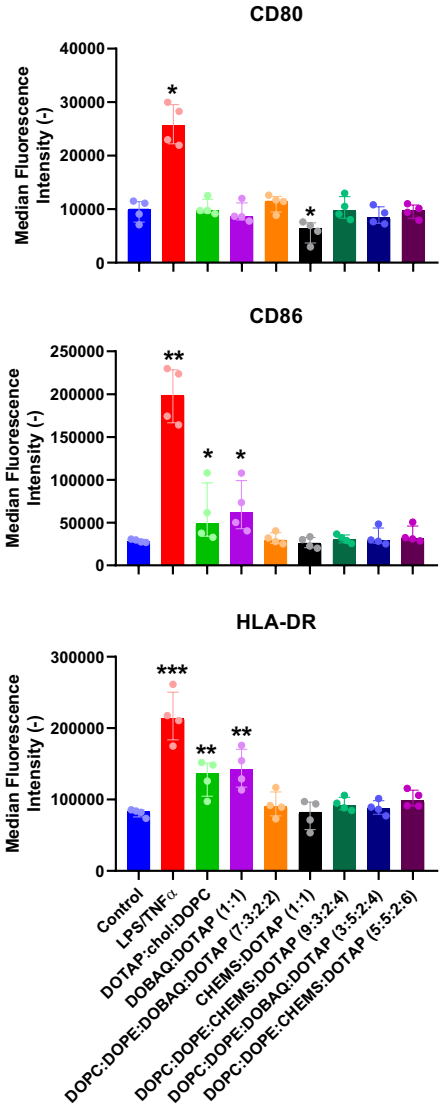

Supplementary Figure S2. Upregulation of surface activation markers and viability of human monocyte-derived dendritic cells (DCs) following exposure to liposomal empty formulations for 1 hour. Cells were incubated with formulations 250 µg/ml lipids, with lipid ratios specified as molar ratios. Median fluorescence intensities (MFI) indicate expression of activation markers CD80, CD86, and HLA-DR (n=4 donors). Formulations were compared to a medium-only control. Results are shown as median ± interquartile range. Statistical significance was determined using the Kruskal-Wallis test with uncorrected Dunn's post-hoc test, with thresholds set at $P < 0.05$ (*$P < 0.05$, **$P < 0.01$, ***$P < 0.001$, ****$P < 0.0001$).

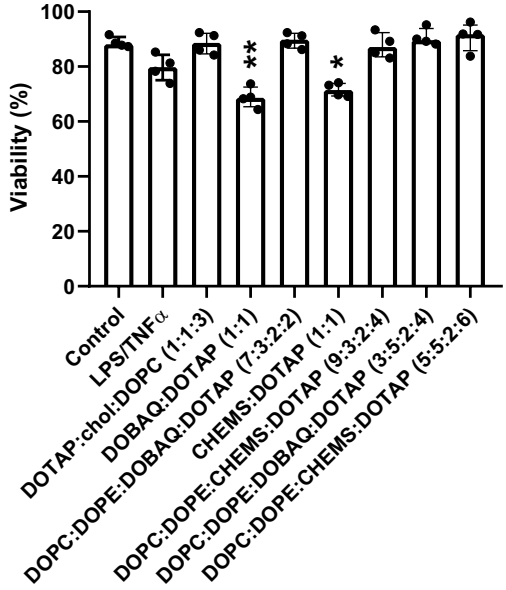

Supplementary Figure S3. Viability of human monocyte-derived dendritic cells following 1-hour incubation with empty liposomal formulations. Viability was calculated as the percentage of SYTOX AADvanced-negative cells relative to the total cell population. Cells were incubated with formulations containing 250 µg/ml lipids, with lipid ratios specified as molar ratios. Results are shown as median ± interquartile range, n = 4 (cell donors). Statistical analysis was performed using the Kruskal-Wallis test with uncorrected Dunn's post-hoc test, with significance thresholds at P < 0.05 (*P < 0.05, **P < 0.01, ***P < 0.001, ****P < 0.0001).

→ **Supplementary Figure S4.** Upregulation of surface activation markers and viability of human monocyte-derived dendritic cells (DCs) following exposure to empty liposomal formulations. Cells were incubated with formulations containing 250 µg/ml lipids, with lipid ratios specified as molar ratios for 1 hour. Median fluorescence intensities (MFI) indicate expression of activation markers CD40, CD80, CD83, CD86, CCR7 and HLA-DR (n=4 donors). Viability was calculated as the percentage of SYTOX AADvanced-negative cells relative to the total cell population. Results are shown as median ± interquartile range.

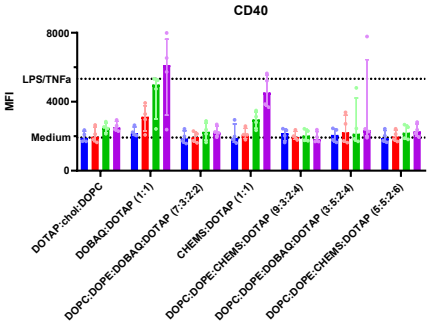
CD40
MFI
8000
LPS/TNFa
4000
Medium
0
DOTAP:chol:DOPC
DOBAQ:DOTAP (1:1)
DOPC:DOPE:DOBAQ:DOTAP (7:3:2:2)
CHEMS:DOTAP (1:1)
DOPC:DOPE:CHEMS:DOTAP (9:3:2:4)
DOPC:DOPE:DOBAQ:DOTAP (3:5:2:4)
DOPC:DOPE:CHEMS:DOTAP (5:5:2:6)

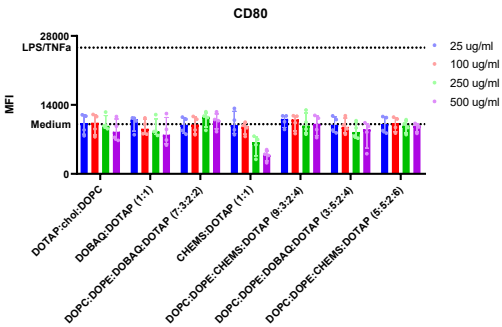
CD80
MFI
28000
LPS/TNFa
14000
Medium
0
25 ug/ml
100 ug/ml
250 ug/ml
500 ug/ml
DOTAP:chol:DOPC
DOBAQ:DOTAP (1:1)
DOPC:DOPE:DOBAQ:DOTAP (7:3:2:2)
CHEMS:DOTAP (1:1)
DOPC:DOPE:CHEMS:DOTAP (9:3:2:4)
DOPC:DOPE:DOBAQ:DOTAP (3:5:2:4)
DOPC:DOPE:CHEMS:DOTAP (5:5:2:6)

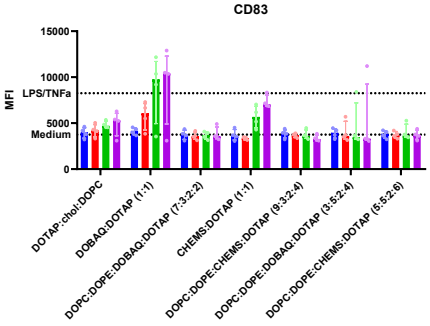
CD83
MFI
15000
10000
LPS/TNFa
5000
Medium
0
DOTAP:chol:DOPC
DOBAQ:DOTAP (1:1)
DOPC:DOPE:DOBAQ:DOTAP (7:3:2:2)
CHEMS:DOTAP (1:1)
DOPC:DOPE:CHEMS:DOTAP (9:3:2:4)
DOPC:DOPE:DOBAQ:DOTAP (3:5:2:4)
DOPC:DOPE:CHEMS:DOTAP (5:5:2:6)

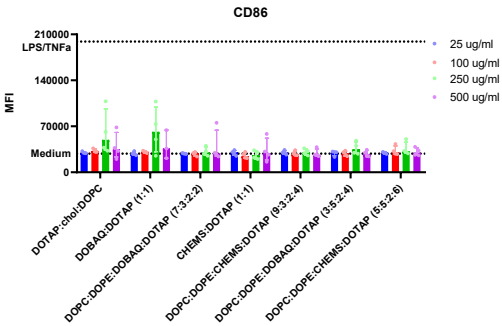
CD86
MFI
210000
LPS/TNFa
140000
70000
Medium
0
25 ug/ml
100 ug/ml
250 ug/ml
500 ug/ml
DOTAP:chol:DOPC
DOBAQ:DOTAP (1:1)
DOPC:DOPE:DOBAQ:DOTAP (7:3:2:2)
CHEMS:DOTAP (1:1)
DOPC:DOPE:CHEMS:DOTAP (9:3:2:4)
DOPC:DOPE:DOBAQ:DOTAP (3:5:2:4)
DOPC:DOPE:CHEMS:DOTAP (5:5:2:6)

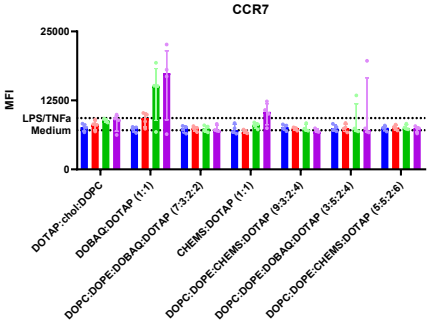
CCR7
MFI
25000
12500
LPS/TNFa
Medium
0
DOTAP:chol:DOPC
DOBAQ:DOTAP (1:1)
DOPC:DOPE:DOBAQ:DOTAP (7:3:2:2)
CHEMS:DOTAP (1:1)
DOPC:DOPE:CHEMS:DOTAP (9:3:2:4)
DOPC:DOPE:DOBAQ:DOTAP (3:5:2:4)
DOPC:DOPE:CHEMS:DOTAP (5:5:2:6)

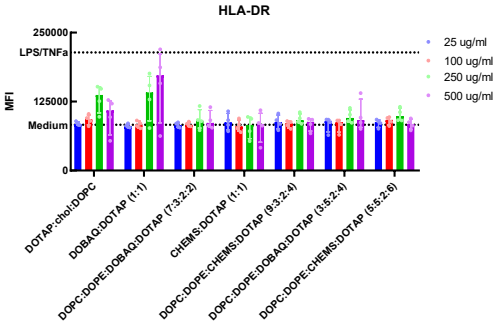
HLA-DR
MFI
250000
LPS/TNFa
125000
Medium
0
25 ug/ml
100 ug/ml
250 ug/ml
500 ug/ml
DOTAP:chol:DOPC
DOBAQ:DOTAP (1:1)
DOPC:DOPE:DOBAQ:DOTAP (7:3:2:2)
CHEMS:DOTAP (1:1)
DOPC:DOPE:CHEMS:DOTAP (9:3:2:4)
DOPC:DOPE:DOBAQ:DOTAP (3:5:2:4)
DOPC:DOPE:CHEMS:DOTAP (5:5:2:6)

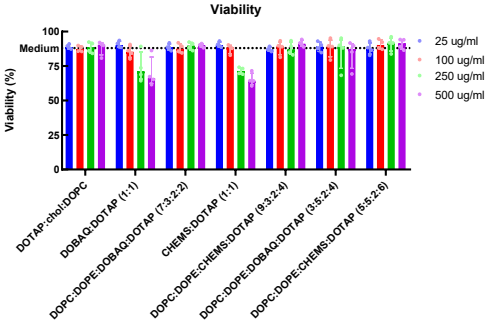
Viability
Viability (%)
100
Medium
75
50
25
0
25 ug/ml
100 ug/ml
250 ug/ml
500 ug/ml
DOTAP:chol:DOPC
DOBAQ:DOTAP (1:1)
DOPC:DOPE:DOBAQ:DOTAP (7:3:2:2)
CHEMS:DOTAP (1:1)
DOPC:DOPE:CHEMS:DOTAP (9:3:2:4)
DOPC:DOPE:DOBAQ:DOTAP (3:5:2:4)
DOPC:DOPE:CHEMS:DOTAP (5:5:2:6)

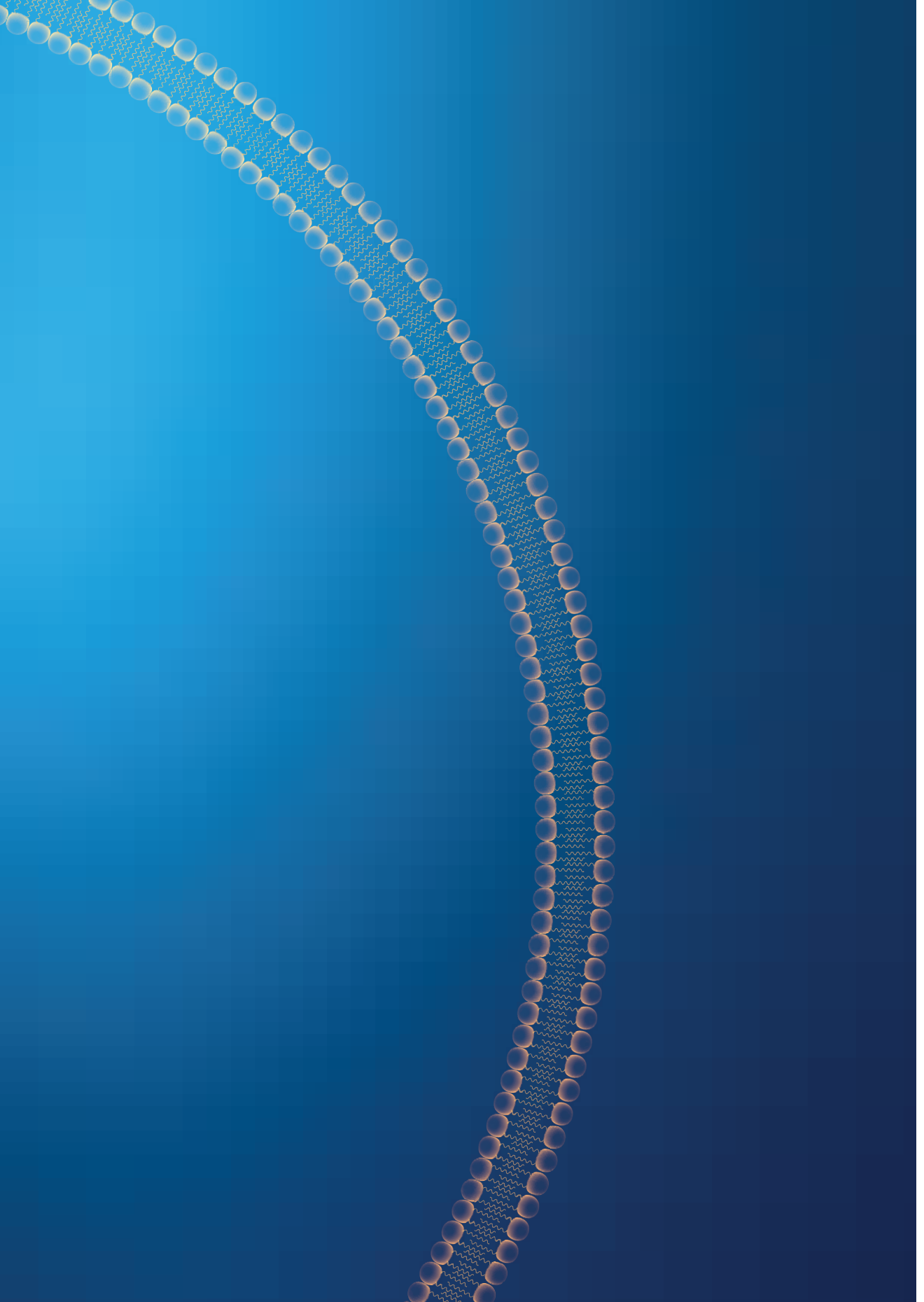

CHAPTER 4

Cationic pH-sensitive liposome-based subunit tuberculosis vaccine induces protection in mice challenged with Mycobacterium tuberculosis

M.M. Szachniewicz, S.J.F. van den Eeden, K.E. van Meijgaarden,
K.L.M.C. Franken, S. van Veen, A. Geluk, J.A. Bouwstra, T.H.M. Ottenhoff

Adapted from European Journal of Pharmaceutics and Biopharmaceutics, 2024, 203: 114437

ABSTRACT

Tuberculosis (TB) has been and still is a global emergency for centuries. Prevention of disease through vaccination would have a major impact on disease prevalence, but the only available current vaccine, BCG, has insufficient impact. In this article, a novel subunit vaccine against TB was developed, using the Ag85B-ESAT6-Rv2034 fusion antigen, two adjuvants – CpG and MPLA, and a cationic pH-sensitive liposome as a delivery system, representing a new TB vaccine delivery strategy not previously reported for TB.

In vitro in human dendritic cells (DCs), the adjuvanted formulation induced a significant increase in the production of (innate) cytokines and chemokines compared to the liposome without additional adjuvants. *In vivo*, the new vaccine administrated subcutaneously significantly reduced *Mycobacterium tuberculosis (Mtb)* bacterial load in the lungs and spleens of mice, significantly outperforming results from mice vaccinated with the antigen mixed with adjuvants without liposomes. In-depth analysis underpinned the vaccine's effectiveness in terms of its capacity to induce polyfunctional $CD4^+$ and $CD8^+$ T-cell responses, both considered essential for controlling Mtb infection. Also noteworthy was the differential abundance of various $CD69^+$ B-cell subpopulations, which included IL17-A-producing B cells. The vaccine stimulated robust antigen-specific antibody titers, further extending its potential as a novel protective agent against TB.

1. INTRODUCTION

TB remains one of the top infectious killers globally for decades. According to the WHO, TB is ranked as the 13th leading cause of all deaths worldwide, only during 2020-2021 second to COVID-19 as the deadliest infectious disease.[1] TB was responsible for 1.3 million deaths in 2022 alone.[2] Goals set by the End TB Strategy involve early TB diagnostics, including new point-of-care tests, safer and shorter medication regimens, safer and more effective therapy of latent TB, and, in particular, effective pre- and post-exposure vaccination.[3] To this day there is only one approved TB vaccine – *Mycobacterium bovis* Bacillus Calmette–Guérin (BCG). The major shortcoming of BCG is its highly variable efficacy, ranging from 0 to 80 %, and its limited induction of protection to infectious pulmonary TB in adults.[4] Therefore, there is a need for novel, more effective vaccines.

Vaccines are prepared using attenuated, inactivated, recombinant pathogens or derived substances from these pathogens, also known as subunit vaccines.[5] The first three categories of vaccines can induce robust immune responses; however, there are also associated health risks, including mutation, reversion, and contamination.[6,7] In contrast, subunit vaccines (proteins, lipids, RNA, DNA, etc.) are less immunogenic, but the safety concerns are significantly reduced thanks to their synthetic nature. Subunit vaccines are versatile, and most aspects can be easily modified and optimized for specific types of immune responses. Weak immunogenicity can be overcome by adjuvants that induce robust and specific types of immune responses and delivery systems that allow increased uptake of antigens and adjuvants by professional antigen-presenting cells (APCs) such as DCs and macrophages.[7]

Vaccine delivery systems are thus excellent tools to increase the immunogenicity of subunit vaccines, increase the uptake of antigens and adjuvants by APCs, and thus help decrease and "spare" vaccine doses and costs. Cationic liposomes are widely researched vaccine delivery systems. They are intrinsically immunogenic, rapidly taken up by APCs, and easy to customize regarding their physicochemical properties like size, charge, bilayer organization, and surface chemistry. They can be formulated with various molecular adjuvants and antigens including peptides, proteins, RNA, and DNA.[8–12]

Cationic pH-sensitive liposomes are a unique type of delivery system characterized by their responsiveness to changes in the pH of the environment. At the physiological pH, the liposomes are stable; however, when internalized by APCs and exposed to decreasing pH inside endosomes, their liposomal bilayer becomes unstable. The destabilized lipid phase fuses with the endosomal membrane, which makes it leaky and allows it to release the content of the endosome into the cytosol.[13–16] This has potential benefits for vaccination. It prevents the degradation of antigens carried by the liposome inside the endosome and consequently facilitates MHC class I antigen presentation leading to increased cytotoxic $CD8^+$ T-cell responses.[13,16–18] pH-sensitive liposomes have not been widely studied for vaccination against infectious diseases. In literature, pH-sensitive liposomes are studied primarily in gene delivery and gene-based cancer vaccines.[13,19–23] Here, we explored the application of pH-sensitive liposomes as a subunit (fusion-protein-based) vaccine delivery system against TB.

In this study, we used cationic pH-sensitive liposomes to deliver a triple fusion antigen protein Ag85B-ESAT6-Rv2034 (AER), and molecular adjuvants cytosine-phosphate-guanine motifs (CpG) (ODN1826) and a synthetic monophosphoryl lipid A (MPLA). Ag85B and ESAT6 are immunodominant antigens abundantly expressed at an early stage of Mtb infection. Both antigens are extensively studied in TB vaccine research.[5,24,25] Notably, both are currently used in vaccines in clinical trials: H1:IC31[25] and H56:IC31 (H56 also contains Rv2660c antigen).[26] Rv2034 has been identified as a potent *in vivo* expressed Mtb antigen.[27] It was shown effective in inducing protection against Mtb in HLA-DR3 transgenic mice.[25] AER fusion protein combined with cationic adjuvant formulation 09 (CAF09) effectively reduced bacterial burden in HLA-DR3 transgenic mice and guinea pigs CpG is a Toll-like receptor (TLR) 9 ligand that induces strong Th1 immune responses in mice, and it was previously shown as an effective adjuvant for the Rv2034-based subunit vaccine.[25] MPLA (PHAD) is a synthetic analog of naturally occurring MPLA, which is a potent TLR4 agonist that induces Th1 as well as Th17 responses.[28–30]

MPLA and CpG have been used together in a liposomal vaccine adjuvant called AS15, which consists of *Quillaja saponaria Molina*, fraction 21 (QS-21), MPLA, and CpG 7909. Intramuscular administration of AS15 in mice induced activation of DCs, as indicated by cell-surface activation markers CD40, CD80, and CD86 on DCs in draining lymph nodes.[31] Several phase II and III clinical trials demonstrated that cancer vaccines (melanoma and non-small-cell lung cancer) utilizing this adjuvant

system were safe and induced robust, specific T-cell and antibody responses.[31–35] Compared to a similar adjuvant AS02B that does not include CpG, AS15 was shown to induce superior immune responses.[34] Further development of these vaccines has been discontinued because of the lack of efficacy in two phase III trials. However, the body of evidence indicates that a combination of MPLA and CpG in a liposomal formulation is an effective and safe system for inducing robust immune responses and it is worth further investigation.

In this work, we developed a new tuberculosis subunit vaccine using DOPC:DOPE:DOBAQ:EPC 3:5:2:4 pH-sensitive liposomes as a delivery system for AER, CpG, and MPLA. We evaluated its efficacy *in vitro* using primary human monocyte-derived dendritic cells to evaluate its immunogenicity and *in vivo* using C57Bl/6 mice mucosal Mtb infection model to investigate induction of protection in terms of reduction of colony forming units (CFUs) in lungs and spleens of mice challenged with H37Rv Mtb strain, and immune responses in vaccinated non-Mtb-challenged mice, using a 27 marker spectral flow cytometry panel for analysis of $CD4^+$, $CD8^+$ T-cells, and B-cell responses, as well as antigen-specific antibody titers in sera. To identify differentially abundant and biologically relevant populations of cells followed by vaccinations, we performed dimension reduction analyses.

2. MATERIALS AND METHODS

2.1 Materials

1,2-dioleoyl-sn-glycero-3-phosphocholine (DOPC), 1,2-dioleoyl-sn-glycero-3-ethyl-phosphocholine chloride salt (EPC), 1,2-dioleoyl-sn-glycero-3-phosphoethanolamine (DOPE), N-(4-carboxybenzyl)-N,N-dimethyl-2,3-bis(oleoyloxy)propan-1-aminium (DOBAQ) and monophosphoryl lipid A (PHAD), synthetic (MPLA) were acquired from Avanti Polar Lipids, Inc. (USA). The chemical structures of the lipids are shown in Figure S1. Class B CpG oligonucleotide ODN1826 was obtained from InvivoGen (the Netherlands). Recombinant fusion protein AER was produced as described previously by Franken et al.[36] In brief, genes obtained from Mtb (lab strain H37Rv) were amplified through polymerase chain reaction (PCR) using genomic DNA. These amplified genes were cloned using Gateway technology (Invitrogen, USA) into bacteria containing an N-terminal hexahistidine (His) tag. The successful insertion of the cloned products was confirmed through sequencing. Next, the antigen AER was

expressed in *Escherichia coli* strain BL21 (DE3) and subsequently purified. Produced AER was subsequently purified. The protein quality, size, purity, and determination of endotoxin concentration were performed as described by Franken et al.[36]

2.2 Liposome preparation

Liposomes were prepared using the thin-film hydration method as described previously.[37] Lipids were dissolved in chloroform, with appropriate lipids diluted from 25 mg/ml stock solutions. A total of 10 mg (10 mg/ml) lipids in chloroform were used per batch. The lipid solution was added into a round-bottom flask, and the chloroform was removed by evaporation for 1 hour using a Buchi rotavapor R210 (Switzerland). The lipid film was flushed with nitrogen for 5 minutes to remove any remaining traces of chloroform and rehydrated with 1 ml of 200 µg/ml AER in 10 mM phosphate buffer (PB) at pH 7.4 to prepare AER-containing liposomes. Following rehydration, the liposomes were downsized using a Branson sonifier 250 (US) with an eight-cycle sonication program. Each cycle comprised 30 seconds of sonication at 10 % amplitude, followed by a 60-second break. The liposomes were subsequently centrifuged at 1500 RPM for 5 minutes (Allegra X-12R, US) to remove any metal particles released by the sonicator. The resulting liposomal suspensions were transferred to new tubes, discarding the pellet, 1 mg/ml CpG in water was added dropwise, and further diluted with PB. The final product contained 40 µg/ml AER, 12 µg/ml CpG, 2 mg/ml lipids, 5 µg/ml MPLA, and 10 mM PB. The liposomes were stored at 4 °C overnight and injected into mice the next day. For each immunization (three per experiment), a new batch of liposomes were produced, and their quality was assessed based on size, size distribution, and zeta-potential prior to injection.

2.3 Liposome characterization (size and zeta-potential)

The intensity-weighted average hydrodynamic diameter (Z-average size) and polydispersity index (PDI) of the liposomal formulations were determined using dynamic light scattering (DLS), while the zeta potential was measured using laser Doppler electrophoresis. The liposomes were diluted to 0.25 mg/mL lipid concentration in 10 mM phosphate buffer (PB) at pH 7.4 to perform the measurements. The diluted liposomes were transferred to 1.5 ml VWR Two-Sided Disposable PS Cuvettes (VWR, the Netherlands). Each batch was measured in triplicates, with a minimum of ten runs per measurement at a temperature of 20 °C. A Nano ZS Zetasizer equipped

with a 633 nm laser and 173° optics (Malvern Instruments, Worcestershire, UK) was employed for the DLS and zeta potential measurements. The acquired data were analyzed using Zetasizer Software v7.13 (Malvern Instruments).

2.4 Mice

C57Bl/6 mice were obtained from The Jackson Laboratory (ME, USA) (stock number SC1300004) and were housed in the animal facilities of the Leiden University Medical Center (LUMC), the Netherlands. Female mice 6-8 weeks old at the start of each experiment were used. All Mtb infections were performed in a biosafety level 3 (BSL-3) facility at the LUMC.

All mouse experiments were individually designed, reviewed, ethically approved, and registered the LUMC's institutional Animal Welfare Body, and executed under the project license number AVD116002017856, which was granted by the Netherlands' authoritative body on animal experimentation, the CCD. These experiments adhered strictly to the Dutch Act on Animal Experimentation regulations and the European Union Directive 2010/63/EU, at the LUMC facility. The mice were kept in separately ventilated cages, maintaining a maximum occupancy of six mice per cage, and the studies commenced only after an acclimatization period of one-week post-transport.

2.5 Immunizations

Mice (6 mice per group per experiment) were vaccinated with either BCG or AER solution mixed with CpG (ODN1826) and MPLA (PHAD) or liposomes. For liposome immunization, mice were injected 3 times with liposomal suspension (each dose containing 8 µg AER, 400 µg total lipids, 2.5 µg CpG ODN1826, and 1 µg MPLA (PHAD) in 200 µl of PB) subcutaneously (s.c.) in the right flank at 2 weeks intervals. Four weeks after the last immunizations, mice were sacrificed or infected with live Mtb. For immunization with AER mixed with adjuvants, mice were injected 3 times s.c. with AER mixed with CpG and MPLA in phosphate-buffered saline (each dose containing 25 µg AER, 50 µg CpG, and 1 µg MPLA in 200 µl PBS) in the right flank at 2 weeks interval, as described by Commandeur et al.[25] The liposomal immunization used a 3 times lower dose of AER and 20 times lower dose of CpG to evaluate whether reducing the dose using vaccine delivery technology is possible and effective compared to work by Commandeur et al.[25] For BCG immunization, mice were once injected s.c. 12 weeks before sacrificing or infection with live Mtb, in the

right flank with 10^6 CFU live BCG (Danish strain 1331) from glycerol stocks, stored at -80 °C. The number of bacteria was determined by plating the suspension used for infection on 7H10 agar plates (Difco, BD, Franklin Lakes, NJ USA) supplemented with BBL Middlebrook OADC enrichment (BD, Franklin Lakes, NJ USA). Colonies were counted after 3 weeks of incubation at 37 °C.

2.6 Intranasal infection with live Mtb

Naïve and immunized mice were infected with live Mtb strain H37Rv 4 weeks after third liposome immunization or 12 weeks after BCG immunization. Mice were anesthetized with isoflurane (2-chloro-2-(difluoromethoxy)-1,1,1-trifluoroethane; Pharmachemie BV, The Netherlands) and intranasally (i.n.) infected with 10^5 CFU Mtb from glycerol stocks, stored at -80 °C.[38] Plating the suspension used for infection on 7H10 agar plates determined the number of bacteria. Colonies were counted after 3 weeks of incubation at 37 °C.

Mice were euthanized with CO_2, 6 weeks post Mtb infection, and spleens and lungs were aseptically removed. The organs were homogenized using 70 µM cell strainers (Corning, USA) in sterile PBS, and the bacterial load was determined by plating in serial dilutions on 7H11 agar plates (BD Bioscience, USA), supplemented with OADC, and PANTA (BD, Franklin Lakes, NJ USA).

2.7 *In vitro* cultures

Splenocytes of immunized uninfected mice were resuspended at 3×10^6 cells/ml in Iscove's Modified Dulbecco's Medium (IMDM) (Gibco, Thermo Fisher Scientific, Belgium), supplemented with 2 mM GlutaMAX Supplement (Gibco, Thermo Fisher Scientific, Belgium), 100 U/100 µg/ml penicillin-streptomycin (Gibco, Paisley, UK), and 8 % heat-inactivated fetal bovine serum (FBS; Greiner, Frickenhausen, Deutschland) and *in vitro* stimulated with 5 µg/mL of fusion protein AER, at 37 °C 5 % CO_2. After 6 days, the splenocytes were restimulated with 5 µg/ml of the same protein as the stimulation for 5 hours, and 2.5 µg/mL Brefeldin A (Sigma, Merck, Darmstadt, Germany) was added for overnight incubation. Next, splenocytes were harvested and stained for intracellular cytokines and surface markers.

For cytokine production by restimulated splenocytes, 3×10^6 cells/ml were resuspended in IMDM, supplemented with 2 mM GlutaMAX Supplement, 100

U/100 µg/ml penicillin-streptomycin, and 8 % heat-inactivated FBS and incubated with the antigen in round bottom 96 wells plates. Supernatants were collected after 6 days.

2.8 Antibody enzyme-linked immunosorbent assay (ELISA)

Blood was collected from immunized uninfected mice via heart puncture upon sacrifice and stored on ice. Sera were obtained by blood centrifugation at 15,000 rpm for 10 minutes. Antibodies against proteins in sera were determined by ELISA: plates were coated overnight at 4 °C with protein (5 µg/ml) or PBS/0.4 % bovine serum albumin (BSA) (Sigma, Merck, Darmstadt, Germany), washed and blocked for 2 h using PBS/1 % BSA/1 % Tween-20. Serum dilutions (100 µl/well) were incubated at 37 °C for 2 h. Plates were washed (PBS, 0.05 % Tween-20) and incubated with 100 µl/well horse radish peroxide (HRP)-labeled, rabbit-anti-mouse total IgG, IgG1, IgG2a, IgG2b, IgG2c, IgG3 and IgM (Dako, Denmark). After 2 h at 37 °C, plates were washed and 100 µl/well tetramethylbenzidine substrate (TMB; Sigma) was added for 15 min at room temperature after which H_2SO_4 (1 M; 100 µl/well) was added and OD450 measured using Spectramax i3x spectrometer (Molecular Devices, CA, USA).

2.9 Antibody staining and flow cytometry

For flow cytometry analysis, the splenocytes were transferred into round-bottom 96-well plates (CELLSTAR, Greiner Bio-One GmbH, Germany) and washed with FACS buffer (PBS containing 0.1 % BSA; Sigma, Merck, Darmstadt, Germany). Next, the Zombie UV Fixable Viability Kit was reconstituted according to the manufacturer's instruction (BioLegend, the Netherlands), and the working solution was diluted 1:250 in PBS. 100 µl of the diluted dye was added to each well, and cells were incubated at room temperature in the dark for 30 minutes. Cells then were washed twice with FACS buffer. After that, cells were blocked with 20 µl of 5 % normal mouse serum (Thermo Fisher Scientific Inc., Bleiswijk, the Netherlands) in FACS buffer for 15 minutes at room temperature. Antibody staining was then performed. The list of antibodies used are listed in Table 1. Briefly, cells were washed once, and stained with CCR7 for 30 minutes at 37 °C. Next, cells were washed twice, and stained with 50 µl/well antibody mix containing remaining cell surface markers in FACS buffer containing 10 µl/well of BD Horizon Brilliant Stain Buffer Plus (BD Biosciences, Belgium). Cells were incubated at 4 °C for 30 minutes. Subsequently, cells were washed twice, and cells were fixated and permeabilized using eBioscience Foxp3/Transcription Factor

Staining Buffer Set (Invitrogen, Thermo Fisher Scientific, Belgium) at 4 °C for 60 minutes according to the manufacturer's instructions. After washing, intracellular staining was performed using an antibody mix diluted in a permeabilization buffer. Cells were incubated with 50 µl/well antibody mix at room temperature for 45 minutes. Afterward, cells were washed twice resuspended in 100 µl/well FACS buffer. Cells were stored at 4 °C until measured with a 5-laser Cytek Aurora spectral flow cytometer (Cytek Biosciences, Fremont, CA, USA) at the Flow cytometry Core Facility of Leiden University Medical Center (LUMC) in Leiden, the Netherlands.

Table 1. List of antibodies used in this study for spectral flow cytometry analysis of $CD4^+$, $CD8^+$, and $CD3^-$ $CD19^+$ B-cells.

Marker	Fluorochrome	Clone	Manufacturer
CCR7 (CD197)	PE/Cyanine5	4B12	BioLegend
CD273	BUV 395	TY25	BD Biosciences
CD8b.2	BUV 496	53-5.8	BD Biosciences
CD80	BUV 661	16-10A1	BD Biosciences
CD69	BUV 737	H1.2F3	BD Biosciences
CD25	BV 480	PC61	BD Biosciences
CD154	Super Bright 436	MR1	Thermo Fisher
IgD	Pacific Blue	11-26c.2a	BioLegend
I-A/I-E (MHC class II)	BV 510	M5/114.15.2	BioLegend
CD44	BV 570	IM7	BioLegend
PD-1 (CD279)	BV 605	29F.1A12	BioLegend
CXCR3 (CD183)	BV 650	CXCR3-173	BioLegend
KLRG1 (MAFA)	BV 711	2F1/KLRG1	BioLegend
CCR6 (CD196)	BV 785	29-2L17	BioLegend
CD4	Spark Blue 550	GK1.5	BioLegend
CCR5 (CD195)	PerCP/Cyanine5.5	HM-CCR5	BioLegend
CD19	PE Fire 640	6D5	BioLegend
CD138	APC	281-2	BioLegend
B220 (CD45R)	Spark NIR 685	RA3-6B2	BioLegend

CD62L (L-selectin)	APC/Fire 750	MEL-14	BioLegend
CD3	APC/Fire 810	17A2	BioLegend
IL-2	APC-R700	JES6-5H4	BD Biosciences
IL-17A	PE	eBio17B7	Thermo Fisher
IgM	FITC	RMM-1	BioLegend
IL-10	PE/Dazzle 594	JES5-16E3	BioLegend
TNFα	PE/Cyanine7	MP6-XT22	BioLegend
IFNγ	Alexa Fluor 647	XMG1.2	BioLegend

2.10 Analysis of flow cytometry data

Data were analyzed using FlowJo v10.8.0 and OMIQ analysis software (www.omiq.ai). The analysis strategy is depicted in Figure S2. Briefly, using FlowJo the data were first manually gated to remove debris, doublets, acquisition-disturbed events, and dead cells. Subsequently, cells were gated on CD3 vs CD19, and $CD3^+$ $CD19^-$ (T-cells) and $CD3^-$ $CD19^+$ (B-cells) were separately exported (minimum 20,000 events each population) and uploaded to the OMIQ platform (Figure S2). Imported data were further cleaned with the FlowAI tool in OMIQ. UMAP was performed on digitally concatenated cells. Subsequently, single marker gates were created for all markers except live/dead stain, CD3 (Figure S3), and CD19 (Figure S4). Using Boolean gating, combinations of gates were created. Afterward, counts for all Boolean gates were exported, and statistical analysis was performed.

2.11 Statistical analysis

Mann-Whitney statistical test with Benjamini Hochberg false discovery rate (FDR) correction was carried out using R[39] and RStudio,[40] to identify differentially abundant populations of cells. In GraphPad Prism, version 8.01 (GraphPad software, Prism, USA) statistical analyses were performed to compare vaccination groups. The results were analyzed with the Kruskal-Wallis test followed by an uncorrected Dunn's post-hoc test when comparing non-parametric data sets of three or more groups to the control group, where $P < 0.05$ was considered as statistically significant (*$P < 0.05$, **$P < 0.01$, ***$P < 0.001$, ****$P < 0.0001$). Graph values represent the median and error bars the interquartile range (IQR) unless indicated otherwise.

3. RESULTS

In this study, DOPC:DOPE:DOBAQ:EPC 3:5:2:4 cationic pH-sensitive liposomal formulation was used to deliver AER antigen, which was previously described as very promising *in vitro* (Szachniewicz, submitted [Chapter 3]). Based on our previous research, this liposome was an excellent candidate for further testing *in vivo*. To further increase the activation of APCs *in vivo*, two TLR agonists CpG and MPLA were incorporated.

3.1 Characterization of the vaccine formulation

The pH-sensitive liposomal formulation with CpG and MPLA was prepared, and its physicochemical properties were measured. The size of the prepared liposomes was 164.6 ± 33.1 nm, PDI 0.30 ± 0.10, and Zeta-potential 21.4 ± 2.5 mV. The values represent a mean and standard deviation of three independent batches.

3.2 Immunogenicity of the vaccine formulation in primary human MDDCs model

First, the effect of DOPC:DOPE:DOBAQ:EPC liposome formulated with AER, CpG, and MPLA on cytokine production in primary human MDDCs was investigated (Figure S5). The adjuvanted formulation induced a significant increase in the production of IL-1RA, IL-6, TNFα, CCL2, CCL3, CCL4, CCL5, CCL8, CCL11, CCL22, CXCL9, and CXCL10. These results supported the hypothesis that the formulation could effectively stimulate APCs and induce innate and also adaptive immune responses (see further below) to AER. Furthermore, the immunogenicity of liposomes containing different doses of AER (5 µg/ml, 1.5 µg/ml, and 0.5 µg/ml), CpG, and MPLA was evaluated using flow cytometry to investigate their effect on the expression of cell surface activation markers (CD40, CD80, CD83, and CD86) and cytotoxicity (Figure S6). All liposome formulations significantly upregulated the expression of these markers, and no cytotoxicity was observed. The effect of incorporating molecular adjuvants CpG and MPLA was further evaluated with this method (Figure S7). The combination of CpG and MPLA significantly increased CD80, CD83, and CD86 expression but not CD40. The adjuvant-free liposomal vaccine increased CD40 and CD83 but did not increase CD80 and CD86. In contrast, the liposome formulated with both CpG and MPLA increased all these cell surface markers, demonstrating the excellent immunogenicity of this formulation *in vitro*.

3.3 pH-sensitive liposome-based vaccine induced protection in mice

The efficacy of the vaccines to induce protection in mice was investigated. Immunization groups are summarized in Table 2. We assessed the bacterial burden in lungs and spleens of mice six weeks after the infection (Figure 1). CFUs from mice vaccinated with the pH-sensitive liposomal vaccine and BCG were significantly reduced compared to unimmunized mice both in lungs and spleens. Compared to the liposomal vaccine, mice immunized with AER mixed with adjuvants without liposomal constituents, showed bacterial reduction only in spleens but not in lungs. Importantly, the liposomal vaccine reduced CFUs significantly better in spleens compared to the non-liposomal formulation. The data show a notable range in the bacterial burden, indicating variable immune responses among the mice. Noteworthy is that in 6 mice of the BCG-vaccinated group and 2 mice of the pH-sensitive liposome group, the CFUs were at the detection limit of 100-200 CFUs, which is over 10^3 times less in lungs and over 10^4 times less in spleens compared to CFUs of unimmunized mice. These results indicate a high level of protection. Only 1 mouse of the AER-adjuvant mix group showed such a level of protection, but it was limited to lungs and not in spleens. Furthermore, the protection using the cationic pH-sensitive formulation was achieved using 3 times lower dose of the antigen and 20 times lower dose of CpG, demonstrating significant benefits using these liposomes.

Table 2. Summary of vaccination groups and doses of vaccine constituents administrated to a mouse per single immunization.

Group	Description	AER (µg)	Liposome (µg)	CpG (µg)	MPLA (µg)
Naïve	Unimmunized	NA	NA	NA	NA
BCG	Applied human vaccine	NA	NA	NA	NA
Ag	Antigen-adjuvant mix	25	NA	50	1
pH	pH-sensitive liposome	8	400	2.5	1

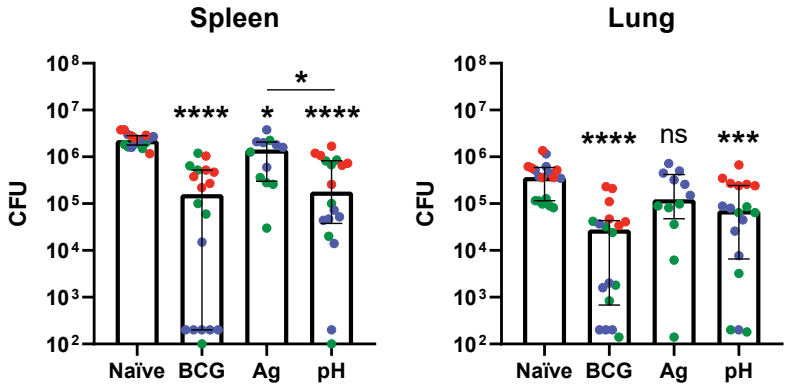

Figure 1. Bacterial burden in spleens (a) and lungs (b) of challenged mice represented with colony forming units (CFU) of Mtb. Each point represents CFU obtained from a single mouse. n = 18 except Ag group n = 12. Median ± IQR. Each dot represents a single mouse and results from the same experiment are shown in one color. Groups represent: naïve – unimmunized mice, BCG – BCG vaccination, Ag – AER/CpG/MPLA mixture vaccination, pH – vaccination with cationic pH-sensitive liposomal formulation of AER/CpG/MPLA. The statistical analysis shown compares to the naïve mice unless otherwise indicated.

3.4 The abundance of polyfunctional CD4⁺ T-cells increased after vaccination

To explore the immune responses induced by the vaccine, we evaluated the phenotypical abundance of various lymphocyte populations. First, we visually investigated differences in the abundance of $CD4^+$ and $CD8^+$ T-cell subsets between different immunization groups by UMAP (Figure 2). To quantitively analyze those differences, a differential subset abundance analysis was performed to identify populations of interest. The criteria for selecting cell subsets were: sufficiently large (> 100 events) and expressed biologically relevant marker profiles, enabling the identification of specific immune response populations. If several subpopulations had overlapping marker expression patterns, we selected one that is defined by more markers or had a lower p-value. We observed several $CD4^+$ T-cell subpopulations with polyfunctional phenotypes (Figure 3). The largest polyfunctional population defined as $CD4^+$ IL-2^+ $IFN\gamma^+$ $TNF\alpha^+$ IL-$17A^-$ IL-10^- $CD44^-$ $CD62L^+$ $CCR7^-$ T-cells. This population was more than twice as abundant in mice vaccinated with AER mixed with adjuvants and with the liposomal formulation, compared to naïve and BCG-vaccinated mice, and, importantly, also displayed a central memory phenotype. Secondly, a much less abundant population of IFNγ-producing $CD4^+$ IL-2^- $IFN\gamma^+$

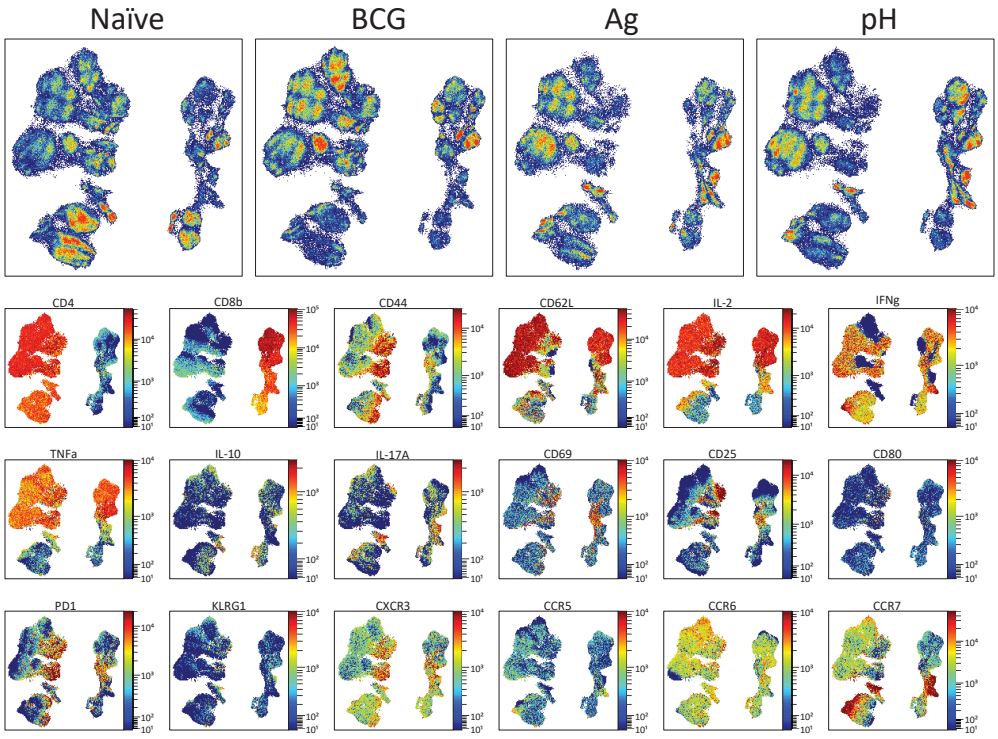

Figure 2. Uniform Manifold Approximation and Projection for Dimension Reduction (UMAP) visualization of spleen-derived CD4⁺, and CD8⁺ T-cells (CD3⁺ CD19⁻) from all tested mice (per group) showing differential abundances of various populations of cells followed by color-continuous plots depicting phenotypical markers distribution. Groups represent: naïve – unimmunized mice, BCG – BCG vaccination, Ag – AER/CpG/MPLA mixture vaccination, pH – vaccination with cationic pH-sensitive liposomal formulation of AER/CpG/MPLA.

TNFα⁻ CCR7⁺ T-cells was differentially enriched, being statistically increased both in AER mixed with CpG/MPLA and AER delivered in the liposomal formulation compared to naïve and BCG-vaccinated mice and displayed a predominant effector memory phenotype. Two monofunctional subpopulations of CD4⁺ T-cells that produced IL-2 were increased in mice vaccinated with BCG. CD4⁺ IL-2⁺ IFNγ⁻ TNFα⁻ IL-17A⁻ IL-10⁻ CD44⁻ CD62L⁺ CCR7⁻ T-cells were significantly increased in the BCG group compared to naïve and both subunit vaccine groups. CD4⁺ IL-2⁺ IFNγ⁻ TNFα⁻ CCR7⁺ T-cells were increased in BCG and AER adjuvant mix compared to naïve and AER delivered in the liposomes. We did not observe any increase in IL-17A production by CD4⁺ T cells followed by any of the immunization.

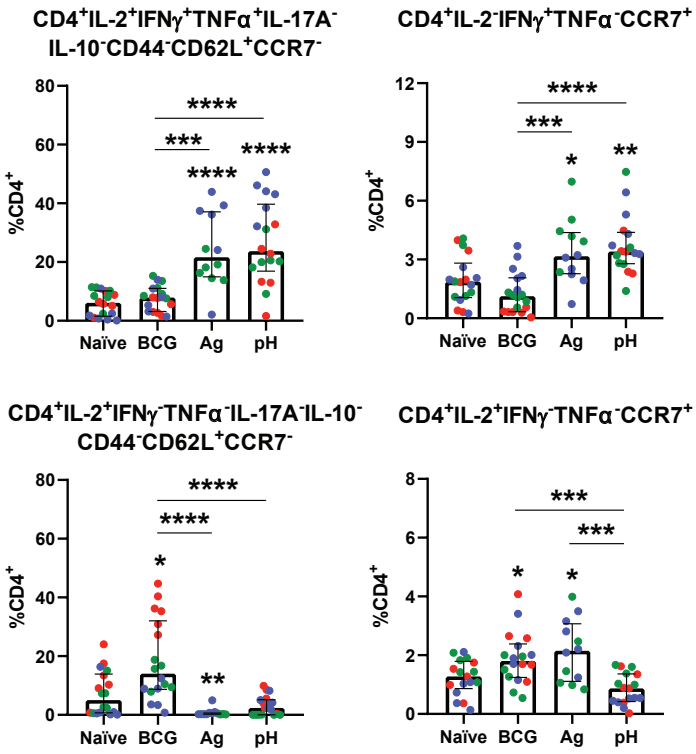

Figure 3. Differentially abundant populations of CD4⁺ T-cells present in restimulated splenocytes from immunized non-Mtb-challenged mice. Markers defining each population are indicated above each graph. Graph values depict percentages of the population as a part of the CD3⁺ CD19⁻ CD4⁺ CD8⁻ cell subset. Each dot represents a single mouse and results from the same experiment are shown in one color. Groups represent: naïve – unimmunized mice, BCG – BCG vaccination, Ag – AER/CpG/MPLA mixture vaccination, pH – vaccination with cationic pH-sensitive liposomal formulation of AER/CpG/MPLA. n = 18 (mice) except Ag group – n =12. Median ± IQR.The minimal number of events used in the analysis was 20,000.

3.5 The abundance of several polyfunctional and monofunctional CD8⁺ T-cell populations increased after immunization

We observed several populations of differentially abundant CD8⁺ T-cells, with the largest subset defined as CD8⁺ IL-2⁺ IFNγ⁺ TNFα⁺ CD44⁻ CD62L⁺ CCR7⁻ (Figure 4). These polyfunctional cells were significantly more abundant in mice vaccinated with AER mixed with CpG/MPLA, and AER in pH-sensitive liposomal adjuvant compared to naïve and BCG-vaccinated mice. We also found a subpopulation that expressed the activation marker CD69 – also known as the activation inducer molecule, a marker of very early activation.[41] This subpopulation

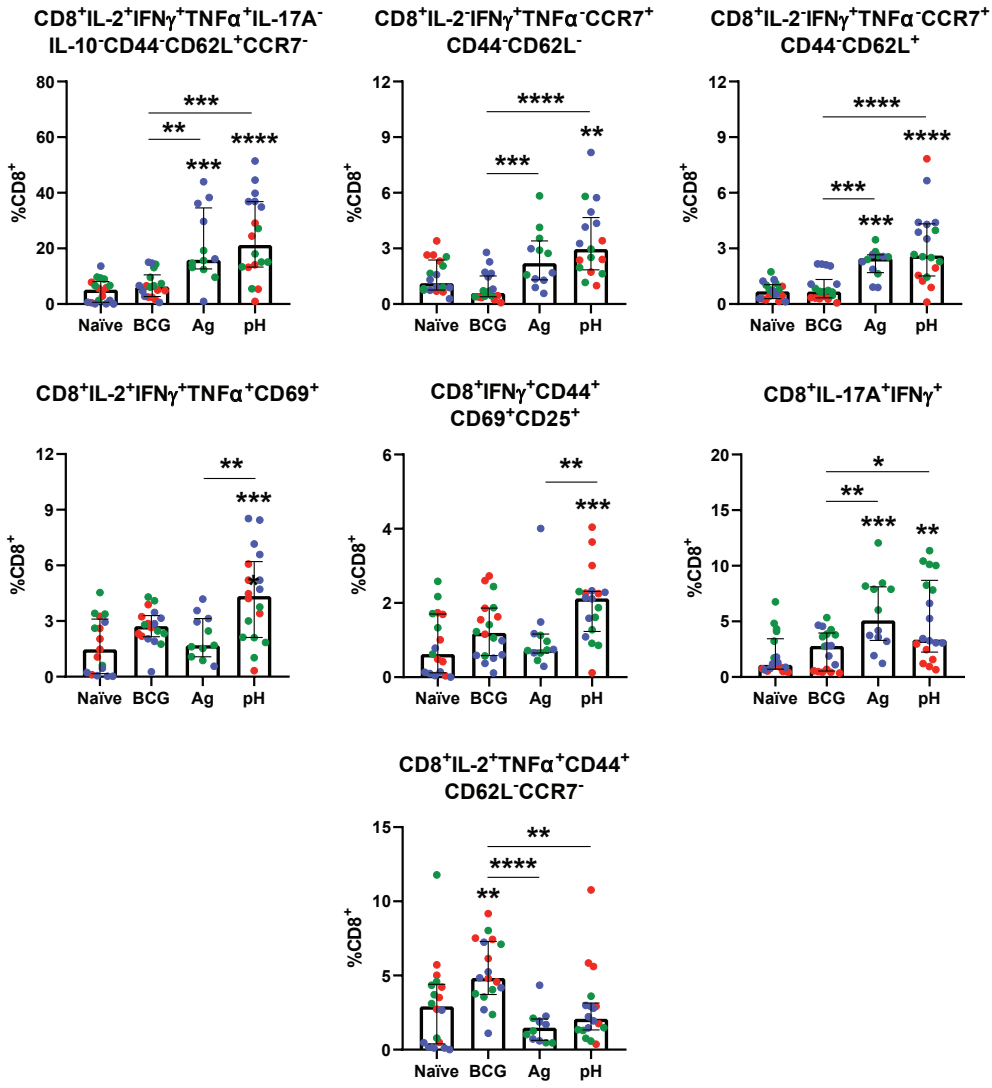

Figure 4. Differentially abundant populations of CD8⁺ T-cells present in restimulated splenocytes from immunized non-Mtb-challenged mice. Markers defining each population are indicated above each graph. Graph values depict percentages of the population as a part of the CD3⁺ CD19⁻ CD4⁻ CD8⁺ cell subset. Each dot represents a percentage value from a single mouse and results from the same experiment are shown in one color. Groups represent: naïve – unimmunized mice, BCG – BCG vaccination, Ag – AER/CpG/MPLA mixture vaccination, pH – vaccination with cationic pH-sensitive liposomal formulation of AER/CpG/MPLA. n = 18 (mice) except Ag group – n =12. Median ± IQR. The minimal number of events used in the analysis was 20,000.

was significantly increased in mice vaccinated with AER in pH-sensitive liposomes compared to naïve mice, and mice vaccinated with AER mixed with CpG/MPLA. We also observed two single functional populations of $CD8^+$ T-cell producing only IFNγ – one expressing CCR7 but not CD44 or CD62L, the other expressing both CCR7 and CD62L but not CD44. Both of these populations were increased after immunization with AER and adjuvant mix, and AER in the pH-sensitive liposomal formulation compared to naïve and BCG groups. $CD8^+$ $IFN\gamma^+$ $CD44^+$ $CD69^+$ $CD25^+$ T-cells were significantly more abundant in the pH-sensitive liposomal formulation group compared to naïve and AER mixed with CpG/MPLA. This population expressed three activation markers, which may imply that IFNγ-producing $CD8^+$ T-cells derived from mice immunized with the liposomal vaccine are more broadly and/or readily activated upon antigen restimulation compared to $CD8^+$ T-cells derived from other groups. Also, the percentage of $CD8^+$ $IL\text{-}17A^+$ $IFN\gamma^+$ T-cells was statistically increased in mice in both AER vaccine arms compared to naïve and BCG groups. The $CD8^+$ $IL\text{-}2^+$ $TNF\alpha^+$ $CD44^+$ $CD62L^-$ $CCR7^-$ population of $CD8^+$ T-cells was more abundant in mice vaccinated with BCG but not with any of the two AER vaccine groups –, which corresponds to activated effector memory phenotype.

3.6 Altered B-cell responses in vaccinated mice

B-cell responses in the concatenated dimensionally reduced data (Figure 5) were visually inspected to determine whether there were differences in the abundance of B-cells in different mice groups. Clear differences in various subsets of cells were observed; therefore, the quantitative analysis used the same approach as in the T-cell data analysis. Several differentially abundant B-cell subsets were identified (Figure 6). Several subpopulations of $CD19^+$ $CD3^-$ cells that expressed the activation marker CD69 were observed: $MHCII^+$ IgM^+ IgD^- $B220^+$ (marginal zone B-cell, transitional 1 B), $MHCII^+$ IgM^+ IgD^+ $B220^+$ (transitional 2B, activated B), $MHCII^+$ IgM^- IgD^- $B220^+$ (germinal center B-cell) and $MHCII^+$ IgM^- IgD^+ $B220^+$ (follicular B/B2).[42,43] The percentages of all these subsets were significantly increased in mice immunized with AER in pH-sensitive liposome formulation, and AER mixed with CpG/MPLA compared to naïve and BCG-immunized mice. A population of B cells defined as $MHCII^-$ IgM^+ IgD^- $B220^-$ was observed which could be a transient subpopulation of plasma cells since it did not express CD138. Also, three subsets of $CD19^+$ $CD3^-$ cells that were significantly more abundant in mice vaccinated with BCG but not with AER

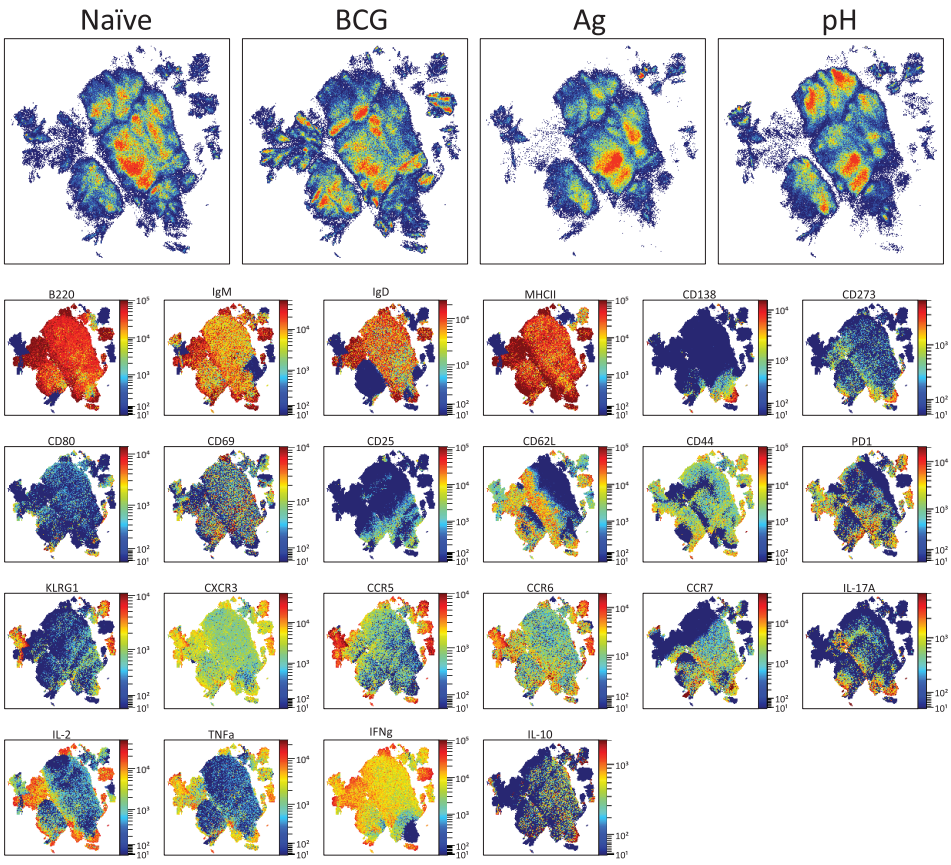

Figure 5. Uniform Manifold Approximation and Projection for Dimension Reduction (UMAP) visualization of concatenated spleen-derived B-cells ($CD3^-$ $CD19^+$) from all tested mice (per group) showing differential abundances of various populations of cells followed by color-continuous plots depicting phenotypical markers distribution. Groups represent: naïve – unimmunized mice, BCG – BCG vaccination, Ag – AER/CpG/MPLA mixture vaccination, pH – vaccination with cationic pH-sensitive liposomal formulation of AER/CpG/MPLA.

CpG/MPLA mix or AER in pH-sensitive liposomes were observed: $CD69^+$ $TNF\alpha^+$ cells $MHCII^+$ $B220^+$ $CD62L^+$ $IL\text{-}17A^+$, and $MHCII^+$ $B220^+$ $CXCR3^+$ $PD\text{-}1^+$.

3.7 High AER-specific antibody titers in vaccinated mice

AER-specific antibody titers in sera of non-Mtb-challenged mice were measured (Figure 7). High total antibody titers and high titers for antibody subclasses were observed: high levels of IgG1, IgG2a, (and IgG2b, IgG2c, and intermediate levels of IgG3 and IgM, Fig S8). Mice vaccinated with AER delivered in pH-sensitive liposomal

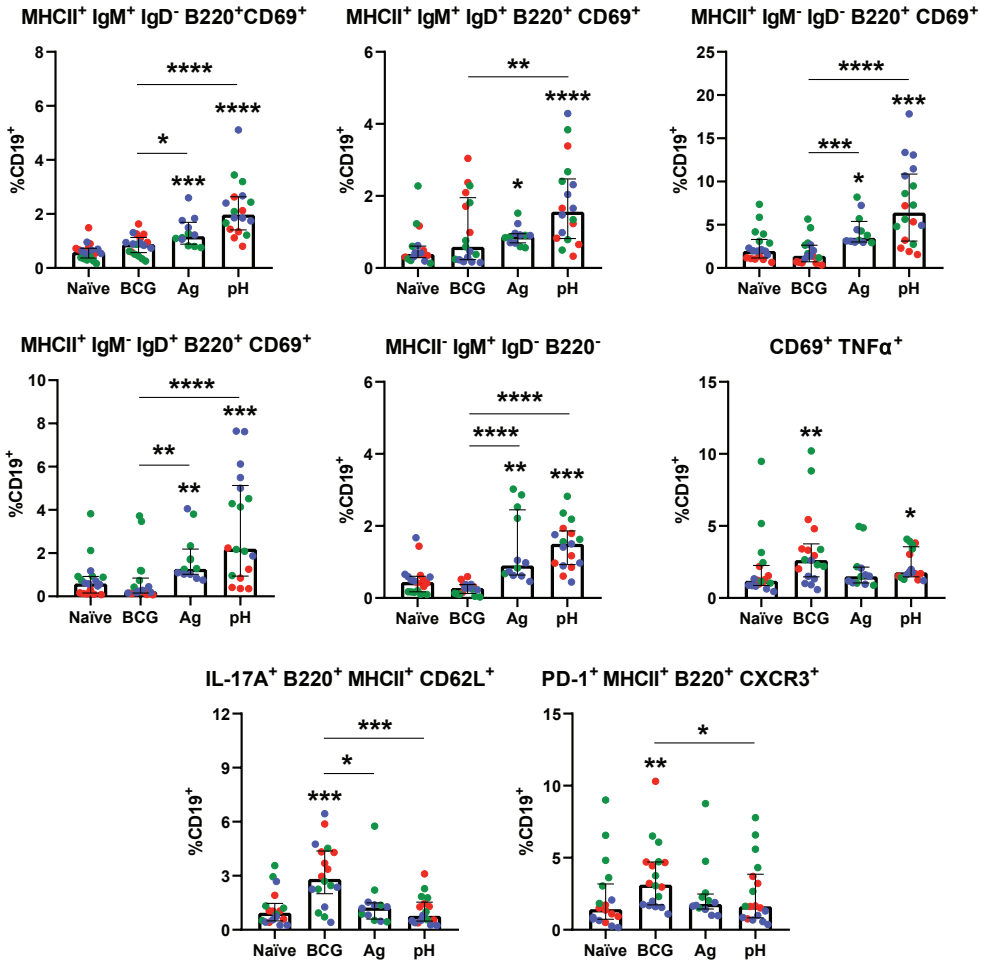

Figure 6. Differentially abundant CD19⁺ B-cell populations present in restimulated splenocytes from immunized non-Mtb-challenged mice. Markers defining each population are indicated above each graph. Graph values depict percentages of the population as a part of the CD3⁻ CD19⁺ cell subset. Each dot represents a percentage value from a single mouse and results from the same experiment are shown in one color. Groups represent: naïve – unimmunized mice, BCG – BCG vaccination, Ag – AER/CpG/MPLA mixture vaccination, pH – vaccination with cationic pH-sensitive liposomal formulation of AER/CpG/MPLA. n = 18 (mice) except Ag group – n =12. Median ± IQR. The minimal number of events used in the analysis was 20,000.

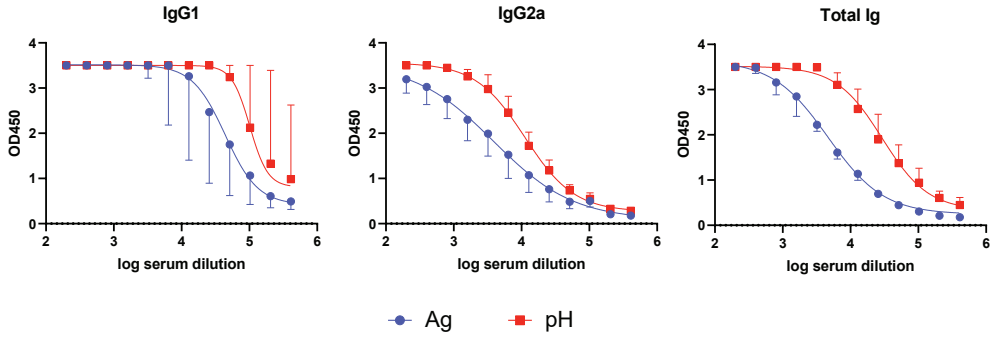

Figure 7. Quantification of serum antibodies to AER. The type of antibody measured is indicated above each graph. Values represent end-point titers. Values of 6 mice. Median ± IQR. ND – titer below detection level.

formulation had higher antibody titers compared to mice immunized with AER mixed with adjuvants. When comparing titers of IgG1 and IgG2a subsets, we observed that the IgG1 titer was higher. Although this might suggest that the balance of immune responses was potentially skewed towards Th2; however, this was not substantiated by the above direct splenocyte T-cell data, where we did not observe any increase in the production of Th2 cytokine IL-10.

4. DISCUSSION

TB for centuries has remained at the top of the deadliest infectious diseases worldwide. One of the reasons why TB poses an immense burden is BCG's variable and incomplete protection against contagious pulmonary TB in adolescents and adults. Despite decades of research, there is no other TB vaccine approved. In this work, we investigated a pH-sensitive liposome-based subunit vaccine that incorporates a triple fusion antigen AER together with two molecular adjuvants CpG and MPLA. pH-sensitive liposomes are a unique class of liposomes that respond to changes in pH in the microenvironment, which has many applications, notably allowing endosomal escape and intracellular delivery of antigens. To the best of our knowledge, this is the first report on the application of pH-sensitive liposomes for protein-based antigen delivery for TB vaccination. In this study, we explored the effectiveness of such a vaccine and whether pH-sensitive liposomes are suitable for further TB vaccine development.

Protection is the main goal of prophylactic vaccination. AER antigen was previously studied by Commandeur et al. and showed the protective effects of a 25 µg AER mixed with CAF09 adjuvant in HLA-DR3 transgenic mice (C57BL/10 background). In

this study, vaccination with AER encapsulated in a DOPC:DOPE:DOBAQ:EPC/MPLA/CpG adjuvant significantly reduced a bacterial load in lungs and spleens of Mtb-infected mice. This vaccine was also more effective than 25 μg AER solution mixed with 50 μg CpG and 1 μg MPLA.

Th1 cells, particularly $CD4^+$ T-cells, play a critical role in immunity against Mtb by producing cytokines and mediating immune responses.[5,44–46] The hallmark cytokine IFNγ is involved in macrophage activation, $CD8^+$ T-cell differentiation, and B-cell activation,[47,48] while TNFα acts synergistically with IFNγ to induce reactive nitrogen species in macrophages, promotes immune cell migration, and modulates granuloma formation.[49] These roles are substantiated by observations of increased susceptibility to BCG infection in infants with IFNγ receptor gene mutations[50] and higher TB reactivation risk in individuals taking TNFα antagonists.[51] IL-2, produced by activated T-cells, stimulates lymphocyte differentiation and proliferation, enhancing cellular immunity,[52] and its low-dose therapy can improve TB symptoms.[53] Vaccination studies in mice[54–56] and humans[57] support the notion of the superior role of polyfunctional T-cells secreting IL-2, TNFα, and IFNγ.[58,59] However, contradicting data question their protective role in TB,[60–63] as well as the association of IFNγ production with vaccine-induced TB protection and Mtb killing.[64–66]

Our data showed higher polyfunctional $CD4^+$ T-cell counts in mice vaccinated with AER mixed with CpG and MPLA, and AER in a pH-sensitive liposomal formulation compared to naïve and BCG-vaccinated mice. These prevalent T-cells expressed CD62L but not CD44 or CCR7, suggesting they may represent a distinct central memory T-cell subset that has shed CD44[67] Such cells were reported to display significant expansion and conferred excellent protection when transferred to $Rag^{-/-}$ mice exposed to Mtb H37Rv aerosol but this was not observed for $CD4^+$ $CD44^{hi}$ $CD62L^{lo}$ cells.[68] $CD4^+$ $CD44^{lo}$ $CD62L^{hi}$ cells likely represent a crucial cell reservoir capable of inducing protection, consistent with a central memory phenotype. We also noted an increase in single functional $IFN\gamma^+$ $CD4^+$ T-cells expressing CCR7, hinting at another central memory subset.[67] In contrast, $CD4^+$ $IL\text{-}2^+$ $IFN\gamma^-$ $TNF\alpha^-$ $CCR7^+$ T-cells were increased by BCG and AER mix, but not by the liposomal vaccine.

Th17 cells, $CD4^+$ T-cells that produce IL-17, play a significant role in the early stages of Mtb protection by recruiting neutrophils and Th1 cells to infection sites, facilitating the formation of mature granuloma and protection.[5,44–46] Despite their contribution

to the initial response in high-dose aerosol Mtb-infected mice,[69] the efficacy of Th17 cells in Mtb protection is disputed. IL-17 deficient or receptor-deficient mice can control Mtb comparably to normal mice, and Th17 responses may not provide adequate protection,[70] and potentially contribute to worsening lung pathology.[71–73] In our data, no increase in Th17 cells was observed following any tested vaccines.

Cytotoxic $CD8^+$ T-cells play a role in protection against Mtb; however, their role is debated. Apart from their main biological function of directly killing infected cells, they also can produce cytokines, modulate host immune response, and work synergistically with Th1 cells.[47,74] It has been proposed that $CD8^+$ T-cells next to Th1 cells are an interesting target for new vaccines against Mtb.[5,75,76] This view is supported by numerous mice studies showing that depletion of $CD8^+$ T-cells using antibodies increased susceptibility to Mtb,[77,78] and genetic knockout experiments demonstrated that they are necessary for the Mtb control.[79–82] In latency, depletion of $CD8^+$ but not $CD4^+$ T-cells resulted in an increase in bacterial burden, signifying their critical role in chronic phases of infection in mice [83] and in non-human primates.[84]

In this study, we observed increased counts of $CD8^+$ T-cells and several populations of polyfunctional cells compared to naïve and BCG-vaccinated mice. The largest population observed was a polyfunctional $CD8^+$ T-cell population that displayed a central memory phenotype similar to that observed in the $CD4^+$ T-cell arm. We also found a subpopulation of these cells that expressed the CD69 marker, which suggests that a fraction of these cells is readily activated upon AER restimulation. Noteworthy, we observed increased IL-17A-producing $CD8^+$ T-cells. It is believed that such cells (Tc17) play a similar role to Th17 cells;[85,86] however, more research is needed to determine their contribution to immune responses against Mtb infection.

B-cell and antibody responses play a role in tuberculosis (TB) immunity, though this is not fully clear yet.[59,87] B-cells may help combat TB through various strategies such as cytokine production, MHC class II antigen presentation, immune regulation and Mtb neutralization, to mention a few.[87] Evidence supporting B-cell involvement includes the high numbers of B-cells in infected lung tissues in mice, non-human primates, and humans,[88,89] heightened susceptibility to Mtb infection in B-cell-depleted mice and non-human primates, resolved after B-cell transfer,[90–92] and B-cell dysfunction

associated with active TB in humans, which normalized after effective treatment.[93] However, this theory faces opposition from genetic knockout results,[90,92,94–99] and different Mtb infection models showing insignificant effects.[97–99]

In our current work, we observed increased subsets of B-cells in splenocyte cultures from mice vaccinated with AER mixed with CpG and MPLA, and the vaccine delivered in a pH-sensitive liposome. These subsets expressed activation marker CD69. We also observed subpopulations of B-cells producing TNFα, and IL-17A. B-cells were shown to influence the expansion and differentiation of Th1[100] and Th2 cells[101] through TNFα production. A study by Deepe et al. demonstrated $CD4^+$ T-cells' inability to clear *Pneumocystis murina* infection without B-cell-derived TNF.[102] B-cells producing IL-17 in response to *Trypanosoma cruzi*, were shown to be important in protection against this parasitic infection.[103] The main IL-17 producers were IgM^+ $CD138^+$ plasmablasts in early infection stages, and were necessary for infection control.[103] IL-17A-producing B-cells could play a crucial role in initial Mtb infection control, which could be further explored in future studies.

Antibodies (Abs) are suggested to contribute to protection against TB. This view is supported by successful serum therapy in Mtb-infected severe combined immunodeficient mice[104] and reduced Mtb burden through high-dose intravenous immunoglobulin in C57Bl/6 mice[105] Transfers of sera from LTBI patients and highly exposed but uninfected individuals also demonstrated protection in mice.[106] Furthermore, monoclonal Abs against specific mycobacterial antigens extended survival,[107,108] limited dissemination,[109] diminished tissue pathology,[110] and decreased mycobacterial burden.[107,110–112] In this study, we observed high total AER-specific Ig titers, as well as subtypes: IgG1, IgG2a, IgG2b, and IgG2c, and intermediate levels of IgG3 and IgM. Mice immunized with AER delivered in pH-sensitive liposomes induced higher antibody titers compared to AER mixed with CpG and MPLA, correlating with the stronger protection afforded by the liposomal vaccine. However, this difference was not statistically significant.

Our study investigated a new tuberculosis subunit vaccine's efficacy, using pH-sensitive liposomes to deliver the AER antigen. We found that it triggered protection in Mtb-challenged C57Bl/6 mice, and induced various immune responses in vaccinated mice, including differentially abundant polyfunctional T- and B-cells, and increased antigen-specific antibody titers. We discovered similar immune responses

using both AER antigen mixed with adjuvants and AER in pH-sensitive liposomes and the latter provided significantly improved protection. Notably, pH-sensitive liposome formulation used three times lower dose of antigen and twenty times lower dose of CpG indicating a significant benefit of using this vaccine delivery system. However, the protection mechanism remains unknown.

The study's key limitation is its single time point assessment, which limits the evaluation of the time-dynamic immune responses and potentially overlooks late or long-term protective effects. In future research, multiple time points should be assessed. The 7-day restimulation of lymphocytes protocol prohibited the study of early immune responses. Our study's reliance on single doses of antigen and liposome restricted understanding of dose-response relationships, and future research should explore varying doses. Likewise, the arbitrary choice and dose of adjuvants may have missed dose-dependent or adjuvant-specific effects. The main strength of this work is the connection of primary human innate responses with adaptive immune responses observed in vaccinated mice, which sheds light on the possibilities of expanding this research to other animal models and translation into human use.

5. CONCLUSIONS

In this research, a novel subunit vaccine was developed targeting TB, which remains at the top of infectious killers globally. The formulation consisted of the Ag85B-ESAT6-Rv2034 fusion antigen, two adjuvants (CpG and MPLA), and a cationic pH-sensitive liposome DOPC:DOPE:DOBAQ:EPC 3:5:2:4 as a delivery system. One of the key contributions of this study is the introduction of pH-sensitive liposomes as a delivery system for TB vaccines, which had not been previously reported. *In vivo* experiments demonstrated that the new vaccine led to a substantial reduction in Mtb bacterial load in the lungs and spleens, outperforming the results observed in mice vaccinated with the antigen mixed with adjuvants but lacking the liposome delivery system. Furthermore, the vaccine induced potent polyfunctional $CD4^+$ and $CD8^+$ T-cell responses. An increase in $CD69^+$ B-cell subpopulations was also observed. In addition to cellular responses, the vaccine stimulated robust antigen-specific antibody titers. Overall, these findings offer new insights into the application of pH-

sensitive liposomes for subunit vaccines against TB. The effectiveness of the vaccine in inducing diverse immune responses underscores its potential as an interesting candidate for future TB vaccine research.

ABBREVIATIONS

AER, Ag85B-ESAT6-Rv2034 antigen; APC, antigen-presenting cell; Ag, antigen(-adjuvant mix group); BCG, Mycobacterium bovis Bacillus Calmette–Guérin; CAF09, cationic adjuvant formulation 09;CCL, chemokine (C-C motif) ligand; CCR, C-C chemokine receptor type; CD, cluster of differentiation; CFU, colony forming unit; CpG ODN, cytosine-phosphorothioate-guanine oligodeoxynucleotides; CXCL, chemokine (C-X-C motif) ligand; CXCR, C-X-C motif chemokine receptor; DC, dendritic cell; DOBAQ, N-(4-carboxybenzyl)-N,N-dimethyl-2,3-bis(oleoyloxy) propan-1-aminium; DOPC, 1,2-dioleoyl-sn-glycero-3-phosphocholine; DOPE, 1,2-dioleoyl-sn-glycero-3-phosphoethanolamine; EPC, 1,2-dioleoyl-sn-glycero-3-ethylphosphocholine; FBS, fetal bovine serum; FDR, false discovery rate; GM-CSF, granulocyte-macrophage colony-stimulating factor; HLA, human leukocyte antigen; HRP, horse radish peroxide; IFN, interferon; Ig, immunoglobulin, IL, interleukin; i.n., intranasal; IQR, interquartile range; KLRG1, killer cell lectin-like receptor subfamily G member 1; MACS, magnetic cell isolation; M-CSF, macrophage colony-stimulating factor; LAL, limulus amebocyte lysate; LUMC, Leiden University Medical Center; MDDC, monocyte-derived dendritic cell; MHC, major histocompatibility complex; MPLA, monophosphoryl lipid A; Mtb, mycobacterium tuberculosis; PAMP, pathogen-associated molecular pattern; PBMC, peripheral blood mononuclear cell; PCR, polymerase chain reaction; PD-1, programmed cell death protein 1; PDI, polydispersity index; PE, phosphatidylethanolamine; pH, pH-sensitive liposome group; rpm, rounds per minute; s.c., subcutaneous; TB, tuberculosis; Th1/Th2/Th17, type 1/2/17 helper T-cell; TLR, Toll-like receptor; TNF, tumor necrosis factor; UMAP, uniform manifold approximation and projection.

APPENDICES

Supplementary materials

CREDIT AUTHOR STATEMENT

M.M. Szachniewicz: Conceptualization, Methodology, Formal Analysis, Investigation, Writing – Original Draft. **S.J.F. van den Eeden**: Conceptualization, Methodology, Investigation, Writing – Original Draft. **K.E. van Meijgaarden**: Conceptualization, Methodology, Writing – Review & Editing, Supervision. **K.L.M.C. Franken**: Methodology, Investigation, Resources. **S. van Veen**: Methodology, Formal Analysis. **A. Geluk**: Conceptualization, Writing – Review & Editing, Project Administration, Funding Acquisition, Supervision. **J.A. Bouwstra**: Conceptualization, Writing – Review & Editing, Project Administration, Funding Acquisition, Supervision. T**.H.M. Ottenhoff**: Conceptualization, Writing – Review & Editing, Project Administration, Funding Acquisition, Primary supervision.

FUNDING

This work was supported by the Dutch Research Council (NWO) Domain Applied and Engineering Sciences grant, project number: 15240.

DECLARATIONS OF INTEREST

None.

REFERENCES

1. World Health Organization. *Global Tuberculosis Report 2022*. (2022).
2. World Health Organization. *Global Tuberculosis Report 2023*. (2023).
3. World Health Organization. The end TB strategy. (2015).
4. Brewer, T. F. Preventing Tuberculosis with Bacillus Calmette-Guérin Vaccine: A Meta-Analysis of the Literature. *Clinical Infectious Diseases* 31, S64–S67 (2000).
5. Ottenhoff, T. H. M. & Kaufmann, S. H. E. Vaccines against Tuberculosis: Where Are We and Where Do We Need to Go? *PLoS Pathogens* 8, e1002607 (2012).
6. Fatima, S. *et al.* Tuberculosis vaccine: A journey from BCG to present. *Life Sciences* 252, 117594 (2020).
7. Andersen, P. & Scriba, T. J. Moving tuberculosis vaccines from theory to practice. *Nature Reviews Immunology* 19:9, 550–562 (2019).
8. Christensen, D. *et al.* Cationic liposomes as vaccine adjuvants. *Expert Review of Vaccines* 10, 513–521 (2011).

9. Liu, X. *et al.* A novel liposome adjuvant DPC mediates Mycobacterium tuberculosis subunit vaccine well to induce cell-mediated immunity and high protective efficacy in mice. *Vaccine* 34, 1370–1378 (2016).
10. Inglut, C. T. *et al.* Immunological and Toxicological Considerations for the Design of Liposomes. *Nanomaterials* 10:2, 190 (2020).
11. Shah, S. *et al.* Liposomes: Advancements and innovation in the manufacturing process. *Advanced Drug Delivery Reviews* 154, 102–122 (2020).
12. Bozzuto, G. & Molinari, A. Liposomes as nanomedical devices. *International Journal of Nanomedicine* 10, 975 (2015).
13. Karanth, H. & Murthy, R. S. R. pH-Sensitive liposomes-principle and application in cancer therapy. *Journal of Pharmacy and Pharmacology* 59, 469–483 (2007).
14. Momekova, D. *et al.* Long-Circulating, pH-Sensitive Liposomes. *Methods in Molecular Biology* 1522, 209–226 (2017).
15. Mu, Y. *et al.* Advances in pH-responsive drug delivery systems. *OpenNano* 5, 100031 (2021).
16. Balamurali, V. *et al.* pH Sensitive Drug Delivery Systems: A Review. *American Journal of Drug Discovery and Development* 1, 24–48 (2010).
17. Fehres, C. M. *et al.* Understanding the biology of antigen cross-presentation for the design of vaccines against cancer. *Frontiers in Immunology* 5, 149 (2014).
18. Melero, I. *et al.* Therapeutic vaccines for cancer: an overview of clinical trials. *Nature Reviews Clinical Oncology 2014 11:9* 11, 509–524 (2014).
19. Paliwal, S. R. *et al.* A review of mechanistic insight and application of pH-sensitive liposomes in drug delivery. *Drug delivery* 22:3, 231–242 (2015).
20. Liu, X. & Huang, G. Formation strategies, mechanism of intracellular delivery and potential clinical applications of pH-sensitive liposomes. *Asian Journal of Pharmaceutical Sciences* 8, 319–328 (2013).
21. Abri Aghdam, M. *et al.* Recent advances on thermosensitive and pH-sensitive liposomes employed in controlled release. *Journal of Controlled Release* 315, 1–22 (2019).
22. Ferreira, D. D. S. *et al.* pH-sensitive liposomes for drug delivery in cancer treatment. *Therapeutic Delivery* 4, 1099–1123 (2013).
23. Gupta, M. *et al.* pH-sensitive liposomes. *Liposomal Delivery Systems: Advances and Challenges* 1, 74–86 (2015).

24. Commandeur, S. *et al.* Double- and monofunctional CD4+ and CD8+ T-cell responses to Mycobacterium tuberculosis DosR antigens and peptides in long-term latently infected individuals. *European Journal of Immunology* 41, 2925–2936 (2011).
25. Commandeur, S. *et al.* The in vivo expressed Mycobacterium tuberculosis (IVE-TB) antigen Rv2034 induces CD4+ T-cells that protect against pulmonary infection in HLA-DR transgenic mice and guinea pigs. *Vaccine* 32, 3580–3588 (2014).
26. Luabeya, A. K. K. *et al.* First-in-human trial of the post-exposure tuberculosis vaccine H56:IC31 in Mycobacterium tuberculosis infected and non-infected healthy adults. *Vaccine* 33, 4130–4140 (2015).
27. Commandeur, S. *et al.* An Unbiased Genome-Wide Mycobacterium tuberculosis Gene Expression Approach To Discover Antigens Targeted by Human T Cells Expressed during Pulmonary Infection. *The Journal of Immunology* 190, 1659–1671 (2013).
28. Ko, E. J. *et al.* MPL and CpG combination adjuvants promote homologous and heterosubtypic cross protection of inactivated split influenza virus vaccine. *Antiviral Research* 156, 107–115 (2018).
29. Todoroff, J. *et al.* Mucosal and Systemic Immune Responses to Mycobacterium tuberculosis Antigen 85A following Its Co-Delivery with CpG, MPLA or LTB to the Lungs in Mice. *PLoS One* 8, e63344 (2013).
30. Meraz, I. M. *et al.* Adjuvant cationic liposomes presenting MPL and IL-12 induce cell death, suppress tumor growth, and alter the cellular phenotype of tumors in a murine model of breast cancer. *Molecular Pharmaceutics* 11, 3484–3491 (2014).
31. Kruit, W. H. J. *et al.* Selection of immunostimulant AS15 for active immunization with MAGE-A3 protein: results of a randomized phase II study of the European Organisation for Research and Treatment of Cancer Melanoma Group in Metastatic Melanoma. *Journal of Clinical Oncology* 31, 2413–2420 (2013).
32. Vansteenkiste, J. F. *et al.* Efficacy of the MAGE-A3 cancer immunotherapeutic as adjuvant therapy in patients with resected MAGE-A3-positive non-small-cell lung cancer (MAGRIT): a randomised, double-blind, placebo-controlled, phase 3 trial. *Lancet Oncology* 17, 822–835 (2016).

33. Dreno, B. *et al.* MAGE-A3 immunotherapeutic as adjuvant therapy for patients with resected, MAGE-A3-positive, stage III melanoma (DERMA): a double-blind, randomised, placebo-controlled, phase 3 trial. *Lancet Oncology* 19, 916–929 (2018).
34. Kruit, W. H. *et al.* Immunization with recombinant MAGE-A3 protein combined with adjuvant systems AS15 or AS02B in patients with unresectable and progressive metastatic cutaneous melanoma: A randomized open-label phase II study of the EORTC Melanoma Group (16032- 18031). *Journal of Clinical Oncology* 26, 9065–9065 (2008).
35. Gutzmer, R. *et al.* Safety and immunogenicity of the PRAME cancer immunotherapeutic in metastatic melanoma: results of a phase I dose escalation study. *ESMO Open* 1, e000068 (2016).
36. Franken, K. L. M. C. *et al.* Purification of His-Tagged Proteins by Immobilized Chelate Affinity Chromatography: The Benefits from the Use of Organic Solvent. *Protein Expression and Purification* 18, 95–99 (2000).
37. Szachniewicz, M. M. *et al.* Intrinsic immunogenicity of liposomes for tuberculosis vaccines: effect of cationic lipid and cholesterol. *European Journal of Pharmaceutical Sciences* 195, 106730 (2024).
38. Geluk, A. *et al.* A multistage-polyepitope vaccine protects against Mycobacterium tuberculosis infection in HLA-DR3 transgenic mice. *Vaccine* 30, 7513–7521 (2012).
39. R Core Team. R: A language and environment for statistical computing. (2023).
40. RStudio Team. RStudio: Integrated Development Environment for R. (2023).
41. Marzio, R., Mauël, J. & Betz-Corradin, S. CD69 and regulation of the immune function. *Immunopharmacology and Immunotoxicology* 21, 565–582 (1999).
42. Pillai, S. & Cariappa, A. The follicular versus marginal zone B lymphocyte cell fate decision. *Nature Reviews Immunology 2009 9:11* 9, 767–777 (2009).
43. Kleiman, E. *et al.* Distinct transcriptomic features are associated with transitional and mature B-cell populations in the mouse spleen. *Frontiers in Immunology* 6, 126060 (2015).
44. Flynn, J. A. L. Immunology of tuberculosis and implications in vaccine development. *Tuberculosis* 84, 93–101 (2004).
45. Ernst, J. D. The immunological life cycle of tuberculosis. *Nature Reviews Immunology 2012 12:8* 12, 581–591 (2012).

46. Ottenhoff, T. H. M. *et al.* Human CD4 and CD8 T Cell Responses to Mycobacterium tuberculosis: Antigen Specificity, Function, Implications and Applications. *Handbook of Tuberculosis* 119–155 (2008).
47. Prezzemolo, T. *et al.* Functional signatures of human CD4 and CD8 T cell responses to Mycobacterium tuberculosis. *Frontiers in Immunology* 5, 83298 (2014).
48. Tau, G. & Rothman, P. Biologic functions of the IFN-γ receptors. *Allergy* 54, 1233–1251 (1999).
49. Cavalcanti, Y. V. N. *et al.* Role of TNF-alpha, IFN-gamma, and IL-10 in the development of pulmonary tuberculosis. *Pulmonary Medicine* 2012:1, 745483 (2012).
50. Ottenhoff, T. H. M. *et al.* Genetics, cytokines and human infectious disease: lessons from weakly pathogenic mycobacteria and salmonellae. *Nature Genetics 2002 32:1* 32, 97–105 (2002).
51. Toussirot, É. & Wending, D. The use of TNF-α blocking agents in rheumatoid arthritis: an update. *Expert Opinion on Pharmacotherapy* 8, 2089–2107 (2007).
52. Kelso, A. *et al.* Interleukin 2 enhancement of lymphokine secretion by T lymphocytes: analysis of established clones and primary limiting dilution microcultures. *The Journal of Immunology* 132, 2932–2938 (1984).
53. Johnson, B. J. *et al.* Clinical and immune responses of tuberculosis patients treated with low-dose IL-2 and multidrug therapy. *Cytokines and Molecular Therapy* 1, 185–196 (1995).
54. Aagaard, C. *et al.* A multistage tuberculosis vaccine that confers efficient protection before and after exposure. *Nature Medicine* 17:2, 189–194 (2011).
55. Derrick, S. C. *et al.* Vaccine-induced anti-tuberculosis protective immunity in mice correlates with the magnitude and quality of multifunctional CD4 T cells. *Vaccine* 29, 2902–2909 (2011).
56. Lindenstrøm, T. *et al.* Tuberculosis Subunit Vaccination Provides Long-Term Protective Immunity Characterized by Multifunctional CD4 Memory T Cells. *The Journal of Immunology* 182, 8047–8055 (2009).
57. Abel, B. *et al.* The Novel Tuberculosis Vaccine, AERAS-402, Induces Robust and Polyfunctional CD4+ and CD8+ T Cells in Adults. *American Journal of Respiratory and Critical Care Medicine* 181, 1407–1417 (2012).

58. Counoupas, C. *et al.* Deciphering protective immunity against tuberculosis: implications for vaccine development. *Expert Review of Vaccines* 18, 353–364 (2019).
59. Duong, V. T. *et al.* Towards the development of subunit vaccines against tuberculosis: The key role of adjuvant. *Tuberculosis* 139, 102307 (2023).
60. Harari, A. *et al.* Dominant TNF-α+ Mycobacterium tuberculosis–specific CD4+ T cell responses discriminate between latent infection and active disease. *Nature Medicine 2011 17:3* 17, 372–376 (2011).
61. Caccamo, N. *et al.* Multifunctional CD4+ T cells correlate with active Mycobacterium tuberculosis infection. *European Journal of Immunology* 40, 2211–2220 (2010).
62. Sutherland, J. S. *et al.* Pattern and diversity of cytokine production differentiates between Mycobacterium tuberculosis infection and disease. *European Journal of Immunology* 39, 723–729 (2009).
63. Lewinsohn, D. A. *et al.* Polyfunctional CD4+ T cells as targets for tuberculosis vaccination. *Frontiers in Immunology* 8, 295382 (2017).
64. Cowley, S. C. & Elkins, K. L. CD4+ T Cells Mediate IFN-γ-Independent Control of Mycobacterium tuberculosis Infection Both In Vitro and In Vivo. *The Journal of Immunology* 171, 4689–4699 (2003).
65. Gallegos, A. M. *et al.* A Gamma Interferon Independent Mechanism of CD4 T Cell Mediated Control of M. tuberculosis Infection in vivo. *PLoS Pathogens* 7, e1002052 (2011).
66. You, Q. *et al.* Subcutaneous Administration of Modified Vaccinia Virus Ankara Expressing an Ag85B-ESAT6 Fusion Protein, but Not an Adenovirus-Based Vaccine, Protects Mice Against Intravenous Challenge with Mycobacterium tuberculosis. *Scandinavian Journal of Immunology* 75, 77–84 (2012).
67. Henao-Tamayo, M. I. *et al.* Phenotypic definition of effector and memory T-lymphocyte subsets in mice chronically infected with mycobacterium tuberculosis. *Clinical and Vaccine Immunology* 17, 618–625 (2010).
68. Kipnis, A. *et al.* Memory T Lymphocytes Generated by Mycobacterium bovis BCG Vaccination Reside within a CD4 CD44lo CD62 Ligandhi Population. *Infection and Immunity* 73, 7759 (2005).
69. Khader, S. A. *et al.* IL-23 and IL-17 in the establishment of protective pulmonary CD4+ T cell responses after vaccination and during Mycobacterium tuberculosis challenge. *Nature Immunology* 8:4, 369–377 (2007).

70. Ashhurst, A. S. *et al.* PLGA particulate subunit tuberculosis vaccines promote humoral and Th17 responses but do not enhance control of Mycobacterium tuberculosis infection. *PLoS One* 13, e0194620 (2018).
71. Cruz, A. *et al.* Pathological role of interleukin 17 in mice subjected to repeated BCG vaccination after infection with Mycobacterium tuberculosis. *Journal of Experimental Medicine* 207, 1609–1616 (2010).
72. Turner, J. *et al.* Effective preexposure tuberculosis vaccines fail to protect when they are given in an immunotherapeutic mode. *Infection and Immunity* 68, 1706–1709 (2000).
73. Taylor, J. L. *et al.* Pulmonary necrosis resulting from DNA vaccination against tuberculosis. *Infection and Immunity* 71, 2192–2198 (2003).
74. Lu, Y. J. *et al.* CD4 T cell help prevents CD8 T cell exhaustion and promotes control of Mycobacterium tuberculosis infection. *Cell Reports* 36, 109696 (2021).
75. Behar, S. M. *et al.* Next generation: tuberculosis vaccines that elicit protective CD8+ T cells. *Expert Review of Vaccines* 6, 441–456 (2007).
76. Boom, W. H. New TB vaccines: is there a requirement for CD8+ T cells? *Journal of Clinical Investigation* 117, 2092–2094 (2007).
77. Woodworth, J. S. *et al.* Mycobacterium tuberculosis-Specific CD8+ T Cells Require Perforin to Kill Target Cells and Provide Protection In Vivo. *The Journal of Immunology* 181, 8595–8603 (2008).
78. Mogues, T. *et al.* The Relative Importance of T Cell Subsets in Immunity and Immunopathology of Airborne Mycobacterium tuberculosis Infection in Mice. *Journal of Experimental Medicine* 193, 271–280 (2001).
79. Orme, I. M. The kinetics of emergence and loss of mediator T lymphocytes acquired in response to infection with Mycobacterium tuberculosis. *The Journal of Immunology* 138, 293–298 (1987).
80. Flynn, J. L. *et al.* Major histocompatibility complex class I-restricted T cells are required for resistance to Mycobacterium tuberculosis infection. *Proceedings of the National Academy of Sciences* 89, 12013–12017 (1992).
81. Sousa, A. O. *et al.* Relative contributions of distinct MHC class I-dependent cell populations in protection to tuberculosis infection in mice. *Proceedings of the National Academy of Sciences* 97, 4204–4208 (2000).

82. Behar, S. M. *et al.* Susceptibility of Mice Deficient in CD1D or TAP1 to Infection with Mycobacterium tuberculosis. *Journal of Experimental Medicine* 189, 1973–1980 (1999).
83. Van Pinxteren, L. A. H. *et al.* Control of latent Mycobacterium tuberculosis infection is dependent on CD8 T cells. *European Journal of Immunology* 30, 3689–3698 (2000).
84. Lin, P. L. *et al.* CD4 T Cell Depletion Exacerbates Acute Mycobacterium tuberculosis While Reactivation of Latent Infection Is Dependent on Severity of Tissue Depletion in Cynomolgus Macaques. *AIDS Research and Human Retroviruses* 28, 1693–1702 (2012).
85. Mills, K. H. G. IL-17 and IL-17-producing cells in protection versus pathology. *Nature Reviews Immunology 2022 23:1* 23, 38–54 (2022).
86. Ciric, B. *et al.* IL-23 Drives Pathogenic IL-17-Producing CD8+ T Cells. *The Journal of Immunology* 182, 5296–5305 (2009).
87. Rijnink, W. F. *et al.* B-Cells and Antibodies as Contributors to Effector Immune Responses in Tuberculosis. *Frontiers in Immunology* 12, 640168 (2021).
88. Phuah, J. Y. *et al.* Activated B Cells in the Granulomas of Nonhuman Primates Infected with Mycobacterium tuberculosis. *American Journal of Pathology* 181, 508–514 (2012).
89. Tsai, M. C. *et al.* Characterization of the tuberculous granuloma in murine and human lungs: cellular composition and relative tissue oxygen tension. *Cell Microbiology* 8, 218–232 (2006).
90. Maglione, P. J. *et al.* B Cells Moderate Inflammatory Progression and Enhance Bacterial Containment upon Pulmonary Challenge with Mycobacterium tuberculosis. *The Journal of Immunology* 178, 7222–7234 (2007).
91. Phuah, J. *et al.* Effects of B cell depletion on early Mycobacterium tuberculosis infection in cynomolgus macaques. *Infection and Immunity* 84, 1301–1311 (2016).
92. Vordermeier, H. M. *et al.* Increase of tuberculous infection in the organs of B cell-deficient mice. *Clinical & Experimental Immunology* 106, 312–316 (2003).
93. Joosten, S. A. *et al.* Patients with Tuberculosis Have a Dysfunctional Circulating B-Cell Compartment, Which Normalizes following Successful Treatment. *PLoS Pathogens* 12, e1005687 (2016).

94. Khera, A. K. *et al.* Role of B Cells in Mucosal Vaccine–Induced Protective CD8+ T Cell Immunity against Pulmonary Tuberculosis. *The Journal of Immunology* 195, 2900–2907 (2015).
95. Kozakiewicz, L. *et al.* B Cells Regulate Neutrophilia during Mycobacterium tuberculosis Infection and BCG Vaccination by Modulating the Interleukin-17 Response. *PLoS Pathogens* 9, e1003472 (2013).
96. Torrado, E. *et al.* Differential and Site Specific Impact of B Cells in the Protective Immune Response to Mycobacterium tuberculosis in the Mouse. *PLoS One* 8, e61681 (2013).
97. Turner, J. *et al.* The progression of chronic tuberculosis in the mouse does not require the participation of B lymphocytes or interleukin-4. *Experimental Gerontology* 36, 537–545 (2001).
98. Bosio, C. M. *et al.* Infection of B Cell-Deficient Mice with CDC 1551, a Clinical Isolate of Mycobacterium tuberculosis: Delay in Dissemination and Development of Lung Pathology. *The Journal of Immunology* 164, 6417–6425 (2000).
99. Johnson, C. M. *et al.* Mycobacterium tuberculosis aerogenic rechallenge infections in B cell-deficient mice. *Tubercle and Lung Disease* 78, 257–261 (1997).
100. Menard, L. C. *et al.* B Cells Amplify IFN-γ Production By T Cells via a TNF-α-Mediated Mechanism. *The Journal of Immunology* 179, 4857–4866 (2007).
101. Wojciechowski, W. *et al.* Cytokine-Producing Effector B Cells Regulate Type 2 Immunity to H. polygyrus. *Immunity* 30, 421–433 (2009).
102. Opata, M. M. *et al.* B Cell Production of Tumor Necrosis Factor in Response to Pneumocystis murina Infection in Mice. *Infection and Immunity* 81, 4252 (2013).
103. Bermejo, D. A. *et al.* Trypanosoma cruzi trans-sialidase initiates a program independent of the transcription factors RORγt and Ahr that leads to IL-17 production by activated B cells. *Nature Immunology* 14:5, 514–522 (2013).
104. Guirado, E. *et al.* Passive serum therapy with polyclonal antibodies against Mycobacterium tuberculosis protects against post-chemotherapy relapse of tuberculosis infection in SCID mice. *Microbes and Infection* 8, 1252–1259 (2006).

105. Roy, E. *et al.* Therapeutic efficacy of high-dose intravenous immunoglobulin in Mycobacterium tuberculosis infection in mice. *Infection and Immunity* 73, 6101–6109 (2005).
106. Li, H. *et al.* Latently and uninfected healthcare workers exposed to TB make protective antibodies against Mycobacterium tuberculosis. *Proceedings of the National Academy of Sciences of the United States of America* 114, 5023–5028 (2017).
107. Hamasur, B. *et al.* A mycobacterial lipoarabinomannan specific monoclonal antibody and its F(ab')2 fragment prolong survival of mice infected with Mycobacterium tuberculosis. *Clinical & Experimental Immunology* 138, 30–38 (2004).
108. Chambers, M. A. *et al.* Antibody bound to the surface antigen MPB83 of Mycobacterium bovis enhances survival against high dose and low dose challenge. *FEMS Immunology and Medical Microbiology* 41, 93–100 (2004).
109. Pethe, K. *et al.* The heparin-binding haemagglutinin of M. tuberculosis is required for extrapulmonary dissemination. *Nature* 412:6843, 190–194 (2001).
110. López, Y. *et al.* Induction of a protective response with an IgA monoclonal antibody against Mycobacterium tuberculosis 16 kDa protein in a model of progressive pulmonary infection. *International Journal of Medical Microbiology* 299, 447–452 (2009).
111. Zimmermann, N. *et al.* Human isotype-dependent inhibitory antibody responses against Mycobacterium tuberculosis. *EMBO Molecular Medicine* 8, 1325–1339 (2016).
112. Balu, S. *et al.* A Novel Human IgA Monoclonal Antibody Protects against Tuberculosis. *The Journal of Immunology* 186, 3113–3119 (2011).

SUPPLEMENTARY MATERIALS

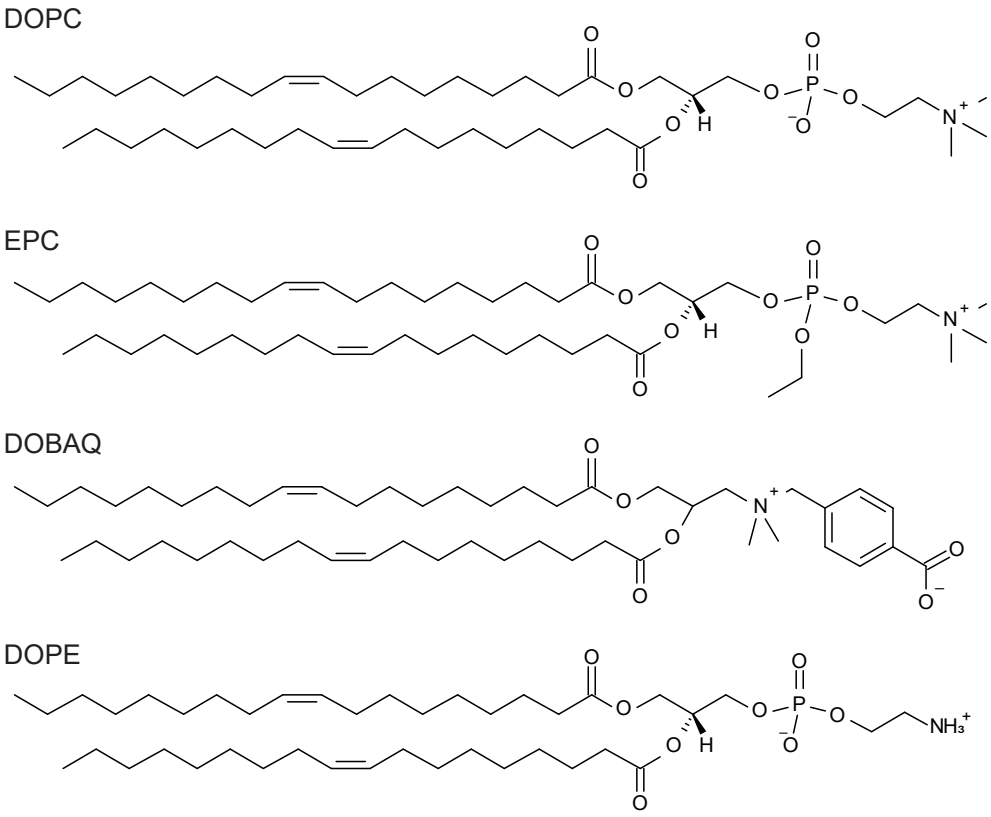

Supplementary Figure S1. Chemical structures of lipids used in the production of pH-sensitive liposomes.

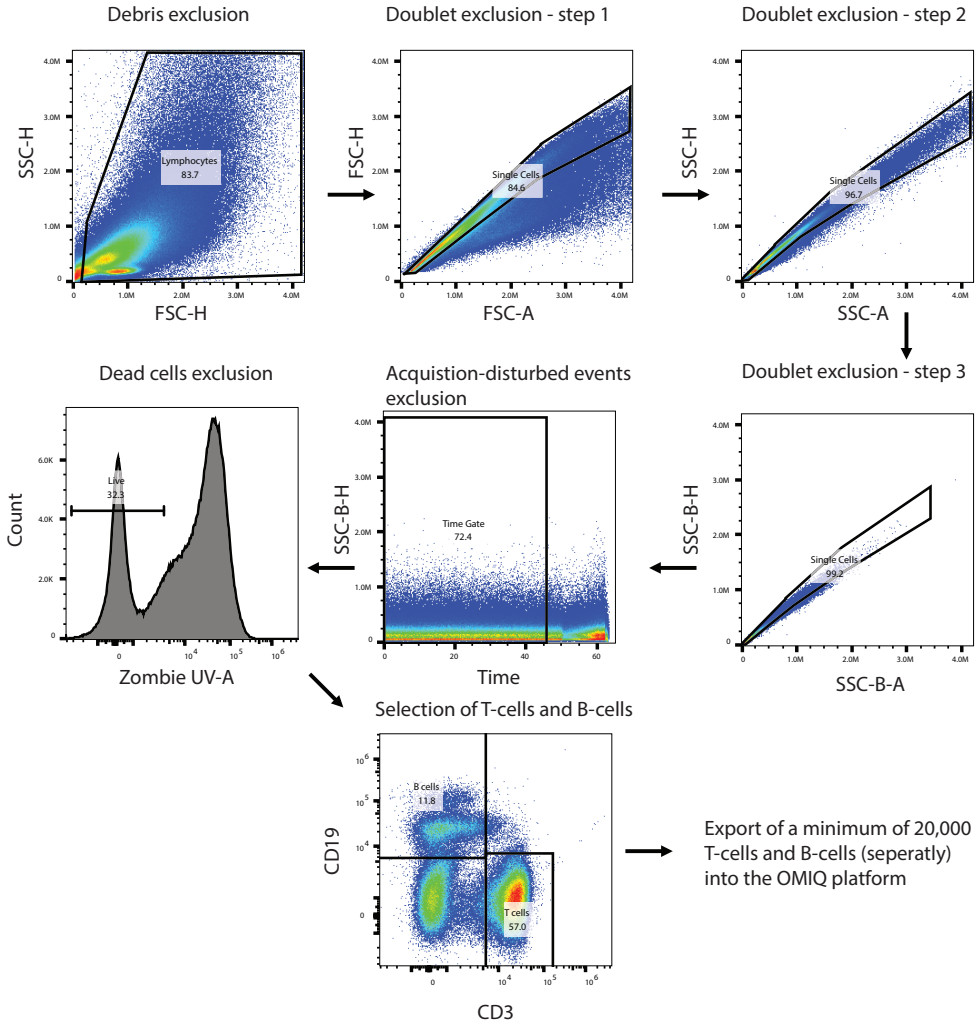

Supplementary Figure S2. Scheme of a gating strategy used to pregate data for further analysis in the OMIQ platform.

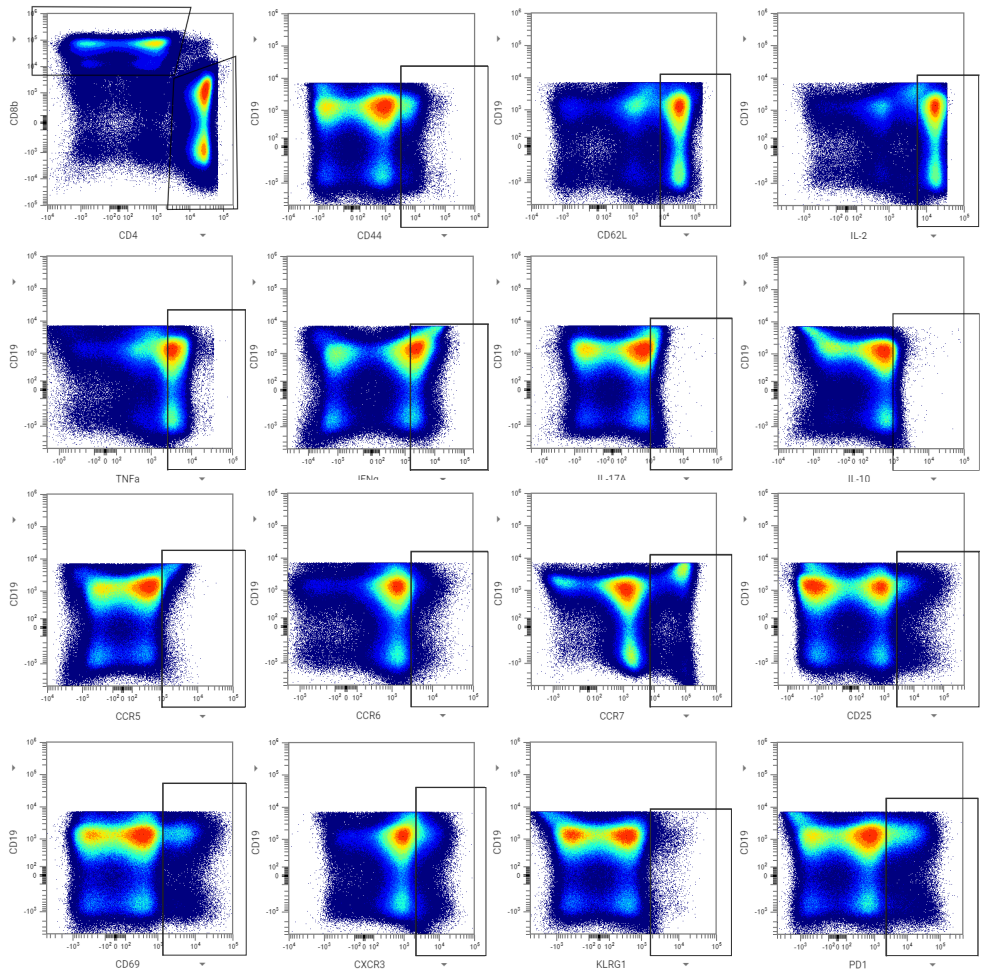

Supplementary Figure S3. Gates used for the creation of Boolean gates for the analysis of T-cell subsets.

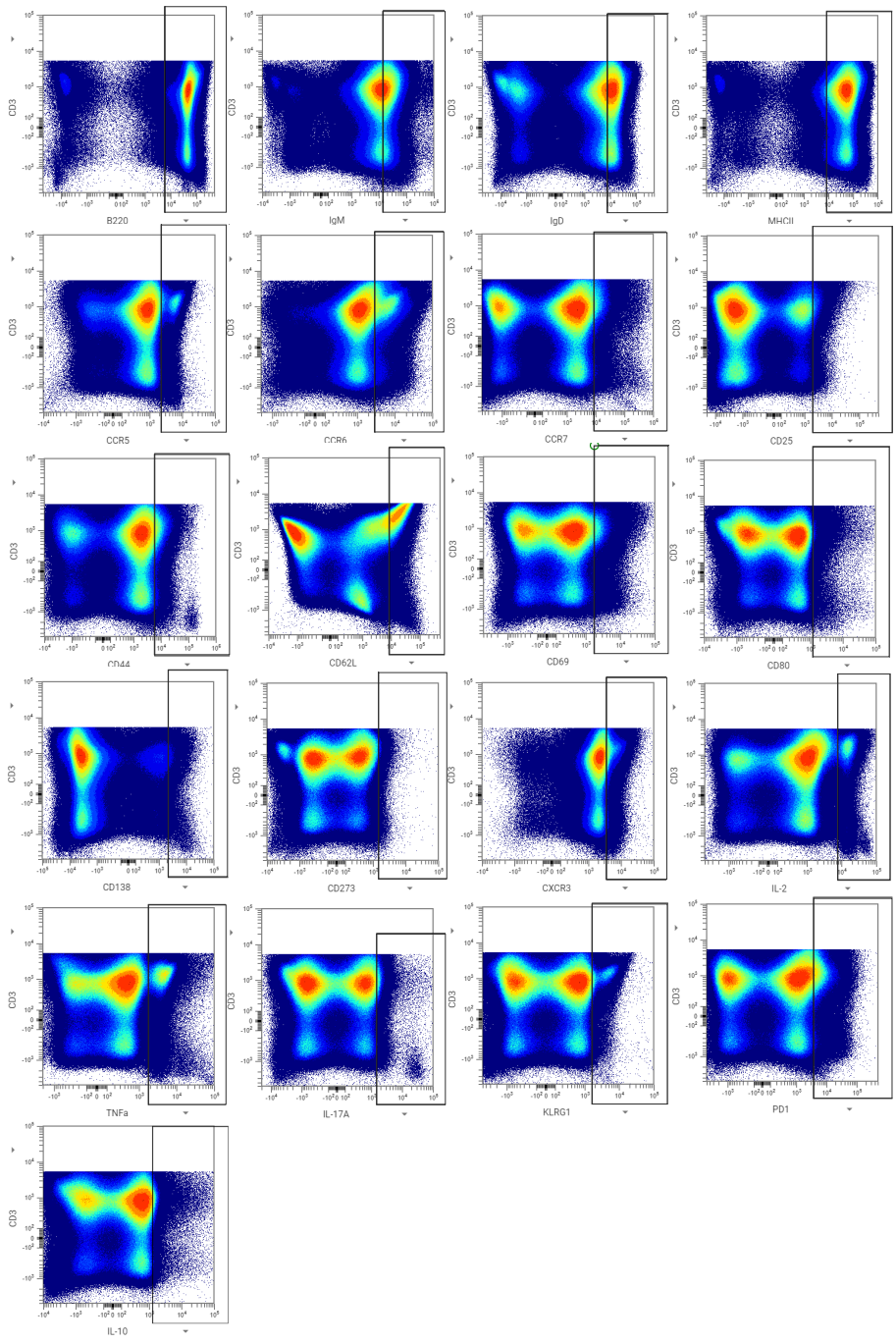

Supplementary Figure S4. Gates used for the creation of Boolean gates for the analysis of B-cell subsets.

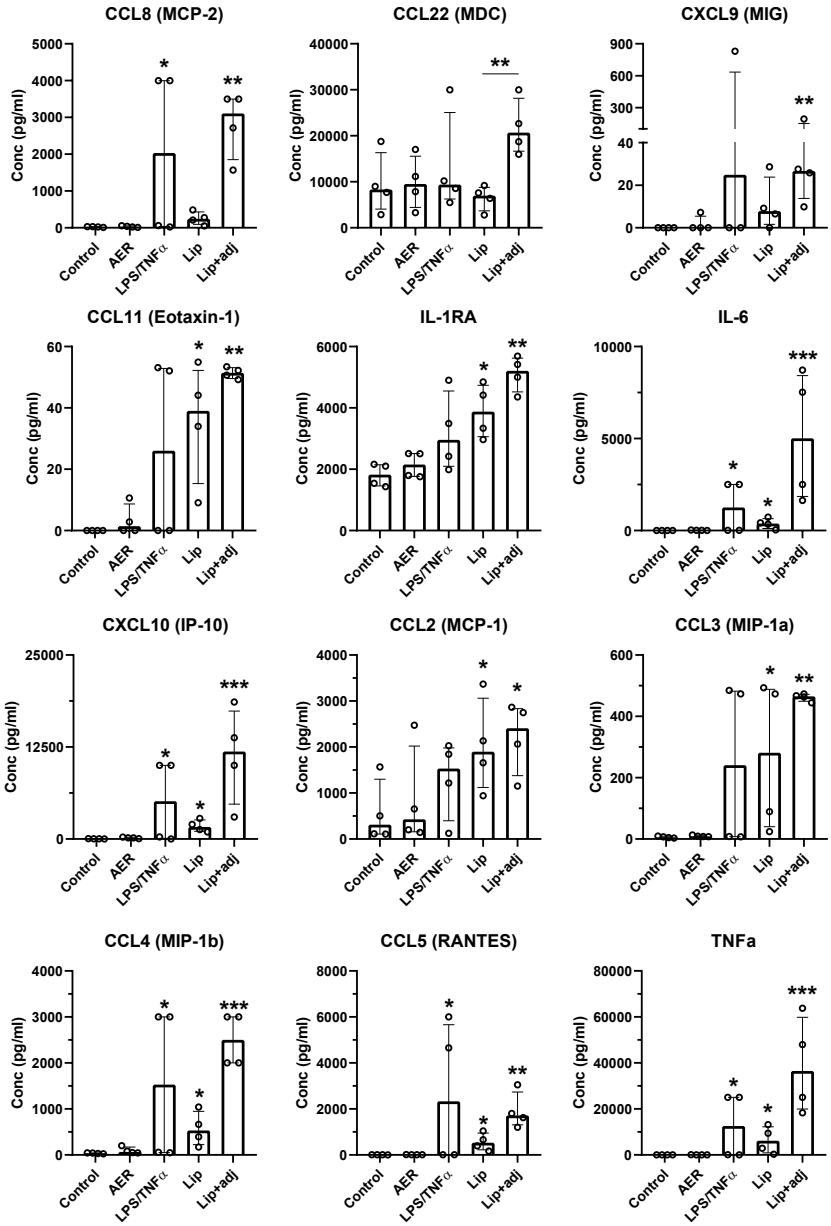

Supplementary Figure S5. Production of cytokines by MDDCs exposed to liposomal formulations (5 µg/ml AER, 250 µg/ml liposomes, exposure 1 h), Lip – unadjuvanted formulation, and Lip+adj – adjuvanted with 12.5 µg/ml CpG, and 5 µg/ml MPLA compared to control (medium only). AER - 5 µg/ml AER, exposure 1 h, LPS/TNFα - 100 and 5 ng/ml respectively, exposure 16 hours (positive control), n = 4 (cell donors). The results represent median ± IQR.

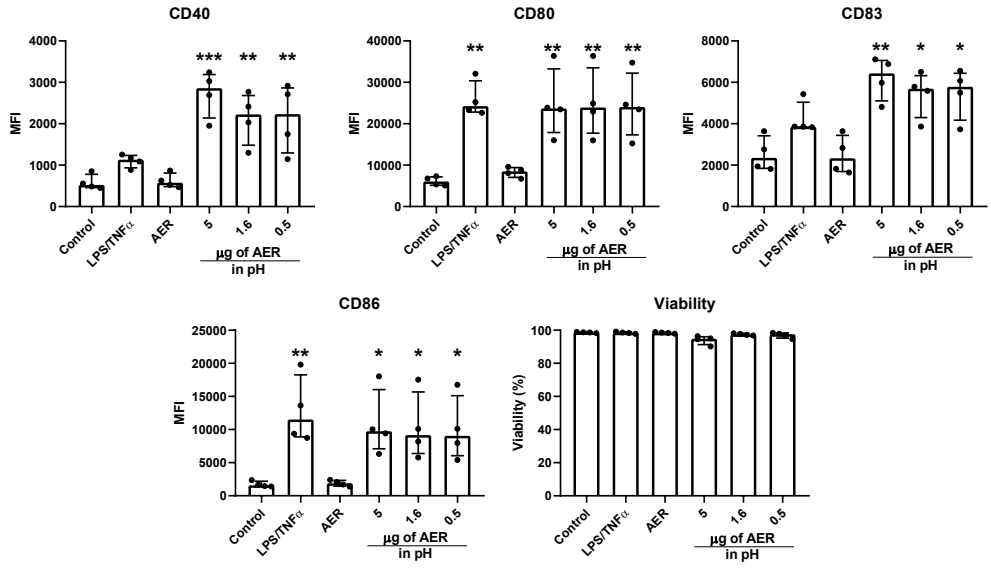

Supplementary Figure S6. Effect of the EPC:DOPE:DOBAQ:DOPC liposomes containing different doses of AER, and CpG and MPLA adjuvants on the expression of cell surface activation markers in primary human monocyte-derived dendritic cells (MDDCs). Median fluorescence intensities (MFI) related to the expression of indicated activation markers: CD40, CD80, CD83, and CD86, n = 4 (cell donors). Cell viability was calculated as a percentage of SYTOX AADvanced -negative cell population in relation to all recorded cells. Formulations were compared to (medium-only) control. The results represent median ± IQR.

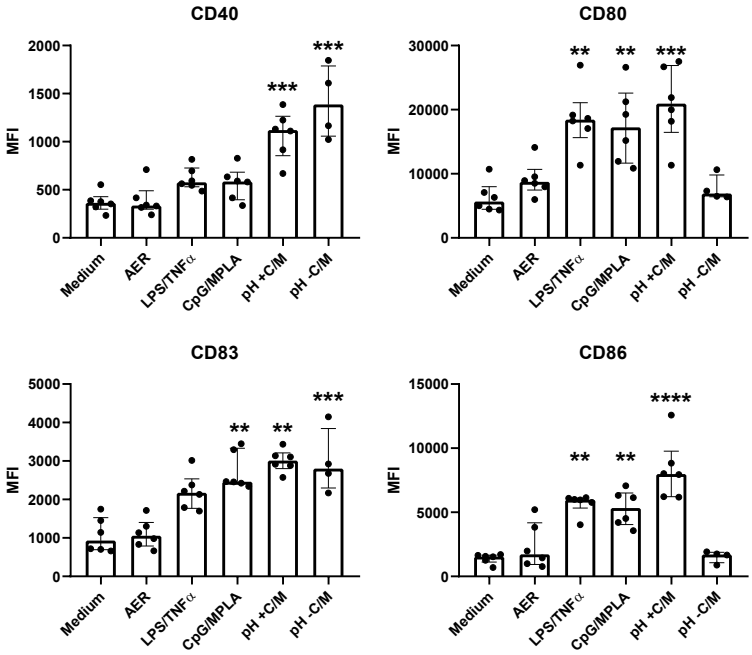

Supplementary Figure S7. Effect of the CpG and MPLA adjuvants on the immunogenicity of EPC:DOPE:DOBAQ:DOPC liposomes containing AER on the expression of cell surface activation markers in primary human monocyte-derived dendritic cells (MDDCs). Median fluorescence intensities (MFI) related to the expression of indicated activation markers: CD40, CD80, CD83, and CD86, n = 6 (cell donors). pH + C/M – liposome containing CpG and MPLA, pH - C/M – liposomes without molecular adjuvants. Formulations were compared to (medium-only) control. The results represent median ± IQR.

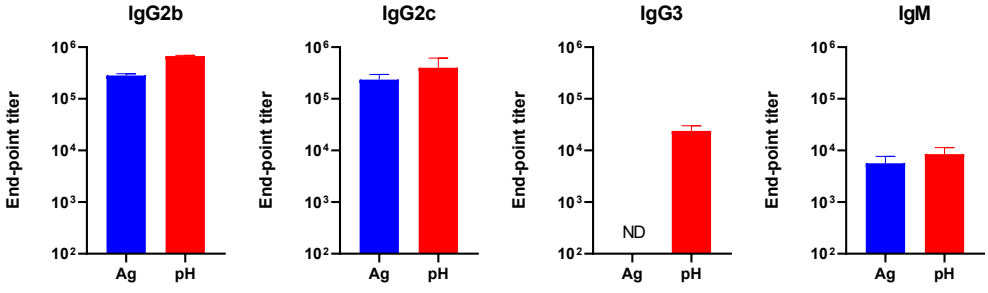

Supplementary Figure S8. Quantification of AER-specific antibodies in sera. The type of antibody measured is indicated above each graph as well as the vaccination group. Values represent end-point titers. Naïve controls were not included because of the undetected (total) AER-specific antibodies (Figure 7). n = 2 (mice).

SUPPLEMENTARY MATERIALS AND METHODS

S1. Generation of Monocyte-derived Dendritic Cells (MDDCs) from Peripheral Blood Mononuclear Cells (PBMCs)

PBMCs were isolated from buffy coats obtained from healthy individuals who provided written informed consent (Sanquin Blood Bank, The Netherlands). The PBMCs were separated using a Ficoll-based density gradient centrifugation method. $CD14^+$ cells were then isolated from the PBMCs using the magnetic cell isolation (MACS) technique with an autoMACS Pro Separator (Miltenyi Biotec BV, the Netherlands).

To generate MDDCs, the isolated $CD14^+$ cells were incubated for six days in the presence of cytokines: 10 ng/ml recombinant human granulocyte-macrophage colony-stimulating factor (GM-CSF; Miltenyi Biotec BV, the Netherlands) and 10 ng/ml recombinant human interleukin-4 (IL-4; Peprotech, USA). The cells were cultured at 37 °C with 5 % CO_2 in complete Roswell Park Memorial Institute (RPMI) 1640 medium, which was supplemented with 10 % fetal bovine serum (FBS), 100 units/ml penicillin, 100 µg/ml streptomycin, and 2mM GlutaMAX (Gibco, Thermo Fisher Scientific, Belgium). MDDCs were harvested by pipetting the medium.

S2. Activation and Viability of MDDCs

To evaluate the cellular toxicity and immunogenicity of AER-containing liposomal formulations in MDDCs flow cytometry analysis was performed. The formulations were added to round-bottom 96-well plates (CELLSTAR, Greiner Bio-One GmbH, Germany) pre-seeded with 30,000 MDDCs per well (250 µg/ml lipids, 0.5-5 µg/ml AER, in 200 µl medium) and incubated for 1 hour at 37 °C with 5 % CO_2. The cells were then washed with complete RPMI medium to remove free liposomes and cultured overnight. The following day, the cells were spun down, and the supernatants were collected and stored at -20 °C to measure cytokine/chemokine production. For flow cytometry staining, the cells were washed with FACS buffer (PBS containing 0.1 % bovine serum albumin; Merck, Germany) and incubated for 5 minutes with 5 % human serum (Sanquin Blood Bank, the Netherlands) in PBS to block non-specific Fc-receptor binding. The cells were then washed, and the cell surface markers on the MDDCs were stained for at least 30 minutes with monoclonal antibodies: CD83-PE (clone HB15e), CD40-APC (clone 5C3), CD80-APC-R700 (clone L307.4)

from BD Biosciences, Belgium, and CD86-BV421 (clone IT2.2) from BioLegend, the Netherlands, in FACS buffer. After staining, the cells were washed and stained with SYTOX AADvanced Dead Cell Stain (Invitrogen, Thermo Fisher Scientific, Belgium) in FACS buffer. Viability was calculated as the percentage of the SYTOX AADvanced-negative cell population relative to all recorded cells. Flow cytometry data acquisition was performed using a BD FACSLyric Flow Cytometer (BD Biosciences, Belgium), and data were analyzed using FlowJo software (version 10.6, FlowJo LLC, BD, USA).

S3. Luminex Assay

Supernatants were analyzed using two Bio-Plex panels (Bio-Rad, Veenendaal, the Netherlands) according to the manufacturer's protocols. A total of 16 analytes were measured. The chemokine panel included CXCL9, CXCL11, CCL8, and CCL22. The cytokine panel consisted of CCL11 (Eotaxin), GM-CSF, IFN-α2, IL-1β, IL-1rα, IL-6, CXCL10, CCL2 (MCP-1), CCL3, CCL4, RANTES, and TNF-α. Samples were acquired on a Bio-Plex 200 system and analyzed using Bio-Plex manager software version 6.1.

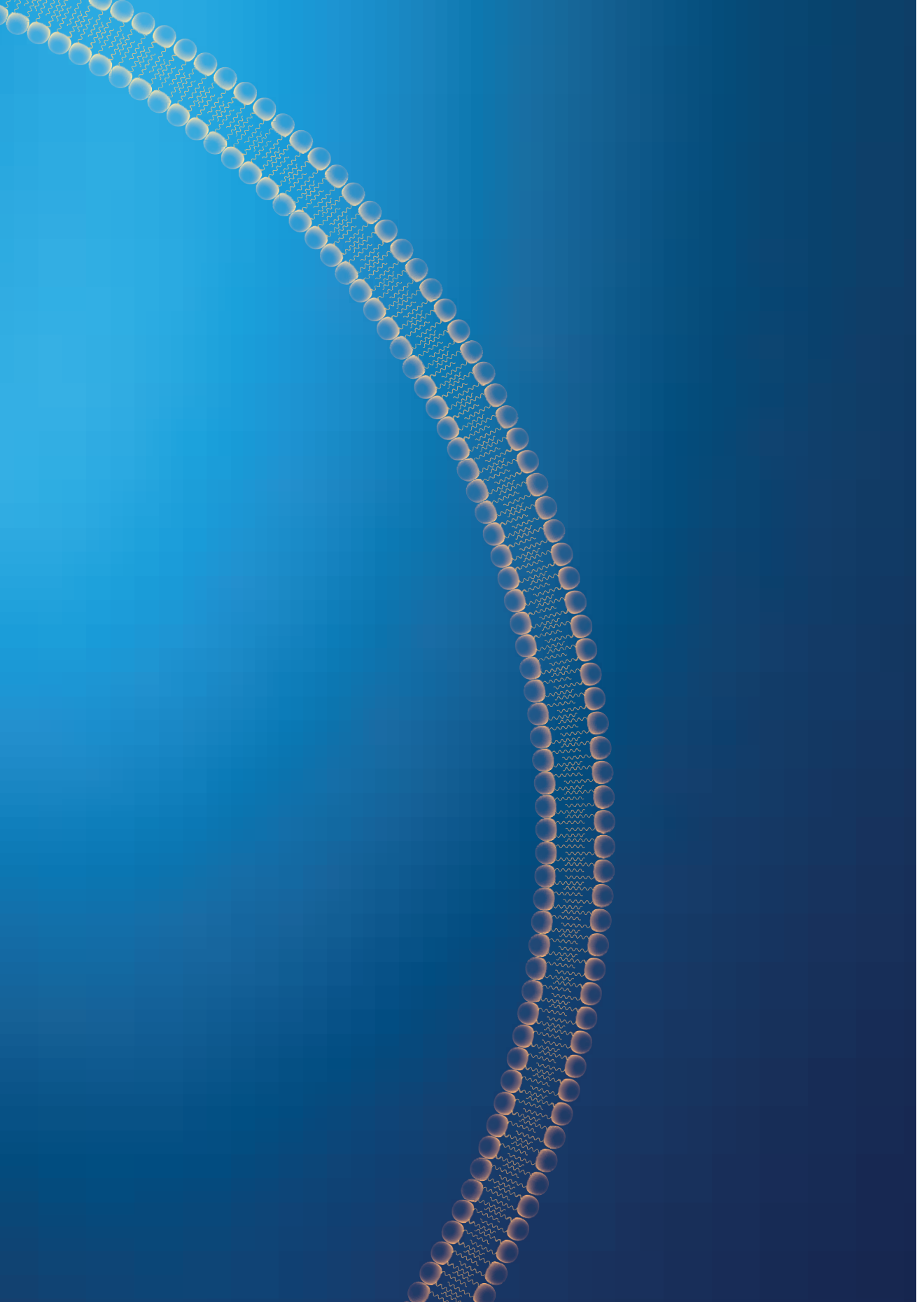

CHAPTER 5

Evaluation of PLGA, lipid-PLGA hybrid nanoparticles, and cationic pH-sensitive liposomes as tuberculosis vaccine delivery systems in a Mycobacterium tuberculosis challenge mouse model – a comparison

M.M. Szachniewicz, M.A. Neustrup, S.J.F. van den Eeden, K.E. van Meijgaarden, Kees L.M.C. Franken, S. van Veen, R.I. Koning, R.W.A.L. Limpens, A. Geluk, J.A. Bouwstra, T.H.M. Ottenhoff

Adapted from International Journal of Pharmaceutics, 2024, 666: 124842

ABSTRACT

Tuberculosis (TB) continues to pose a global threat for millennia, currently affecting over 2 billion people and causing 10.6 million new cases and 1.3 million deaths annually. The only existing vaccine, *Mycobacterium Bovis* Bacillus Calmette-Guérin (BCG), provides highly variable and inadequate protection in adults and adolescents. This study explores newly developed subunit tuberculosis vaccines that use a multistage protein fusion antigen Ag85b-ESAT6-Rv2034 (AER). The protection efficacy, as well as *in vivo* induced immune responses, were compared for five vaccines: BCG; AER-CpG/MPLA mix; poly(D,L-lactic-co-glycolic acid) (PLGA); lipid-PLGA hybrid nanoparticles (NPs); and cationic pH-sensitive liposomes (the latter three delivering AER together with CpG and MPLA). All vaccines, except the AER-adjuvant mix, induced protection in *Mycobacterium tuberculosis* (Mtb)-challenged C57/Bl6 mice as indicated by a significant reduction in bacterial burden in lungs and spleens of the animals. Four AER-based vaccines significantly increased the number of circulating multifunctional $CD4^+$ and $CD8^+$ T-cells producing IL-2, IFNγ, and TNFα, exhibiting a central memory phenotype. Furthermore, AER-based vaccines induced an increase in $CD69^+$ B-cell counts as well as high antigen-specific antibody titers. Unexpectedly, none of the observed immune responses were associated with the bacterial burden outcome, such that the mechanism responsible for the observed vaccine-induced protection of these vaccines remains unclear. These findings suggest the existence of non-classical protective mechanisms for Mtb infection, which could, once identified, provide interesting targets for novel vaccines.

1. INTRODUCTION

The WHO estimates that approximately one quarter of the world's human population is latently infected with TB.[1] Dubbed the 'white plague', pulmonary TB is the primary transmissible form caused by *Mycobacterium tuberculosis* (Mtb).[2] In 2022, 1.3 million died from TB, including 167,000 with HIV, making it a leading cause of death in this group of patients, and the second leading infectious disease killer after COVID-19, with the major cause of death due to antibiotic resistance.[1] TB is curable and preventable, but multidrug-resistant TB (MDR-TB) is an increasing public health threat.[1] The WHO aims to end the TB epidemic by 2030 as part of the United Nations' Sustainable Development Goals (SDGs).[3,4] As outlined by the End TB Strategy and the Western Pacific regional framework to end TB: 2021-2030,[5] the main tools to achieve this goal involve point-of-care approaches, early and easily accessible diagnostics, shorter and more effective treatment regiments, comprehensive treatment of all people with TB, including those with MDR-TB, management of co-morbidities, preventative treatment, and vaccination.[3,5]

Vaccination is indispensable for preventing infectious diseases like TB. Vaccines have enabled the eradication of smallpox and rinderpest and, more recently, have been essential in the fight against SARS-CoV-2.[6–8] The only licensed TB vaccine *Mycobacterium Bovis* Bacillus Calmette-Guérin (BCG), unfortunately offers highly variable and often insufficient protection.[9–11] Therefore, there is an unmet demand for better vaccines against TB.[9]

Subunit vaccines, produced with synthesized or purified antigens, DNA, or RNA, are safe and suitable for use in wide populations, including those with compromised immunity.[12,13] This broad applicability is especially important for TB in countries with high HIV rates.[5] However, they often lack immunogenicity, making further improved delivery system development essential for subunit vaccines.[14,15] Vaccine delivery systems use biocompatible nanoparticles (NPs) that prevent or limit antigen degradation and elimination, allow co-encapsulation of antigens with (molecular) adjuvants, and enhance uptake by antigen-presenting cells (APCs).[16–19] The work presented in this paper investigates and compares the immunological and biological effects of poly(D,L-lactic-co-glycolic acid) (PLGA), lipid-PLGA hybrid NPs, and cationic pH-sensitive liposomes as particulate delivery systems for protein-based TB vaccines.

PLGA is one of the most extensively studied polymers for numerous biomedical applications. It is available in varied compositions and molecular weights. Its versatile characteristics make it suitable for tissue engineering and sustained-release drug and vaccine delivery systems. PLGA has excellent safety records, tunable degradation, release properties, and high versatility. This has led to its wide adoption in several biomedical applications and longstanding approval by the US Food and Drug Administration for human use including drug delivery, and various biomedical products ranging from sutures to implants.[16,20–25] It biodegrades through hydrolysis into non-toxic metabolic by-products lactic and glycolic acid.[22] Previous studies have demonstrated the efficacy of antigen- and adjuvant-loaded PLGA nanoparticles in enhancing cell-mediated immune response in mice.[26–33]

Cationic liposomes are potent delivery systems that serve as particulate adjuvants.[12,18,34–36] Several liposome-based vaccines have been approved for clinical use.[37–39] Specifically, cationic liposomes can enhance immune responses, inducing the maturation of DCs and triggering T-cell responses, making them a versatile vaccination platform.[40–42]

pH-sensitive liposomes are a subclass of (cationic) liposomes that respond to pH changes by altering their molecular bilayer organization upon a decrease in pH. When exposed to an acidic environment, bilayers destabilize, which results in a fusion of the liposome with the endosomal membrane, thus releasing their cargo. This allows them to deliver antigens and adjuvants into a cell's cytosol, avoiding endosomal degradation.[43–47] This unique ability to escape rapid degradation has potential vaccination benefits.[48] Unlike non-pH-sensitive liposomes that degrade inside the endosome,[49,50] pH-sensitive liposomes can protect antigens and facilitate cross-priming,[49,51] which could significantly impact the type of immune responses induced by a vaccine.[52]

Lipid-PLGA hybrid NPs are complex nanostructures that have been successfully used in drug and vaccine delivery in preclinical research.[53–57] These hybrid NPs comprise a biodegradable PLGA core enveloped in a lipid shell that encapsulates drugs or antigens. They combine the properties of both PLGA NPs and liposomes. PLGA provides a rigid and solid core that allows sustained controlled release of antigens and adjuvants whereas the (cationic) lipid shell overcomes the lack of the immunogenicity of PLGA, facilitates uptake by APCs, reduces the degradation

rate of the PLGA core by limiting water diffusion into the particle, thus ensuring controlled release kinetics.[56–59] In vaccine applications, cationic lipid-PLGA hybrid NPs have demonstrated enhanced immunogenicity and induced humoral and cellular immune responses.[59–65]

In this study, the immunogenicity and effectiveness of tuberculosis vaccines prepared with NP-based delivery systems were compared to the antigen-adjuvant mixture in mice. The fusion protein antigen Ag85B-ESAT6-Rv2034 (AER) combined with adjuvants monophosphoryl lipid A (MPLA), cytosine-phosphate-guanine motifs oligodeoxynucleotides (CpG ODN) were used in the formulation. AER consists of Ag85B, an immunodominant antigen rich in epitopes offering enhanced protection when combined with other antigens;[66] ESAT6 which is a potent immunomodulatory antigen that is not expressed by BCG;[21,67] both used in vaccines currently in clinical trials: H1:IC31,[68] and H56:IC31;[69] and Rv2034 which is a potent *in vivo* expressed Mtb antigen.[70] AER mixed with CAF09 adjuvant induced protection in HLA-DR3 transgenic mice and in guinea pigs.[71] CpG is a Toll-like receptor (TLR) 9 ligand that induces robust Th1 responses, and MPLA, a TLR4 agonist, induces Th1 and Th17 responses.[72–74] A combination of both has been successfully used in several phase II and III clinical trials, and it was demonstrated safe and effective in the induction of robust T-cell and antibody responses.[75–79] The novel tuberculosis subunit vaccines developed in this research were tested *in vitro* on primary human APCs for immunogenicity and *in vivo* on C57Bl/6 mice with intranasal H37Rv Mtb infection to quantify protection, specifically CFU reduction in lungs and spleens. Immune responses in vaccinated, non-Mtb challenged mice were analyzed using a 27-marker spectral flow cytometry for $CD4^+$, $CD8^+$ T-cells, and B-cell responses. Additionally, serum antigen-specific antibody titers were measured.

2. MATERIALS AND METHODS

2.1 Materials

1,2-dioleoyl-sn-glycero-3-phosphocholine (DOPC), 1,2-dioleoyl-sn-glycero-3-ethyl-phosphocholine chloride salt (EPC), 1,2-dioleoyl-sn-glycero-3-phosphoethanolamine (DOPE), N-(4-carboxybenzyl)-N,N-dimethyl-2,3-bis(oleoyloxy)propan-1-aminium (DOBAQ), and monophosphoryl lipid A, PHAD (MPLA) were purchased from Avanti

Polar Lipids, Inc. in the USA. Figure S1 illustrates the chemical structures of these lipids. Class B CpG oligonucleotide ODN1826 was acquired from InvivoGen (the Netherlands).

PLGA (acid terminated, lactide:glycolide 50:50, Mw 24,000-38,000) was purchased from Merck Chemicals B.V. (the Netherlands). Interconnect tees for use with 360 µm outer diameter capillaries, one-piece fittings (for 360 µm capillaries and for 1/16" tubings), two-piece adapters (360- µm-to-1.6-mm and 1.6-mm-to-360- µm), and Luer-lock adapters (for use with 360 µm capillaries and 1/16" tubings), were obtained from Mengel Engineering (Denmark). Polyether ether ketone capillary tubing (inner diameter of 0.02" and outer diameter of 1/16"), was bought from Fisher Emergo B.V. (the Netherlands). A Teflon tube (1/16") was sourced from Waters Chromatography B.V. (the Netherlands). TSP Standard polyimide-coated fused silica tubings, (75 µm and 250 µm inner diameters, and 360 µm outer diameter) were obtained from BGB Analytik Benelux B.V. (the Netherlands). Polytetrafluoroethylene Leur-lock Hamilton gastight (1710TLL 100 µL, 1001TLL 1 ml, and 1010TLL 10 ml) syringes were purchased from Merck (Germany).

Recombinant fusion protein AER was produced as described by Franken et al.[80] Briefly, genes from Mtb (lab strain H37Rv) were amplified using PCR with genomic DNA. The amplified genes were cloned into bacteria using an N-terminal hexa-histidine (His) tag utilizing Gateway technology (Invitrogen, USA), and their successful insertion was confirmed through sequencing. The antigen AER was then expressed in *Escherichia coli* strain BL21 (DE3) and purified. Its quality was assessed through gel electrophoresis followed by Coomassie brilliant blue staining and with an anti-His antibody (Invitrogen, USA) Western blotting, which evaluated the size and purity of the protein. The ToxinSensor Chromogenic Limulus Amebocyte Lysate (LAL) Endotoxin Assay Kit (GenScript, USA) was employed to determine the endotoxin contamination level in the protein, revealing levels below 50 endotoxin units per 1 mg of protein.

2.2 Liposome production

Liposomes were made using the thin-film hydration method, as described previously.[81] Lipids were dissolved in chloroform and diluted from 25 mg/ml stocks to 10 mg per batch. The composition used was DOPC:DOPE:DOBAQ:EPC in a molar ratio 3:5:2:4. The lipid solution was placed in a flask and chloroform was removed

using a Buchi rotavapor R210 (Switzerland). The lipid film was then rehydrated with 1 ml of 200 µg/ml AER in 10 mM phosphate buffer (PB) at pH 7.4 to create AER-containing liposomes. These were downsized with Branson sonifier 250 (US) using an eight-cycle sonication program comprising 30 seconds of sonication at 10 % amplitude, followed by a 60-second break, and centrifuged (at 500 g for 3 min) to remove metal particles. The liposomal suspensions (5 mg/ml lipids) were transferred to new tubes and stored at 4 °C overnight. The final product contained 40 µg/ml AER and 2 mg/ml lipids after dilution with 10 mM PB.

2.3 PLGA NP preparation

The PLGA NPs were produced using a modular microfluidic system. A three-component system was used for PLGA NPs. Briefly, the contents of two syringes, Syringe 1 and 2, met each other in a T-flow, subsequently, the combined fluid met the contents of a third syringe, Syringe 3, in a co-flow, where the combined fluid constitutes the inner flow and the content of Syringe 3 constitutes the outer flow. The three syringes contained: 1) 3.33 mg/ml AER solution and 1 mg/ml CpG in water for injection, 2) 5 mg/ml PLGA and 12.5 µg/ml MPLA in acetonitrile, and 3) water for injection. The flow rates for the fluids in Syringe 1, 2, and 3 were set to 37.5, 1250, and 4955 µl/min, respectively, obtaining a total flow rate of 6242.5 µl/min, and final concentrations of 20 µg/ml AER, 6 µg/ml CpG, 2 mg/ml PLGA, and 2.5 µg/ml MPLA. The suspensions were set under a stream of nitrogen to evaporate the acetonitrile and concentrate the formulations. Before the characterization of particles and further use *in vitro* and *in vivo*, a concentrated solution of PB was added to obtain a concentration of 10 mM PB in the final product (40 µg/ml AER, 12 µg/ml CpG, 2 mg/ml PLGA, and 5 µg/ml MPLA).

2.4 Lipid-PLGA hybrid NP preparation

The lipid-PLGA NPs were produced using the same method as PLGA NPs with modifications. A four-component system was used in this case. As described above, AER solution with CpG was combined with PLGA (without MPLA) solution in an interconnected tee. The combined flow (1287.5 µl/minute) was then directed into another tee, where it was combined with water for injection (at 3712 µl/minute), and 5 mg/ml lipid solution of DOPC:DOPE:DOBAQ:EPC (3:5:2:4) containing 12.5 µg/ml MPLA in ethanol at a flow rate of 1250 µl/minute. The total flow rate was 6249.5 µl/

minute. The produced suspension was then evaporated and twice up-concentrated under nitrogen flow. The final product contained 40 µg/ml AER, 12 µg/ml CpG, 2 mg/ml PLGA, 2 mg/ml lipids, 5 µg/ml MPLA, and 10 mM PB.

2.5 Determination of size and Zeta-potential

The hydrodynamic diameter (Z-average size) and polydispersity index (PDI) of the liposomal formulations were determined with dynamic light scattering (DLS), and zeta potential was measured using laser Doppler electrophoresis as described previously.[81] Liposomes were diluted to 0.25 mg/ml lipid in 10 mM PB at pH 7.4 and added to 1.5 ml VWR Two-Sided Disposable PS Cuvettes (VWR, the Netherlands). Measurements, conducted in triplicates with at least ten runs at 20 °C, were performed using a Nano ZS Zetasizer with 633 nm laser and 173° optics (Malvern Instruments, UK). The data were analyzed with Zetasizer Software v7.13 (Malvern Instruments).

2.6 Differentiation of human monocyte-derived dendritic cells (MDDCs) and macrophages (MDMFs)

After written informed consent, PBMCs were obtained from healthy donors' buffy coats (Sanquin Blood Bank, Netherlands) as described previously.[81] Using the Ficoll-based density gradient centrifugation method, PBMCs were separated, and $CD14^+$ cells were isolated via the magnetic cell isolation method (MACS) with an autoMACS Pro Separator (Miltenyi Biotec BV, the Netherlands). These cells were then differentiated into DCs, and type 1 and 2 (M1 and M2, respectively) macrophages over six days using cytokines. MDDCs were generated with 10 ng/ml recombinant human granulocyte-macrophage colony-stimulating factor (GM-CSF; Miltenyi Biotec BV, the Netherlands) and 10 ng/ml recombinant human interleukin 4 (IL-4; Peprotech, USA). For M1 macrophages we used 5 ng/ml GM-CSF, and for M2 macrophages we used 50 ng/ml macrophage colony-stimulating factor (M-CSF; Miltenyi Biotec BV, the Netherlands) (Verreck et al., 2006). Cells were cultured at 37 °C / 5 % CO_2 in Roswell Park Memorial Institute (RPMI) 1640 medium, supplemented with 10 % fetal bovine serum (FBS), penicillin (100 units/ml), streptomycin (100 µg/ml), and 2mM GlutaMAX (Gibco, Belgium). MDDCs were harvested through pipetting, while for macrophages, we used trypsinization (Gibco, Belgium).

2.7 Uptake study

To assess the uptake of liposome, MDDCs, M1, and M2 MDMFs were cultured in 96-well plates with round bottoms (CELLSTAR, Greiner Bio-One GmbH, Germany), each well containing 30,000 cells. These cells were then treated with 1 % (v/v) empty fluorescent liposomes containing 0.1 % mol% of 1,2-dioleoyl-sn-glycero-3-phosphoethanolamine-N-(Cyanine 5) (18:2 PE-Cy5) sourced from Avanti Polar Lipids, Inc., USA, for 1 hour. Following exposure, the cells were washed three times with FACS buffer to eliminate any free liposomes. Flow cytometry data collection was collected using a BD FACSLyric Flow Cytometer (BD Biosciences, Belgium), and the analysis of this data was conducted using the FlowJo software, version 10.6 (FlowJo LLC, BD, USA).[81]

2.8 Activation study

The adjuvant properties of formulations loaded with AER were investigated using MDDCs as described previously.[83] To 30,000 cells/well in MDDCs seeded in 96-well plates with round bottoms (CELLSTAR, Greiner Bio-One GmbH, Germany), at a density of 30,000 cells per well, with lipid concentrations ranging from 25 to 250 µg/ml in 200 µl of medium. The cells were incubated for 1 hour at 37 °C / 5 % CO_2. Subsequent to this incubation, cells were rinsed with a complete RPMI medium and then cultured overnight. The following day, cells were centrifuged, the supernatants collected and stored at -20 °C for later use. For flow cytometry, cells were washed with FACS buffer (PBS with 0.1 % bovine serum albumin; Merck, Germany) and blocked for 5 minutes with 5 % human serum (Sanquin Blood Bank, the Netherlands) in PBS to prevent non-specific Fc-receptor binding. After blocking, cells were stained for 30 minutes with monoclonal antibodies targeting various cell surface markers: CCR7-BB515 (clone 3D12, catalog 565870), CD83-PE (clone HB15e, catalog 556855), CD40-APC (clone 5C3, 555591), CD80-APC-R700 (clone L307.4, catalog 565157), HLA-DR-V500 (clone G46-6, 561225) from BD Biosciences, Belgium, and CD86-BV421 (clone IT2.2, 305426) from BioLegend, the Netherlands, all at a dilution of 1:200 in FACS buffer. Post-staining, cells were again washed three times and resuspended in FACS buffer. Flow cytometry data was acquired using a BD FACSLyric Flow Cytometer and analyzed with FlowJo software.

2.9 Luminex assay

According to the manufacturer's protocols, supernatants were tested in two Bio-Plex panels (Bio-Rad, Veenendaal, the Netherlands). In total, 16 analytes were measured. The chemokine panel consisted of CXCL9, CXCL11, CCL8, and CCL22. The cytokine panel included CCL11 (Eotaxin), GM-CSF, IFN-α2, IL-1β, IL-1rα, IL-6, CXCL10, CCL2(MCP-1), CCL3, CCL4, RANTES and TNF-α. Samples were acquired on a Bio-Plex 200 system and analyzed with Bio-Plex manager software version 6.1.

2.10 Mice

All mouse experiments were individually designed, reviewed, ethically approved, and registered by the institutional Animal Welfare Body of the Leiden University Medical Center (LUMC). The study was conducted under project license AVD116002017856, issued by the Netherlands's Central Authority for Scientific Procedures on Animals (CCD). The experiments adhered to the Dutch Act on Animal Experimentation and EU Directive 2010/63/EU for animal experiments.

The Jackson Laboratory (USA) provided C57Bl/6 mice (stock number SC1300004), which were housed in the LUMC animal facility. Female mice, aged 6-8 weeks and matched for age (17-18 g weight), were utilized for each experiment. Mice were housed in a specific pathogen-free, temperature-controlled environment (20 °C ± 1 °C; humidity 55 % ± 15 %) including a controlled day-night cycle (12 hours per day; 60-300 lux), in individually ventilated cages containing bedding and nesting materials and as enrichment a tunnel and gnawing wood with no more than six mice per cage. Food and drinking water *ad libitum*. Mice were acclimatized for one week following transport before the experiments began.

Two independent experiments were performed. The experimental groups, summarized in Table 1, included naïve (unimmunized) mice as a negative control and a BCG immunized group as a control group using the licensed TB vaccine. Each mouse was considered an experimental unit, and mice in the same experimental group were housed together in one cage. Each group consisted of six mice, and a total of 36 mice were used per experiment. The results from the two experiments were combined for statistical analysis, increasing the number of mice to 12 per group and 72 in total.

2.11 Immunizations

C57Bl/6 mice were randomly allocated to six groups (6 mice per group). The naïve group served as the unimmunized control. Mice in the remaining groups were vaccinated with either BCG or AER combined with CpG (ODN1826) and MPLA (PHAD) or with AER together with CpG and MPLA delivered in PLGA NPs, cationic pH-sensitive liposomes or pH-sensitive lipid PLGA hybrid NPs. For immunizations that involved nanoparticle-based delivery systems, mice were given 3 subcutaneous (s.c.) injections in the right flank every 2 weeks with appropriate formulations (Table 1). Four weeks post-final immunization, mice were either sacrificed or infected with live Mtb. When AER was mixed with adjuvants, mice received 3 injections every 2 weeks with a solution of 25 µg AER, 50 µg CpG, and 1 µg MPLA in 200 µl PBS. For BCG vaccination, mice were given a single s.c. injection with 10^6 CFU live BCG (Danish strain 1331) 12 weeks prior to sacrifice or Mtb infection. BCG bacterial counts were determined by placing the suspension on 7H10 agar plates (Difco, BD, Franklin Lakes, NJ USA) supplemented with BBL Middlebrook OADC enrichment (BD, Franklin Lakes, NJ USA) and counting colonies after a 3-week incubation at 37 °C. Doses, frequency, and routes of administration were selected based on previous research.[71,81,84]

Table 1. Summary of vaccination groups and doses of vaccine constituents administrated to a mouse in a single immunization. Each group consists of 6 mice per experiment. All adjuvanted systems also contained CpG and MPLA.

Group	Description	AER (µg)	Lipid (µg)	PLGA (µg)	CpG (µg)	MPLA (µg)
Naïve	Unimmunized	NA	NA	NA	NA	NA
BCG	Approved vaccine	NA	NA	NA	NA	NA
Ag	Antigen-adjuvant mix	25	NA	NA	50	1
PLGA	PLGA NPs	8	NA	400	2.5	1
Hybrid	Lipid-PLGA hybrid NPs	8	400	400	2.5	1
pH	pH-sensitive liposome	8	400	NA	2.5	1

2.12 Intranasal infection with H37Rv Mtb

Unimmunized and immunized mice were infected with live Mtb H37Rv either 4 weeks post-AER vaccination or 12 weeks after BCG vaccination. Mice were sedated using isoflurane (Pharmachemie BV, The Netherlands) and received an intranasal

dose of 10^5 CFU Mtb sourced from glycerol stocks kept at at -80 °C.[85] The bacterial count was measured using 7H10 agar plates. The bacterial colonies were counted after incubation for 3 weeks at 37 °C.

Six weeks following the Mtb infection, the mice were humanely euthanized using CO_2. Their spleens and lungs were aseptically extracted. These tissues were then processed using 70 µM mesh strainers (Corning, USA) in a sterile PBS solution. The counts of bacteria were evaluated by serial dilutions on 7H11 agar plates (procured from BD Bioscience, USA), which were supplemented with OADC and PANTA (sourced from BD, Franklin Lakes, NJ USA).

2.13 Splenocyte cultures

Splenocytes from immunized uninfected mice were resuspended at 3×10^6 cells/ml in Iscove's Modified Dulbecco's Medium (IMDM; Lonza, Switzerland) with 2 mM GlutaMAX™, 100 U/100 µg/ml penicillin-streptomycin (both purchased from Gibco, Paisley, UK), and 8 % heat-inactivated fetal bovine serum (FBS; Greiner, Frickenhausen, Deutschland), and stimulated *in vitro* with 5 µg/ml of AER or its single components at 37 °C and 5 % CO_2. After 6 days, the splenocytes were restimulated with the same protein for 5 hours, and 2.5 µg/ml Brefeldin A (Sigma, Merck, Darmstadt, Germany) was added overnight. They were then harvested and stained for intracellular cytokines and surface markers the next day, as described previously.[84]

2.14 Antibody enzyme-linked immunosorbent assay (ELISA)

Blood was drawn from immunized, uninfected mice via heart puncture and cooled on ice. It was then centrifuged at 15,000 rpm for 10 minutes to obtain sera. ELISA was used to determine antibodies against proteins in sera, as described previously.[84] Plates were coated overnight with AER (5 µg/ml) or PBS/0.4 % BSA (Sigma, Merck, Darmstadt, Germany) at 4 °C and blocked for 2 hours with PBS/1 % BSA/1 % Tween-20. Serum dilutions (100 µl/well) were kept at 37 °C for 2 hours, followed by a wash (PBS, 0.05 % Tween-20) and incubation with horse radish peroxide (HRP)-labeled rabbit-anti-mouse antibodies: total IgG, IgG1, IgG2a, IgG2b, IgG2c, IgG3 and IgM (Dako, Denmark). After a 2-hour incubation at 37 °C, plates were washed and treated with 100 µl/well tetramethylbenzidine substrate (TMB; Sigma) for 15 minutes. Then H_2SO_4 was added, and OD450 was measured using a Spectramax i3x spectrometer Molecular Devices, CA, USA).

2.15 Antibody staining and flow cytometry

Surface and intracellular staining procedures were described elsewhere.[84] In short, splenocytes were transferred to 96-well plates and washed with PBS. They were stained with Zombie UV Fixable Viability Kit (BioLegend, the Netherlands), diluted 1:250 in PBS, and incubated with 100 µl of dye per well for 30 minutes. The cells were washed twice with FACS buffer (PBS with 0.1 % BSA), blocked with 20 µl of 5 % normal mouse serum (Thermo Fisher Scientific Inc., Bleiswijk, the Netherlands) in FACS buffer, then washed and stained with CCR7 for 30 minutes at 37 °C. The full list of antibodies used is summarized in Table S1. Lastly, the cells were washed twice and stained with a 50 µl/well antibody mix containing 10 µl/well of BD Horizon Brilliant Stain Buffer Plus (BD Biosciences, Belgium). Cells were incubated at 4 °C for 30 minutes, washed twice with FACS buffer, and then fixated and permeabilized with eBioscience Foxp3/Transcription Factor Staining Buffer Set (Invitrogen, Thermo Fisher Scientific, Belgium) at 4 °C for 60 minutes. Following a wash, intracellular staining was performed using a diluted antibody mix in permeabilization buffer. Cells were incubated with 50 µl/well antibody mix for 45 minutes, washed twice with FACS buffer, and resuspended in 100 µl/well FACS buffer. They were then stored at 4 °C until measured with a Cytek Aurora spectral flow cytometer (Cytek Biosciences, Fremont, CA, USA) at the Flow Cytometry Core Facility of Leiden University Medical Center in the Netherlands.

2.16 Flow cytometry data analysis

Data were analyzed with FlowJo v10.8.0 and OMIQ (www.omiq.ai) software, as described previously.[84] The analysis strategy is shown in Figure S2. In brief, data were first manually gated in FlowJo to remove debris, doublets, and acquisition-disturbed cells. Cells were then gated on CD3 vs CD19, and T-cells ($CD3^+$ $CD19^-$) and B-cells ($CD3^-$ $CD19^+$) were separately exported (min. 20,000 events each) to OMIQ. The imported data were further cleaned with FlowAI in OMIQ, and single marker gates were created. Using Boolean gating, gate combinations were made. Counts for all Boolean gates were exported, and statistical analysis was conducted. Uniform manifold approximation and projection (UMAP) was performed on digitally concatenated cells from all mice in each group.

2.17 Cryo-Electron Microscopy

Cryo-electron microscopy was performed as described previously.[86] Quantifoil 2/2 electron microscopy grids were glow discharged in 0.2 mbar air, at 25 mA, and for 30 seconds using an Easyglow (Pelco). A 3 µl droplet of the sample was added to the glow discharged grids, and blotted away using filter paper (Whatman no.4) for 3 seconds at 85-95 % humidity and room temperature, using an EM GP (Leica). The grid was subsequently plunged into liquid ethane/propane (2:1) at -196 °C. Grids were transferred into a Talos Arctica (Thermo Fisher Scientific) and images were acquired using EPU (Thermo Fisher Scientific) in multi-grid mode, at 0.55 nm/pixel, 15000x nominal magnification. Images were recorded on a K3 direct electron detector (Gatan) in counting mode and ZLP imaging in movie mode, a defocus of -5 micron, and an electron dose of ~4 e/A2/s with 8 seconds exposure time (corresponding to a total dose of 35 e/A2). Using this magnification/pixel size and electron dose, the full 2-micron hole is visible in one image, and the vesicle bilayer (at 4 nm) can be discerned. Movies (80 frames in total) were aligned using MotionCor2 and converted to tiff using EMAN2.

2.18 Statistical analysis

Mann-Whitney statistical test with Benjamini Hochberg FDR correction was carried out using R[87] and RStudio,[88] to identify differentially abundant populations of cells. Statistical analyses to compare vaccination groups were performed in GraphPad Prism, version 8.01 (GraphPad Software, Prism, USA), using the Kruskal-Wallis test and an uncorrected Dunn's posthoc test for non-parametric comparisons of three or more groups to the control group, where cutoff of $P < 0.05$ was selected as statistically significant (*$P < 0.05$, **$P < 0.01$, ***$P < 0.001$, ****$P < 0.0001$). Bar values represent the median and error bars the interquartile range (IQR) unless indicated otherwise.

3. RESULTS

3.1 In vitro testing of vaccine formulations

Formulations were prepared using three types of nanoparticle-based vaccine delivery systems: PLGA NPs, lipid-PLGA hybrid NPs, and cationic pH-sensitive

liposomes. Both hybrid NPs and liposomes shared the same lipid composition DOPC:DOPE:DOBAQ:EPC (3:5:2:4). We performed the initial immunogenicity tests in primary human MDDCs, including the performance of PLGA NPs.

First, we examined the uptake of PLGA NPs (Figure S2). The uptake was assessed using primary human MDDCs (IL-4 and GM-CSF-induced), as well as pro-inflammatory M1 (GM-CSF-induced) and anti-inflammatory (M-CSF-induced) MDMFs. The uptake of empty PLGA NPs in MDDCs was much lower compared to the uptake observed in type 1 and 2 MDMFs (Figure S2a). Because the PLGA NPs were not positively charged and no targeting moieties were used, it was expected that the uptake in DCs would be low. Subsequently, the uptake of empty PLGA and empty cationic lipid-PLGA hybrid NPs was compared in MDDCs only (the primary APCs of our interest) (Figure S2b). A significantly higher uptake was measured for the lipid-PLGA hybrid NPs compared to the PLGA NPs. Similarly to our previous work, pH-sensitive liposomes were efficiently taken up by all three types of APCs (manuscript submitted). These results thus show that professional APCs relatively poorly take up PLGA NPs without any adjuvants.

Subsequently, we examined the activation of primary human MDDCs in terms of the expression of cell-surface activation markers and cytokine production (Figure S3 and S4). Unadjuvanted PLGA, lipid-PLGA NPs, and pH-sensitive liposomes were tested, as well as their counterparts formulated with CpG and MPLA adjuvants. Unadjuvanted PLGA NPs, as expected, were weakly immunogenic, failed to increase activation marker expression, and induced weak or non-detectable cytokine production. Unadjuvanted lipid-PLGA hybrid NPs were more efficient in activating MDDCs in terms of cell surface markers and cytokine production than the PLGA NPs.

Table 2. Physicochemical properties of liposomes used for immunization of mice. Results represent a mean of n = 6 batches (3 batches used in 2 experiments, each batch value is a mean of a triplicate) and standard deviation.

Formulation	Z-average size (nm)	PDI (-)	Zeta-potential (mV)
AER/PLGA	83.9 ± 17.8	0.25 ± 0.10	-49.6 ± 11.2
AER/DOPC:DOPE:DOBAQ:EPC/PLGA	139.7 ± 8.0	0.19 ± 0.03	25.1 ± 1.8
AER/DOPC:DOPE:DOBAQ:EPC	166.9 ± 41.6	0.34 ± 0.09	21.5 ± 3.2

Cationic pH-sensitive liposomes induced CD40, CD83, and CCR7 expression but did not induce cytokine production. However, PLGA and lipid-PLGA NPs adjuvanted with CpG and MPLA induced both cell-surface markers expression and cytokine production. These results indicated that inert PLGA NPs, when formulated with potent adjuvants, can induce robust immune responses in vitro and, therefore, are promising delivery systems.

3.2 Physicochemical characterization of vaccine formulations and mouse study design

PLGA, lipid-PLGA hybrid NPs, and cationic pH-sensitive liposomes formulated with AER antigen, CpG, and MPLA adjuvants were prepared and characterized (Table 2). PLGA NPs had the smallest size about 85 nm, and very low Zeta-potential of about -50 mV. Lipid-PLGA hybrid NPs and liposomes had higher sizes of about 140 nm and 170 nm, respectively, as well as Zeta-potential between 20 ÷ 25 mV. Cryo-electron microscopy (Figure S5A) revealed spherical PLGA NPs in the size range between 50 and 100 nm with unsharp edges. Cryo-electron images of lipid-PLGA hybrid NPs (Figure S5B) revealed spherical NPs with clear lipid bilayer-resembling features. Subsequently, formulations were administrated subcutaneously to mice three times two weeks apart. Naïve (unimmunized) mice and BCG and AER mixed with CpG and MPLA were used as control groups. The immunization groups are summarized in Table 1. In the AER-adjuvant mix group, higher doses of antigen (25 μg compared to 8 μg) and CpG (50 μg compared to 2.5 μg) were used.

3.3 Nanoparticle-based subunit vaccines induce protection against Mtb in mice

The bacterial burden in lungs and spleens of infected mice was examined six weeks after the infection, which corresponds to ten weeks after the last immunizations (Figure 1). Bacterial counts from mice vaccinated with PLGA, lipid-PLGA, and pH-sensitive liposomal formulations as well as BCG were all significantly reduced compared to unimmunized mice and mice vaccinated with AER-adjuvant mix both in lungs and spleens, mounting to 2-3 log differences. Mice vaccinated with PLGA NPs had lower median CFUs, both in spleens and lungs, compared to BCG and the other two NP-based vaccines; however, the difference was not statistically significant between these groups. Noteworthy, NP-based vaccines used much lower doses of the antigen (8 μg vs 25 μg) and CpG (2.5 μg vs 50 μg) compared to the antigen-adjuvant mix.

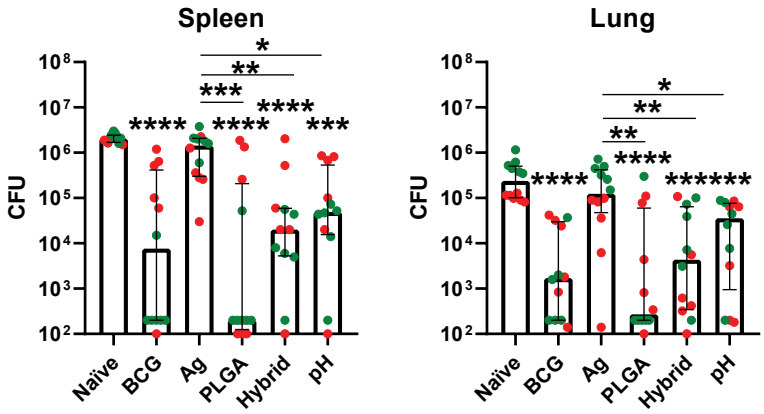

Figure 1. Bacterial burden in spleens (a) and lungs (b) of challenged mice represented by colony forming units (CFU) of Mtb. Each point represents CFU obtained from a single mouse. Colors indicate mice used in the same experiment. Groups: naïve – unimmunized mice; BCG – live BCG; Ag –antigen (25 µg Ag85B-ESAT6-Rv2034, AER) adjuvant mix (50 µg CpG, 1 µg MPLA), NP-free; PLGA – antigen (8 µg AER) and adjuvants (2.5 µg CpG, 1 µg MPLA) delivered in PLGA (400 µg) NPs; Hybrid – antigen (8 µg AER) and adjuvants (2.5 µg CpG, 1 µg MPLA) delivered in lipid (400 µg DOPC:DOPE:DOBAQ:EPC, 3:5:2:4)-PLGA (400 µg) NPs; pH – (8 µg AER) antigen and adjuvants (2.5 µg CpG, 1 µg MPLA) delivered in cationic pH-sensitive liposomes (400 µg DOPC:DOPE:DOBAQ:EPC, 3:5:2:4). n = 12. Bars represent median ± IQR. *p < 0.05, **p< 0.01, ***p < 0.001, ****p < 0.0001 (Kruskal-Wallis with an uncorrected Dunn's posthoc test).

3.4 AER-specific CD4⁺ and CD8⁺ T-cell responses in splenocytes ex vivo

Splenocytes from immunized (but non-Mtb-challenged mice) were collected and restimulated with AER. The cells were then stained with a 27-color panel and analyzed using spectral flow cytometry to evaluate the immune responses. Concatenated flow cytometry events of $CD3^+$ $CD19^-$ T-cells were examined following uniform manifold approximation and projection (UMAP) dimensionality reduction (Figure 2). UMAP was employed to evaluate global qualitative changes across experimental groups, utilizing all $CD3^+$ $CD19^-$ events simultaneously. The visual inspection of the data revealed differences in the abundance of T-cells between the groups. Major differences in the abundances of $CD4^+$ and $CD8^+$ cells, especially cells expressing IL-2, INFγ, and TNFα, were observed when comparing UMAPs of vaccinated mice compared to naïve mice. Subsequently, differential subset abundance analysis was performed to identify populations of interest and perform quantitative comparisons. We then selected sufficiently large cell populations (>100 events) and exhibited

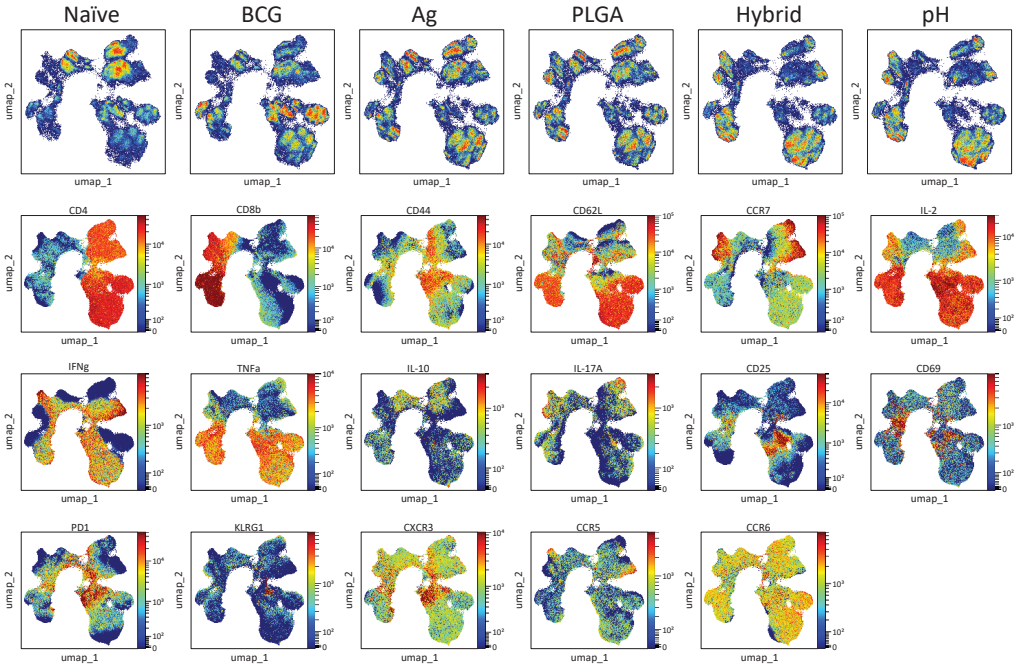

Figure 2. UMAP visualization of concatenated, AER-restimulated spleen-derived $CD4^+$, and $CD8^+$ T-cells ($CD3^+$ $CD19^-$) from all tested mice (per group) showing differential abundances of various populations of cells followed by color-continuous plots depicting phenotypical markers distribution. Groups: naïve – unimmunized mice; BCG – live BCG; Ag –antigen (25 µg Ag85B-ESAT6-Rv2034, AER) adjuvant mix (50 µg CpG, 1 µg MPLA), NP-free; PLGA – antigen (8 µg AER) and adjuvants (2.5 µg CpG, 1 µg MPLA) delivered in PLGA (400 µg) NPs; Hybrid – antigen (8 µg AER) and adjuvants (2.5 µg CpG, 1 µg MPLA) delivered in lipid (400 µg DOPC:DOPE:DOBAQ:EPC, 3:5:2:4)-PLGA (400 µg) NPs; pH – (8 µg AER) antigen and adjuvants (2.5 µg CpG, 1 µg MPLA) delivered in cationic pH-sensitive liposomes (400 µg DOPC:DOPE:DOBAQ:EPC, 3:5:2:4).

specific phenotypic markers that not only differentiated them from other cell subsets but also provided insights into their functional role. If several subsets were characterized by overlapping marker expression patterns, we selected one that was defined by more markers and was still large enough. We observed several $CD4^+$ T-cell subpopulations that were differentially abundant (Figure 3). The largest population was a polyfunctional population defined as $CD4^+$ IL-2^+ IFNγ^+ TNFα^+ IL-$17A^-$ IL-10^- $CD44^-$ $CD62L^+$ $CCR7^-$ T-cells. All AER-based vaccination groups increased this population, displaying a central memory phenotype, but interestingly, this was not the case for BCG. Similarly, a monofunctional Th1 cell subset defined

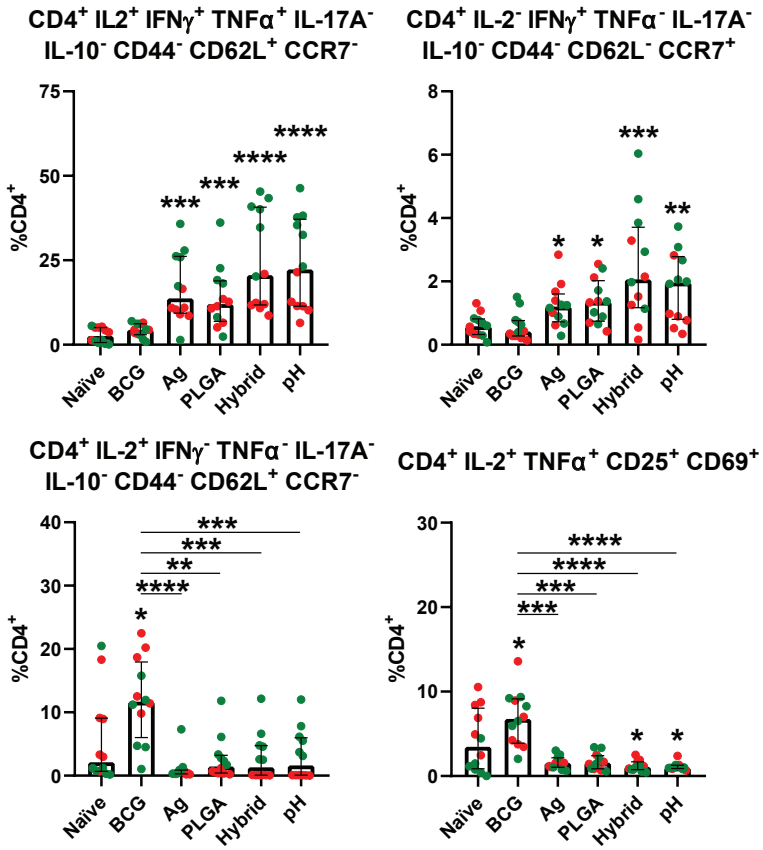

Figure 3. Differential abundance of CD4⁺ T-cells present in AER restimulated splenocytes from immunized non-Mtb-challenged mice. Markers defining each population are indicated above each graph. Graph values depict percentages of the population as a part of the CD3⁺ CD19⁻ CD4⁺ CD8⁻ cell subset. Each dot represents a single mouse and results from the same experiment are shown in one color. Groups: naïve – unimmunized mice; BCG – live BCG; Ag –antigen (25 μg Ag85B-ESAT6-Rv2034, AER) adjuvant mix (50 μg CpG, 1 μg MPLA), NP-free; PLGA – antigen (8 μg AER) and adjuvants (2.5 μg CpG, 1 μg MPLA) delivered in PLGA (400 μg) NPs; Hybrid – antigen (8 μg AER) and adjuvants (2.5 μg CpG, 1 μg MPLA) delivered in lipid (400 μg DOPC:DOPE:DOBAQ:EPC, 3:5:2:4)-PLGA (400 μg) NPs; pH – (8 μg AER) antigen and adjuvants (2.5 μg CpG, 1 μg MPLA) delivered in cationic pH-sensitive liposomes (400 μg DOPC:DOPE:DOBAQ:EPC, 3:5:2:4). n = 12 (mice). The minimal number of events used in the analysis was 20,000. Bars represent median ± IQR. *p < 0.05, **p < 0.01, ***p < 0.001, ****p < 0.0001 (Kruskal-Wallis with an uncorrected Dunn's posthoc test).

as $CD4^+$ IL-2^- $IFN\gamma^+$ $TNF\alpha^-$ IL-$17A^-$ IL-10^- $CD44^-$ $CD62L^-$ $CCR7^+$ T-cells displaying an effector memory phenotype was also differentially enriched. On the other hand, two subpopulations of $CD4^+$ T-cells were increased following BCG vaccination but not AER-based vaccines: a monofunctional central memory population of $CD4^+$ IL-2^+ $IFN\gamma^-$ $TNF\alpha^-$ IL-$17A^-$ IL-10^- $CD44^-$ $CD62L^+$ $CCR7^-$ T-cells as well as a population $CD4^+$ IL-2^+ $TNF\alpha^+$ $CD25^+$ $CD69^+$. Th17 responses were not observed in this study.

Similarly, we analyzed $CD8^+$ T-cell populations (Figure 4). The largest population was a polyfunctional central memory T-cell subset defined as $CD8^+$ IL-2^+ $IFN\gamma^+$ $TNF\alpha^+$ IL-$17A^-$ IL-10^- $CD44^-$ $CD62L^+$ $CCR7^-$ T-cells. It was significantly increased in all groups immunized with AER-based vaccines but not in the case of BCG. We also observed two other subsets that were increased by AER-based vaccines: a monofunctional central memory $CD4^+$ IL-2^- $IFN\gamma^+$ $TNF\alpha^-$ IL-$17A^-$ IL-10^- $CD62L^+$ $CCR7^+$ T-cells and T-cells defined as $CD8^+$ IL-$17A^+$ $IFN\gamma^+$. One population increased following BCG immunization, but none of the AER-based vaccines defined as $CD8^+$ IL-2^+ $TNF\alpha^+$ $CD44^+$ $CD62L^-$ $CCR7^-$ displayed predominantly an effector memory phenotype.

3.5 Differentially abundant B-cell populations

Similar to the analysis of T-cell responses, B-cell data were dimensionally reduced and UMAPs were analyzed (Figure 5). The UMAPs revealed the presence of differentially abundant populations of cells between different groups. Subsequently, differential subset abundance analysis was carried out, and statistically significant subsets were analyzed using univariate plots (Figure 6). Three B-cell populations expressing activation marker CD69 were found in AER-restimulated splenocytes. The largest population was a subset identified as $MHCII^+$ IgM^- IgD^- $B220^+$ $CD69^+$ B-cells corresponding to germinal center B-cells, followed by $MHCII^+$ IgM^- IgD^+ $B220^+$ $CD69^+$ (follicular B/B2 cells), and $MHCII^+$ IgM^+ IgD^- $B220^+$ $CD69^+$ (marginal zone B-cell, transitional 1 B cells) follicular B/B2.[89,90] All three B-cell subsets were more abundant in mouse groups vaccinated with AER-based vaccines compared to naïve mice. Moreover, mice vaccinated with lipid-PLGA hybrid NPs as well as pH-sensitive liposomes had higher counts of these B-cells compared to mice vaccinated with AER mixed with CpG and MPLA. B-cells defined as IL-$17A^+$ $B220^+$ $MHCII^+$ B-cells were increased in mice vaccinated with BCG compared to naïve mice and mice vaccinated with AER-based vaccines.

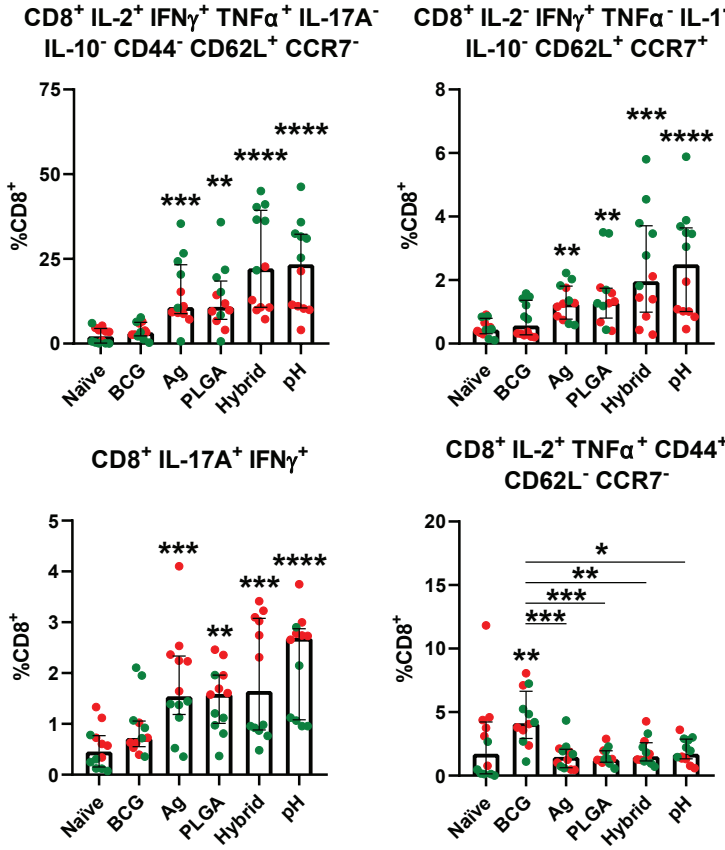

Figure 4. Differential abundance of CD8⁺ T-cell populations present in AER restimulated splenocytes from immunized non-Mtb-challenged mice. Markers defining each population are indicated above each graph. Graph values depict percentages of the population as a part of the CD3⁺ CD19⁻ CD4⁻ CD8⁺ cell subset. Each dot represents a percentage value from a single mouse and results from the same experiment are shown in one color. Groups: naïve – unimmunized mice; BCG – live BCG; Ag –antigen (25 μg Ag85B-ESAT6-Rv2034, AER) adjuvant mix (50 μg CpG, 1 μg MPLA), NP-free; PLGA – antigen (8 μg AER) and adjuvants (2.5 μg CpG, 1 μg MPLA) delivered in PLGA (400 μg) NPs; Hybrid – antigen (8 μg AER) and adjuvants (2.5 μg CpG, 1 μg MPLA) delivered in lipid (400 μg DOPC:DOPE:DOBAQ:EPC, 3:5:2:4)-PLGA (400 μg) NPs; pH – (8 μg AER) antigen and adjuvants (2.5 μg CpG, 1 μg MPLA) delivered in cationic pH-sensitive liposomes (400 μg DOPC:DOPE:DOBAQ:EPC, 3:5:2:4). n = 12 (mice). The minimal number of events used in the analysis was 20,000. Bars represent median ± IQR. *p < 0.05, **p< 0.01, ***p < 0.001, ****p < 0.0001 (Kruskal-Wallis with an uncorrected Dunn's posthoc test).

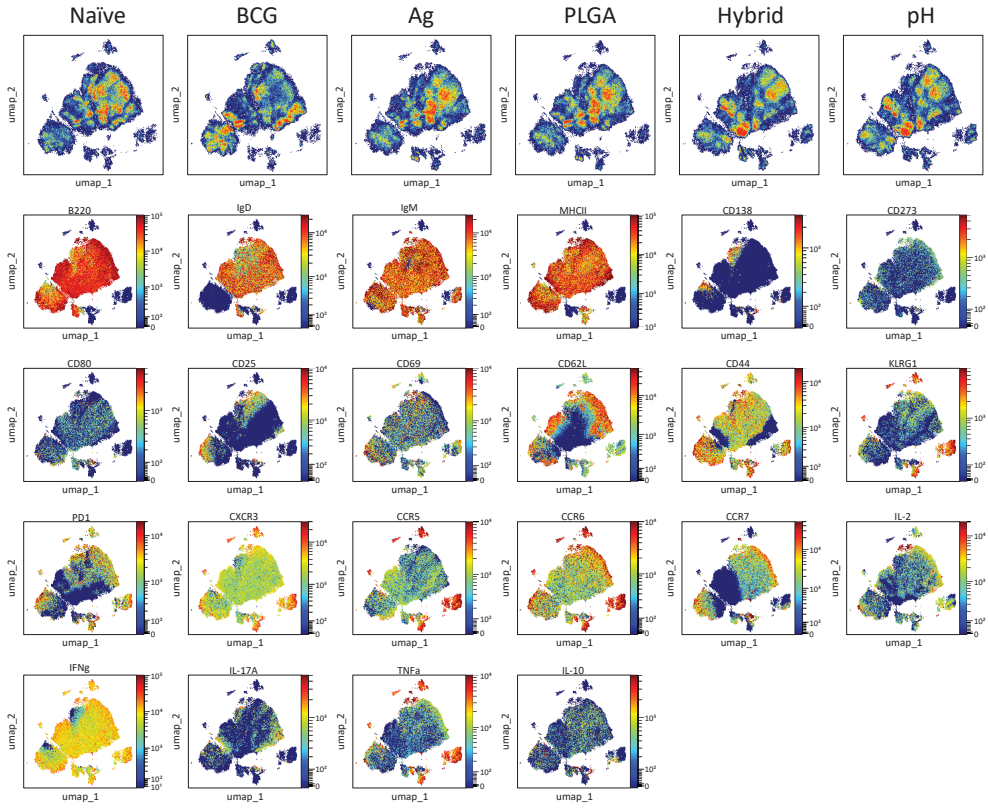

Figure 5. UMAP visualization of concatenated, AER-restimulated spleen-derived B-cells ($CD3^{-}$ $CD19^{+}$) from all tested mice (per group) showing differential abundances of various populations of cells followed by color-continuous plots depicting phenotypical markers distribution. Groups: naïve – unimmunized mice; BCG – live BCG; Ag –antigen (25 µg Ag85B-ESAT6-Rv2034, AER) adjuvant mix (50 µg CpG, 1 µg MPLA), NP-free; PLGA – antigen (8 µg AER) and adjuvants (2.5 µg CpG, 1 µg MPLA) delivered in PLGA (400 µg) NPs; Hybrid – antigen (8 µg AER) and adjuvants (2.5 µg CpG, 1 µg MPLA) delivered in lipid (400 µg DOPC:DOPE:DOBAQ:EPC, 3:5:2:4)-PLGA (400 µg) NPs; pH – (8 µg AER) antigen and adjuvants (2.5 µg CpG, 1 µg MPLA) delivered in cationic pH-sensitive liposomes (400 µg DOPC:DOPE:DOBAQ:EPC, 3:5:2:4).

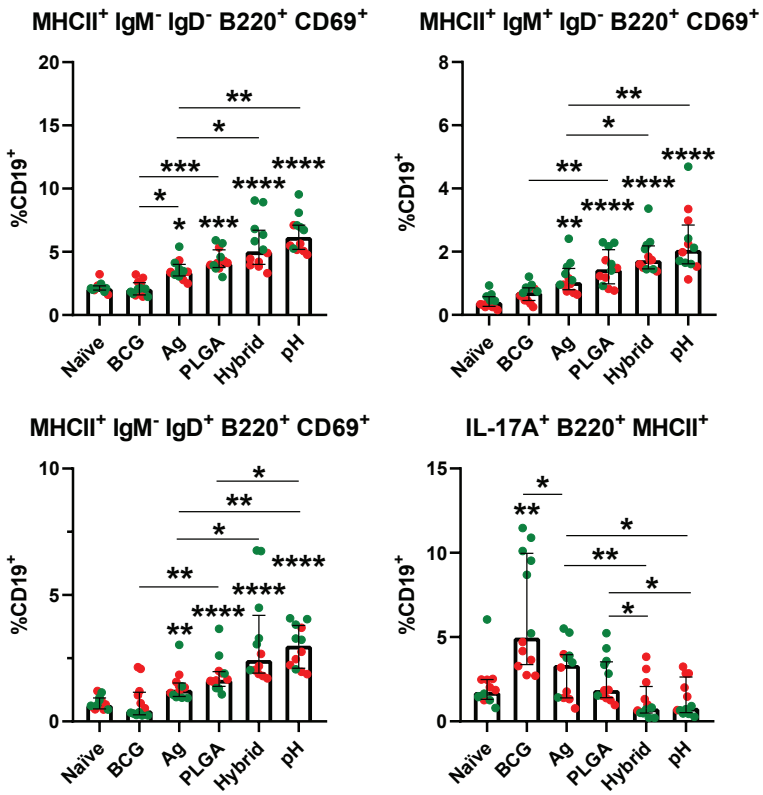

Figure 6. Differential abundance of CD19⁺ B-cell populations present in AER restimulated splenocytes from immunized non-Mtb-challenged mice. Markers defining each population are indicated above each graph. Graph values depict percentages of the population as a part of the CD3⁻ CD19⁺ cell subset. Each dot represents a percentage value from a single mouse and results from the same experiment are shown in one color. Groups: naïve – unimmunized mice; BCG – live BCG; Ag –antigen (25 μg Ag85B-ESAT6-Rv2034, AER) adjuvant mix (50 μg CpG, 1 μg MPLA), NP-free; PLGA – antigen (8 μg AER) and adjuvants (2.5 μg CpG, 1 μg MPLA) delivered in PLGA (400 μg) NPs; Hybrid – antigen (8 μg AER) and adjuvants (2.5 μg CpG, 1 μg MPLA) delivered in lipid (400 μg DOPC:DOPE:DOBAQ:EPC, 3:5:2:4)-PLGA (400 μg) NPs; pH – (8 μg AER) antigen and adjuvants (2.5 μg CpG, 1 μg MPLA) delivered in cationic pH-sensitive liposomes (400 μg DOPC:DOPE:DOBAQ:EPC, 3:5:2:4). n = 12 (mice). The minimal number of events used in the analysis was 20,000. Bars represent median ± IQR. *$p < 0.05$, **$p < 0.01$, ***$p < 0.001$, ****$p < 0.0001$. (Kruskal-Wallis with an uncorrected Dunn's posthoc test).

3.6 AER-specific antibody production

AER-specific antibody titers were investigated to explore humoral immune responses after vaccination. All four AER-based vaccines resulted in high antibody titers (Figure 7). However, in sera from naïve and BCG-vaccinated mice, AER-specific total Ig titers were below the detection limit. The highest total as well as IgG1 and IgG2 antibody titers were observed in mice vaccinated with cationic pH-sensitive liposomes and the lowest in mice immunized with the AER-adjuvant mix. Moreover, we also observed titers of other subtypes: high IgG2b and IgG2c as well as moderate-low levels of IgG3 and IgM (Figure S6).

4. DISCUSSION

TB remains a global epidemic, as a highly contagious airborne infectious disease that remains one of the foremost causes of death worldwide for centuries. According to the 2022 WHO Global Tuberculosis Report, approximately a quarter of the global population is latently infected with Mtb. Between 2000 and 2021, TB claimed the lives of 1.4 to 2 million individuals annually, with a peak mortality between 2000

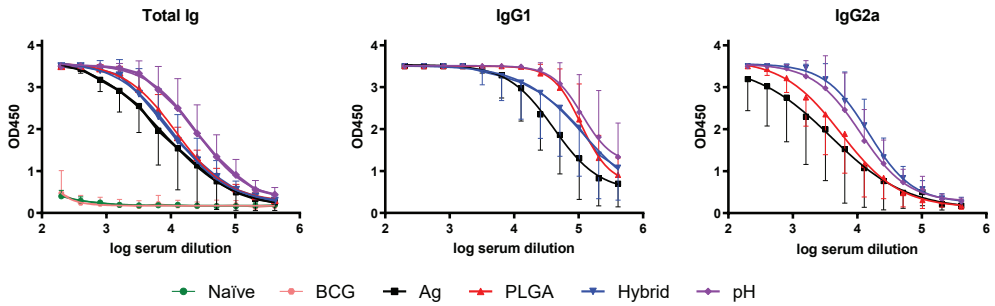

Figure 7. Quantification of AER-specific antibodies in sera. The type of antibody measured is indicated above each graph. Values represent OD450 ELISA, and serum dilutions are shown on the x-axis. Groups are indicated in the legend. Groups: naïve – unimmunized mice; BCG – live BCG; Ag –antigen (25 μg Ag85B-ESAT6-Rv2034, AER) adjuvant mix (50 μg CpG, 1 μg MPLA), NP-free; PLGA – antigen (8 μg AER) and adjuvants (2.5 μg CpG, 1 μg MPLA) delivered in PLGA (400 μg) NPs; Hybrid – antigen (8 μg AER) and adjuvants (2.5 μg CpG, 1 μg MPLA) delivered in lipid (400 μg DOPC:DOPE:DOBAQ:EPC, 3:5:2:4)-PLGA (400 μg) NPs; pH – (8 μg AER) antigen and adjuvants (2.5 μg CpG, 1 μg MPLA) delivered in cationic pH-sensitive liposomes (400 μg DOPC:DOPE:DOBAQ:EPC, 3:5:2:4). n = 6 (mice). Values represent mean ± standard deviation.

and 2010. In 2022 alone, TB was responsible for over one million deaths, surpassing fatalities from any other single infectious agent before the COVID-19 pandemic. Despite intense research efforts, the world still lacks a licensed effective TB vaccine, especially for adolescents and adults. The only licensed vaccine, BCG, offers moderate protection to infants and children but falls short for adult populations with the highest TB incidence, emphasizing the urgent need for a new vaccine.[1]

NPs are very effective delivery systems for subunit vaccines, offering several advantages in enhancing their efficacy. Firstly, NPs function as adjuvants, enhancing the antigenicity of associated antigens, and can mimic some properties of pathogens like viruses. Secondly, NPs can trigger both innate and adaptive immune responses, acting as effective antigen carriers that enhance antigen processing and presentation. Their nanoscale size promotes efficient uptake by phagocytic cells and facilitates robust innate immune responses. This positions NPs as pivotal tools in next-generation vaccine development.[91–93]

The physicochemical properties of NPs dictate their recognition, uptake, and immune responses.[94–96] Key properties such as size, charge, hydrophobicity, and rigidity affect interactions with interstitial matrix and antigen-presenting cells (APCs).[97,98] Small particles (<20 nm) drain to blood capillaries and are eliminated, while particles 20 ÷ 100 nm drain into lymph nodes (LNs) and are taken up by LN-resident APCs. Larger NPs (>100 nm) remain at the injection site (SOI) until transported to LNs by resident APCs.[99,100] Surface charge affects interactions with the interstitial matrix and cellular membranes.[95] Neutral and negatively charged NPs drain more easily into LNs,[101,102] while positively charged particles are more efficiently taken up by APCs[103,104] and form depots, facilitating immune responses.[41] The depot effect allows precise targeting of APCs, controlled antigen release, and antigens retention at the SOI. This leads to prolonged exposure to the immune system and continuous stimulation of the APCs in the vicinity of the SOI. Rigid NPs are more efficiently taken up by APCs and facilitate depot formation at the SOI[105,106] compared to soft NPs.[107,108] Hydrophilic NPs may accumulate more in LNs than hydrophobic ones of similar size.[109,110]

In this study, PLGA NPs (85 nm, -50 mV) with a hydrophilic, acid-terminated surface likely exhibited short retention at the SOI and efficient transport to LNs, which resulted in strong immune responses possibly due to slow release of antigens and adjuvants from the NP core. Hybrid lipid-PLGA NPs and liposomes (140-170 nm, 20-

25 mV) with hydrophilic surfaces formed palpable depots at the SOI, likely resulting in extended antigen presentation. Although hybrid NPs most likely offered a slow release of antigens and adjuvants compared to the expected burst release from liposomes, both types of NPs induced comparable protection and immune response.

To date, no clear immune correlates of protection against tuberculosis have been established. Therefore, it remains a challenge to identify types of immune responses that should be induced by a vaccine that would result in protection against Mtb. Historically, T helper 1 responses were deemed essential for a successful TB vaccination, and this notion was supported by ample evidence. [9,111–113] However, over time a conventional strategy aiming to induce predominant Th1/Th17 responses and minimize Th2/Treg immunity is being complemented by a more balanced approach that would lead to the interplay between Th1 and Th2 responses as well as B-cell responses. Such a diverse immune response repertoire is supposed to be more beneficial for the host.

All of the AER-containing vaccines induced primarily polyfunctional $CD4^+$ and $CD8^+$ T-cells that produced IL-2, IFNγ, and TNFα, as well as monofunctional IFNγ-producing T-cells, which both displayed a central memory phenotype.[114] The observed polyfunctional T-cells expressed CD62L but not CD44 or CCR7, which could mean that they belong to a separate central memory T-cell subset that has lost CD44, as shown by Henao-Tamayo et al.[114] $CD4^+$ T-cells with such a phenotype were observed to possess a significant expansion potential and induced excellent protection when transferred to $Rag^{-/-}$ mice challenged with Mtb H37Rv but not $CD4^+$ $CD44^{hi}$ $CD62L^{lo}$ cells.[115] $CD44^{lo}$ $CD62L^{hi}$ T-cells could significantly contribute to the protective responses like T-cells with $CD62L^{hi}$ $CCR7^{hi}$ central memory phenotype. Central memory $CD4^+$ T-cells rather than effector memory T-cells mediate long-term protection, and it has been suggested that inadequate protection conferred by BCG in adults and adolescents may be (partially) attributed to insufficient central memory T-cell responses.[116]

Noteworthy, we observed a significant increase in $CD8^+$ T-cells compared to naïve mice, especially in mice vaccinated with lipid-PLGA hybrid NPs, and cationic pH-sensitive liposomes. The significance of cytotoxic $CD8^+$ T-cells in Mtb protection is debated. Beyond directly killing infected cells, they produce cytokines, modulate the immune response, and work together with Th1 cells.[117,118] Recent research suggests

$CD8^+$ T-cells, alongside Th1 cells, are promising vaccine targets against Mtb.[9,119,120] Mouse studies support their importance in controlling Mtb.[121–124] Specifically, $CD8^+$ T-cell depletion increases bacterial load during latent phases in both mice[125] and non-human primates.[126] Interestingly, we observed elevated counts of IL-17A-producing $CD8^+$ T-cells but not $CD4^+$ T-cells. These $CD8^+$ T-cells, referred to as Tc17, are postulated to exhibit functions comparable to Th17 cells.[127,128] Th17 cells contribute to protective responses in the early stages of Mtb infection by engaging neutrophils and Th1 cells to infection sites and play a role in the formation of mature granuloma, which is crucial for the control of the disease.[9,129] However, further investigations are necessary to elucidate the specific role of Tc17 cells in immune responses against Mtb infection.

An increase in three subsets of CD69-expressing B-cells and high total AER-specific and Ig subtypes were observed in mice immunized with AER-based vaccines, which could contribute to the protection. B-cell and antibody responses are believed to contribute to TB immunity, but their exact role remains ambiguous.[130,131] Evidence for B-cell involvement is substantiated by increased vulnerability to Mtb in B-cell-depleted subjects restored post-B-cell transfer[132–134] and B-cell dysfunction in active TB patients rectifying post-treatment.[135] However, some genetic knockout studies and Mtb infection models challenge this perspective.[136–138] The protective role of antibody responses is supported by research on sera transfers from LTBI patients showing protective effects in mice[139] as well as treatment with monoclonal antibodies against Mtb antigens has been shown to improve survival, reduce spread, decrease tissue damage, and decrease mycobacterial load in animals.[140–143] Differential antibody responses between LTBI and ATB patients have also been shown. Antibodies from LTBI patients exhibited enhanced FC receptor profiles and enhanced macrophage killing of intracellular Mtb.[144]

All delivery-system-based AER vaccines (PLGA, lipid-PLGA hybrid NPs, and pH-sensitive liposomes) induced protection in intranasal Mtb challenge mouse model but not AER-adjuvant mix, despite overall similar immune responses induced by all AER vaccines. Importantly, the immunological effects induced by the NP-based vaccine were achieved at significantly lower doses of the antigen and adjuvants. This highlights the substantial advantage of using these nanoparticles for vaccine delivery, as they lead to better immunological outcomes and can reduce costs associated with antigens. $CD4^+$, $CD8^+$ T-cell, and B-cell responses that we observed

have been previously linked with protective outcomes by others; however, they do not explain the induced protection by these vaccines. The protection mechanism remains unknown because there are no established correlates of Mtb protection, and none of the immune responses observed in this study were associated with bacterial burden outcomes. This knowledge gap is a major hurdle in developing effective TB vaccines, and this issue has been raised in the literature before.[145,146]

The study's primary limitation is its single time point assessment, missing dynamic immune responses, and potential long-term effects. Future research should investigate multiple time points and explore various doses of the antigen, NPs, and adjuvants. The 7-day lymphocyte restimulation limited early immune responses study. The lack of immune response data from Mtb-challenged mice limits direct protection correlation. However, the study's strength lies in linking human innate responses with adaptive immune responses in vaccinated mice, finding NP-based vaccines that outperform BCG, hinting at broader applicability to other models and human use.

5. CONCLUSIONS

In this study, three types of NP-based potential TB vaccines were compared *in vivo*: PLGA, lipid-PLGA hybrid NPs, and cationic pH-sensitive liposomes. The formulations used Ag85B-ESAT6-Rv2034 AER fusion antigen, and two adjuvants (CpG and MPLA). Lipids used in the production of the hybrid NPs and liposomes comprised of DOPC:DOPE:DOBAQ:EPC at 3:5:2:4 molar ratio. This study describes the side-by-side comparison of three types of delivery systems in terms of protection (Mtb burden reduction in lungs and spleens) as well as a comprehensive exploration of immune responses: $CD4^+$/$CD8^+$ T-cell, B-cell, and antigen-specific antibody production. Vaccines that used NP-based delivery systems induced protection in intranasal Mtb-challenged mice as indicated by a significant CFU reduction compared to NP-free vaccination (AER mixed with CpG and MPLA). Moreover, NP-based vaccines induced a significant increase in polyfunctional $CD4^+$, and $CD8^+$ T-cells, as well as $CD69^+$ B-cell subsets, and high antigen-specific antibody titers. NP-based vaccines induced protection and protective immune responses at much lower doses of the antigen and molecular adjuvants than the NP-free vaccine. Our study's strength lies in linking human innate with adaptive immune responses in immunized mice,

thereby identifying NP-based vaccines that outperform BCG. PLGA, lipid-PLGA hybrid NPs, and cationic pH-sensitive liposomes are excellent promising vaccine delivery candidates, and their application should be further explored.

ABBREVIATIONS

AER, Ag85B-ESAT6-Rv2034 antigen; APC, antigen-presenting cell; Ag, antigen(-adjuvant mix group); BCG, *Mycobacterium bovis* Bacillus Calmette–Guérin; CCL, chemokine (C-C motif) ligand; CCR, C-C chemokine receptor type; CD, cluster of differentiation; CFU, colony forming unit; CpG ODN, cytosine-phosphorothioate-guanine oligodeoxynucleotides; CXCL, chemokine (C-X-C motif) ligand; CXCR, C-X-C motif chemokine receptor; DC, dendritic cell; DOBAQ, N-(4-carboxybenzyl)-N,N-dimethyl-2,3-bis(oleoyloxy)propan-1-aminium; DOPC, 1,2-dioleoyl-*sn*-glycero-3-phosphocholine; DOPE, 1,2-dioleoyl-sn-glycero-3-phosphoethanolamine; EPC, 1,2-dioleoyl-*sn*-glycero-3-ethylphosphocholine; FBS, fetal bovine serum; FDR, false discovery rate; GM-CSF, granulocyte-macrophage colony-stimulating factor; HLA, human leukocyte antigen; HRP, horse radish peroxide; IFN, interferon; Ig, immunoglobulin, IL, interleukin; i.n., intranasal; IQR, interquartile range; KLRG1, killer cell lectin-like receptor subfamily G member 1; MACS, magnetic cell isolation; M-CSF, macrophage colony-stimulating factor; LAL, limulus amebocyte lysate; LN, lymph node; LUMC, Leiden University Medical Center; MDDC, monocyte-derived dendritic cell; MDMF, monocyte-derived macrophages; MDR-TB, multidrug-resistant tuberculosis; MHC, major histocompatibility complex; MPLA, monophosphoryl lipid A; Mtb, mycobacterium tuberculosis; NP, nanoparticle; PBMC, peripheral blood mononuclear cell; PCR, polymerase chain reaction; PD-1, programmed cell death protein 1; PDI, polydispersity index; PE, phosphatidylethanolamine; pH, pH-sensitive liposome group; PLGA, poly(D,L-lactic-co-glycolic acid); rpm, rounds per minute; s.c., subcutaneous; SDGs, Sustainable Development Goals; SOI, site of injection; TB, tuberculosis; Th1/Th2/Th17, type 1/2/17 helper T-cell; TLR, Toll-like receptor; TNF, tumor necrosis factor; UMAP, uniform manifold approximation and projection.

APPENDICES

Supplementary materials

FUNDING

This work was supported by the Dutch Research Council (NWO) Domain Applied and Engineering Sciences grant, project number: 15240.

CREDIT AUTHOR STATEMENT

M.M. Szachniewicz: Conceptualization, Methodology, Formal Analysis, Investigation, Writing – Original Draft. **M. A. Neustrup**: Conceptualization, Methodology. **S.J.F. van den Eeden**: Conceptualization, Methodology, Investigation, Writing – Original Draft. **K.E. van Meijgaarden**: Conceptualization, Methodology, Writing – Review & Editing, Supervision. **K.L.M.C. Franken**: Methodology, Investigation, Resources. **S. van Veen**: Methodology, Formal Analysis. **R.I. Koning**: Methodology, Investigation. **R.W.A.L. Limpens**: Methodology, Investigation. **A. Geluk**: Conceptualization, Writing – Review & Editing, Project Administration, Funding Acquisition, Supervision. **J.A. Bouwstra**: Conceptualization, Writing – Review & Editing, Project Administration, Funding Acquisition, Supervision. **T.H.M. Ottenhoff**: Conceptualization, Writing – Review & Editing, Project Administration, Funding Acquisition, Primary supervision.

DECLARATIONS OF INTEREST

None.

REFERENCES

1. World Health Organization. *Global Tuberculosis Report 2023*. (2023).
2. Coppola, M. & Ottenhoff, T. H. Genome wide approaches discover novel Mycobacterium tuberculosis antigens as correlates of infection, disease, immunity and targets for vaccination. *Seminars in Immunology* 39, 88–101 (2018).
3. World Health Organization. *The End TB Strategy* (2015).
4. World Health Organization. *Implementing the End TB Strategy: The Essentials* (2015).
5. World Health Organization. *Western Pacific Regional Framework to End TB: 2021-2030* (2022).
6. Pollard, A. J. & Bijker, E. M. A guide to vaccinology: from basic principles to new developments. *Nature Reviews Immunology* 21:2, 83–100 (2020).
7. Rémy, V. *et al.* Vaccination: the cornerstone of an efficient healthcare system. *Journal of Market Access & Health Policy* 3, 27041 (2015).
8. Pérez-Alós, L. *et al.* Modeling of waning immunity after SARS-CoV-2 vaccination and influencing factors. *Nature Communications* 13:1, 1–11 (2022).
9. Ottenhoff, T. H. M. & Kaufmann, S. H. E. Vaccines against Tuberculosis: Where Are We and Where Do We Need to Go? *PLoS Pathogens* 8, e1002607 (2012).
10. Brewer, T. F. Preventing Tuberculosis with Bacillus Calmette-Guérin Vaccine: A Meta-Analysis of the Literature. *Clinical Infectious Diseases* 31, S64–S67 (2000).
11. Trunz, B. B. *et al.* Effect of BCG vaccination on childhood tuberculous meningitis and miliary tuberculosis worldwide: a meta-analysis and assessment of cost-effectiveness. *Lancet* 367, 1173–1180 (2006).
12. Christensen, D. *et al.* Cationic liposomes as vaccine adjuvants. *Expert Review of Vaccines* 10, 513–521 (2011).
13. Moyle, P. M. & Toth, I. Modern Subunit Vaccines: Development, Components, and Research Opportunities. *ChemMedChem* 8, 360–376 (2013).
14. Tandrup Schmidt, S. *et al.* Liposome-Based Adjuvants for Subunit Vaccines: Formulation Strategies for Subunit Antigens and Immunostimulators. *Pharmaceutics* 8, 7 (2016).
15. Barnier-Quer, C. *et al.* Adjuvant Effect of Cationic Liposomes for Subunit Influenza Vaccine: Influence of Antigen Loading Method, Cholesterol and

Immune Modulators. *Pharmaceutics* 5, 392–410 (2013).

16. Silva, A. L. *et al.* PLGA particulate delivery systems for subunit vaccines: Linking particle properties to immunogenicity. *Human Vaccines & Immunotherapeutics* 12, 1056–1069 (2016).
17. Parveen, S. *et al.* Nanoparticles: A Boon to Drug Delivery, Therapeutics, Diagnostics and Imaging. *Nanomedicine in Cancer* 47–98 (2017).
18. Marasini, N. *et al.* Liposomes as a Vaccine Delivery System. *Micro- and Nanotechnology in Vaccine Development* 221–239 (2017).
19. Storni, T., *et al.* Immunity in response to particulate antigen-delivery systems. *Advanced Drug Delivery Reviews* 57, 333–355 (2005).
20. Ignjatovic, N. L., *et al.* Size effect of calcium phosphate coated with poly-DL-lactide- co-glycolide on healing processes in bone reconstruction. *Journal of Biomedical Materials Research Part B: Applied Biomaterials* 94B, 108–117 (2010).
21. Duong, V. T. *et al.* Towards the development of subunit vaccines against tuberculosis: The key role of adjuvant. *Tuberculosis* 139, 102307 (2023).
22. Jain, R. A. The manufacturing techniques of various drug loaded biodegradable poly(lactide-co-glycolide) (PLGA) devices. *Biomaterials* 21, 2475–2490 (2000).
23. Danhier, F. *et al.* PLGA-based nanoparticles: An overview of biomedical applications. *Journal of Controlled Release* 161, 505–522 (2012).
24. Lü, J. M. *et al.* Current advances in research and clinical applications of PLGA-based nanotechnology. *Expert Review of Molecular Diagnostics* 9, 325–341 (2014).
25. Allahyari, M. & Mohit, E. Peptide/protein vaccine delivery system based on PLGA particles. *Human Vaccines & Immunotherapeutics* 12, 806–828 (2016).
26. Chong, C. S. W. *et al.* Enhancement of T helper type 1 immune responses against hepatitis B virus core antigen by PLGA nanoparticle vaccine delivery. *Journal of Controlled Release* 102, 85–99 (2005).
27. Schlosser, E. *et al.* TLR ligands and antigen need to be coencapsulated into the same biodegradable microsphere for the generation of potent cytotoxic T lymphocyte responses. *Vaccine* 26, 1626–1637 (2008).
28. Akagi, T. *et al.* Biodegradable nanoparticles as vaccine adjuvants and delivery systems: Regulation of immune responses by nanoparticle-based vaccine. *Advances in Polymer Science* 247, 31–64 (2012).
29. Hamdy, S. *et al.* Co-delivery of cancer-associated antigen and Toll-like receptor

4 ligand in PLGA nanoparticles induces potent CD8+ T cell-mediated anti-tumor immunity. *Vaccine* 26, 5046–5057 (2008).

30. Ashhurst, A. S. *et al.* PLGA particulate subunit tuberculosis vaccines promote humoral and Th17 responses but do not enhance control of Mycobacterium tuberculosis infection. *PLoS One* 13, e0194620 (2018).
31. Liang, Z. *et al.* CFP10–loaded PLGA nanoparticles as a booster vaccine confer protective immunity against Mycobacterium bovis. *Bioimpacts* 12, 395 (2022).
32. Ni, J. *et al.* Recombinant ArgF PLGA nanoparticles enhances BCG induced immune responses against Mycobacterium bovis infection. *Biomedicine & Pharmacotherapy* 137, 111341 (2021).
33. Malik, A. *et al.* Single-dose Ag85b-ESAT6–loaded poly(Lactic-co-glycolic acid) nanoparticles confer protective immunity against tuberculosis. *International Journal of Nanomedicine* 14, 3129–3143 (2019).
34. Latif, N. & Bachhawat, B. K. The effect of surface charges of liposomes in immunopotentiation. *Bioscience Reports* 4, 99–107 (1984).
35. Liu, X. *et al.* A novel liposome adjuvant DPC mediates Mycobacterium tuberculosis subunit vaccine well to induce cell-mediated immunity and high protective efficacy in mice. *Vaccine* 34, 1370–1378 (2016).
36. Heuts, J. *et al.* Cationic Liposomes: A Flexible Vaccine Delivery System for Physicochemically Diverse Antigenic Peptides. *Pharmacological Research* 35, 1–9 (2018).
37. Khademi, F. *et al.* Potential of cationic liposomes as adjuvants/delivery systems for tuberculosis subunit vaccines. in *Reviews of Physiology, Biochemistry and Pharmacology* vol. 175 47–69 (2018).
38. Luwi, N. E. M. *et al.* Liposomes as immunological adjuvants and delivery systems in the development of tuberculosis vaccine: A review. *Asian Pacific Journal of Tropical Medicine* 15:1, 7–16 (2022).
39. Tretiakova, D. S. & Vodovozova, E. L. Liposomes as Adjuvants and Vaccine Delivery Systems. *Biochemistry (Moscow), Supplement Series A: Membrane and Cell Biology* 16:1, 1–20 (2022).
40. Du, G. *et al.* Intradermal vaccination with hollow microneedles: A comparative study of various protein antigen and adjuvant encapsulated nanoparticles. *Journal of Controlled Release* 266, 109–118 (2017).
41. Henriksen-Lacey, M. *et al.* Liposomes based on dimethyldioctadecylammonium promote a depot effect and enhance immunogenicity of soluble antigen.

Journal of Controlled Release 142, 180–186 (2010).

42. Nakanishi, T. *et al.* Positively charged liposome functions as an efficient immunoadjuvant in inducing cell-mediated immune response to soluble proteins. *Journal of Controlled Release* 61, 233–240 (1999).
43. Karanth, H. & Murthy, R. S. R. pH-Sensitive liposomes-principle and application in cancer therapy. *Journal of Pharmacy and Pharmacology* 59, 469–483 (2007).
44. Balamurali, V. *et al.* pH Sensitive Drug Delivery Systems: A Review. *American Journal of Drug Discovery and Development* 1, 24–48 (2010).
45. Liu, X. & Huang, G. Formation strategies, mechanism of intracellular delivery and potential clinical applications of pH-sensitive liposomes. *Asian Journal of Pharmaceutical Sciences* 8, 319–328 (2013).
46. Zhuo, S. *et al.* pH-Sensitive Biomaterials for Drug Delivery. *Molecules* 25, (2020).
47. Mu, Y. *et al.* Advances in pH-responsive drug delivery systems. *OpenNano* 5, 100031 (2021).
48. Chang, J. S. *et al.* Development of Th1-mediated CD8+ effector T cells by vaccination with epitope peptides encapsulated in pH-sensitive liposomes. *Vaccine* 19, 3608–3614 (2001).
49. Fehres, C. M. *et al.* Understanding the biology of antigen cross-presentation for the design of vaccines against cancer. *Frontiers in Immunology* 5, 149 (2014).
50. Andersen, B. M. & Ohlfest, J. R. Increasing the efficacy of tumor cell vaccines by enhancing cross priming. *Cancer Letters* 325, 155–164 (2012).
51. Melero, I. *et al.* Therapeutic vaccines for cancer: an overview of clinical trials. *Nature Reviews Clinical Oncology* 11:9, 509–524 (2014).
52. Wang, C. *et al.* Self-adjuvanted nanovaccine for cancer immunotherapy: Role of lysosomal rupture-induced ROS in MHC class I antigen presentation. *Biomaterials* 79, 88–100 (2016).
53. Hadinoto, K. *et al.* Lipid–polymer hybrid nanoparticles as a new generation therapeutic delivery platform: A review. *European Journal of Pharmaceutics and Biopharmaceutics* 85, 427–443 (2013).
54. Tan, S. *et al.* Lipid-enveloped hybrid nanoparticles for drug delivery. *Nanoscale* 5, 860–872 (2013).
55. Sah, H. *et al.* Concepts and practices used to develop functional PLGA-based nanoparticulate systems. *International Journal of Nanomedicine* 8, 747–765

(2013).

56. Pandita, D. *et al.* Hybrid poly(lactic-co-glycolic acid) nanoparticles: design and delivery prospectives. *Drug Discovery Today* 20, 95–104 (2015).
57. Alsaab, H. O. *et al.* PLGA-Based Nanomedicine: History of Advancement and Development in Clinical Applications of Multiple Diseases. *Pharmaceutics* 14:12, 2728 (2022).
58. Ghitman, J. *et al.* Review of hybrid PLGA nanoparticles: Future of smart drug delivery and theranostics medicine. *Materials & Design* 193, 108805 (2020).
59. Rose, F. *et al.* Engineering of a novel adjuvant based on lipid-polymer hybrid nanoparticles: A quality-by-design approach. *Journal of Controlled Release* 210, 48–57 (2015).
60. Khademi, F. *et al.* Induction of strong immune response against a multicomponent antigen of Mycobacterium tuberculosis in BALB/c mice using PLGA and DOTAP adjuvant. *APMIS* 126, 509–514 (2018).
61. Khademi, F. *et al.* A novel antigen of Mycobacterium tuberculosis and MPLA adjuvant co-entrapped into PLGA:DDA hybrid nanoparticles stimulates mucosal and systemic immunity. *Microbial Pathogenesis* 125, 507–513 (2018).
62. Moon, J. J. *et al.* Antigen-Displaying Lipid-Enveloped PLGA Nanoparticles as Delivery Agents for a Plasmodium vivax Malaria Vaccine. *PLoS One* 7, e31472 (2012).
63. Liu, L. *et al.* Hyaluronic Acid-Modified Cationic Lipid-PLGA Hybrid Nanoparticles as a Nanovaccine Induce Robust Humoral and Cellular Immune Responses. *ACS Applied Materials & Interfaces* 8, 11969–11979 (2016).
64. Liu, L. *et al.* Immune responses to vaccines delivered by encapsulation into and/or adsorption onto cationic lipid-PLGA hybrid nanoparticles. *Journal of Controlled Release* 225, 230–239 (2016).
65. Rose, F. *et al.* A strong adjuvant based on glycol-chitosan-coated lipid-polymer hybrid nanoparticles potentiates mucosal immune responses against the recombinant Chlamydia trachomatis fusion antigen CTH522. *Journal of Controlled Release* 271, 88–97 (2018).
66. Karbalaei Zadeh Babaki, M. *et al.* Antigen 85 complex as a powerful Mycobacterium tuberculosis immunogene: Biology, immune-pathogenicity, applications in diagnosis, and vaccine design. *Microbial Pathogenesis* 112, 20–29 (2017).
67. Li, W. *et al.* A recombinant adenovirus expressing CFP10, ESAT6, Ag85A and

Ag85B of Mycobacterium tuberculosis elicits strong antigen-specific immune responses in mice. *Molecular Immunology* 62, 86–95 (2014).

68. Mearns, H. *et al.* H1:IC31 vaccination is safe and induces long-lived TNF-α+IL-2+CD4 T cell responses in M. tuberculosis infected and uninfected adolescents: A randomized trial. *Vaccine* 35, 132–141 (2017).
69. Luabeya, A. K. K. *et al.* First-in-human trial of the post-exposure tuberculosis vaccine H56:IC31 in Mycobacterium tuberculosis infected and non-infected healthy adults. *Vaccine* 33, 4130–4140 (2015).
70. Commandeur, S. *et al.* An Unbiased Genome-Wide Mycobacterium tuberculosis Gene Expression Approach To Discover Antigens Targeted by Human T Cells Expressed during Pulmonary Infection. *The Journal of Immunology* 190, 1659–1671 (2013).
71. Commandeur, S. *et al.* The in vivo expressed Mycobacterium tuberculosis (IVE-TB) antigen Rv2034 induces CD4+ T-cells that protect against pulmonary infection in HLA-DR transgenic mice and guinea pigs. *Vaccine* 32, 3580–3588 (2014).
72. Ko, E. J. *et al.* MPL and CpG combination adjuvants promote homologous and heterosubtypic cross protection of inactivated split influenza virus vaccine. *Antiviral Research* 156, 107–115 (2018).
73. Todoroff, J. *et al.* Mucosal and Systemic Immune Responses to Mycobacterium tuberculosis Antigen 85A following Its Co-Delivery with CpG, MPLA or LTB to the Lungs in Mice. *PLoS One* 8, e63344 (2013).
74. Meraz, I. M. *et al.* Adjuvant cationic liposomes presenting MPL and IL-12 induce cell death, suppress tumor growth, and alter the cellular phenotype of tumors in a murine model of breast cancer. *Molecular Pharmaceutics* 11, 3484–3491 (2014).
75. Vansteenkiste, J. F. *et al.* Efficacy of the MAGE-A3 cancer immunotherapeutic as adjuvant therapy in patients with resected MAGE-A3-positive non-small-cell lung cancer (MAGRIT): a randomised, double-blind, placebo-controlled, phase 3 trial. *Lancet Oncology* 17, 822–835 (2016).
76. Dreno, B. *et al.* MAGE-A3 immunotherapeutic as adjuvant therapy for patients with resected, MAGE-A3-positive, stage III melanoma (DERMA): a double-blind, randomised, placebo-controlled, phase 3 trial. *Lancet Oncology* 19, 916–929 (2018).
77. Kruit, W. H. J. *et al.* Selection of immunostimulant AS15 for active immunization

with MAGE-A3 protein: results of a randomized phase II study of the European Organisation for Research and Treatment of Cancer Melanoma Group in Metastatic Melanoma. *Journal of Clinical Oncology* 31, 2413–2420 (2013).

78. Kruit, W. H. *et al.* Immunization with recombinant MAGE-A3 protein combined with adjuvant systems AS15 or AS02B in patients with unresectable and progressive metastatic cutaneous melanoma: A randomized open-label phase II study of the EORTC Melanoma Group (16032- 18031). *Journal of Clinical Oncology* 26, 9065–9065 (2008).
79. Gutzmer, R. *et al.* Safety and immunogenicity of the PRAME cancer immunotherapeutic in metastatic melanoma: results of a phase I dose escalation study. *ESMO Open* 1, e000068 (2016).
80. Franken, K. L. M. C. *et al.* Purification of His-Tagged Proteins by Immobilized Chelate Affinity Chromatography: The Benefits from the Use of Organic Solvent. *Protein Expression and Purification* 18, 95–99 (2000).
81. Szachniewicz, M. M. *et al.* Intrinsic immunogenicity of liposomes for tuberculosis vaccines: Effect of cationic lipid and cholesterol. *European Journal of Pharmaceutical Sciences* 195, 106730 (2024).
82. Verreck, F. A. W. *et al.* Phenotypic and functional profiling of human proinflammatory type-1 and anti-inflammatory type-2 macrophages in response to microbial antigens and IFN-γ- and CD40L-mediated costimulation. *Journal of Leukocyte Biology* 79, 285–293 (2006).
83. Szachniewicz, M. M. *et al.* Cationic pH-sensitive liposomes as tuberculosis subunit vaccine delivery systems: Effect of liposome composition on cellular innate immune responses. *International Immunopharmacology* 145, 113782 (2025).
84. Szachniewicz, M. M. *et al.* Cationic pH-sensitive liposome-based subunit tuberculosis vaccine induces protection in mice challenged with Mycobacterium tuberculosis. *European Journal of Pharmaceutics and Biopharmaceutics* 203, 114437 (2024).
85. Geluk, A. *et al.* A multistage-polyepitope vaccine protects against Mycobacterium tuberculosis infection in HLA-DR3 transgenic mice. *Vaccine* 30, 7513–7521 (2012).
86. Ali, M. *et al.* Physical and Functional Characterization of PLGA Nanoparticles Containing the Antimicrobial Peptide SAAP-148. *International Journal of Molecular Sciences* 24, 2867 (2023).

87. R Core Team. R: A language and environment for statistical computing, (2023).
88. RStudio Team. RStudio: Integrated Development Environment for R, (2023).
89. Pillai, S. & Cariappa, A. The follicular versus marginal zone B lymphocyte cell fate decision. *Nature Reviews Immunology* 9:11, 767–777 (2009).
90. Kleiman, E. *et al.* Distinct transcriptomic features are associated with transitional and mature B-cell populations in the mouse spleen. *Frontiers in Immunology* 6, 126060 (2015).
91. Reed, S. G. *et al.* Key roles of adjuvants in modern vaccines. *Nature Medicine* 9:12, 1597–1608 (2013).
92. Zhao, L. *et al.* Nanoparticle vaccines. *Vaccine* 32, 327–337 (2014).
93. Demento, S. L. *et al.* Role of sustained antigen release from nanoparticle vaccines in shaping the T cell memory phenotype. *Biomaterials* 33, 4957–4964 (2012).
94. Jia, J. *et al.* Interactions Between Nanoparticles and Dendritic Cells: From the Perspective of Cancer Immunotherapy. *Frontiers in Oncology* 8, 410678 (2018).
95. Wang, Y. *et al.* Effect of physicochemical properties on in vivo fate of nanoparticle-based cancer immunotherapies. *Acta Pharmaceutica Sinica B* 11, 886–902 (2021).
96. Liu, J. *et al.* Nanoparticle cancer vaccines: Design considerations and recent advances. *Asian Journal of Pharmaceutical Sciences* 15, 576–590 (2020).
97. Moyano, D. F. *et al.* Modulation of Immune Response Using Engineered Nanoparticle Surfaces. *Small* 12, 76–82 (2016).
98. Getts, D. R. *et al.* Harnessing nanoparticles for immune modulation. *Trends in Immunology* 36, 419–427 (2015).
99. Fan, Y. & Moon, J. J. Nanoparticle Drug Delivery Systems Designed to Improve Cancer Vaccines and Immunotherapy. *Vaccines* 3, 662–685 (2015).
100. Correia-Pinto, J. F. *et al.* Vaccine delivery carriers: Insights and future perspectives. *International Journal of Pharmaceutics* 440, 27–38 (2013).
101. Doddapaneni, B. S. *et al.* A three-drug nanoscale drug delivery system designed for preferential lymphatic uptake for the treatment of metastatic melanoma. *Journal of Controlled Release* 220, 503–514 (2015).
102. Min, Y. *et al.* Antigen-capturing nanoparticles improve the abscopal effect and cancer immunotherapy. *Nature Nanotechnology* 12:9, 877–882 (2017).
103. Henriksen-Lacey, M. *et al.* Liposomal cationic charge and antigen adsorption are important properties for the efficient deposition of antigen at the injection

site and ability of the vaccine to induce a CMI response. *Journal of Controlled Release* 145, 102–108 (2010).

104. Foged, C. *et al.* Particle size and surface charge affect particle uptake by human dendritic cells in an in vitro model. *International Journal of Pharmaceutics* 298, 315–322 (2005).
105. Christensen, D. *et al.* A cationic vaccine adjuvant based on a saturated quaternary ammonium lipid have different in vivo distribution kinetics and display a distinct CD4 T cell-inducing capacity compared to its unsaturated analog. *Journal of Controlled Release* 160, 468–476 (2012).
106. Merkel, T. J. *et al.* Using mechanobiological mimicry of red blood cells to extend circulation times of hydrogel microparticles. *Proceedings of the National Academy of Sciences of the United States of America* 108, 586–591 (2011).
107. Anselmo, A. C. *et al.* Elasticity of nanoparticles influences their blood circulation, phagocytosis, endocytosis, and targeting. *ACS Nano* 9, 3169–3177 (2015).
108. Sun, J. *et al.* Tunable Rigidity of (Polymeric Core)–(Lipid Shell) Nanoparticles for Regulated Cellular Uptake. *Advanced Materials* 27, 1402–1407 (2015).
109. Moyano, D. F. *et al.* Nanoparticle hydrophobicity dictates immune response. *Journal of the American Chemical Society* 134, 3965–3967 (2012).
110. Rao, D. A. *et al.* Biodegradable PLGA based nanoparticles for sustained regional lymphatic drug delivery. *Journal of Pharmaceutical Sciences* 99, 2018–2031 (2010).
111. Griffiths, K. L. & Khader, S. A. Novel vaccine approaches for protection against intracellular pathogens. *Current Opinion in Immunology* 28, 58–63 (2014).
112. Flynn, J. A. L. Immunology of tuberculosis and implications in vaccine development. *Tuberculosis* 84, 93–101 (2004).
113. Ottenhoff, T. H. M. *et al.* Human CD4 and CD8 T Cell Responses to Mycobacterium tuberculosis: Antigen Specificity, Function, Implications and Applications. *Handbook of Tuberculosis* 119–155 (2008).
114. Henao-Tamayo, M. I. *et al.* Phenotypic definition of effector and memory T-lymphocyte subsets in mice chronically infected with mycobacterium tuberculosis. *Clinical and Vaccine Immunology* 17, 618–625 (2010).
115. Kipnis, A. *et al.* Memory T Lymphocytes Generated by Mycobacterium bovis BCG Vaccination Reside within a CD4 CD44lo CD62 Ligandhi Population. *Infection and Immunity* 73, 7759 (2005).

116. Orme, I. M. The Achilles heel of BCG. *Tuberculosis* 90, 329–332 (2010).
117. Prezzemolo, T. *et al.* Functional signatures of human CD4 and CD8 T cell responses to Mycobacterium tuberculosis. *Frontiers in Immunology* 5, 83298 (2014).
118. Lu, Y. J. *et al.* CD4 T cell help prevents CD8 T cell exhaustion and promotes control of Mycobacterium tuberculosis infection. *Cell Reports* 36, 109696 (2021).
119. Behar, S. M. *et al.* Next generation: tuberculosis vaccines that elicit protective CD8+ T cells. *Expert Review of Vaccines* 6, 441–456 (2007).
120. Boom, W. H. New TB vaccines: is there a requirement for CD8+ T cells? *Journal of Clinical Investigation* 117, 2092–2094 (2007).
121. Orme, I. M. The kinetics of emergence and loss of mediator T lymphocytes acquired in response to infection with Mycobacterium tuberculosis. *The Journal of Immunology* 138, 293–298 (1987).
122. Flynn, J. L. *et al.* Major histocompatibility complex class I-restricted T cells are required for resistance to Mycobacterium tuberculosis infection. *Proceedings of the National Academy of Sciences* 89, 12013–12017 (1992).
123. Sousa, A. O. *et al.* Relative contributions of distinct MHC class I-dependent cell populations in protection to tuberculosis infection in mice. *Proceedings of the National Academy of Sciences* 97, 4204–4208 (2000).
124. Behar, S. M. *et al.* Susceptibility of Mice Deficient in CD1D or TAP1 to Infection with Mycobacterium tuberculosis. *Journal of Experimental Medicine* 189, 1973–1980 (1999).
125. Van Pinxteren, L. A. H. *et al.* Control of latent Mycobacterium tuberculosis infection is dependent on CD8 T cells. *European Journal of Immunology* 30, 3689–3698 (2000).
126. Lin, P. L. *et al.* CD4 T Cell Depletion Exacerbates Acute Mycobacterium tuberculosis While Reactivation of Latent Infection Is Dependent on Severity of Tissue Depletion in Cynomolgus Macaques. *AIDS Research and Human Retroviruses* 28, 1693–1702 (2012).
127. Mills, K. H. G. IL-17 and IL-17-producing cells in protection versus pathology. *Nature Reviews Immunology 2022 23:1* 23, 38–54 (2022).
128. Ciric, B. *et al.* IL-23 Drives Pathogenic IL-17-Producing CD8+ T Cells. *The Journal of Immunology* 182, 5296–5305 (2009).
129. Ernst, J. D. The immunological life cycle of tuberculosis. *Nature Reviews*

Immunology 12:8, 581–591 (2012).

130. Rijnink, W. F. *et al.* B-Cells and Antibodies as Contributors to Effector Immune Responses in Tuberculosis. *Frontiers in Immunology* 12, 640168 (2021).
131. Duong, V. T. *et al.* Towards the development of subunit vaccines against tuberculosis: The key role of adjuvant. *Tuberculosis* 139, 102307 (2023).
132. Maglione, P. J. *et al.* B Cells Moderate Inflammatory Progression and Enhance Bacterial Containment upon Pulmonary Challenge with Mycobacterium tuberculosis. *The Journal of Immunology* 178, 7222–7234 (2007).
133. Phuah, J. *et al.* Effects of B cell depletion on early Mycobacterium tuberculosis infection in cynomolgus macaques. *Infection and Immunity* 84, 1301–1311 (2016).
134. Vordermeier, H. M. *et al.* Increase of tuberculous infection in the organs of B cell-deficient mice. *Clinical & Experimental Immunology* 106, 312–316 (2003).
135. Joosten, S. A. *et al.* Patients with Tuberculosis Have a Dysfunctional Circulating B-Cell Compartment, Which Normalizes following Successful Treatment. *PLoS Pathogens* 12, e1005687 (2016).
136. Turner, J. *et al.* The progression of chronic tuberculosis in the mouse does not require the participation of B lymphocytes or interleukin-4. *Experimental Gerontology* 36, 537–545 (2001).
137. Bosio, C. M. *et al.* Infection of B Cell-Deficient Mice with CDC 1551, a Clinical Isolate of Mycobacterium tuberculosis: Delay in Dissemination and Development of Lung Pathology. *The Journal of Immunology* 164, 6417–6425 (2000).
138. Johnson, C. M. *et al.* Mycobacterium tuberculosis aerogenic rechallenge infections in B cell-deficient mice. *Tubercle and Lung Disease* 78, 257–261 (1997).
139. Li, H. *et al.* Latently and uninfected healthcare workers exposed to TB make protective antibodies against Mycobacterium tuberculosis. *Proceedings of the National Academy of Sciences of the United States of America* 114, 5023–5028 (2017).
140. Zimmermann, N. *et al.* Human isotype-dependent inhibitory antibody responses against Mycobacterium tuberculosis. *EMBO Molecular Medicine* 8, 1325–1339 (2016).
141. Balu, S. *et al.* A Novel Human IgA Monoclonal Antibody Protects against Tuberculosis. *The Journal of Immunology* 186, 3113–3119 (2011).

142. Hamasur, B. *et al.* A mycobacterial lipoarabinomannan specific monoclonal antibody and its F(ab')2 fragment prolong survival of mice infected with Mycobacterium tuberculosis. *Clinical & Experimental Immunology* 138, 30–38 (2004).
143. López, Y. *et al.* Induction of a protective response with an IgA monoclonal antibody against Mycobacterium tuberculosis 16 kDa protein in a model of progressive pulmonary infection. *International Journal of Medical Microbiology* 299, 447–452 (2009).
144. Lu, L. L. *et al.* A Functional Role for Antibodies in Tuberculosis. *Cell* 167, 433-443.e14 (2016).
145. Mittrücker, H. W. *et al.* Poor correlation between BCG vaccination-induced T cell responses and protection against tuberculosis. *Proceedings of the National Academy of Sciences of the United States of America* 104, 12434–12439 (2007).
146. Kagina, B. M. N. *et al.* Specific T Cell Frequency and Cytokine Expression Profile Do Not Correlate with Protection against Tuberculosis after Bacillus Calmette-Guérin Vaccination of Newborns. *American Journal of Respiratory and Critical Care Medicine* 182, 1073–1079 (2012).

SUPPLEMENTARY MATERIALS

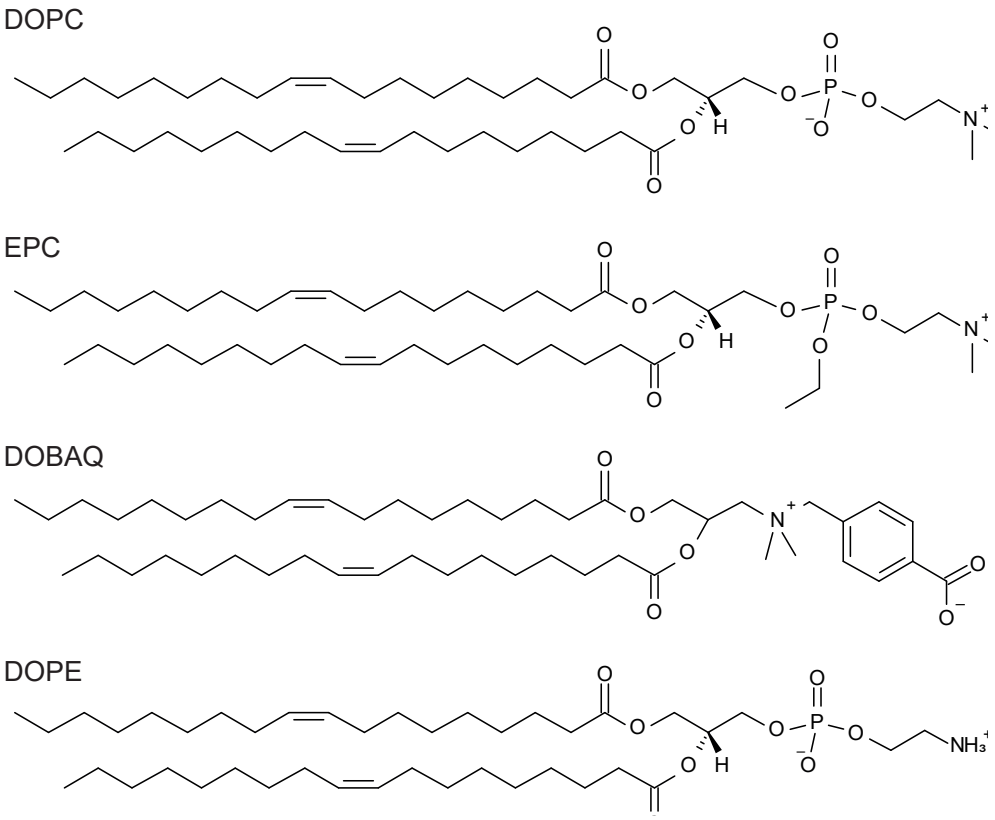

Figure S1. Chemical structures of lipids used in the production of pH-sensitive liposomes and lipid-PLGA hybrid NPs.

Table S1. List of antibodies used for spectral flow cytometry analysis of $CD4^+$, $CD8^+$, and $CD3^-$ $CD19^+$ cells.

Marker	Fluorochrome	Clone	Catalog	Manufacturer
CCR7 (CD197)	PE/Cyanine5	4B12	120113	BioLegend
CD273	BUV 395	TY25	565102	BD Biosciences
CD8b.2	BUV 496	53-5.8	741049	BD Biosciences
CD80	BUV 661	16-10A1	741515	BD Biosciences
CD69	BUV 737	H1.2F3	612793	BD Biosciences
CD25	BV 480	PC61	566120	BD Biosciences
CD154	Super Bright 436	MR1	62-1541-82	Thermo Fisher
IgD	Pacific Blue	11-26c.2a	405711	BioLegend
I-A/I-E (MHC II)	BV 510	M5/114.15.2	107636	BioLegend
CD44	BV 570	IM7	103037	BioLegend
PD-1 (CD279)	BV 605	29F.1A12	135220	BioLegend
CXCR3 (CD183)	BV 650	CXCR3-173	126531	BioLegend
KLRG1 (MAFA)	BV 711	2F1/KLRG1	138427	BioLegend
CCR6 (CD196)	BV 785	29-2L17	129823	BioLegend
CD4	Spark Blue 550	GK1.5	100474	BioLegend
CCR5 (CD195)	PerCP/Cyanine5.5	HM-CCR5	107015	BioLegend
CD19	PE Fire 640	6D5	115574	BioLegend
CD138	APC	281-2	142505	BioLegend
B220 (CD45R)	Spark NIR 685	RA3-6B2	103267	BioLegend
CD62L (L-selectin)	APC/Fire 750	MEL-14	104449	BioLegend
CD3	APC/Fire 810	17A2	100267	BioLegend
IL-2	APC-R700	JES6-5H4	565186	BD Biosciences
IL-17A	PE	eBio17B7	12-7177-81	Thermo Fisher
IgM	FITC	RMM-1	406505	BioLegend
IL-10	PE/Dazzle 594	JES5-16E3	505033	BioLegend
TNFα	PE/Cyanine7	MP6-XT22	506323	BioLegend
IFNγ	Alexa Fluor 647	XMG1.2	505816	BioLegend

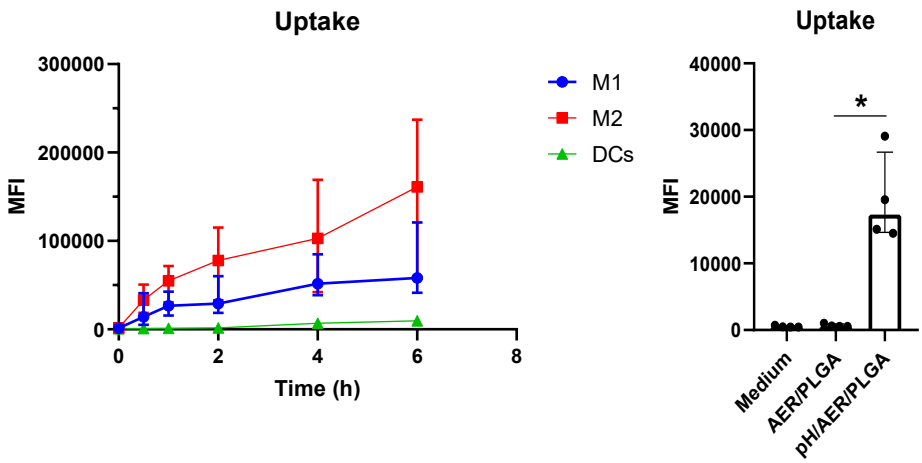

Figure S2. Uptake of (DiI-stained) PLGA NPs and lipid-PLGA hybrid NPs. A) Uptake kinetics of PLGA NPs by MDDCs, pro-inflammatory (M1), and anti-inflammatory M2 MDMFs between 1 and 6 hours of exposure. n = 4 (MDMFs), n =2 (MDDCs) donors. B) Uptake of PLGA NPs and lipid-PLGA hybrid NPs by MDDCs after 1 hour of exposure. n = 4 donors. Results represent median fluorescence intensity (MFI) ± IQR.

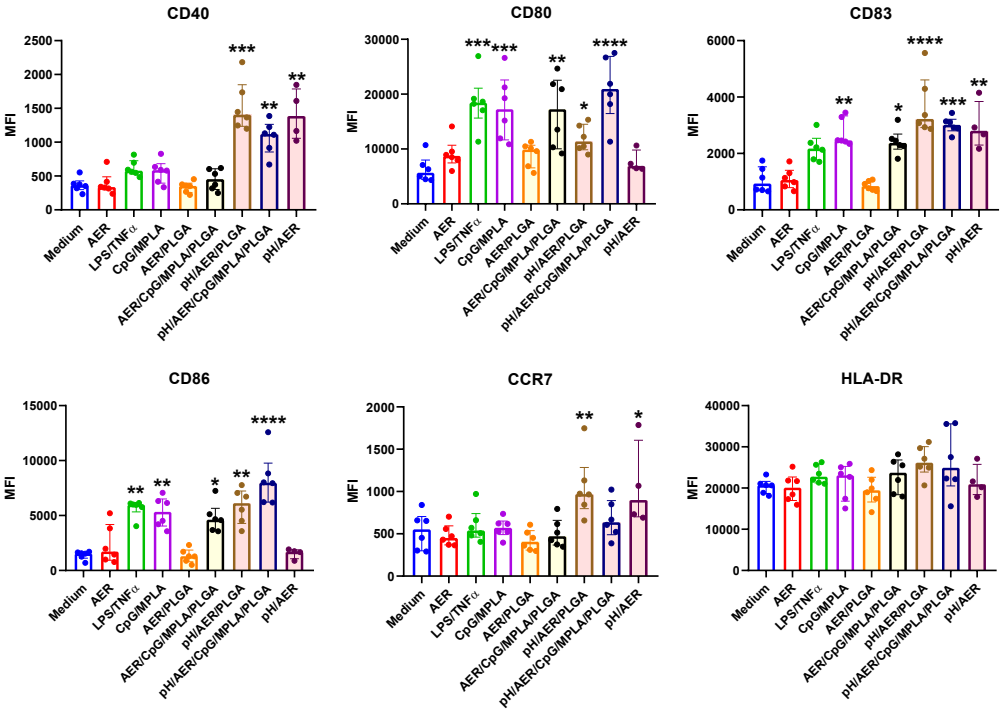

Figure S3. Cell surface activation marker expression levels in MDDCs after stimulation with medium, unadjuvanted AER (5 µg/ml), a combination of LPS and TNFα (100 and 5 ng/ml, respectively), CpG and MPLA (1.56 and 0.625 µg/ml, respectively) as the positive controls, and vaccine formulations: PLGA NPs (5 µg/ml AER, 250 µg/ml PLGA), lipid-PLGA hybrid NPs (5 µg/ml AER, 250 µg/ml lipids, 250 µg/ml PLGA), and (pH) liposomal formulation (5 µg/ml AER, 250 µg/ml liposomes), and their adjuvanted counterparts (containing additionally 1.56 and 0.625 µg/ml CpG and MPLA, respectively). Median fluorescence intensities (MFI) related to the expression of indicated activation markers. The formulations are compared to the medium in the significance testing. The results represent median ± IQR. n = 4 or 6 (cell donors).

→ **Figure S4**. Production of cytokines by MDDCs exposed to vaccine formulations. Concentrations used: 5 µg/ml AER, 100 ng/ml LPS and 5 ng/ml TNFα, 1.56 µg/ml CpG and 0.625 µg/ml MPLA, 250 µg/ml PLGA, 250 µg/ml liposomes/lipids, exposure 1 hour, n = 4 (cell donors). The results represent median ± IQR.

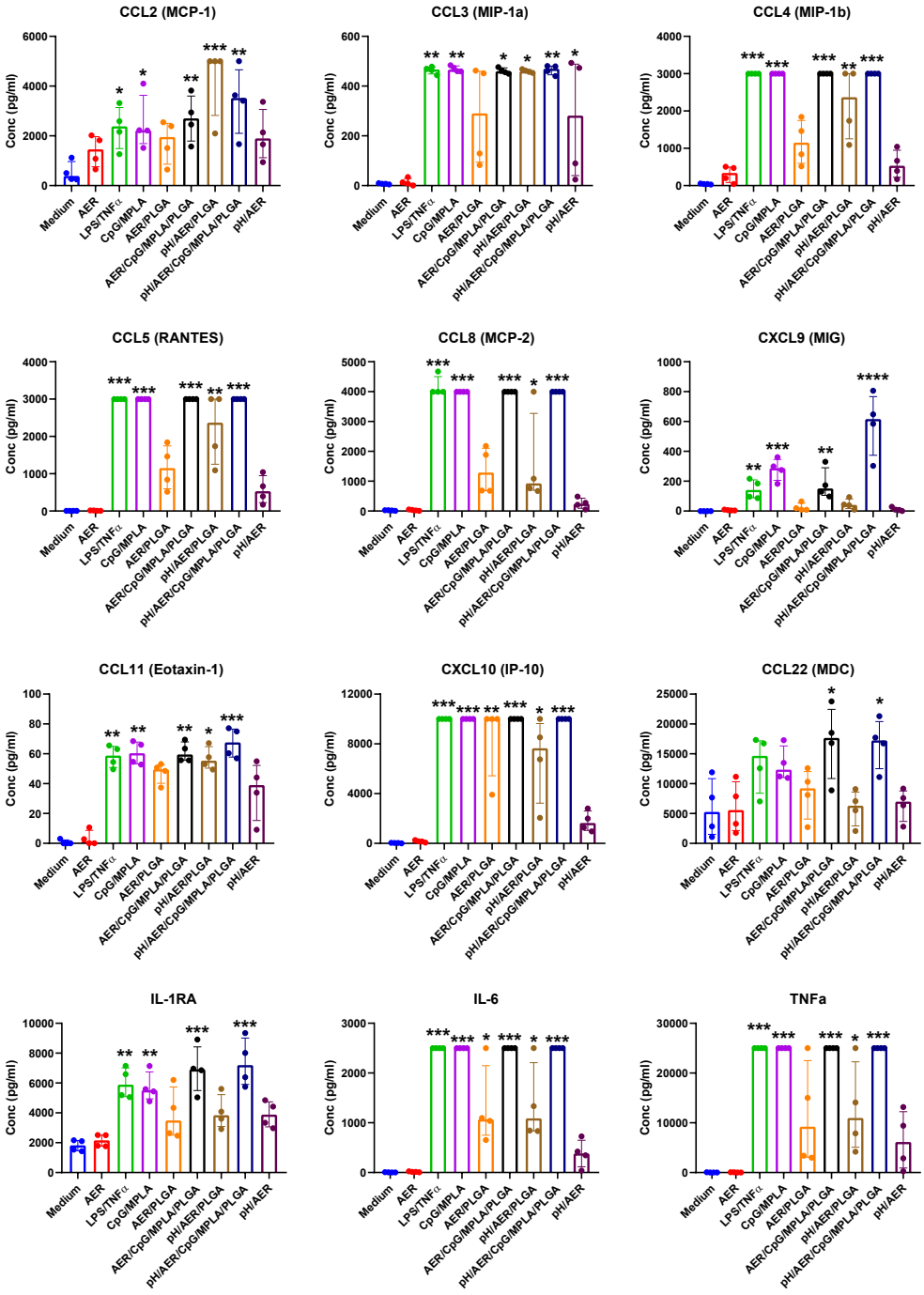
CCL2 (MCP-1)
CCL3 (MIP-1a)
CCL4 (MIP-1b)
CCL5 (RANTES)
CCL8 (MCP-2)
CXCL9 (MIG)
CCL11 (Eotaxin-1)
CXCL10 (IP-10)
CCL22 (MDC)
IL-1RA
IL-6
TNFa
Conc (pg/ml)
Medium
AER
LPS/TNFα
CpG/MPLA
AER/PLGA
AER/CpG/MPLA/PLGA
pH/AER/PLGA
pH/AER/CpG/MPLA/PLGA
pH/AER

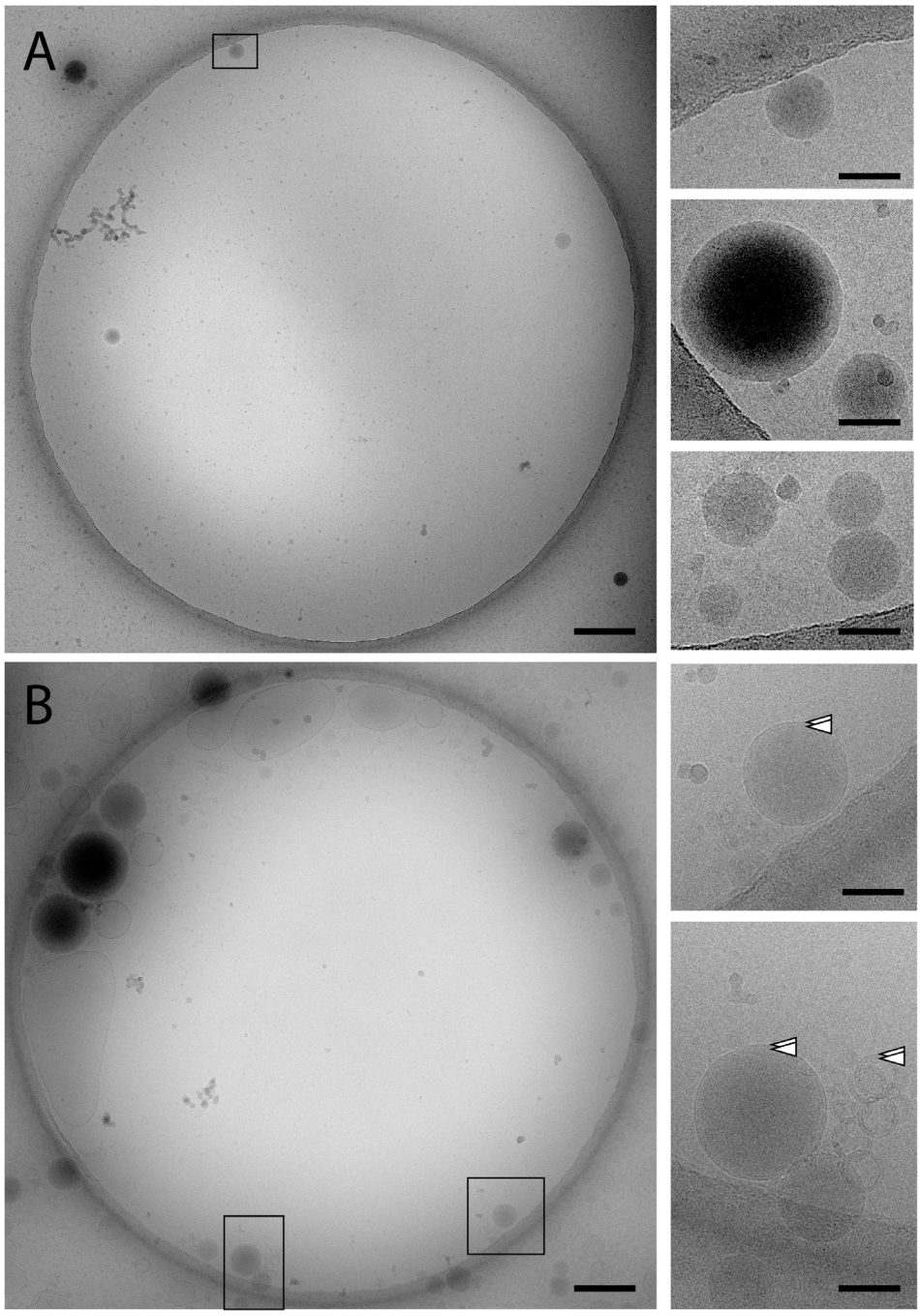
A
B

← **Figure S5.** A) PLGA NPs (without lipids added). CryoEM overview image of a typical 2-micron diameter hole in the carbon film with three PLGA spheres. The box's area is magnified on the top right. Several other spheres from other images are shown below that image. The edges of the spheres are not sharply defined.

B) Lipid-PLGA hybrid NPs. CryoEM overview of a typical 2-micron diameter hole in the carbon film showing multiple lipid-PLGA spheres. Irregularly shaped lipid vesicles were found occasionally. The boxes' areas are magnified and show PLGA spheres with clear lipid bilayer-resembling features, which can also be observed in small lipid vesicles (arrowheads). The borders of the spheres are more distinctive.

In both A and B scale bars are 200 nm (overview images) and 50 nm (insets).

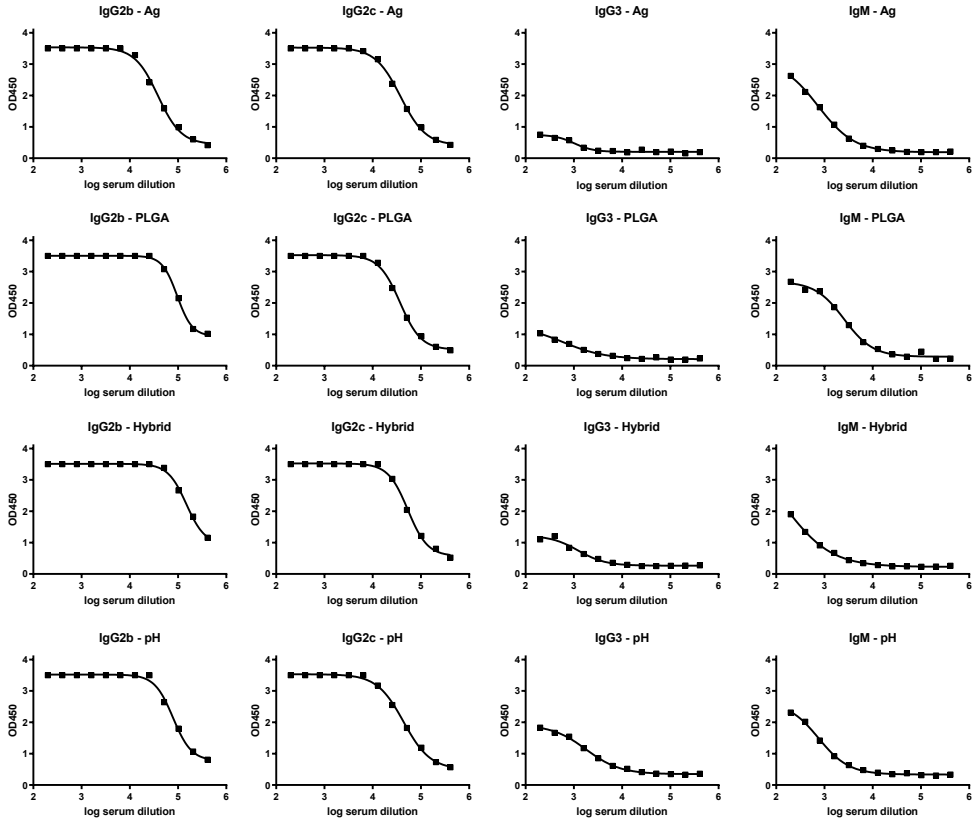

Figure S6. Quantification of AER-specific antibodies in sera. The type of antibody measured is indicated above each graph as well as the vaccination group. Values represent OD450 ELISA, and serum dilutions are shown on the x-axis. Groups are indicated in the legend. Naïve controls were not included because of the undetected (total) AER-specific antibodies (Figure 7). n = 2 (mice).

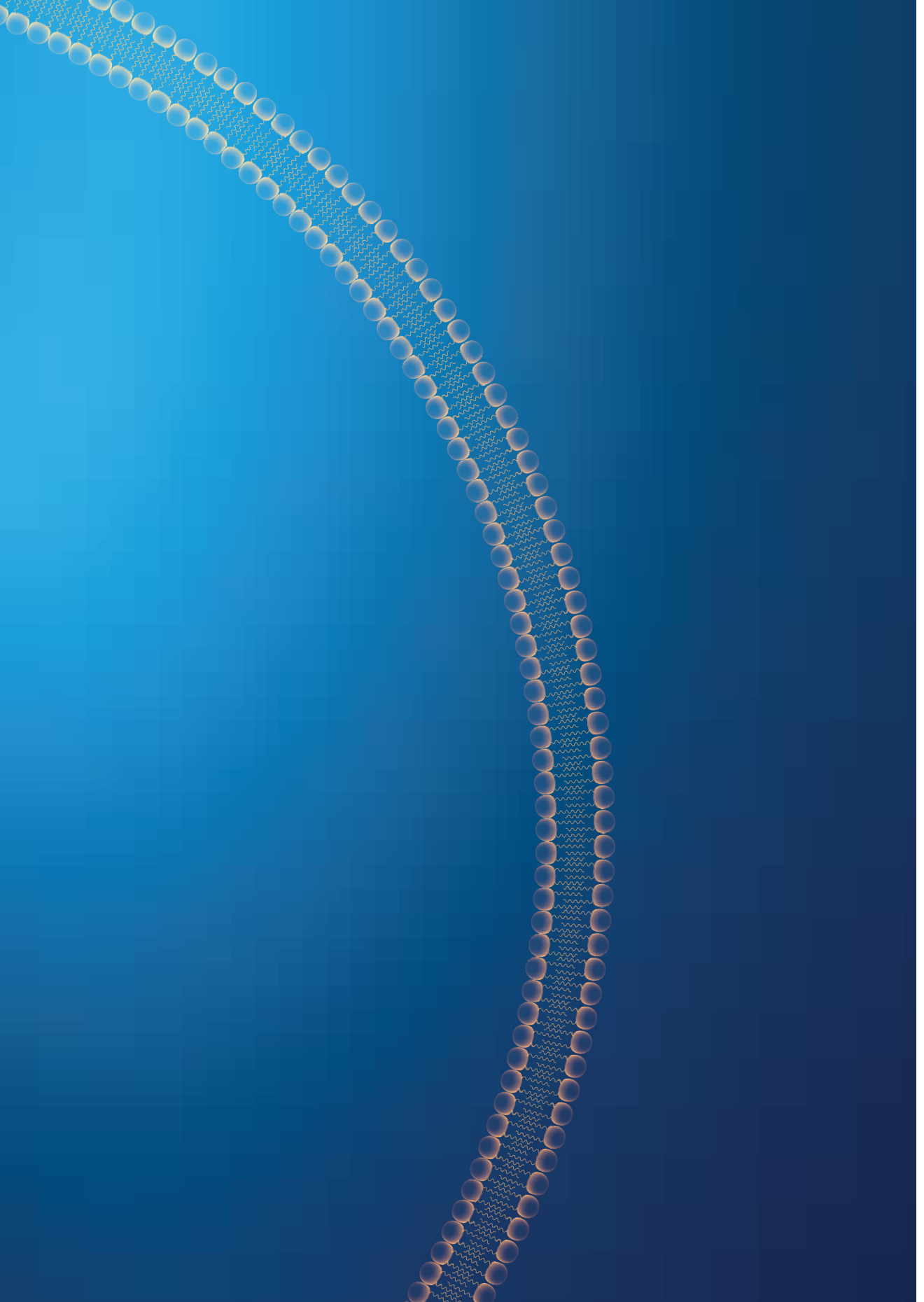

CHAPTER 6

Intradermal Versus Subcutaneous Immunization: Effects of Administration Route using a Lipid-PLGA Hybrid Nanoparticle Tuberculosis Vaccine

M.M. Szachniewicz, S.J.F. van den Eeden, K.E. van Meijgaarden, K.L.M.C. Franken, S. van Veen, A. Geluk, J.A. Bouwstra, T.H.M. Ottenhoff

Adapted from European Journal of Pharmaceutical Sciences, 2025, 205: 106995

ABSTRACT

Tuberculosis (TB) remains a significant global health challenge, latently affecting around a quarter of the global population. The sole licensed TB vaccine, *Mycobacterium bovis* Bacillus Calmette-Guérin (BCG), shows variable efficacy, particularly among adolescents and adults, underscoring the pressing need for more effective vaccination strategies. The administration route is crucial for vaccine efficacy, and administration via the skin, being rich in immune cells, may offer advantages over conventional subcutaneous routes, which lack direct access to abundant antigen-presenting cells.

This study compared the immunogenic effects of intradermal versus subcutaneous administration of a candidate TB vaccine delivering a Ag85B-ESAT6-Rv2034 (AER) multiphase fusion recombinant protein, in lipid-poly(D,L-lactic-co-glycolic acid) (lipid-PLGA) nanoparticles in mice. In-depth evaluation of immune responses in splenocytes was performed using 27-marker spectral flow cytometry. Both routes elicited significant T-cell responses. However, intradermal administration uniquely increased polyfunctional $CD4^+$ and $CD8^+$ T-cells producing IL-2, IFNγ, and TNFα, associated with protection against TB. Additionally, it significantly increased $CD69^+$ B-cell counts and induced higher AER-specific antibody titers, particularly IgG2a. These results underscore the superior immunogenic potential of intradermal vaccine administration by effectively inducing immune cells associated with TB protection, highlighting its significance in the development of new vaccine strategies.

1. INTRODUCTION

Tuberculosis (TB), caused by the bacterium *Mycobacterium tuberculosis* (Mtb), is one of humanity's oldest and deadliest infectious diseases.[1] It remains a major global health problem, primarily affecting the lungs but capable of impacting other body systems. TB is widespread globally, especially in low-middle income countries and in marginalized communities.[2] It is estimated that about a quarter of the entire human population is latently infected with Mtb. Despite advances in medicine, TB continues to pose a significant threat, aggravated by factors such as inadequate healthcare systems, social inequality, concurrent type-2 diabetes and co-infection with HIV/AIDS.[1] In 2021, 10.6 million people fell ill, and 1.6 million people died because of TB.[3] These statistics highlight the urgent need for improved public health strategies, increased awareness, and access to effective treatment and prevention measures such as vaccines.

The Bacillus Calmette-Guérin (BCG) vaccine, derived from *Mycobacterium bovis*, is currently the only licensed vaccine for TB. Its efficacy against pulmonary TB in adults and adolescents varies substantially, ranging from 0 to 80 %.[4] Yet, it remains extensively utilized due to its proven effectiveness in preventing various forms of TB in children.[5]

Subunit vaccines, formulated using synthesized or purified antigens, DNA, or RNA, are noted for their safety and broad applicability, including for individuals with weakened immune systems.[6] Despite their safety profile, these vaccines often face challenges in terms of immunogenicity, highlighting the need for enhanced delivery strategies.[7] To address this, the study described here focuses on using biocompatible nanoparticles (NPs) in vaccine delivery. These NPs are designed to protect antigens from degradation and premature elimination. Simultaneous encapsulation of antigens and adjuvants may improve the uptake efficacy by antigen-presenting cells (APCs).

In preclinical vaccine delivery research, lipid-PLGA hybrid NPs have emerged as highly effective nanostructures, as evidenced in various studies.[8–13] These NPs are engineered with a biodegradable poly(lactic-co-glycolic acid) (PLGA) core surrounded by a lipid layer. The hybrid nature of these NPs leverages the benefits of two commonly researched types of nanoparticles: PLGA NPs and liposomes. The

PLGA core provides a stable and solid structure for the prolonged and controlled release of antigens and adjuvants, while the lipid shell, often cationic, addresses PLGA's limited immunogenicity. This shell enhances uptake by antigen-presenting cells (APCs), slows down the degradation of the PLGA core by restricting water infiltration, and thus ensures a more controlled release of the cargo.[14–17] In vaccine development, these cationic lipid-PLGA hybrid NPs have shown promising results, significantly boosting immunogenicity and triggering both humoral and cellular immune responses.[11–13,18]

Alternative routes of vaccine administration may potentially further improve the effectiveness of vaccines. Intradermal vaccination is an alternative to intramuscular and subcutaneous routes and offers several advantages. The skin is easily accessible, and, in contrast to muscle and subcutaneous (s.c.) tissues, contains many immune cells, especially APCs such as dendritic cells and Langerhans cells.[19,20] Intradermal immunization was shown to be as effective as the conventional immunization schemes but at lower doses, thus reducing costs and sparing antigen.[21–24] Another advantage is that intradermal (i.d.) injections allow for the possibility of vaccinating less painfully compared to intramuscular and s.c. injections, which may translate to better compliance, especially in children.[25]

This study explored the effect of the administration route (s.c. vs. i.d.) in mice on the immunogenicity of a candidate TB vaccine. The fusion protein antigen, Ag85B-ESAT6-Rv2034 (AER), combined with adjuvants like monophosphoryl lipid A (MPLA) and cytosine-phosphate-guanine motifs oligodeoxynucleotides (CpG ODN) was used in the formulation. This vaccine was delivered using pH-sensitive lipid-PLGA hybrid NPs. The AER antigen is a fusion of three proteins: Ag85B, an epitope-rich immunodominant Mtb antigen;[26] ESAT6, a potent immunomodulatory antigen not expressed by BCG;[27,28] and Rv2034, a potent antigen expressed by Mtb *in vivo*.[29] Murine immune responses were assessed using a 27-marker spectral flow cytometry, focusing on $CD4^+$, $CD8^+$ T-cell, and B-cell responses. Additionally, serum antigen-specific antibody levels were measured.

2. MATERIALS AND METHODS

2.1 Materials

The phospholipids 1,2-dioleoyl-sn-glycero-3-phosphocholine (DOPC), 1,2-dioleoyl-sn-glycero-3-ethylphosphocholine chloride salt (EPC), 1,2-dioleoyl-sn-glycero-3-phosphoethanolamine (DOPE), monophosphoryl lipid A (PHAD), synthetic (MPLA), and N-(4-carboxybenzyl)-N,N-dimethyl-2,3-bis(oleoyloxy)propan-1-aminium (DOBAQ) were procured from Avanti Polar Lipids, Inc., (USA). Class B CpG oligonucleotide ODN1826 was purchased from InvivoGen (the Netherlands). Poly(lactic-co-glycolic acid) (PLGA) (acid terminated), a copolymer ratio of lactide to glycolide of 50:50, and a molecular weight range of 24,000 to 38,000 was acquired from Merck Chemicals B.V. (the Netherlands). Hardware for microfluidic connections, including interconnect tees compatible with capillaries of 360 µm (outer diameter), one-piece (for 360 µm capillaries and for 1/16" tubings), and two-piece fittings (360- µm-to-1.6-mm and 1.6-mm-to-360- µm) for capillaries and tubings of specified dimensions, along with Luer-lock adapters (for use with 360 µm capillaries and 1/16" tubings), were supplied by Mengel Engineering (Denmark). Capillary tubing made of polyether ether ketone (PEEK) (inner diameter of 0.02" and outer diameter of 1/16") as well as a Teflon tube (1/16"), were sourced from Fisher Emergo B.V. and Waters Chromatography B.V., respectively (the Netherlands). Standard polyimide-coated fused silica tubing of 75 µm and 250 µm inner diameters and an external diameter of 360 µm was obtained from BGB Analytik Benelux B.V. (the Netherlands). Polytetrafluoroethylene (PTFE) Luer-lock Hamilton gastight syringes of varying volumes (1710TLL 100 µL, 1001TLL 1 ml, and 1010TLL 10 ml) were purchased from Merck (Germany).

The recombinant fusion protein AER was prepared following the protocol outlined by Franken et al.[30] The genetic material from the Mycobacterium tuberculosis (Mtb) laboratory strain H37Rv was amplified via polymerase chain reaction (PCR) utilizing genomic DNA as the template. The resulting gene products were subsequently cloned into a bacterial vector (*Escherichia coli* strain BL21 DE3) employing an N-terminal hexahistidine (His) tag via Gateway technology (Invitrogen, USA), with sequencing confirming the accuracy of the insertions. Produced AER was subsequently purified as described previously.[30] AER is a 519-amino acid protein with a molecular mass of 56.13 kDa, an isoelectric point (pI) of 5.60, and an aliphatic index of 73.64. The protein

quality was evaluated using gel electrophoresis, Coomassie brilliant blue staining, and Western blot analysis using an anti-His antibody (Invitrogen, USA) to confirm protein size and purity was found to be >95 %. The ToxinSensor Chromogenic Limulus Amebocyte Lysate (LAL) Endotoxin Assay Kit (GenScript, USA) was utilized to quantify endotoxin levels within the protein preparation, confirming contamination levels were below 5 endotoxin units per milligram of protein. Cellular toxicity and non-specific T-cell activation were assessed and excluded using in vitro assays with human peripheral blood mononuclear cells (non-responsive to stimulation with purified protein derivative (PPD) of Mtb) obtained from healthy Dutch donors (recruited at the Sanquin Blood Bank, Leiden, the Netherlands).

2.2 Production of lipid-PLGA hybrid NPs

Lipid-PLGA hybrid NPs were produced by employing a previously described modular microfluidic system.[31] This system utilized a four-component approach (Figure 1). In brief, two flows from Syringe 1 (PLGA in acetonitrile) and Syringe 2 (AER/CpG in water for injection) were combined at a T-junction, creating a T-flow. This mixture was subsequently combined with a flow from Syringe 3 (water for injection) at a subsequent junction, forming a co-flow arrangement where the merged stream from Syringes 1 and 2 served as the inner flow, and the stream from Syringe 3 acted as the outer flow. The flow from this assembly was directed into another T-junction, where it was combined with a lipid mixture consisting of DOPC:DOPE:DOBAQ:EPC in molar ratio 3:5:2:4 (the optimization of the lipid formulation was described previously[32]) and MPLA (in ethanol) from Syringe 4. The flow rates were precisely controlled, with Syringe 1, 2, 3, and 4 delivering fluids at 37.5, 1250, 3712, and 1250 µl/min, respectively, achieving a cumulative flow rate of 6249.5 µl/min. Three different batches were prepared for each immunization, as explained in section *2.5 Immunizations*. The contents of the syringes are summarized in Table 1.

After production, the nanoparticle suspension underwent evaporation and was concentrated twofold for s.c. immunization and tenfold for i.d. immunizations under a stream of nitrogen to accommodate for different injection volume requirements. The volume was adjusted using water for injections and phosphate buffer (PB) concentrate so that the end PB concentration was 10 mM, and pH 7.4. The concentrations of constituents of the resulting suspensions are summarized in Table 2.

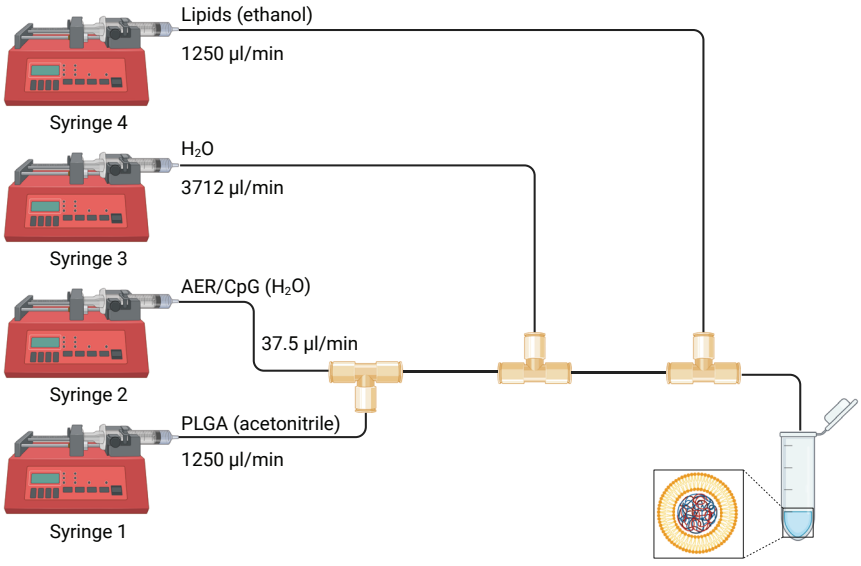

Figure 1. Schematic representation of microfluidic system used for the production of hybrid lipid-PLGA NPs. Syringes 1-4 contain PLGA, AER/CpG, H_2O, and lipids (DOPC:DOPE:DOBAQ:EPC 3:5:2:4 + MPLA), respectively. Solvents are indicated in parentheses as well as output flow rates. Created with BioRender.com.

Table 1. Summary of the concentrations of constituents in syringes 1-4 used in the microfluidic system for each immunization group. AER – Ag85B-ESAT6-Rv2034 protein, lipids -DOPC:DOPE:DOBAQ:EPC 3:5:2:4 (molar ratio).

Group	1) PLGA (mg/ml)	2) AER/CpG (mg/ml)	3) H_2O (mg/ml)	4) Lipids/MPLA (mg/ml)
2.5 µg s.c.	5.00	1.05/1.05	—	5.00/0.0125
0.5 µg i.d.	6.40	0.28/1.40	—	6.40/0.0170
2.5 µg i.d.	6.40	1.40/1.40	—	6.40/0.0170

Table 2. Summary of the end concentrations (after evaporation and volume adjustment) of constituents in each formulation. AER – Ag85B-ESAT6-Rv2034 protein, lipids -DOPC:DOPE:DOBAQ:EPC 3:5:2:4 (molar ratio).

Formulation	PLGA (mg/ml)	AER/CpG (mg/ml)	H_2O (mg/ml)	Lipids/MPLA (mg/ml)
2.5 µg s.c.	2000	12.5/12.5	—	2000/5
0.5 µg i.d.	13400	16.8/84.0	—	13400/34
2.5 µg i.d.	13400	84.0/84.0	—	13400/34

2.3 Physicochemical properties of NPs

The characterization of liposomal formulations, specifically their hydrodynamic diameter (Z-average size) and polydispersity index (PDI), was conducted through dynamic light scattering (DLS), while their zeta potential was assessed via laser Doppler electrophoresis as described previously.[33] Briefly, the NPs were diluted to 0.25 mg/mL lipid concentration in a 10 mM PB at a pH of 7.4 for these analyses. This solution was then transferred into 1.5 ml VWR Two-Sided Disposable Polystyrene (PS) Cuvettes (VWR, the Netherlands) for measurements. The evaluation was carried out in triplicate, using a minimum of ten individual runs at a controlled temperature of 20 °C, utilizing a Nano ZS Zetasizer equipped with a 633 nm laser and optics positioned at 173° (Malvern Instruments, UK). Data processing and analysis were performed using the Zetasizer Software version 7.13 (Malvern Instruments).

2.4 Mice

C57Bl/6 mice (stock number SC1300004) were supplied by The Jackson Laboratory (USA) and housed within the animal care facilities of Leiden University Medical Center (LUMC). Female mice aged 6 to 8 weeks and age-matched were selected for each experiment.

All mouse experiments were individually designed, reviewed, and ethically approved by the institutional Animal Welfare Body at the LUMC, and carried out under project license number AVD116002017856, issued by the Netherlands' authoritative body on animal experimentation, the CCD. These experiments strictly followed the Dutch Act on Animal Experimentation and the European Union Directive 2010/63/EU within the LUMC facility. Mice were housed in separately ventilated cages with no more than seven mice per cage, and experiments began only after a one-week acclimatization period following transport.

2.5 Immunizations

Mice received vaccinations utilizing pH-sensitive lipid-PLGA hybrid NPs as delivery systems for AER protein antigen and molecular adjuvants MPLA and CpG. Lipid-PLGA hybrid NPs consist of DOPC:DOPE:DOBAQ:EPC 3:5:2:4 (lipid layer) and PLGA (core). The vaccination protocol entailed administering three subcutaneous (s.c.) or intradermal (i.d.) injections. S.C. injections (200 µl) were performed in the right

flank, and i.d. injections (30 µl) in the tail base area. Immunizations were performed biweekly, using formulations as detailed in Table 3. Vaccine formulations were freshly prepared a day prior to each immunization and stored at 4 °C to ensure quality and consistency. Four weeks following the final vaccination, the mice were humanely euthanized with CO_2. The timeline of the experiment is summarized in Figure 2.

Table 3. Summary of vaccination groups and doses of vaccine constituents administered to a mouse in a single immunization. AER – Ag85B-ESAT6-Rv2034 protein, lipid -DOPC:DOPE:DOBAQ:EPC 3:5:2:4 (molar ratio).

Group	Route	AER (µg)	Lipid (µg)	PLGA (µg)	CpG (µg)	MPLA (µg)
Naïve	NA	NA	NA	NA	NA	NA
2.5 µg s.c.	subcutaneous	2.5	400	400	2.5	1
0.5 µg i.d.	intradermal	0.5	400	400	2.5	1
2.5 µg i.d.	intradermal	2.5	400	400	2.5	1

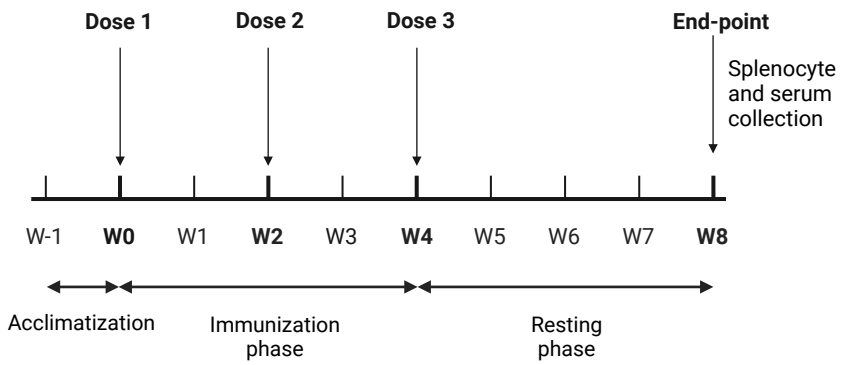

Figure 2. Overview of the immunization experiment timeline. Created with BioRender.com.

2.6 Splenocyte cultures

Splenocytes harvested from immunized mice were suspended at a density of 3×10^6 cells/ml in Iscove's Modified Dulbecco's Medium (IMDM; Lonza, Switzerland), supplemented with 2 mM GlutaMAX™ and 100 U/100 µg/ml of penicillin-streptomycin (both sourced from Gibco, Paisley, UK), along with 8 % heat-inactivated fetal bovine serum (FBS; Greiner, Frickenhausen, Germany). These cells were then restimulated *in vitro* using 5 µg/ml of AER at 37 °C / 5 % CO_2. Six days later, the splenocytes received a second stimulation with the identical antigen for 5 hours, followed by

adding 2.5 µg/ml Brefeldin A (Sigma, Merck, Darmstadt, Germany) and incubation overnight. Subsequently, these cells were harvested and used for flow cytometry analysis.

2.7 Antibody enzyme-linked immunosorbent assay (ELISA)

Blood samples were collected from immunized mice via cardiac puncture following humane euthanasia with CO_2 and were immediately placed on ice for preservation. Subsequent centrifugation at 15,000 rpm for 10 minutes facilitated the separation of sera. The presence of antibodies specific to proteins within the sera was quantified using ELISA, as described previously.[31,34,35] For this purpose, Microlon 96-well plates (Greiner Bio-One GmbH, Germany) were coated overnight at 4 °C with either AER (5 µg/ml) or a control solution of PBS / 0.4 % bovine serum albumin (BSA; Sigma, Merck, Darmstadt, Germany), followed by a blocking phase of 2 hours with PBS containing 1 % BSA and 1 % Tween-20. Serum samples were diluted to 100 µl per well using a series of serial dilutions starting at 1:200 and incubated at 37 °C for 2 hours. After washing with PBS/0.05 % Tween-20, the plates were incubated with horseradish peroxidase (HRP)-conjugated rabbit anti-mouse antibodies targeting total IgG, IgG1, and IgG2a (Dako, Denmark) for another 2 hours at 37 °C. After washing, 100 µl of tetramethylbenzidine (TMB; Merck, Germany) substrate was added to each well for 15 minutes. The reaction was halted by adding 1M H_2SO_4, and the optical density at 450 nm (OD450) was measured using a Spectramax i3x spectrometer (Molecular Devices, CA, USA).

2.8 Flow cytometry

The surface and intracellular staining methodology was detailed in prior publications.[31,35] The list of antibodies is summarized in Table 4. Briefly, splenocytes were transferred to 96-well plates and washed with PBS. The cells were stained using the Zombie UV Fixable Viability Kit (BioLegend, the Netherlands) at a dilution of 1:250 in PBS, with each well receiving 100 µl of the dye solution for 30 minutes. Subsequently, the cells were washed with FACS buffer (PBS supplemented with 0.1 % BSA). The cells were then blocked with 20 µl of 5 % normal mouse serum (Thermo Fisher Scientific Inc., Bleiswijk, the Netherlands) in FACS buffer, followed by additional washes before staining with CCR7 for 30 minutes at 37 °C. After another two washes, cells were incubated with 50 µl per well of an antibody mixture, which included

Table 4. List of antibodies used in for spectral flow cytometry analysis of $CD4^+$, $CD8^+$, and $CD3^-$ $CD19^+$ cells.

Marker	Fluorochrome	Clone	Manufacturer
CCR7 (CD197)	PE/Cyanine5	4B12	BioLegend
CD273	Brilliant Ultra Violet (BUV) 395	TY25	BD Biosciences
CD8b.2	BUV 496	53-5.8	BD Biosciences
CD80	BUV 661	16-10A1	BD Biosciences
CD69	BUV 737	H1.2F3	BD Biosciences
CD25	Brilliant Violet (BV) 480	PC61	BD Biosciences
CD154	Super Bright 436	MR1	Thermo Fisher
IgD	Pacific Blue	11-26c.2a	BioLegend
I-A/I-E (MHC class II)	BV 510	M5/114.15.2	BioLegend
CD44	BV 570	IM7	BioLegend
PD-1 (CD279)	BV 605	29F.1A12	BioLegend
CXCR3 (CD183)	BV 650	CXCR3-173	BioLegend
KLRG1 (MAFA)	BV 711	2F1/KLRG1	BioLegend
CCR6 (CD196)	BV 785	29-2L17	BioLegend
CD4	Spark Blue 550	GK1.5	BioLegend
CCR5 (CD195)	PerCP/Cyanine5.5	HM-CCR5	BioLegend
CD19	PE Fire 640	6D5	BioLegend
CD138	APC	281-2	BioLegend
B220 (CD45R)	Spark NIR 685	RA3-6B2	BioLegend
CD62L (L-selectin)	APC/Fire 750	MEL-14	BioLegend
CD3	APC/Fire 810	17A2	BioLegend
IL-2	APC-R700	JES6-5H4	BD Biosciences
IL-17A	PE	eBio17B7	Thermo Fisher
IgM	FITC	RMM-1	BioLegend
IL-10	PE/Dazzle 594	JES5-16E3	BioLegend
TNFα	PE/Cyanine7	MP6-XT22	BioLegend
IFNγ	Alexa Fluor 647	XMG1.2	BioLegend

10 µl per well of BD Horizon Brilliant Stain Buffer Plus (BD Biosciences, Belgium), for 30 minutes at 4 °C. Following two more washes with FACS buffer, cells were fixed and permeabilized using the eBioscience Foxp3/Transcription Factor Staining Buffer Set (Invitrogen, Thermo Fisher Scientific, Belgium) at 4 °C for an hour. After washing, intracellular staining was conducted with an antibody mix diluted in permeabilization buffer, with a 45-minute incubation in 50 µl per well of the antibody mixture. After two final washes in FACS buffer, cells were resuspended in 100 µl per well of FACS buffer and stored at 4 °C until analysis. The samples were analyzed using a Cytek Aurora spectral flow cytometer (Cytek Biosciences, Fremont, CA, USA) at the Flow Cytometry Core Facility of Leiden University Medical Center, the Netherlands.

2.9 Flow cytometry data analysis

Data was analyzed using FlowJo version 10.8.0 (FlowJo LLC, BD, USA) and OMIQ (www.omiq.ai) platforms. Initially, manual gating was performed in FlowJo to exclude debris, doublets, and cells affected by acquisition disturbances. Subsequent gating focused on the distinction between CD3 and CD19 markers, enabling the separation of T-cells ($CD3^+$ $CD19^-$) and B-cells ($CD3^-$ $CD19^+$), with each subgroup being exported with a minimum of 20,000 events into OMIQ for further analysis. Within OMIQ, the data underwent additional cleaning via FlowAI, followed by establishing single marker gates. Boolean gating techniques were then applied to derive combinations of gates. The counts derived from all Boolean gating were retrieved for further analysis, and statistical analysis was carried out.

2.10 Statistical analysis

With the Benjamini-Hochberg false discovery rate (FDR) adjustment, the Mann-Whitney U test was employed to discern differentially abundant cell populations, utilizing the R[36] and RStudio,[37] interface for analysis. For comparisons among vaccination cohorts, statistical assessments were executed in GraphPad Prism, version 8.01 (GraphPad Software, Prism, USA), using the Kruskal-Wallis test followed by Dunn's posthoc test without correction for multiple comparisons. This non-parametric test was used to evaluate differences across three or more groups in relation to a control group. A significance threshold was established at $P < 0.05$, with specific notation indicating levels of statistical significance: *$P < 0.05$, **$P < 0.01$, ***$P < 0.001$, ****$P < 0.0001$. Graphs show median ± interquartile range (IQR).

3. RESULTS

3.1 Characterization of lipid-PLGA hybrid NPs and study design

Lipid-PLGA hybrid NPs were used to deliver AER antigen with CpG and MPLA adjuvants. The produced NPs were characterized, and the results are summarized in Table 5. All the produced formulations had very similar physicochemical characteristics – size 145-155 nm, PDI 0.16, and Zeta-potential 25 mV. These results assure that the differences in immunological responses are unlikely to be caused by differences in the formulations. The day after the formulations were produced and characterized, the vaccines were administered to mice. Three immunizations were administered two weeks apart, with a fresh batch of vaccines prepared for each immunization. Any remaining vaccine from each batch was discarded. Two different routes of administration were tested: subcutaneous (s.c.) and intradermal (i.d.). The immunization groups are detailed in Table 3.

Table 5. Physicochemical properties of pH-sensitive lipid-PLGA hybrid NPs used for immunization of mice. Results represent an average of n = 6 batches (3 batches used in 2 experiments). Lipid-PLGA hybrid NPs consisting of AER, DOPC:DOPE:DOBAQ:EPC 3:5:2:4 (lipid layer) and PLGA (core).

Formulation	Z-average size (nm)	PDI (-)	Zeta-potential (mV)
2.5 µg/mouse AER s.c.	143.9 ± 18.5	0.16 ± 0.02	25.8 ± 1.1
2.5 µg/mouse AER i.d.	143.1 ± 18.5	0.16 ± 0.01	25.1 ± 2.8
0.5 µg/mouse AER i.d.	156.4 ± 14.7	0.17 ± 0.01	25.7 ± 0.6

3.2 AER-specific T-cell responses in splenocytes ex vivo

Splenocytes from immunized mice were harvested and restimulated with AER. Subsequently, splenocytes were stained and spectral flow cytometry was performed to evaluate immune responses. To investigate T-cell populations, uniform manifold approximation and projection (UMAP) was employed for dimensionality reduction and global qualitative analysis across experimental groups. UMAP analysis included all $CD3^+$ $CD19^-$ events to provide a comprehensive overview of T-cell distributions (Figure 3). Visual inspection of the UMAP plots revealed prominent variations

in T-cell abundance between experimental groups. Immunized groups showed increased abundance of several $CD4^+$ and $CD8^+$ T-cell subpopulations compared to the unimmunized control.

The color-gradient plots highlighted that many of the increased T-cell populations in the immunized groups expressed cytokines IL-2, TNFα, and IFNγ, as well as the surface marker CD62L, indicative of functional immune activation. Furthermore, a distinct difference in the abundance of $IFN\gamma^+$ $CD4^+$ and $IFN\gamma^+$ $CD8^+$ T-cells was observed when comparing the subcutaneous group (2.5 µg dose) with the intradermal group, suggesting route-dependent immune responses.

These qualitative findings prompted further analysis to identify differentially abundant T-cell subsets, which were subsequently subjected to quantitative univariate analysis to reveal the immune responses elicited in the experimental groups.

Criteria for selection included populations exceeding 100 events and possessing distinct phenotypic markers that not only set them apart from other subsets but also provided insights into their potential functional roles.

T-cells, especially $CD4^+$ T-cells, are crucial immune components in protection against Mtb infection.[38,39] The differential abundance analysis revealed several differentially abundant $CD4^+$ T-cell subsets (Figure 4). Notably, three distinct populations were observed that produced one, two, or three cytokines simultaneously. Two Th1 subsets were significantly increased in vaccinated mice compared to naïve mice: trifunctional $CD4^+$ $IL\text{-}2^+$ $IFN\gamma^+$ $TNF\alpha^+$ $IL\text{-}17A^-$ $IL\text{-}10^-$ $CD44^-$ $CD62L^+$ $CCR7^-$, and bifunctional $CD4^+$ $IL\text{-}2^+$ $IFN\gamma^+$ $TNF\alpha^-$ $IL\text{-}17A^-$ $IL\text{-}10^-$ $CD44^-$ $CD62L^+$ $CCR7^-$, both exhibiting central memory-like phenotypes. Trifunctional Th1 cells were increased only in mice vaccinated i.d. but not s.c. Moreover, mice vaccinated with 2.5 µg AER i.d. had significantly higher counts of the trifunctional Th1 cells compared to the corresponding group vaccinated s.c. It should be noted that although the data patterns were consistent, there was a substantial spread within the data from the two experiments. Interestingly, the highest cell counts in s.c. vaccinated mice were observed for a monofunctional subset of $CD4^+$ $IL\text{-}2^+$ $IFN\gamma^-$ $TNF\alpha^-$ $IL\text{-}17A^-$ $IL\text{-}10^-$ $CD44^-$ $CD62L^+$ $CCR7^-$ cells.No Th17 responses were observed. $CD4^+$ T-cell responses in lower and higher AER i.d. vaccinated groups were very similar.

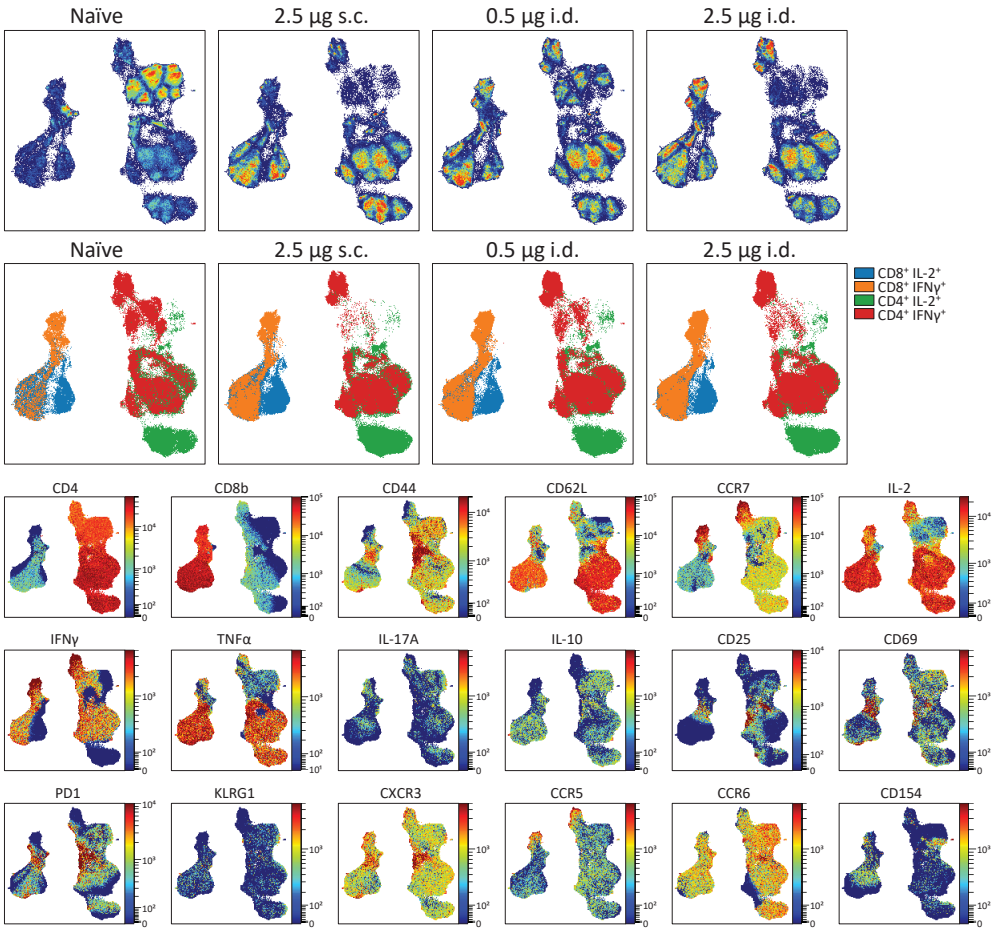

Figure 3. UMAP plots visualize dimensionally reduced phenotypes of spleen-derived $CD4^+$ and $CD8^+$ T-cells ($CD3^+$ $CD19^-$) from all tested mice in each group, demonstrating differences in cell population abundances. Additionally, color-continuous plots were employed to illustrate the distribution of phenotypical markers. Groups represent: naïve – unimmunized mice, 2.5 µg s.c. – immunization with 2.5 µg AER subcutaneously, 0.5 µg i.d. – immunization with 0.5 µg AER intradermally, 2.5 µg i.d. – immunization with 2.5 µg AER intradermally.

Similarly, differentially abundant $CD8^+$ T-cells were found (Figure 5), which play a role in chronic stages of Mtb infection. The largest group of $CD8^+$ T-cells identified in this study was a trifunctional type of central memory T-cells, characterized as$CD8^+$ $IL\text{-}2^+$ $IFN\gamma^+$ $TNF\alpha^+$ $IL\text{-}17A^-$ $IL\text{-}10^-$ $CD44^-$ $CD62L^+$ $CCR7^-$. This subset was significantly increased in all i.d. vaccinated groups, unlike those vaccinated s.c. Additionally,

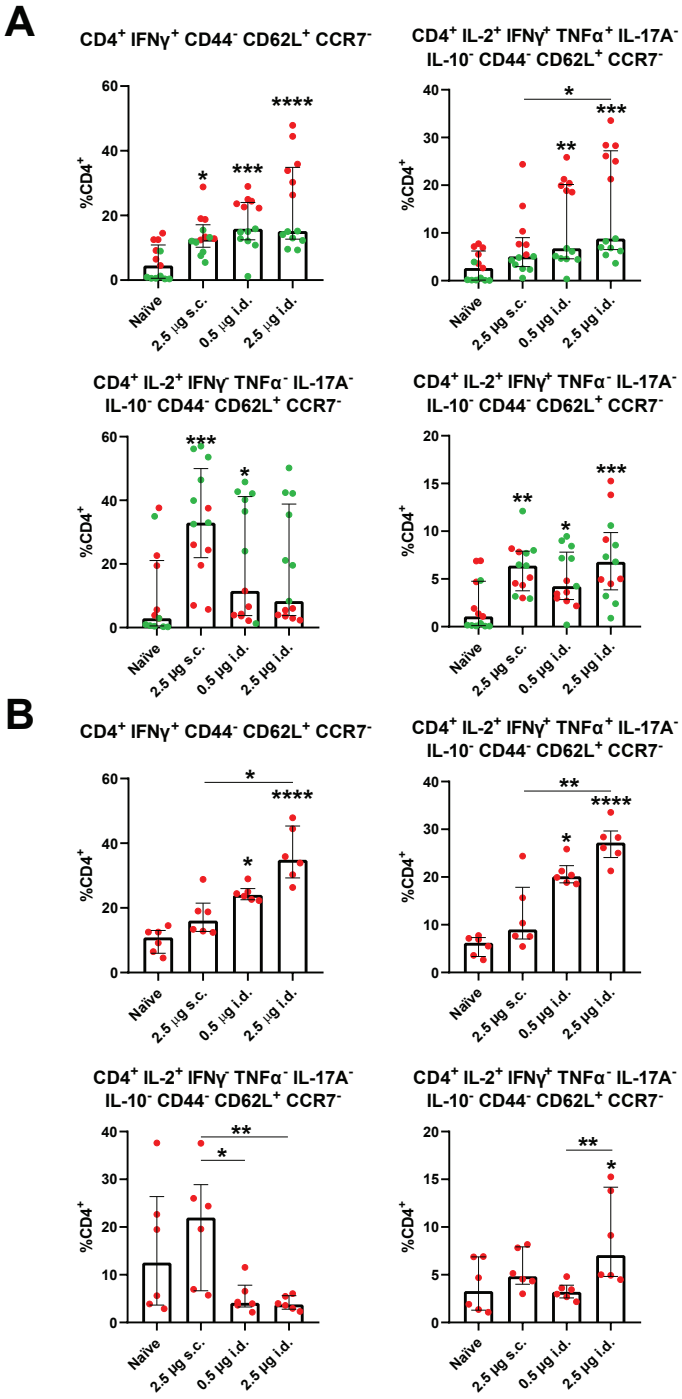
A
CD4+ IFNγ+ CD44- CD62L+ CCR7-
CD4+ IL-2+ IFNγ+ TNFα+ IL-17A- IL-10- CD44- CD62L+ CCR7-
CD4+ IL-2+ IFNγ- TNFα- IL-17A- IL-10- CD44- CD62L+ CCR7-
CD4+ IL-2+ IFNγ+ TNFα- IL-17A- IL-10- CD44- CD62L+ CCR7-
B
CD4+ IFNγ+ CD44- CD62L+ CCR7-
CD4+ IL-2+ IFNγ+ TNFα+ IL-17A- IL-10- CD44- CD62L+ CCR7-
CD4+ IL-2+ IFNγ- TNFα- IL-17A- IL-10- CD44- CD62L+ CCR7-
CD4+ IL-2+ IFNγ+ TNFα- IL-17A- IL-10- CD44- CD62L+ CCR7-
%CD4+
Naïve
2.5 µg s.c.
0.5 µg i.d.
2.5 µg i.d.

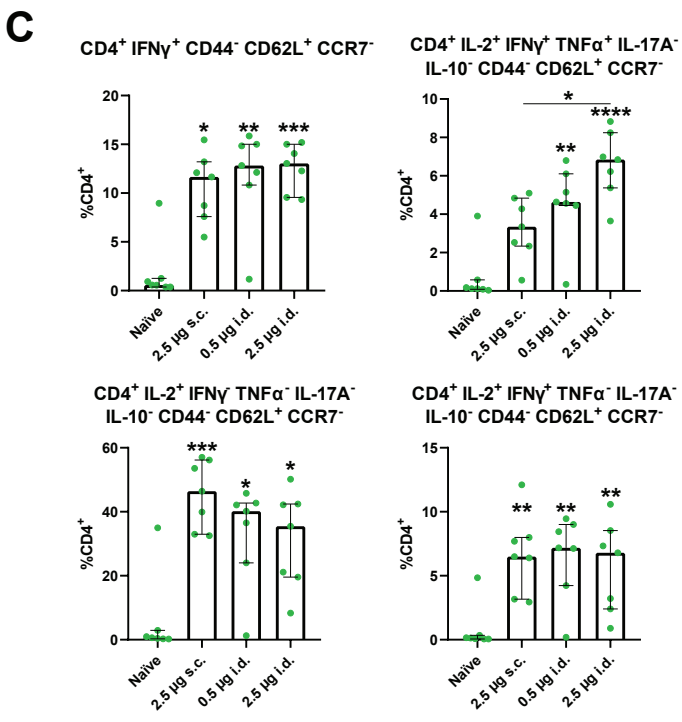

←↑ **Figure 4.** Variations in the abundance of CD4⁺ T-cell populations within restimulated splenocytes from immunized mice. Each graph identifies the markers characterizing the respective populations and displays the percentage values of these populations as median ± IQR within the CD3⁺ CD19⁻ CD4⁺ CD8⁻ cell subset. A) Combined results from both experiments. Each dot represents a single mouse, and the results of the same experiment are shown in one color. n = 13 (mice). B) Results from the first experiment. n = 6 (mice). C) Results from the second experiment. n = 7 (mice). The minimal number of events used in the analysis was 20,000. Groups represent: naïve – unimmunized mice, 2.5 µg s.c. – immunization with 2.5 µg AER subcutaneously, 0.5 µg i.d. – immunization with 0.5 µg AER intradermally, 2.5 µg i.d. – immunization with 2.5 µg AER intradermally.

a bifunctional central memory T-cell subset CD8⁺ IL-2⁺ IFNγ⁺ TNFα⁻ CD44⁻ CD62L⁺ was increased in both the s.c. and i.d. vaccinated groups. No differences in lower and higher AER i.d. vaccinated groups were found. Like for CD4⁺ T cells, also here, although patterns were consistent, there was a substantial spread within the data from the two experiments.

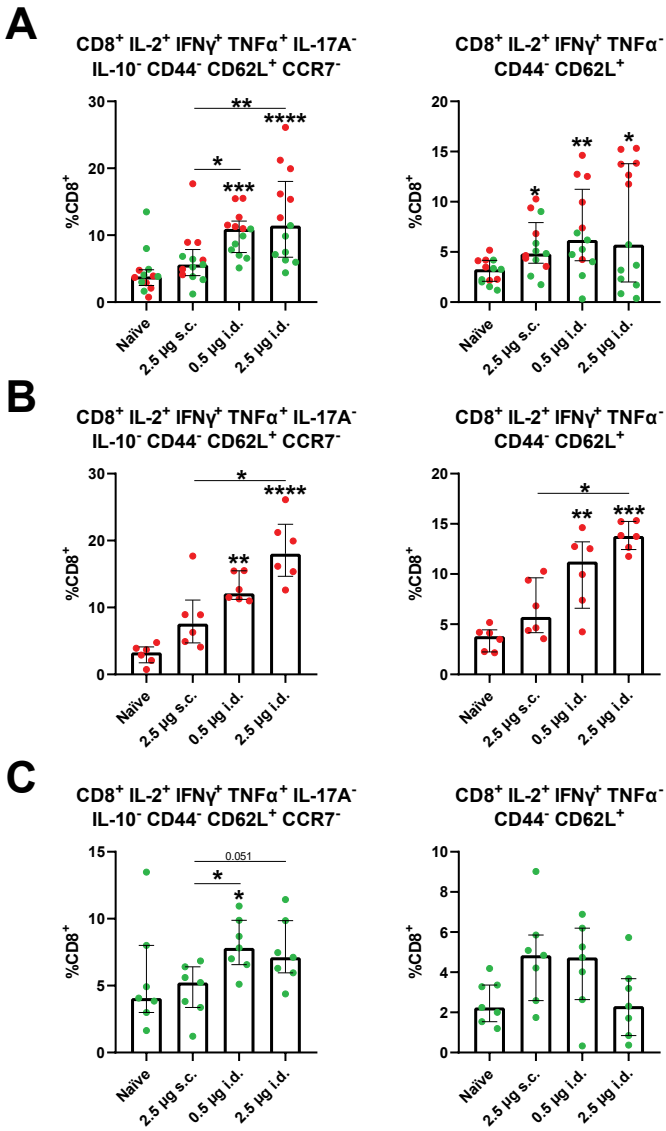

Figure 5. Variations in the abundance of CD8⁺ T-cell populations within restimulated splenocytes from immunized mice. Each graph identifies the markers characterizing the respective populations and displays the percentage values of these populations as median ± IQR within the CD3⁺ CD19⁻ CD4⁻CD8⁺ cell subset. A) Combined results from both experiments. Each dot represents a single mouse, and the results of the same experiment are shown in one color. n = 13 (mice). B) Results from the first experiment. n = 6 (mice). C) Results from the second experiment. n = 7 (mice). The minimal number of events used in the analysis was 20,000. Groups represent: naïve – unimmunized mice, 2.5 µg s.c. – immunization with 2.5 µg AER subcutaneously, 0.5 µg i.d. – immunization with 0.5 µg AER intradermally, 2.5 µg i.d. – immunization with 2.5 µg AER intradermally.

3.3 Differentially abundant AER-specific B-cells from splenocytes ex vivo

B-cells are believed to play a supportive role in immune responses through several mechanisms, including antigen presentation, immune regulation, and antibody production.[40] B-cell data ($CD3^-$ $CD19^+$) were analyzed using the UMAP algorithm for dimensionality reduction and visual assessment of global changes across experimental groups (Figure 6). The UMAP plots revealed subtle differences in the abundance of B-cell subpopulations between the groups. Notably, color-gradient plots indicated that the most pronounced differences were observed in B-cell populations expressing IgM, IgD, and CD69 markers.

To confirm these observations and further investigate the differences, a quantitative analysis was conducted. Differential abundance analysis identified statistically significant B-cell subsets, which were subsequently examined in detail using univariate plots (Figures 7 and 8). Three distinct populations were identified among the AER-restimulated B-cells, all expressing the activation marker CD69 (Figure 7). The predominant population was characterized as $MHCII^+$ IgM^- IgD^- $B220^+$ $CD69^+$ B-cells, indicative of germinal center B-cells. This was followed by $MHCII^+$ IgM^- IgD^+ $B220^+$ $CD69^+$ B-cells, resembling follicular B/B2 cells, and $MHCII^+$ IgM^+ IgD^- $B220^+$ $CD69^+$ B-cells, akin to marginal zone B-cell and transitional 1 B-cells (follicular B/B2). These three B-cell subsets exhibited higher abundance in the groups vaccinated i.d. compared to s.c. We also observed three subsets of B-cells that were $MHCII^-$, expressed B220, and varied in IgM and IgD levels (Figure 8). MHCII is downregulated as B-cells differentiate into antibody-producing B-cells.[41] We can speculate that these cells might be transitional subsets of antibody-producing B-cells. All three subsets were significantly increased in the i.d. but not s.c. groups, suggesting that i.d. immunization led to better B-cell stimulation and, consequently, humoral responses. There were no differences between i.d. vaccinated groups.

To further explore the humoral immune response, AER-specific antibody titers in sera of immunized mice were quantified (Figure 9). Total AER-specific antibody titers in sera from naïve mice were below the detection limit, preventing the assessment of antibody subtypes in these samples. In line with the flow cytometry results, significantly higher total antibody titers in both i.d. groups compared to the s.c. group were observed. Analyzing the antibody subtypes, no difference in IgG1 levels

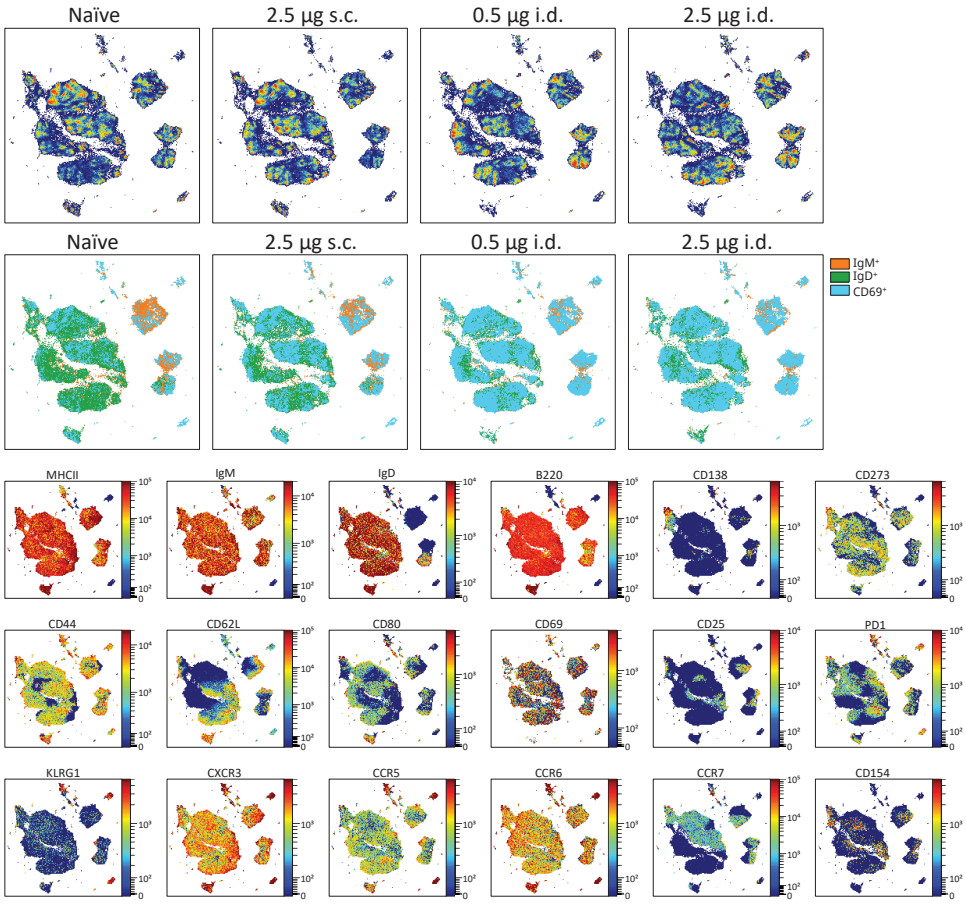

Figure 6. UMAP visualization displays concatenated spleen-derived B-cells ($CD3^-$ $CD19^+$) from all tested mice in each group, highlighting differences in the abundance of various cell populations. This was complemented by color-continuous plots showing the distribution of cellular markers. Groups represent: naïve – unimmunized mice, 2.5 µg s.c. – immunization with 2.5 µg AER subcutaneously, 0.5 µg i.d. – immunization with 0.5 µg AER intradermally, 2.5 µg i.d. – immunization with 2.5 µg AER intradermally.

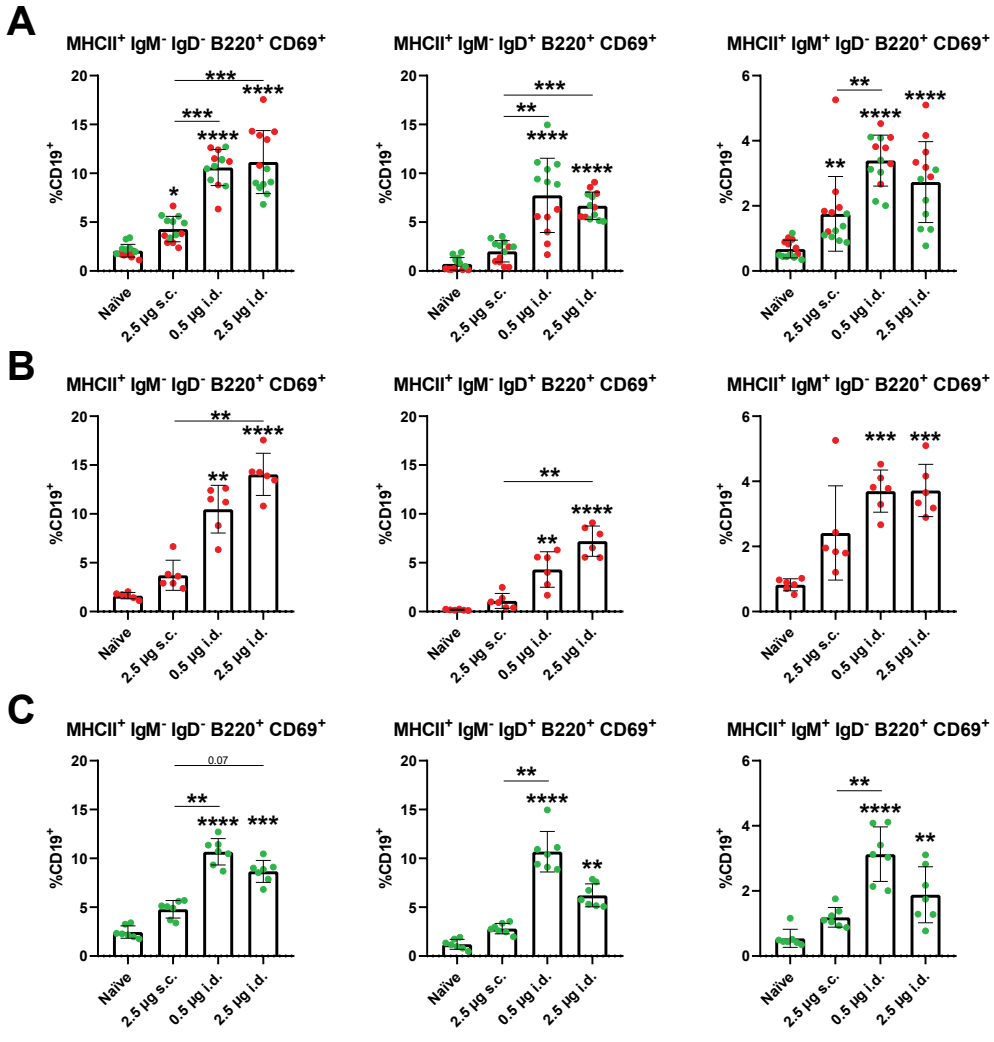

Figure 7. Differentially abundant populations of $CD3^{-}$ $CD19^{+}$ B-cells expressing CD69 in restimulated splenocytes from immunized mice. The markers defining each population are specified above the respective graphs, which present the percentages of these populations as median ± IQR within the overall cell subset. A) Combined results from both experiments. Each dot represents a single mouse, and the results of the same experiment are shown in one color. n = 13 (mice). B) Results from the first experiment. n = 6 (mice). C) Results from the second experiment. n = 7 (mice). The minimal number of events used in the analysis was 20,000. Groups represent: naïve – unimmunized mice, 2.5 µg s.c. – immunization with 2.5 µg AER subcutaneously, 0.5 µg i.d. – immunization with 0.5 µg AER intradermally, 2.5 µg i.d. – immunization with 2.5 µg AER intradermally.

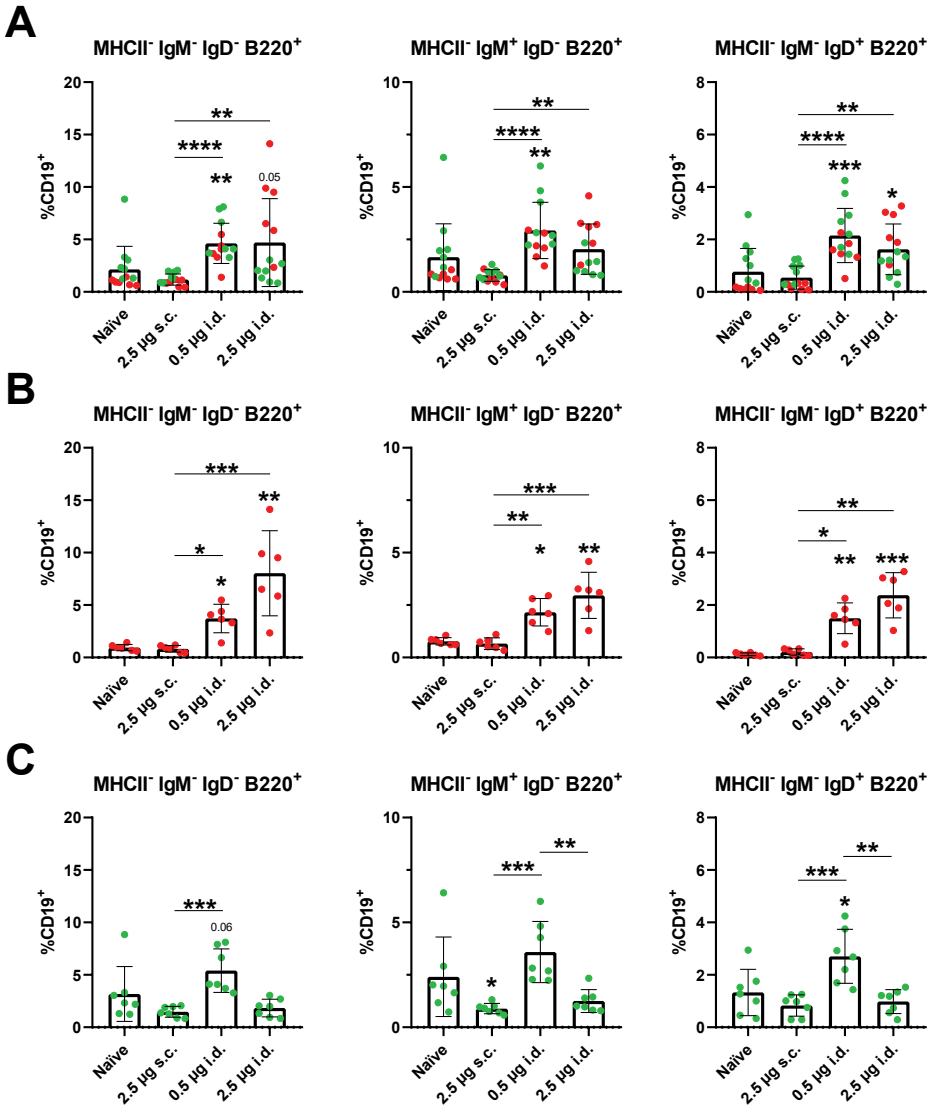

Figure 8. Differentially abundant populations of CD3⁻ CD19⁺ B-cells in restimulated splenocytes from immunized mice. The markers defining each population are specified above the respective graphs, which present the percentages of these populations as median ± IQR within the overall cell subset. A) Combined results from both experiments. Each dot represents a single mouse, and the results of the same experiment are shown in one color. n = 13 (mice). B) Results from the first experiment. n = 6 (mice). C) Results from the second experiment. n = 7 (mice). The minimal number of events used in the analysis was 20,000. Groups represent: naïve – unimmunized mice, 2.5 µg s.c. – immunization with 2.5 µg AER subcutaneously, 0.5 µg i.d. – immunization with 0.5 µg AER intradermally, 2.5 µg i.d. – immunization with 2.5 µg AER intradermally.

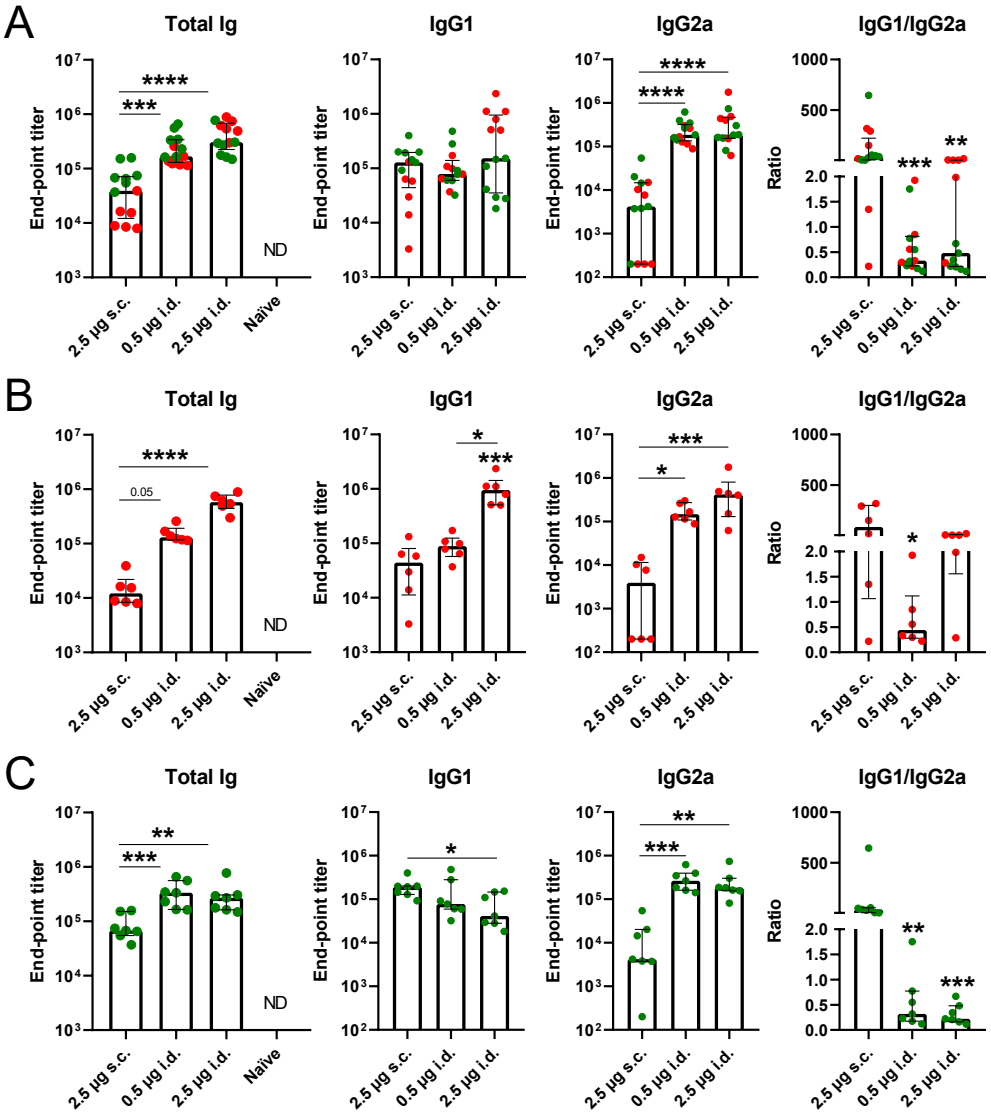

Figure 9. Quantification of AER-specific serum antibodies. The type of antibody measured is indicated above each graph. Values represent end-point titers. A) Combined results from both experiments. Each dot represents a single mouse, and the results of the same experiment are shown in one color. n = 13 (mice). B) Results from the first experiment. n = 6 (mice). C) Results from the second experiment. n = 7 (mice). Groups represent: 2.5 µg s.c. – immunization with 2.5 µg AER subcutaneously, 0.5 µg i.d. – immunization with 0.5 µg AER intradermally, 2.5 µg i.d. – immunization with 2.5 µg AER intradermally, naïve – unimmunized mice.

was detectable; however, IgG2a titers were significantly increased in i.d. groups. These findings might be indicative of overall dominant T-helper responses. Increased IgG2 levels are related to more robust Th1-like immunity, while higher IgG1 levels compared to IgG2 can be linked to Th2-like responses. This shift in T-helper response balance is reflected in the IgG1/IgG2a ratio. However, no increased Th2 subsets were identified in the spectral flow cytometry data in the s.c. group. The Ig ratio in s.c. group is possibly related to suboptimal IFNγ production that led to less efficient antibody class switching. The antibody titters were very similar in lower and higher AER groups vaccinated i.d.

4. DISCUSSION

TB continues to be a global health challenge, particularly in economically disadvantaged and marginalized populations.[1] Innovations in vaccine technology, such as subunit vaccines and biocompatible NP-based vaccine delivery systems, offer promise for safer, more effective immunization strategies.[7] This includes exploring i.d. vaccination routes. I.d. vaccination offers several benefits over traditional methods by delivering vaccines into the skin's dermis, which is rich in APCs.[19,20] This approach often leads to robust immune responses with smaller doses, which is crucial for expanding accessibility, especially in middle- and low-income countries as well as dose sparing.[21–24] Reduced vaccine dosages lower costs, and the shorter needles used with this method reduce discomfort, potentially improving patient compliance and better vaccination coverage.[25] Novel technologies such as microneedle patches may allow for self-administration, which could simplify vaccination efforts. Solid vaccine formulation may potentially improve stability during storage and shelf-life as well as allow for storage at room temperatures. I.d. vaccination emerges as an efficient, cost-effective, and safe strategy that may lead to improved global public health outcomes. This work compared the immunological effects of i.d. administration of low-dose lipid-PLGA hybrid NP-based TB vaccine to the conventional s.c. route.

$CD4^+$ T-cells, especially Th1 cells, are essential in host defence against Mtb through their cytokine production and facilitation of immune responses.[38,39] A key cytokine, IFNγ, plays a significant role in activating macrophages, differentiating $CD8^+$ T-cells, and stimulating B-cells.[42] Concurrently, TNFα synergizes with IFNγ to enhance the production of reactive oxygen and nitrogen species in macrophages, support the migration of immune cells, and facilitate granuloma formation.[43] Comparing the

two routes of administration, both significantly increased the magnitude of IFNγ-producing $CD4^+$ T-cells. However, only i.d. immunizations induced polyfunctional $CD4^+$ T-cells expressing IL-2, IFNγ, and TNFα. In our previous studies,[31,35] AER-based vaccines (at an 8 μg AER dose) formulated with liposomes composed of DOPC:DOPE:DOBAQ:EPC in a 3:5:2:4 ratio (the same lipid ratio used in this study for hybrid NPs), PLGA NPs, and lipid-PLGA hybrid NPs induced high levels of polyfunctional $CD4^+$ T-cells. Coincidentally, these vaccines provided protection against intranasal challenge with live H37Rv Mtb, as evidenced by a significant and immunologically relevant reduction in Mtb bacterial burden in the lungs and spleens of the challenged mice. Other studies in mice[44,45] and humans[46] suggest that these polyfunctional $CD4^+$ T-cells play a crucial and superior role in vaccine induced immunity against Mtb. Nevertheless, some studies challenged this hypothesis.[47,48] In contrast, s.c. immunization induced single positive IL-2-producing T-cells. These results indicate that i.d. immunization induced favorable and protection-associated T-cell subsets, whereas s.c. did not.

The role of cytotoxic $CD8^+$ T-cells in protection against Mtb remains debated. Besides directly eliminating infected cells, these cells also produce cytokines, influence the immune response, and enhance the function of Th1 cells.[49] Studies suggest $CD8^+$ T-cells and Th1 cells are promising targets for new TB vaccines.[38,50] Experiments in mice[51] and non-human primates[52] demonstrate that depletion of $CD8^+$ T-cells increases vulnerability to TB, highlighting their necessity for optimal control of infection, and underscores their vital role during the chronic infection stages.[53] In this study, two differentially abundant $CD8^+$ T-cell subsets were found. The abundance of polyfunctional $CD8^+$ T-cells was increased only in i.d. immunized mice, similarly to the $CD4^+$ counterpart. In our previous work,[31,35] the abundance of polyfunctional CD8+ T-cells was significantly increased, potentially contributing to the observed protection against Mtb infection. Less abundant double-positive IL-2- and IFNγ-producing CD8+ T-cells were increased using both methods.

All the differentially abundant T-cells were found to express CD62L without expressing CD44 or CCR7, indicating they could be a unique subset of central memory T-cells that have lost CD44[54] or could consist of transitional subsets. T-cells with such a profile were shown to offer beneficial anti-Mtb responses, displayed considerable expansion, and provided substantial protection when transferred into $Rag^{-/-}$ mice infected with aerosolized Mtb H37Rv, in contrast to the $CD4^+$ $CD44^{hi}$ $CD62L^{lo}$ cells.[55]

The $CD4^{+}$ $CD44^{lo}$ $CD62L^{hi}$ cells may be an important reservoir of memory cells, potentially offering protection in a manner aligned with the characteristics of central memory T-cells.[55]

Though complex and not fully understood, the role of B-cell and antibody responses in TB immunity is increasingly acknowledged.[56,57] B-cells may contribute to protective immune responses against TB through mechanisms like cytokine release, antigen presentation, immune regulation, opsonization, and direct neutralization of Mtb.[40] Support for their involvement comes from the observation of increased B-cell numbers in infected tissues across species,[58,59] worsened TB susceptibility in B-cell-depleted models reversed by B-cell reintroduction,[60,61] and the normalization of B-cell function after TB treatment.[57] Despite this, some studies using genetic knockouts[62–64] and different infection models[65–67] have questioned their significance in TB immunity. Therefore, the B-cell arm of immune responses was also investigated in this study. Six differentially abundant B-cell subsets were identified, of which three expressed CD69 activation marker. In all six identified subsets, i.d. immunized groups showed a significantly higher abundance of B-cells compared to the s.c. route, indicating that the B-cell arm of immunity was better activated by i.d. immunization.

Antibodies are also postulated to offer protection against TB, evidenced e.g. by successful serum therapy in immunodeficient mice[68] and reduced Mtb load through high-dose immunoglobulin treatments.[69] Protective effects were further demonstrated through serum transfers from latently infected patients and exposure-resistant individuals,[70] as well as monoclonal antibodies targeting specific mycobacterial antigens, which improved survival, limited spread, reduced tissue damage, and lowered bacterial counts.[71–76] In this study, significant total AER-specific antibody responses were observed in all immunized mice, though i.d. immunization induced significantly higher titers compared to s.c. route. Antibody subtype analysis revealed that AER-specific IgG1 titers were similar in all immunized mice; however, IgG2a titers were significantly higher in both lower and higher AER dose i.d. immunized groups compared to the s.c. one. Moreover, in four out of thirteen mice in the s.c. group, IgG2a titers were below the detection level, indicating suboptimal antibody class switching in these mice.

The results from all of the evaluated cellular and humoral immune responses indicated that i.d. immunization provided superior outcomes compared to s.c. immunization. This finding is in line with previously published research demonstrating that i.d. immunization provides the same or improved immune responses to vaccines.[22,23,77,78] Future research will evaluate the effectiveness of these vaccines in Mtb challenge studies.

5. CONCLUSIONS

This study assessed the immunogenicity of a novel subunit TB vaccine, focusing on the impact of different immunization routes. The vaccine formulation included the Ag85B-ESAT6-Rv2034 fusion antigen, adjuvants CpG and MPLA, and a cationic lipid (DOPC:DOPE:DOBAQ:EPC in a 3:5:2:4 ratio) combined with PLGA in a hybrid nanoparticle delivery system. *In vivo* experiments revealed that the vaccine elicited enhanced T-cell responses across both immunization routes. Notably, mice immunized via the i.d. route exhibited significant increases in polyfunctional $CD4^+$ and $CD8^+$ T-cell responses compared to the s.c. one, which are considered crucial for protection against Mtb. In contrast, s.c. administration resulted in increased monofunctional (IL-2-producing) T-cells and no polyfunctional responses. Also, the i.d. route led to a rise in $CD69^+$ B-cell subpopulations, which were higher compared to s.c. vaccinated mice. While both immunization routes increased antigen-specific antibody titers, the i.d. route resulted in markedly higher total Ig and IgG2a titers compared to the s.c. route. The comprehensive analysis of cellular and humoral responses indicates that i.d. immunization is superior to s.c. immunization. These results provide insights into the differential effects of vaccine administration routes and underscore the potential of the tested vaccine as a promising candidate for further TB vaccine development. Further research, including Mtb challenge studies, is necessary to confirm the efficacy of this vaccine approach.

ABBREVIATIONS

AER, Ag85B-ESAT6-Rv2034 antigen; APC, antigen-presenting cell; Ag, antigen(-adjuvant mix group); BCG, Mycobacterium bovis Bacillus Calmette–Guérin; CCR, C-C chemokine receptor type; CD, cluster of differentiation; CpG ODN, cytosine-phosphorothioate-guanine oligodeoxynucleotides; CXCR, C-X-C motif chemokine receptor; DC, dendritic cell; DOBAQ, N-(4-carboxybenzyl)-N,N-dimethyl-2,3-bis(oleoyloxy)propan-1-aminium; DOPC, 1,2-dioleoyl-sn-glycero-3-phosphocholine;

DOPE, 1,2-dioleoyl-sn-glycero-3-phosphoethanolamine; EPC, 1,2-dioleoyl-sn-glycero-3-ethylphosphocholine; FBS, fetal bovine serum; FDR, false discovery rate; HLA, human leukocyte antigen; HRP, horse radish peroxide; IFN, interferon; Ig, immunoglobulin, IL, interleukin; i.d., intradermal; IQR, interquartile range; KLRG1, killer cell lectin-like receptor subfamily G member 1; LUMC, Leiden University Medical Center; MDR-TB, multidrug-resistant tuberculosis; MHC, major histocompatibility complex; MPLA, monophosphoryl lipid A; Mtb, *Mycobacterium tuberculosis*; NP, nanoparticle; PCR, polymerase chain reaction; PD-1, programmed cell death protein 1; PDI, polydispersity index; PE, phosphatidylethanolamine; pH, pH-sensitive liposome group; PLGA, poly(D,L-lactic-co-glycolic acid); rpm, rounds per minute; s.c., subcutaneous; TB, tuberculosis; Th1/Th2, type 1/2 helper T-cell; TLR, Toll-like receptor; TNF, tumor necrosis factor; UMAP, uniform manifold approximation and projection.

FUNDING

This work was supported by the Dutch Research Council (NWO) Domain Applied and Engineering Sciences grant, project number: 15240.

CREDIT AUTHOR STATEMENT

M.M. Szachniewicz: Conceptualization, Methodology, Formal Analysis, Investigation, Writing – Original Draft. **S.J.F. van den Eeden**: Conceptualization, Methodology, Investigation, Writing – Original Draft. **K.E. van Meijgaarden**: Conceptualization, Methodology, Writing – Review & Editing, Supervision. **K.L.M.C. Franken**: Methodology, Investigation, Resources. **S. van Veen**: Methodology, Formal Analysis. **A. Geluk**: Conceptualization, Writing – Review & Editing, Project Administration, Funding Acquisition, Supervision. **J.A. Bouwstra**: Conceptualization, Writing – Review & Editing, Project Administration, Funding Acquisition, Supervision. **T.H.M. Ottenhoff**: Conceptualization, Writing – Review & Editing, Project Administration, Funding Acquisition, Primary supervision.

DECLARATIONS OF INTEREST

None.

REFERENCES

1. Bloom, B. R. A half-century of research on tuberculosis: Successes and challenges. *Journal of Experimental Medicine* 220, (2023).
2. Schrager, L. K. *et al.* The status of tuberculosis vaccine development. *Lancet Infectious Diseases* 20, e28–e37 (2020).
3. World Health Organization. *Global Tuberculosis Report 2023*. (2023).
4. Brewer, T. F. Preventing Tuberculosis with Bacillus Calmette-Guérin Vaccine: A Meta-Analysis of the Literature. *Clinical Infectious Diseases* 31, S64–S67 (2000).
5. Trunz, B. B. *et al.* Effect of BCG vaccination on childhood tuberculous meningitis and miliary tuberculosis worldwide: a meta-analysis and assessment of cost-effectiveness. *Lancet* 367, 1173–1180 (2006).
6. Moyle, P. M. & Toth, I. Modern Subunit Vaccines: Development, Components, and Research Opportunities. *ChemMedChem* 8, 360–376 (2013).
7. Christensen, D. *et al.* Cationic liposomes as vaccine adjuvants. *Expert Review of Vaccines* 10, 513–521 (2011).
8. Alsaab, H. O. *et al.* PLGA-Based Nanomedicine: History of Advancement and Development in Clinical Applications of Multiple Diseases. *Pharmaceutics* 14, 2728 (2022).
9. Khademi, F. *et al.* Induction of strong immune response against a multicomponent antigen of Mycobacterium tuberculosis in BALB/c mice using PLGA and DOTAP adjuvant. *APMIS* 126, 509–514 (2018).
10. Khademi, F. *et al.* A novel antigen of Mycobacterium tuberculosis and MPLA adjuvant co-entrapped into PLGA:DDA hybrid nanoparticles stimulates mucosal and systemic immunity. *Microbial Pathogenesis* 125, 507–513 (2018).
11. Moon, J. J. *et al.* Antigen-Displaying Lipid-Enveloped PLGA Nanoparticles as Delivery Agents for a Plasmodium vivax Malaria Vaccine. *PLoS One* 7, e31472 (2012).
12. Liu, L. *et al.* Hyaluronic Acid-Modified Cationic Lipid-PLGA Hybrid Nanoparticles as a Nanovaccine Induce Robust Humoral and Cellular Immune Responses. *ACS Applied Materials & Interfaces* 8, 11969–11979 (2016).
13. Liu, L. *et al.* Immune responses to vaccines delivered by encapsulation into and/or adsorption onto cationic lipid-PLGA hybrid nanoparticles. *Journal of Controlled Release* 225, 230–239 (2016).

14. Hadinoto, K. *et al.* Lipid–polymer hybrid nanoparticles as a new generation therapeutic delivery platform: A review. *European Journal of Pharmaceutics and Biopharmaceutics* 85, 427–443 (2013).
15. Sah, H. *et al.* Concepts and practices used to develop functional PLGA-based nanoparticulate systems. *International Journal of Nanomedicine* 8, 747–765 (2013).
16. Pandita, D. *et al.* Hybrid poly(lactic-co-glycolic acid) nanoparticles: design and delivery prospectives. *Drug Discovery Today* 20, 95–104 (2015).
17. Ghitman, J. *et al.* Review of hybrid PLGA nanoparticles: Future of smart drug delivery and theranostics medicine. *Materials & Design* 193, 108805 (2020).
18. Rose, F. *et al.* A strong adjuvant based on glycol-chitosan-coated lipid-polymer hybrid nanoparticles potentiates mucosal immune responses against the recombinant Chlamydia trachomatis fusion antigen CTH522. *Journal of Controlled Release* 271, 88–97 (2018).
19. Kashem, S. W. *et al.* Antigen-Presenting Cells in the Skin. *Annual Review of Immunology* 35, 469–499 (2017).
20. Levin, C. *et al.* Tailored immunity by skin antigen-presenting cells. *Human Vaccines & Immunotherapeutics* 11, 27–36 (2015).
21. Fabrizi, F. *et al.* Meta-analysis: intradermal vs. intramuscular vaccination against hepatitis B virus in patients with chronic kidney disease. *Alimentary Pharmacology & Therapeutics* 24, 497–506 (2006).
22. Schnyder, J. L. *et al.* Fractional dose of intradermal compared to intramuscular and subcutaneous vaccination - A systematic review and meta-analysis. *Travel Medicine and Infectious Disease* 37, 101868 (2020).
23. Schnyder, J. L. *et al.* Comparison of equivalent fractional vaccine doses delivered by intradermal and intramuscular or subcutaneous routes: A systematic review. *Travel Medicine and Infectious Disease* 41, 102007 (2021).
24. Egunsola, O. *et al.* Immunogenicity and Safety of Reduced-Dose Intradermal vs Intramuscular Influenza Vaccines: A Systematic Review and Meta-analysis. *JAMA Network Open* 4, e2035693–e2035693 (2021).
25. Witting, N. *et al.* Intramuscular and intradermal injection of capsaicin: a comparison of local and referred pain. *Pain* 84, 407–412 (2000).
26. Karbalaei Zadeh Babaki, M. *et al.* Antigen 85 complex as a powerful Mycobacterium tuberculosis immunogene: Biology, immune-pathogenicity, applications in diagnosis, and vaccine design. *Microbial Pathogenesis* 112, 20–29 (2017).

27. Li, W. *et al.* A recombinant adenovirus expressing CFP10, ESAT6, Ag85A and Ag85B of Mycobacterium tuberculosis elicits strong antigen-specific immune responses in mice. *Molecular Immunology* 62, 86–95 (2014).
28. You, Q. *et al.* Subcutaneous Administration of Modified Vaccinia Virus Ankara Expressing an Ag85B-ESAT6 Fusion Protein, but Not an Adenovirus-Based Vaccine, Protects Mice Against Intravenous Challenge with Mycobacterium tuberculosis. *Scandinavian Journal of Immunology* 75, 77–84 (2012).
29. Commandeur, S. *et al.* An Unbiased Genome-Wide Mycobacterium tuberculosis Gene Expression Approach To Discover Antigens Targeted by Human T Cells Expressed during Pulmonary Infection. *The Journal of Immunology* 190, 1659–1671 (2013).
30. Franken, K. L. M. C. *et al.* Purification of His-Tagged Proteins by Immobilized Chelate Affinity Chromatography: The Benefits from the Use of Organic Solvent. *Protein Expression and Purification* 18, 95–99 (2000).
31. Szachniewicz, M. M. *et al.* Evaluation of PLGA, lipid-PLGA hybrid nanoparticles, and cationic pH-sensitive liposomes as tuberculosis vaccine delivery systems in a Mycobacterium tuberculosis challenge mouse model – A comparison. *International Journal of Pharmaceutics* 666, 124842 (2024).
32. Szachniewicz, M. M. *et al.* Cationic pH-sensitive liposomes as tuberculosis subunit vaccine delivery systems: Effect of liposome composition on cellular innate immune responses. *International Immunopharmacology* 145, 113782 (2025).
33. Szachniewicz, M. M. *et al.* Intrinsic immunogenicity of liposomes for tuberculosis vaccines: Effect of cationic lipid and cholesterol. *European Journal of Pharmaceutical Sciences* 195, 106730 (2024).
34. Geluk, A. *et al.* A multistage-polyepitope vaccine protects against Mycobacterium tuberculosis infection in HLA-DR3 transgenic mice. *Vaccine* 30, 7513–7521 (2012).
35. Szachniewicz, M. M. *et al.* Cationic pH-sensitive liposome-based subunit tuberculosis vaccine induces protection in mice challenged with Mycobacterium tuberculosis. *European Journal of Pharmaceutics and Biopharmaceutics* 203, 114437 (2024).
36. R Core Team. R: A language and environment for statistical computing, (2023).
37. RStudio Team. RStudio: Integrated Development Environment for R, (2023).
38. Ottenhoff, T. H. M. & Kaufmann, S. H. E. Vaccines against Tuberculosis: Where Are We and Where Do We Need to Go? *PLoS Pathogens* 8, e1002607 (2012).

39. Ottenhoff, T. H. M. *et al.* Human CD4 and CD8 T Cell Responses to Mycobacterium tuberculosis: Antigen Specificity, Function, Implications and Applications. *Handbook of Tuberculosis* 119–155 (2008.
40. Rijnink, W. F. *et al.* B-Cells and Antibodies as Contributors to Effector Immune Responses in Tuberculosis. *Frontiers in Immunology* 12, 640168 (2021).
41. Giles, J. R. *et al.* B Cell–Specific MHC Class II Deletion Reveals Multiple Nonredundant Roles for B Cell Antigen Presentation in Murine Lupus. *The Journal of Immunology* 195, 2571–2579 (2015).
42. Prezzemolo, T. *et al.* Functional signatures of human CD4 and CD8 T cell responses to Mycobacterium tuberculosis. *Frontiers in Immunology* 5, 83298 (2014).
43. Cavalcanti, Y. V. N. *et al.* Role of TNF-alpha, IFN-gamma, and IL-10 in the development of pulmonary tuberculosis. *Pulmonary Medicine* 2012:1, 745483 (2012).
44. Aagaard, C. *et al.* A multistage tuberculosis vaccine that confers efficient protection before and after exposure. *Nature Medicine* 17:2, 189–194 (2011).
45. Lindenstrøm, T. *et al.* Tuberculosis Subunit Vaccination Provides Long-Term Protective Immunity Characterized by Multifunctional CD4 Memory T Cells. *The Journal of Immunology* 182, 8047–8055 (2009).
46. Abel, B. *et al.* The Novel Tuberculosis Vaccine, AERAS-402, Induces Robust and Polyfunctional CD4+ and CD8+ T Cells in Adults. *American Journal of Respiratory and Critical Care Medicine* 181, 1407–1417 (2012).
47. Harari, A. *et al.* Dominant TNF-α+ Mycobacterium tuberculosis–specific CD4+ T cell responses discriminate between latent infection and active disease. *Nature Medicine* 17:3, 372–376 (2011).
48. Lewinsohn, D. A., Lewinsohn, D. M. & Scriba, T. J. Polyfunctional CD4+ T cells as targets for tuberculosis vaccination. *Frontiers in Immunology* 8, 295382 (2017).
49. Lu, Y. J. *et al.* CD4 T cell help prevents CD8 T cell exhaustion and promotes control of Mycobacterium tuberculosis infection. *Cell Reports* 36, 109696 (2021).
50. Boom, W. H. New TB vaccines: is there a requirement for CD8+ T cells? *Journal of Clinical Investigation* 117, 2092–2094 (2007).
51. Woodworth, J. S. *et al.* Mycobacterium tuberculosis-Specific CD8+ T Cells Require Perforin to Kill Target Cells and Provide Protection In Vivo. *The Journal of Immunology* 181, 8595–8603 (2008).

52. Lin, P. L. *et al.* CD4 T Cell Depletion Exacerbates Acute Mycobacterium tuberculosis While Reactivation of Latent Infection Is Dependent on Severity of Tissue Depletion in Cynomolgus Macaques. *AIDS Research and Human Retroviruses* 28, 1693–1702 (2012).
53. Van Pinxteren, L. A. H. *et al.* Control of latent Mycobacterium tuberculosis infection is dependent on CD8 T cells. *European Journal of Immunology* 30, 3689–3698 (2000).
54. Henao-Tamayo, M. I. *et al.* Phenotypic definition of effector and memory T-lymphocyte subsets in mice chronically infected with mycobacterium tuberculosis. *Clinical and Vaccine Immunology* 17, 618–625 (2010).
55. Kipnis, A. *et al.* Memory T Lymphocytes Generated by Mycobacterium bovis BCG Vaccination Reside within a CD4 CD44lo CD62 Ligandhi Population. *Infection and Immunity* 73, 7759 (2005).
56. Duong, V. T. *et al.* Towards the development of subunit vaccines against tuberculosis: The key role of adjuvant. *Tuberculosis* 139, 102307 (2023).
57. Joosten, S. A. *et al.* Patients with Tuberculosis Have a Dysfunctional Circulating B-Cell Compartment, Which Normalizes following Successful Treatment. *PLoS Pathogens* 12, e1005687 (2016).
58. Phuah, J. Y. *et al.* Activated B Cells in the Granulomas of Nonhuman Primates Infected with Mycobacterium tuberculosis. *American Journal of Pathology* 181, 508–514 (2012).
59. Tsai, M. C. *et al.* Characterization of the tuberculous granuloma in murine and human lungs: cellular composition and relative tissue oxygen tension. *Cell Microbiology* 8, 218–232 (2006).
60. Maglione, P. J. *et al.* B Cells Moderate Inflammatory Progression and Enhance Bacterial Containment upon Pulmonary Challenge with Mycobacterium tuberculosis. *The Journal of Immunology* 178, 7222–7234 (2007).
61. Phuah, J. *et al.* Effects of B cell depletion on early Mycobacterium tuberculosis infection in cynomolgus macaques. *Infection and Immunity* 84, 1301–1311 (2016).
62. Khera, A. K. *et al.* Role of B Cells in Mucosal Vaccine–Induced Protective CD8+ T Cell Immunity against Pulmonary Tuberculosis. *The Journal of Immunology* 195, 2900–2907 (2015).
63. Torrado, E. *et al.* Differential and Site Specific Impact of B Cells in the Protective Immune Response to Mycobacterium tuberculosis in the Mouse. *PLoS One* 8, e61681 (2013).

64. Vordermeier, H. M. *et al.* Increase of tuberculous infection in the organs of B cell-deficient mice. *Clinical & Experimental Immunology* 106, 312–316 (2003).
65. Turner, J. *et al.* The progression of chronic tuberculosis in the mouse does not require the participation of B lymphocytes or interleukin-4. *Experimental Gerontology* 36, 537–545 (2001).
66. Bosio, C. M. *et al.* Infection of B Cell-Deficient Mice with CDC 1551, a Clinical Isolate of Mycobacterium tuberculosis: Delay in Dissemination and Development of Lung Pathology. *The Journal of Immunology* 164, 6417–6425 (2000).
67. Johnson, C. M. *et al.* Mycobacterium tuberculosis aerogenic rechallenge infections in B cell-deficient mice. *Tubercle and Lung Disease* 78, 257–261 (1997).
68. Guirado, E. *et al.* Passive serum therapy with polyclonal antibodies against Mycobacterium tuberculosis protects against post-chemotherapy relapse of tuberculosis infection in SCID mice. *Microbes and Infection* 8, 1252–1259 (2006).
69. Roy, E. *et al.* Therapeutic efficacy of high-dose intravenous immunoglobulin in Mycobacterium tuberculosis infection in mice. *Infection and Immunity* 73, 6101–6109 (2005).
70. Li, H. *et al.* Latently and uninfected healthcare workers exposed to TB make protective antibodies against Mycobacterium tuberculosis. *Proceedings of the National Academy of Sciences of the United States of America* 114, 5023–5028 (2017).
71. Zimmermann, N. *et al.* Human isotype-dependent inhibitory antibody responses against Mycobacterium tuberculosis. *EMBO Molecular Medicine* 8, 1325–1339 (2016).
72. Balu, S. *et al.* A Novel Human IgA Monoclonal Antibody Protects against Tuberculosis. *The Journal of Immunology* 186, 3113–3119 (2011).
73. Lu, L. L. *et al.* A Functional Role for Antibodies in Tuberculosis. *Cell* 167, 433-443. e14 (2016).
74. Davies, L. R. L. *et al.* Age and sex influence antibody profiles associated with tuberculosis progression. *Nature Microbiology* 9:6, 1513-1525 (2024).
75. Grace, P. S. *et al.* Antibody Subclass and Glycosylation Shift Following Effective TB Treatment. *Frontiers in Immunology* 12, 679973 (2021).
76. Alter, G. *et al.* Antibody glycosylation in inflammation, disease and vaccination. *Seminars in Immunology* 39, 102–110 (2018).

77. Leone, M. *et al.* Hyaluronan-based dissolving microneedles with high antigen content for intradermal vaccination: Formulation, physicochemical characterization and immunogenicity assessment. *European Journal of Pharmaceutics and Biopharmaceutics* 134, 49–59 (2019).
78. Ogai, N. *et al.* Enhanced immunity in intradermal vaccination by novel hollow microneedles. *Skin Research and Technology* 24, 630–635 (2018).

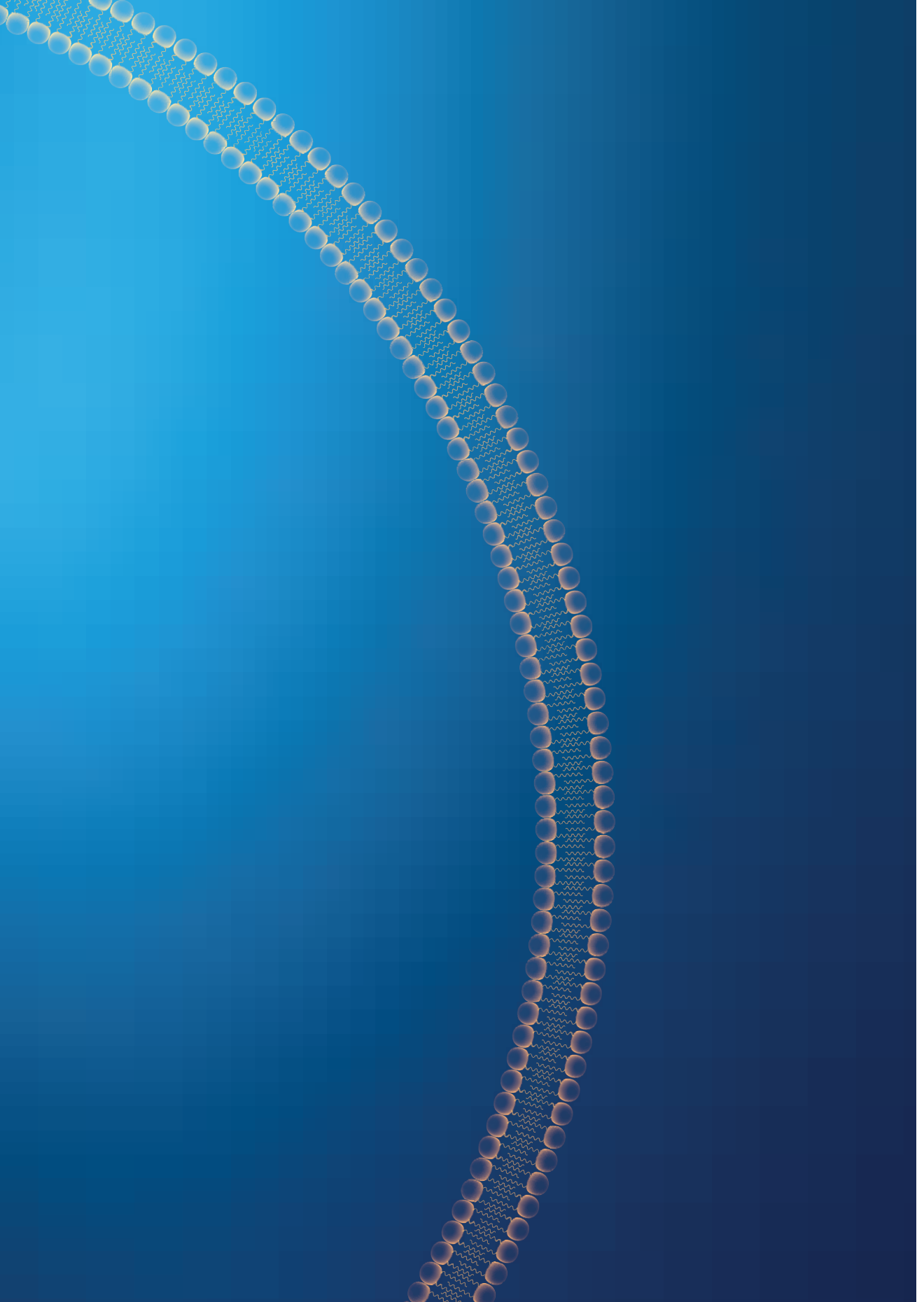

CHAPTER 7

General discussion and future perspectives

1. INTRODUCTION: THE URGENT NEED FOR NEW TB VACCINES

Tuberculosis (TB), caused by the bacterium *Mycobacterium tuberculosis* (Mtb), remains one of the most devastating infectious diseases globally. In 2023, TB regained its position as the leading cause of death from a single infectious agent, surpassing the annual toll of the COVID-19 pandemic. According to the World Health Organization (WHO), approximately 10.8 million people developed TB in 2023, and 1.25 million died from the disease, including 161,000 individuals co-infected with HIV. Furthermore, about 400,000 individuals developed multidrug-resistant or rifampicin-resistant TB (MDR/RR-TB), significantly complicating treatment options and outcomes.[1] These numbers not only highlight the persistent global burden of TB but also underscore the urgent need for more effective public health interventions, especially early diagnosis, host-directed approaches that are not affected by rising drug resistance, like vaccines.

TB disproportionately affects populations in low- and middle-income countries and is closely linked with poverty, undernutrition, and weakened healthcare systems. Moreover, individuals living with HIV are particularly vulnerable due to their compromised immunity, and TB remains the leading cause of death among people with HIV. The global situation is further complicated by the high prevalence of latent TB infection, estimated to affect about a quarter of the world population, posing a vast reservoir for future disease.[1,2]

The Bacillus Calmette-Guérin (BCG) vaccine, derived from *Mycobacterium bovis*, remains the only approved vaccine against TB. While BCG provides reliable protection against severe pediatric TB forms, such as miliary and meningeal TB, its efficacy in preventing pulmonary TB in adolescents and adults is highly variable and generally poor.[3] This limited efficacy, combined with BCG's unsuitability for use in immunocompromised populations and its inability to prevent reactivation from latent TB infection, underscores the critical need for improved vaccination strategies.

To meet the WHO's End TB Strategy goals and the United Nations' Sustainable Development Goals, there is an urgent demand for next-generation TB vaccines that are safe, effective in all age groups, affordable, and suitable for use in resource-limited settings.[4] The recent successes of novel vaccine platforms, including protein subunits, mRNA, and viral vectors, have reinvigorated TB vaccine research. In

particular, subunit vaccines are emerging as highly promising candidates due to their safety profile and the possibility of rational antigen selection.[5,6] When combined with advanced delivery systems such as nanoparticles (NPs), which enhance antigen stability, cellular uptake, and immune activation, these vaccines may overcome the limitations of both BCG and first-generation subunit formulations.[7,8]

This thesis explores the design and evaluation of NP-based subunit vaccine formulations targeting TB, with a focus on enhancing immunogenicity through optimized antigen delivery. In the context of growing antimicrobial resistance and high global comorbidity with HIV, the development of safe and potent vaccine platforms is more critical than ever. This work aims to contribute to this urgent global challenge by investigating novel delivery strategies that could improve TB vaccine efficacy and offer broader insights for future vaccine development.

2. LIMITATIONS OF BCG AND THE CURRENT TB VACCINE DEVELOPMENT LANDSCAPE

Despite being used for over a century, the BCG vaccine remains inadequate for controlling TB, particularly adult pulmonary forms of the disease that drive transmission. Its protective efficacy ranges from 0 % to 80 %, with most studies in high-burden countries reporting poor effectiveness in adolescents and adults.[3] This variability is attributed to multiple factors, including geographic differences, environmental mycobacterial interference, and host genetic background. Importantly, BCG does not reliably protect against reactivation of latent TB infection or multidrug-resistant TB, and it cannot be safely administered to immunocompromised individuals, such as those living with HIV.[3,9]

In response to the limitations of BCG, significant efforts have been made to develop improved TB vaccines. These include a range of technological platforms, each with distinct advantages and challenges:

- **Live-attenuated vaccines**: These aim to improve upon BCG by retaining its ability to stimulate robust immune responses while enhancing antigen expression or attenuating virulence.[10] Examples include VPM1002 and MTBVAC, both in advanced clinical trials.[11] Safety concerns, particularly in immunocompromised populations, remain a possible limitation.[10]

- **Whole-cell inactivated vaccines**: These formulations use killed mycobacteria, such as *Mycobacterium obuense* (DAR-901) or *Mycobacterium indicus pranii* (Immuvac), to stimulate broad immune responses.[11] While generally safe, their immunogenicity is typically weaker, requiring potent adjuvants and repeated administration.[12]

- **Subunit vaccines**: These consist of defined antigens, typically proteins or peptides, combined with adjuvants. Their safety and flexibility make them attractive, especially for vulnerable populations. However, they often suffer from low immunogenicity unless integrated into effective delivery systems.[13] Notable candidates include M72/AS01E, which showed ~50 % efficacy in preventing progression from latent TB infection in a phase IIb trial.[14] Despite growing interest, there are still relatively few adjuvants and delivery systems in late-stage clinical development for TB subunit vaccines. This gap significantly contributes to the translational bottlenecks in the field.[15]

- **Viral vector-based vaccines**: These use replication-deficient viral platforms such as adenoviruses or Modified Vaccinia Ankara (MVA) to deliver TB antigens. They elicit strong T-cell responses and are suitable for prime-boost regimens.[16] Candidates include ChAdOx1.85A and MVA85A.[11] However, there are safety concerns, including rare but serious adverse effects, as seen in other viral vector-based vaccines, and some vectors face pre-existing immunity in target populations, which can limit efficacy.[17]

- **mRNA vaccines**: Building on the success of COVID-19 vaccines, mRNA-based TB vaccine candidates such as BNT164a1 and BNT164b1 (developed by BioNTech) are currently in early-phase clinical trials.[18] These vaccines offer rapid development timelines and flexibility in antigen design. Nonetheless, this approach is in its infancy for TB, and there are still many unknowns regarding how to design mRNA vaccines that are optimized for TB-specific immune responses. More broadly, TB vaccinology remains challenging due to the complex host-pathogen interactions and the lack of well-defined correlates of protection.[19]

Overall, the current TB vaccine pipeline is more diverse and active than ever before. However, no new vaccine has yet replaced or supplemented BCG in routine immunization programs. Continued innovation in antigen selection, formulation,

and delivery is necessary to meet the unique immunological and logistical demands of TB vaccination, particularly in the most affected regions. The research presented in this thesis contributes to this evolving field by investigating NP-based delivery strategies that could enhance the performance of subunit vaccines and offer scalable, safe, and effective solutions for global TB control.

3. RESEARCH RATIONALE AND STUDY OBJECTIVES

While the global TB vaccine pipeline has expanded to include diverse technological platforms, the development of effective subunit vaccines remains constrained by a lack of optimized antigen delivery systems.[8,15,20] Subunit vaccines are among the safest and most adaptable platforms, particularly suited for use in immunocompromised populations and regions with high HIV prevalence. However, their clinical translation has been hindered by inherently low immunogenicity, which necessitates sophisticated delivery systems to achieve robust, durable immune responses. Despite the promise of NPs in enhancing antigen stability, cellular uptake, and immune activation, few NP-based formulations for TB vaccines have advanced beyond early-stage research.[8,15] Compared to the fields of oncology or COVID-19, the TB field still suffers from a significant lag in delivery system innovation and characterization.

This thesis directly addresses this critical bottleneck. It contributes a systematic investigation into how distinct NP platforms, specifically cationic liposomes, PLGA NPs, and hybrid lipid–PLGA systems, can be tailored to improve subunit TB vaccine performance. While both liposomes and PLGA NPs have been individually studied in other biomedical areas, few comparative studies exist within TB vaccinology that examine their relative efficacy, mode of action, and compatibility with rationally designed fusion protein antigens. This work is among the first to perform a side-by-side analysis of these platforms using a consistent antigen and harmonized evaluation criteria.

The antigen used throughout this research Ag85B-ESAT6-Rv2034 (AER), is a rationally selected fusion protein that combines three Mtb-derived antigens known to induce strong T-cell responses.[21–23] By anchoring the delivery system development to this antigen, the thesis ensures biological relevance and translational potential, particularly since AER has already demonstrated protective efficacy in preclinical models.

This research explores several under-investigated aspects of NP design in TB vaccine development. First, it examines the influence of different cationic lipids on immunogenicity, an area where most studies have focused merely on charge, overlooking the potential immunomodulatory effects of specific lipid chemistries.[24] Second, it develops and characterizes pH-sensitive liposomes, which may facilitate improved antigen release in the acidic endosomal compartments of APCs, yet have rarely been tested in TB models.[25] Third, the study introduces a hybrid NP system combining lipid and polymer components to synergize the advantages of both platforms, namely, the endosomal escape capacity of the lipids and the structural rigidity and controlled release of PLGA.[23]

All formulations were tested in murine models using both common subcutaneous and alternative intradermal routes of immunization, with subsequent challenge by the virulent Mtb H37Rv strain delivered intranasally. This approach not only mirrors the pulmonary route of natural infection but also enables rigorous assessment of protective efficacy and immune correlates.[26] The combination of intradermal and subcutaneous vaccination strategies aligns with a growing interest in heterologous prime-boost regimens, which may be essential for achieving sterilizing immunity in TB.[27]

By integrating antigen design with state-of-the-art delivery systems and *in vivo* efficacy testing, this thesis positions itself at the interface of fundamental immunological research and translational vaccine development. It complements existing clinical efforts by addressing a neglected area of the TB vaccine field, the delivery science, and proposes NP-based solutions that could accelerate the development of potent, scalable, and safe vaccines not only for TB, but also for other intracellular pathogens requiring robust cellular immunity.

4. SUMMARY OF THE RESEARCH OF THIS THESIS

To achieve effective immune activation against Mtb, this thesis systematically explored how different NP-based platforms can improve immunogenicity, promote antigen-specific T-cell responses, and ultimately offer protection in preclinical TB models. By synthesizing the insights from both *in vitro* and in vivo studies, the study provides a comprehensive overview of how formulation chemistry, adjuvant co-delivery, particle characteristics, and administration routes collectively shape vaccine efficacy. The summary below highlights how these variables influenced antigen

presentation, immune polarization, memory formation, and protection outcomes, and reflects on their broader implications for the development of next-generation TB vaccines.

In the research described in **Chapter 2**, a broad panel of cationic liposomes was screened to evaluate how different cationic lipids and cholesterol content affect human APC activation and T-cell priming. This study showed that liposomes based on DOTAP and EPC, especially those with cholesterol, exhibited enhanced uptake by dendritic cells and stimulated superior antigen-specific $CD4^+$ T-cell activation *in vitro*. Importantly, the findings highlighted that the immunostimulatory effects of cationic lipids go beyond their net charge and involve structural determinants that modulate membrane rigidity and immune cell engagement. This chapter underscored the significance of careful lipid selection in designing effective vaccine carriers and established DOTAP- and EPC-based formulations as promising candidates.

Building on these findings, in **Chapter 3**, the development and *in vitro* assessment of pH-sensitive liposomes designed to destabilize under acidic endosomal conditions and promote cytosolic antigen release is discussed. These formulations, particularly DOPC:DOPE:DOBAQ:EPC liposomes, showed favorable uptake by APCs and induced robust activation of human MDDCs, leading to efficient presentation to antigen-specific T-cells. The superior cytokine and chemokine induction observed for this pH-sensitive formulation marked it as a promising vector for cross-presentation and $CD8^+$ T-cell priming–an essential but often elusive goal in TB subunit vaccine design.

In the study described in **Chapter 4**, the immunological potential of the optimized pH-sensitive liposomes was validated in a murine TB challenge model. When co-loaded with CpG and MPLA adjuvants, the DOPC:DOPE:DOBAQ:EPC liposomes induced potent polyfunctional $CD4^+$ and $CD8^+$ T-cell responses, increased activation of IL-17A-producing B- and T-cells, and significantly reduced Mtb bacterial burden in the lungs and spleens. Notably, the vaccine achieved protection at antigen and adjuvant doses much lower than those used in the soluble formulation. These findings provided *in vivo* confirmation that delivery system design can critically influence vaccine potency, antigen dose efficiency, and immune polarization.

In **Chapter 5**, the immunological performance of three nanoparticle platforms: PLGA NPs, pH-sensitive liposomes, and lipid-PLGA hybrid NPs, was compared in a head-to-head preclinical study. All three AER-loaded NP vaccines significantly

reduced Mtb burden in the lungs and spleens compared to the antigen-adjuvant mix, which conferred no protection. Although no statistically significant differences were observed between the NP groups, a consistent trend emerged: PLGA NPs showed the greatest median CFU reduction, exceeding BCG by one logarithmic unit, followed by hybrid NPs, then liposomes. This suggests a potential superiority of PLGA-based systems in mediating protective efficacy. Interestingly, immunological data did not fully correlate with protection. The liposomal formulation, which induced the weakest protection, paradoxically generated the highest abundance of T-cell responses, while the antigen-adjuvant mix elicited similar T-cell levels to PLGA NPs but did not confer protection. These findings imply that the magnitude of conventional immune readouts does not directly predict protection, highlighting the unresolved complexity of immune correlates in TB. Similar observations were made for B-cell responses and antibody titers, which did not align with protection outcomes. This chapter underscored the need for better understanding of the qualitative features of vaccine-induced immunity that are mechanistically linked to protection, rather than relying solely on the quantitative expression of specific immune markers.

The study described in **Chapter 6** assessed how the route of administration influences immune responses to a hybrid NP-based TB vaccine. Using intradermal (i.d.) delivery of the lipid–PLGA hybrid NP formulation, this study demonstrated superior induction of polyfunctional $CD4^+$ and $CD8^+$ T-cells, central memory-like phenotypes, and stronger B-cell activation compared to the conventional subcutaneous (s.c.) route. Moreover, i.d. immunization led to significantly higher AER-specific antibody titers and class switching toward IgG2a. These findings align with the increasing recognition of dermal APC richness and dose-sparing advantages of i.d. vaccination, suggesting that strategic delivery routes can further amplify the benefits conferred by NP-based vaccines.

Together, these five chapters demonstrate how careful modulation of NP formulation parameters, lipid composition, pH-sensitivity, polymer-lipid hybridization, adjuvant co-delivery, and administration route can shape the immune response to subunit TB vaccines in distinct and sometimes unexpected ways. While strong immunogenicity was necessary, it was not sufficient to predict protection, emphasizing the need for more refined and/or additional immunological correlates in TB vaccine research, including e.g. innate immunity markers and cell types such as NK cells.

Ultimately, this thesis contributes to a growing body of evidence that immune engineering through tailored NP design can overcome longstanding limitations in TB subunit vaccine development. It lays the groundwork for future work to identify correlates of protection, refine delivery strategies for clinical use, and extend these technologies to other intracellular pathogens requiring strong cell-mediated immunity.

5. KEY INSIGHTS

Bringing together the findings from all experimental chapters, several key take-home messages emerge that go beyond the scope of individual formulations or isolated results. While each chapter addressed specific research questions, several consistent themes and integrative insights became evident across the thesis. These cross-cutting observations highlight the broader scientific relevance of this work and help position it within the larger field of TB vaccine research and NP-based immunization strategies.

1. Delivery System Matters More Than Antigen or Adjuvants Alone

A consistent pattern observed throughout this work is that the mode of antigen delivery, whether via liposomes, PLGA NPs, or hybrid systems, has a decisive impact on both the immunological and protective outcomes. Formulations in which the same antigen (AER) and adjuvants (CpG and MPLA) were delivered in solution failed to confer protection, despite inducing T- and B-cell responses similar in magnitude to some NP-based vaccines. In contrast, all NP-based vaccines significantly reduced bacterial loads *in vivo*. This indicates that antigen delivery vehicles do more than enhance uptake; they fundamentally shape how antigens are processed and presented, which downstream immune pathways are activated, and ultimately, whether protective immunity is achieved.

2. Immune Magnitude Does Not Equate to Immune Efficacy

A second important insight is the dissociation between the magnitude of immune responses and actual protective efficacy. For instance, cationic liposomes often induced the highest T-cell abundances *in vivo* but consistently offered the weakest protection in challenge models. Meanwhile, PLGA NPs, which triggered similar or even lower T-cell frequencies, outperformed liposomes in bacterial clearance, even exceeding the licensed standard BCG vaccine in some instances. These discrepancies

suggest that qualitative aspects of the immune response, such as spatial localization, cellular phenotype, antigen persistence, or functional potential, are more important determinants of protection than bulk measurements of immune magnitude alone.

3. NP Properties Dictate Immune Quality and Protection

Physicochemical properties of NPs, including surface charge, hydrophobicity, rigidity, and particle size, emerged as powerful modulators of immune function. The depot-forming behavior of cationic lipid-containing NPs favors prolonged antigen retention at the injection site, potentially supporting extended antigen presentation.[28,29] Meanwhile, the smaller, negatively charged PLGA NPs likely drained efficiently to lymph nodes, facilitating a different mode of immune priming.[8,30] These formulation-dependent differences not only influenced DC activation and T-cell polarization but also correlated with distinct patterns of bacterial control. Importantly, the type of NP appeared to direct not just *how much* of an immune response was generated, but *what kind* of response predominated.

4. Protection Is Not Driven by a Single Cell Type or Marker

Another cross-cutting finding is that protection could not be linked to a singular immune cell type, cytokine, or antibody isotype. While polyfunctional $CD4^+$ and $CD8^+$ T-cells were consistently observed following NP vaccination, and are widely considered correlates of protection, they were also present in non-protected groups. Similarly, high levels of IgG2a antibodies, often associated with Th1-biased immunity, did not guarantee bacterial clearance. Even B-cell activation markers, which correlated with strong immunogenicity, failed to map clearly with protection outcomes. These results align with the broader consensus that TB immunity is multifactorial and likely requires a constellation of immune features rather than a single hallmark biomarker.

5. pH-Sensitive and Biodegradable Carriers Enable Dose Sparing

The incorporation of pH-sensitive liposomes or biodegradable polymeric NPs enabled substantial dose reduction without compromising efficacy. Vaccines using these delivery platforms were able to reduce the required amount of antigen and adjuvants by several folds while still inducing robust immunity and protection. This

finding has important translational implications for scalable vaccine manufacturing, cost-effective distribution, and dose-sparing strategies, especially in settings where vaccine accessibility remains a challenge.

6. I.d. Administration Enhances Immune Efficiency

Finally, i.d. delivery of hybrid NPs demonstrated superior immunogenicity over s.c. administration, especially considering very low doses of antigens, producing higher frequencies of polyfunctional T- and B-cells and increased antibody titers at reduced doses. This highlights the underutilized potential of i.d. immunization routes and supports ongoing efforts to develop minimally invasive, self-administered, or needle-free delivery systems, particularly relevant for global TB vaccine roll-out.

Conclusion

Taken together, these cross-cutting insights underscore the importance of delivery system design in determining not just immune response magnitude, but also its quality, durability, and protective potential. They also reinforce the central premise of this thesis: that rational engineering of NP-based vaccine platforms, coupled with systematic comparative evaluation, offers a powerful strategy to overcome the immunological challenges posed by TB and other intracellular pathogens. Future work should continue to explore the mechanistic basis of NP-driven immunity, optimize the route of vaccine delivery, and refine correlates of protection, paving the way for the next generation of effective TB vaccines.

6. BROADER IMPLICATIONS FOR TB VACCINE AND DELIVERY SYSTEM DEVELOPMENT

Beyond generating formulation-specific findings, this thesis provides strategic insights that may inform the broader field of vaccinology, particularly in TB but also extending to other infectious and immune-related diseases. The integrated research pipeline developed here offers a structured approach to early-stage vaccine development. This framework enhances the predictive power of preclinical studies and can be adapted across delivery technologies and disease contexts.

Importantly, several key implications emerged that go beyond the immediate study objectives:

1. For Vaccine Design and Immunology

- **Immune Magnitude ≠ Protection**: The consistent disconnect between the magnitude of immune responses (e.g., IFNγ-producing T-cells or high antibody titers) and actual protection challenges long-held assumptions in TB vaccine design. Our findings reinforce the need to identify immune responses with functional relevance, such as tissue-localized memory, recall capacity, or antigen persistence sensing, rather than relying on standard peripheral readouts.
- **Polyfunctionality Is not Predictive Alone**: Despite liposomes inducing the strongest polyfunctional $CD4^+$ and $CD8^+$ T-cell responses, they provided the weakest protection. This decouples polyfunctionality from protection and emphasizes the complexity of protective immunity in TB.
- **Delivery Platform Modulates Mechanism**: The fact that NP-based vaccines induced distinct immune profiles compared to BCG or antigen-adjuvant mixtures suggests that the delivery system actively shapes the quality and trajectory of the immune response. This finding supports a more mechanistically tailored approach to vaccine design, where innate training, mucosal targeting, or antigen persistence can be modulated intentionally.

2. For NP and Adjuvant Technology

- **Formulation as an Immunoengineering Tool**: Even minor chemical modifications, such as swapping DOTAP for EPC or altering cholesterol content, led to significant shifts in uptake, activation, and toxicity. This supports the view of NP formulation as a highly tunable lever for shaping immune responses.
- **Dose Sparing and Antigen Economy**: NP-based systems achieved protection with significantly reduced antigen and adjuvant doses. This not only enhances safety and feasibility for global immunization campaigns, but also addresses one of the main hurdles in TB vaccinology: the need for scalable, cost-effective solutions.

- **pH-Sensitive Systems Beyond Oncology**: While often used in cancer therapy, this work demonstrates that pH-sensitive liposomes can also be effective in infectious disease contexts, supporting the relevance of endosomal escape, efficient cross-presentation, and $CD8^+$ T-cell activation. This may open new avenues for applying these systems to pathogens that require strong cytosolic responses.

3. For TB Research and Correlates of Protection

- **Need for New Biomarkers**: Traditional readouts such as IFNγ levels or polyfunctional T-cells did not consistently correlate with protection. This highlights the pressing need for better-defined biomarkers, potentially involving cell localization, metabolic state, or non-classical immune subsets.
- **Focus on Underexplored T-Cell Subsets**: $CD4^+$ and $CD8^+$ T-cells with a $CD44^{lo}$ $CD62L^{hi}$ phenotype emerged repeatedly in our studies as being enriched in protected animals. These may represent a functionally superior central memory subset and warrant focused investigation in future research.
- **Emerging Role of B-Cells**: We observed IL-17A- and TNFα-producing B-cell subsets, supporting a more nuanced role for B-cells in TB. These findings contribute to growing evidence that B-cells should be included in mechanistic models of protection and correlates of efficacy.

4. For Vaccine Delivery and Clinical Translation

- **Undervalued Potential of I.d. Route**: I.d. delivery yielded superior T- and B-cell responses and improved antibody subclass switching compared to the subcutaneous route, using lower doses. This suggests broader application of i.d. administration in next-generation TB vaccines, particularly in resource-constrained settings.
- **Delivery Can Rescue Antigen Performance**: The AER antigen provided no protection when delivered in solution with adjuvants, yet conferred significant protection in NP formulations. This reaffirms that antigen efficacy is not solely intrinsic but can be unlocked through optimized delivery.

- **Translatable to Other Pathogens**: The platforms and principles validated here, including cationic liposomes, pH-sensitive systems, and hybrid PLGA-lipid NPs, are readily adaptable to vaccines against other intracellular pathogens (e.g., Leishmania, HIV, Chlamydia) or even therapeutic cancer vaccines requiring potent cytotoxic responses.

5. For Experimental Design and Preclinical Strategy

- **Head-to-Head Comparisons Clarify Value**: Conducting standardized, parallel comparisons of different formulations, delivery systems, and administration routes allowed for robust identification of performance trends. This contrasts with many fragmented studies in the field and strengthens decision-making for further development.
- **Early Human-Relevant Screening Increases Predictive Value**: By incorporating human MDDC and T-cell models early in the pipeline, we enhanced the translational relevance of our candidate selection. This step could improve the efficiency and accuracy of preclinical screening in other vaccine pipelines.

A key contribution of this work is the stepwise framework developed for the design, optimization, and evaluation of NP-based vaccines:

1. Rational selection of formulation components, including antigens, lipids, polymers, and adjuvants, based on their known or hypothesized immunological properties and physicochemical compatibility.
2. Formulation development and optimization, guided by physicochemical characterization (e.g., size, charge, stability) and human in vitro immunological readouts. These assays, including APC uptake, activation, cytokine production, and T-cell stimulation, allow for early screening of immunopotency in a human-relevant system.
3. Iterative refinement, where suboptimal candidates are reformulated, e.g., by adjusting lipid composition or adjuvant content, and re-assessed to enhance desired characteristics, particularly those related to immune activation and cellular viability.

4. In vivo evaluation in a relevant small animal model, focusing not only on bacterial load reduction but also on dissecting the nature of the induced immune response, including $CD4^+$, $CD8^+$, B-cell, and memory subsets, to explore potential mechanisms of protection.

5. Comparative studies across multiple delivery systems, routes of administration, or dosing regimens to determine the most promising configuration for translation to more advanced models, such as guinea pigs or non-human primates, and to inform the design of early-phase clinical trials.

Together, these insights argue for a shift in focus across the vaccine development pipeline – from antigen discovery alone to a more holistic strategy that incorporates immuno-engineering, delivery and adjuvant science, and immunology. This work contributes both concrete data and methodological scaffolding to guide the development of next-generation vaccines, particularly those targeting difficult pathogens such as Mtb. The tools and lessons developed here can inform not only the future of TB vaccines but also be broadly applicable across infectious disease and immunotherapy fields.

7. APPLICABILITY BEYOND TB

The delivery platforms and immunological insights developed in this thesis hold significant translational potential far beyond the context of TB. Their versatility, safety, and capacity to fine-tune immune responses make them valuable for diverse biomedical challenges in both infectious and non-infectious settings.

Infectious Disease Vaccinology. The NP-based delivery platforms, especially pH-sensitive liposomes and lipid-PLGA hybrid systems, can be applied to a wide array of intracellular pathogens. These include *Salmonella*, *Leishmania*, *Chlamydia*, and HIV, for which cell-mediated immunity is essential. Moreover, their adaptability enables the design of rapid-response vaccines for emerging pathogens, supporting pandemic preparedness initiatives. The mucosal immune enhancement potential of these formulations also makes them suitable for respiratory and enteric vaccines delivered via intranasal or oral routes.

Cancer Immunotherapy. The platform's ability to induce polyfunctional $CD8^+$ T-cell responses and support antigen-specific recall responses suggests its use in delivering tumor neoantigens. pH-sensitive and depot-forming NPs could be

tailored for endosomal escape, enhancing cytosolic delivery of peptide antigens, mRNA, or siRNA for therapeutic cancer vaccines or immunomodulation of the tumor microenvironment.

Autoimmune Disease and Immune Tolerance. Rationally designed NPs could be repurposed to induce antigen-specific tolerance by co-delivering autoantigens with tolerogenic agents.

Allergy and Asthma Immunotherapy. NP systems could deliver allergens in controlled doses to promote immune tolerance rather than hypersensitivity, offering a safer alternative to conventional desensitization. Depot-forming intradermal or microneedle-based administration routes could improve adherence and reduce adverse effects.

Drug Delivery and Gene Therapy. The principles demonstrated here, particularly pH-sensitivity and controlled release, are applicable to intracellular delivery of antimicrobials, nucleic acid-based therapies, or cytokine delivery for immune modulation. These technologies could be extended into hormone therapies or long-acting injectables requiring depot-like performance.

Trained Immunity and Immunosenescence. NP platforms could be adapted to train innate immune cells via agents like BCG derivatives, helping protect immunocompromised or elderly individuals. Intradermal delivery of immune rejuvenating agents may offer a new strategy to combat immunosenescence.

Preclinical and Translational Research Tools. The structured pipeline developed here, from rational antigen and adjuvant selection, through *in vitro* human cell testing, to *in vivo* efficacy screening, serves as a broadly applicable model for vaccine and immunotherapy development. It offers a more predictive and efficient framework for early-stage screening across disease models.

Global One Health Applications. Solid, thermostable NP-based formulations enable room temperature storage, simplifying logistics in low-resource settings. Combined with needle-free intradermal administration (e.g., microneedles or jet injectors), these vaccines could improve compliance and access, especially in mass campaigns or outbreak control settings.

In summary, the modularity and efficacy of the vaccine platforms developed in this work open a range of translational opportunities. By combining innovative materials science with rational immunological design, these systems have the potential to revolutionize how we approach prevention and treatment in a broad spectrum of medical fields.

8. LIMITATIONS OF THE STUDY

While this thesis provides important insights into NP-based subunit vaccine design for TB, several limitations should be acknowledged to contextualize the scope and impact of the findings.

A key limitation of this work is the evaluation of immune responses and protection at a single post-challenge time point. This approach restricts insights into the time dynamics of vaccine-induced immunity and may overlook critical events associated with either early clearance or long-term protection. Similarly, the use of a 7-day *in vitro* lymphocyte restimulation protocol precluded the characterization of early activation events and innate-like recall responses. Future studies incorporating longitudinal sampling at multiple time points will be necessary to capture the full trajectory of immune induction, contraction, and memory formation.

Another limitation lies in the fixed antigen and adjuvant doses used throughout the experiments. While this design allowed for direct comparison across formulations, it limits the understanding of dose–response relationships. The choice of adjuvants and their dosages, particularly CpG and MPLA, was based on literature precedent rather than systematic optimization, potentially obscuring synergistic or dose-dependent effects. Exploring a broader range of adjuvant types and concentrations could yield improved immunogenicity and better safety profiles, especially when translating these systems to clinical settings.

Additionally, although the study involved rational design of delivery platforms and incorporated multiple NP systems (PLGA, liposomes, lipid–PLGA hybrids), the chemical diversity of tested materials remained limited. Further structural modifications and mechanistic studies would be valuable to refine delivery kinetics and target cell specificity.

From an immunological standpoint, the study emphasized systemic immune responses (e.g., splenocyte analysis) and peripheral markers of T- and B-cell

activation. However, site-specific immune activity in the lungs and draining lymph nodes, crucial compartments in Mtb pathogenesis and vaccine efficacy, was not assessed. Nor were tissue-resident memory T-cells, mucosal antibody production (e.g., secretory IgA), or innate training responses characterized, all of which are increasingly recognized as important correlates of protection against respiratory pathogens. Importantly, the lack of immune response data from Mtb-challenged animals limits the ability to directly correlate protection outcomes (i.e., bacterial burden reduction) with specific immunological signatures. Without this, mechanistic conclusions regarding how each formulation mediates protection remain speculative.

The reliance on a single preclinical model – C57BL/6 mice – also limits generalizability. This strain, while convenient for mechanistic immunology studies, does not develop human-like granulomas and does not fully recapitulate latency, reactivation, or vaccine-driven pathology modulation. Validation in more predictive models, such as guinea pigs, non-human primates, or human challenge studies, will be essential to assess translational relevance.

Lastly, practical considerations relevant to future clinical deployment, such as cold-chain stability, storage conditions, needle-free delivery options (e.g., microneedle patches), and large-scale manufacturability, were not evaluated in this study. These aspects, while beyond the current thesis' scope, are vital for the ultimate implementation of new TB vaccine candidates, particularly in low-resource settings.

In summary, while the current research advances our understanding of NP-based TB vaccine strategies, its limitations underscore the need for continued optimization of formulation, dose, delivery route, immunological readouts, and model systems. Addressing these gaps will enhance the translational potential of next-generation vaccines and strengthen their pathway toward clinical development.

9. FUTURE DIRECTIONS

The findings of this work open multiple avenues for future research that span mechanistic exploration, formulation refinement, and translational advancement. While not all directions are required to move this technology forward into clinical development, each represents a unique opportunity to answer distinct scientific questions or optimize the vaccine platform for different use cases. The appropriate

next steps will depend on the specific research goals, whether they relate to elucidating mechanisms of protection, optimizing immune responses, or advancing toward clinical application.

1. Deeper Immunological Characterization

As stated above, one key limitation of this study was the single post-vaccination time point used for immune assessment. Future studies should incorporate longitudinal analyses to track the kinetics of immune priming, contraction, and memory formation over time. Additionally, sampling from mucosal tissues, particularly the lung, could provide insights into tissue-resident responses that may be more relevant for TB control than those observed in peripheral lymphoid organs. Analysis of mucosal IgA, bronchoalveolar lavage samples, and lung-resident T-cell subsets could provide valuable information on localized immunity. Expanding B-cell and antibody profiling to include affinity maturation, class switching, and functional assays may also help clarify their contributions to protection.

2. Mechanistic Studies and Correlates of Protection

Further mechanistic dissection is warranted to define the immune pathways responsible for protection. Immune subset depletion experiments (e.g., $CD4^+$, $CD8^+$, B-cells, or IL-17-producing cells) and adoptive transfer studies could help clarify the relative importance of different cell types. Additionally, transcriptomic and proteomic profiling of lymphocytes or APCs after vaccination could reveal novel pathways linked to efficacy. Evaluating markers of trained immunity or metabolic reprogramming in myeloid cells may uncover non-classical correlates of protection beyond canonical Th1 immunity.

3. Formulation and Antigen Optimization

While this study explored select formulations and adjuvant combinations, a broader screen could identify improved variants. Future work could involve systematic dose titration studies to determine the minimum effective doses of antigen and adjuvants. Incorporation of novel immunostimulants (e.g., cGAMP, QS-21, or TLR7/8 agonists) into the existing platforms could enhance immunogenicity or skew responses toward specific profiles. Modular antigen design, including epitope mapping or combining more antigens targeting both latent and active Mtb stages, may further improve the breadth and depth of immune coverage.

4. Delivery Route and System Innovation

The demonstrated advantages of intradermal delivery suggest that future studies should explore its broader applicability, including via microneedle patches or solid-form vaccines for thermostable, field-ready use. Rational engineering of NP surfaces, e.g., using receptor-targeting ligands or optimizing lipid composition, could improve cellular targeting, endosomal escape, and depot effects. Additionally, exploring mucoadhesive delivery systems could help target mucosal immune compartments more effectively.

5. Advanced Preclinical Studies

To bridge the translational gap between murine models and human tuberculosis, evaluation in more predictive animal models is essential. Non-human primates provide superior physiological and immunological relevance, especially for studying granuloma architecture, latency, and reactivation. Other intermediate models, such as rabbits and humanized mice, may also offer valuable insights, particularly in capturing aspects of human-like immune responses or pathophysiological features absent in conventional mouse models. Performing comparative challenge studies against leading clinical-stage vaccines (e.g., M72/AS01$_E$) could help benchmark performance and support go/no-go decisions for clinical development.

6. Toward Clinical Translation

If lead formulations continue to show promise, future work should focus on manufacturing under GMP conditions and evaluating formulation stability under different temperature and humidity conditions. Scalability, batch-to-batch reproducibility, and shelf-life under non-refrigerated conditions will be critical for deployment in low-resource settings. Early dialogue with regulatory agencies and global health organizations (e.g., WHO) can help define development milestones and trial readiness. Dose-sparing, intradermal, or even self-administrable formats may offer logistical advantages that accelerate real-world implementation.

These future directions represent a flexible roadmap for further development of the NP-based TB subunit vaccines described in this thesis. Depending on the chosen

research priorities, mechanistic insight, formulation innovation, or translational readiness, different branches of this pipeline may be pursued independently or in combination.

10. FINAL CONCLUSIONS

This thesis presents a comprehensive body of work on the rational design, development, and evaluation of NP-based subunit vaccines for TB. By combining antigen engineering, smart delivery systems, *in vitro* human immune models, and mouse challenge studies, this research demonstrates how formulation science can significantly enhance vaccine efficacy and provide a path forward for next-generation TB vaccines.

The findings illustrate that NP delivery systems, specifically PLGA NPs, pH-sensitive liposomes, and lipid–PLGA hybrid particles, offer not only enhanced antigen delivery but also allow precise modulation of immune responses. All three NP platforms significantly reduced Mtb bacterial burden in mice, with PLGA NPs showing the greatest reduction, even outperforming the benchmark BCG vaccine in median lung protection. This underscores the potential of subunit vaccines when paired with well-engineered delivery vehicles.

Importantly, the data challenge traditional assumptions in vaccinology. High frequencies of polyfunctional T-cells or elevated antibody titers did not reliably predict protection, revealing a disconnect between immune magnitude and functional efficacy.[31] These findings advocate for a shift toward identifying more mechanistically relevant correlates of protection, including central memory-like T-cell subsets, B-cell-derived cytokines, and tissue-resident immunity.

This work also proposes and validates a translational research pipeline that begins with rational formulation design, progresses through *in vitro* human immunological assessment, and culminates in comparative *in vivo* studies that inform clinical strategy. This iterative framework can be adapted for other infectious diseases and even non-infectious indications where immune precision and antigen sparing are critical.

Beyond TB, the platforms and design principles established here are broadly applicable to vaccine development against other intracellular pathogens, as well as

for cancer immunotherapy and mucosal vaccines. The study highlights the utility of i.d. delivery and pH-sensitive systems as underutilized yet powerful strategies for improving vaccine accessibility, efficacy, and global deployment.

In conclusion, this thesis provides both concrete advances in TB vaccine research and generalizable insights for immunoengineering. It reinforces that subunit vaccines, when paired with intelligent delivery platforms, are a viable and scalable path forward for combating TB and potentially many other diseases where conventional vaccine approaches have fallen short.

11. REFERENCES

1. World Health Organization. *Global Tuberculosis Report 2024*. (2024).
2. Schrager, L. K., *et al.* The status of tuberculosis vaccine development. *Lancet Infectious Diseases* 20, e28–e37 (2020).
3. Brewer, T. F. Preventing Tuberculosis with Bacillus Calmette-Guérin Vaccine: A Meta-Analysis of the Literature. *Clinical Infectious Diseases* 31, S64–S67 (2000).
4. World Health Organization. *The End TB Strategy*. (2015).
5. Christensen, D. *et al.* Cationic liposomes as vaccine adjuvants. *Expert Review of Vaccines* 10, 513–521 (2011).
6. Moyle, P. M. & Toth, I. Modern Subunit Vaccines: Development, Components, and Research Opportunities. *ChemMedChem* 8, 360–376 (2013).
7. Lai, R. *et al.* Key advances in vaccine development for tuberculosis—success and challenges. *NPJ Vaccines 2023 8:1* 8, 1–10 (2023).
8. Duong, V. T. *et al.* Towards the development of subunit vaccines against tuberculosis: The key role of adjuvant. *Tuberculosis* 139, 102307 (2023).
9. Ottenhoff, T. H. M. & Kaufmann, S. H. E. Vaccines against Tuberculosis: Where Are We and Where Do We Need to Go? *PLoS Pathogens* 8, e1002607 (2012).
10. Minor, P. D. Live attenuated vaccines: Historical successes and current challenges. *Virology* 479–480, 379–392 (2015).
11. Tuberculosis Vaccine Initiative. Pipeline of vaccines - TBVI. https://www.tbvi.eu/what-we-do/pipeline-of-vaccines/.
12. William Tong, C. Y. Different Types of Vaccines. *Tutorial Topics in Infection for the Combined Infection Training Programme* (2019).
13. Ghattas, M. *et al.* Vaccine Technologies and Platforms for Infectious Diseases: Current Progress, Challenges, and Opportunities. *Vaccines* 9:12, 1490 (2021).

14. Tait, D. R. *et al.* Final Analysis of a Trial of M72/AS01 E Vaccine to Prevent Tuberculosis. *New England Journal of Medicine* 381, 2429–2439 (2019).
15. Franco, A. R. & Peri, F. Developing New Anti-Tuberculosis Vaccines: Focus on Adjuvants. *Cells* 10:1, 78 (2021).
16. Ewer, K. J. *et al.* Viral vectors as vaccine platforms: from immunogenicity to impact. *Current Opinion in Immunology* 41, 47–54 (2016).
17. Lundstrom, K. Viral Vectors in Gene Therapy: Where Do We Stand in 2023? *Viruses* 15:3, 698 (2023).
18. BioNTech. Safety and Immune Responses After Vaccination With Two Investigational RNA-based Vaccines Against Tuberculosis in BCG Vaccinated Volunteers, Trial ID BNT164-02. https://clinicaltrials.biontech.com/trials/BNT164-02.
19. Larsen, S. E. *et al.* Tuberculosis vaccines update: Is an RNA-based vaccine feasible for tuberculosis? *International Journal of Infectious Diseases* 130, S47–S51 (2023).
20. O'Hagan, D. T. *et al.* Towards an evidence based approach for the development of adjuvanted vaccines. *Current Opinion in Immunology* 47, 93–102 (2017).
21. Commandeur, S. *et al.* The in vivo expressed Mycobacterium tuberculosis (IVE-TB) antigen Rv2034 induces CD4+ T-cells that protect against pulmonary infection in HLA-DR transgenic mice and guinea pigs. *Vaccine* 32, 3580–3588 (2014).
22. Szachniewicz, M. M. *et al.* Cationic pH-sensitive liposome-based subunit tuberculosis vaccine induces protection in mice challenged with Mycobacterium tuberculosis. *European Journal of Pharmaceutics and Biopharmaceutics* 203, 114437 (2024).
23. Szachniewicz, M. M. *et al.* Evaluation of PLGA, lipid-PLGA hybrid nanoparticles, and cationic pH-sensitive liposomes as tuberculosis vaccine delivery systems in a Mycobacterium tuberculosis challenge mouse model – A comparison. *International Journal of Pharmaceutics* 666, 124842 (2024).
24. Szachniewicz, M. M. *et al.* Intrinsic immunogenicity of liposomes for tuberculosis vaccines: Effect of cationic lipid and cholesterol. *European Journal of Pharmaceutical Sciences* 195, 106730 (2024).
25. Szachniewicz, M. M. *et al.* Cationic pH-sensitive liposomes as subunit vaccine delivery systems against tuberculosis: effect of liposome composition on cellular innate immune responses. *International Immunopharmacology. Manuscript submitted for publication* (2024).

26. Geluk, A. *et al.* A multistage-polyepitope vaccine protects against Mycobacterium tuberculosis infection in HLA-DR3 transgenic mice. *Vaccine* 30, 7513–7521 (2012).
27. Szachniewicz, M. M. *et al.* Intradermal versus subcutaneous immunization: Effects of administration route using a lipid-PLGA hybrid nanoparticle tuberculosis vaccine. *European Journal of Pharmaceutical Sciences* 205, 106995 (2025).
28. Henriksen-Lacey, M. *et al.* Liposomes based on dimethyldioctadecylammonium promote a depot effect and enhance immunogenicity of soluble antigen. *Journal of Controlled Release* 142, 180–186 (2010).
29. Henriksen-Lacey, M. *et al.* Comparison of the depot effect and immunogenicity of liposomes based on dimethyldioctadecylammonium (DDA), 3β-[N-(N′,N′-dimethylaminoethane)carbomyl] cholesterol (DC-Chol), and 1,2-dioleoyl-3-trimethylammonium propane (DOTAP): Prolonged liposome retention mediates stronger Th1 responses. *Molecular Pharmaceutics* 8, 153–161 (2011).
30. Rao, D. A., Forrest, M. L., Alani, A. W. G., Kwon, G. S. & Robinson, J. R. Biodegradable PLGA based nanoparticles for sustained regional lymphatic drug delivery. *Journal of Pharmaceutical Sciences* 99, 2018–2031 (2010).
31. Caccamo, N. *et al.* Multifunctional CD4+ T cells correlate with active Mycobacterium tuberculosis infection. *European Journal of Immunology* 40, 2211–2220 (2010).

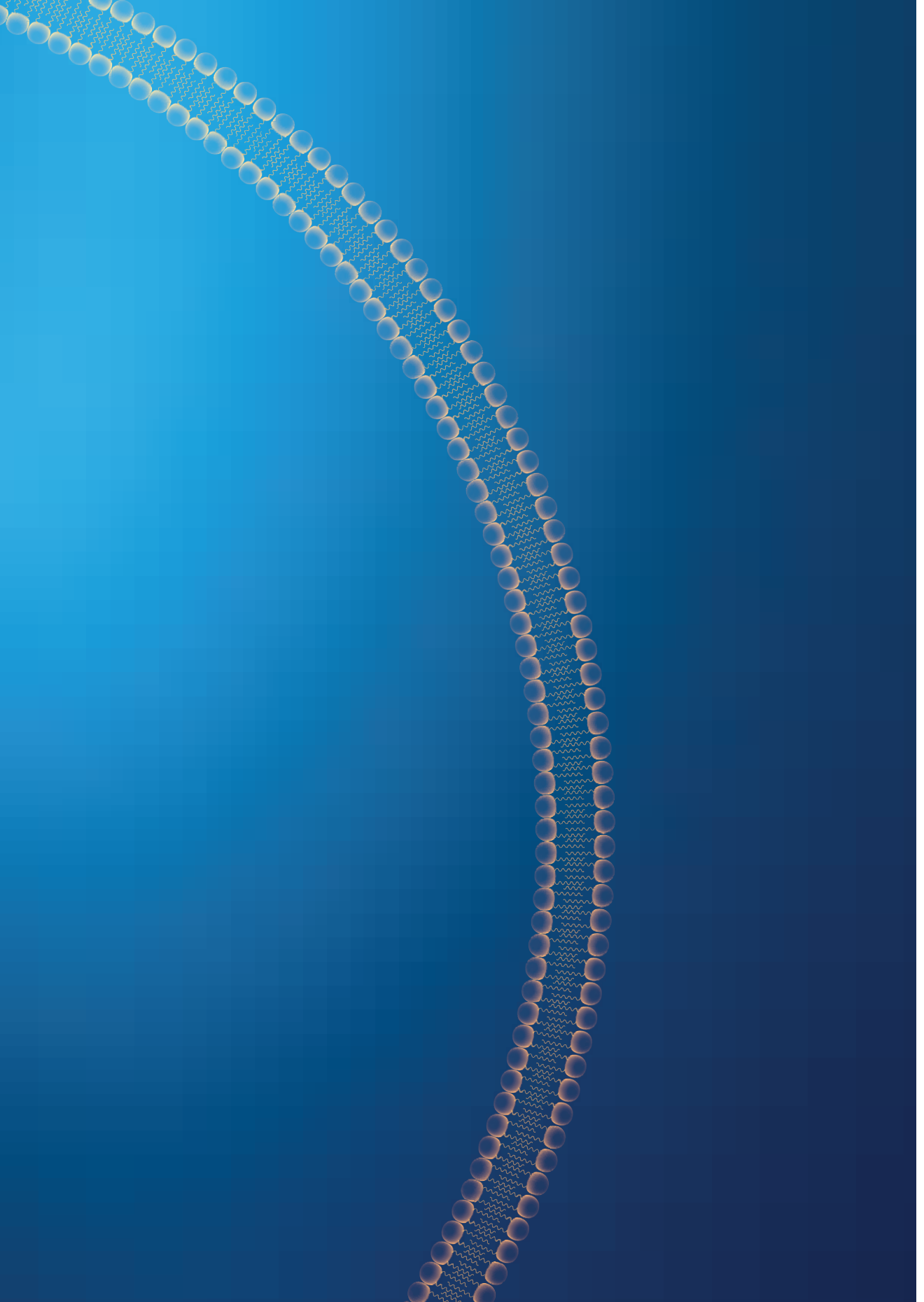

CHAPTER A

Appendices:
Nederlandse samenvatting, Curriculum Vitae,
List of publications, and Acknowledgments

NEDERLANDSE SAMENVATTING

Tuberculose (TB) blijft een van de grootste gezondheidsuitdagingen wereldwijd, veroorzaakt jaarlijks meer dan een miljoen doden en treft naar schatting elk jaar 10 miljoen mensen.[1] De End-TB-strategie van de Wereldgezondheidsorganisatie (WHO) streeft naar een vermindering van het aantal TB-gevallen met 90 % en het aantal TB-gerelateerde sterfgevallen met 95 % tegen 2035.[2] Echter schieten de huidige controlemethoden tekort om deze ambitieuze doelen te behalen. Ondanks de grootschalige toepassing biedt het enige goedgekeurde TB-vaccin, Bacillus Calmette-Guérin (BCG), zeer variabele en vaak onvoldoende bescherming, vooral tegen pulmonale TB bij adolescenten en volwassenen.[3] Deze beperkingen benadrukken de dringende behoefte aan nieuwe TB-vaccins met verbeterde werkzaamheid, in het bijzonder vaccins die langdurige cellulaire immuniteit opwekken.

In het afgelopen decennium is er toenemende belangstelling voor subunitvaccins gebaseerd op goed gedefinieerde antigenen die worden toegediend via geavanceerde platforms zoals nanodeeltjes (NPs). Deze strategieën beogen een verbeterde antigeen afgifte, verhoogde immunogeniciteit en veiligheid, zijn opschaalbaar en bieden tevens flexibiliteit qua formulering. Verschillende subunitvaccinkandidaten tegen TB bevinden zich momenteel in klinische trials, waaronder M72/AS01E en ID93+GLA-SE, wat het potentieel benadrukt van het combineren van immunodominante antigenen met krachtige adjuvantia. Deze thesis sluit aan bij deze inspanningen en richt zich op het ontwerp, de optimalisatie en evaluatie van NP-gebaseerde afgiftesystemen, specifiek liposomen, poly(D,L-melkzuur-co-glycolzuur) (PLGA)-nanodeeltjes, en hybride lipid-PLGA-systemen, voor de toediening van een multistage fusie-eiwitantigeen, Ag85B-ESAT6-Rv2034 (AER).

In **Hoofdstuk 2** wordt onderzoek beschreven waarin een breed panel van kationische liposomen wordt gescreend om te onderzoeken hoe kationische lipiden en cholesterolinhoud de activatie van menselijke antigeen presenterende cellen (APC's) en T-cel priming beïnvloeden. Deze studie toonde aan dat liposomen gebaseerd op 1,2-dioleoyl-3-trimethylammonium-propane (DOTAP) en 1,2-dioleoyl-sn-glycero-3-ethylphosphocholine (EPC), vooral die met cholesterol, verbeterde opname door dendritische cellen induceerden een superieure antigeen-specifieke $CD4^+$ T-cel activatie in vitro. Belangrijk is dat de resultaten aantoonden dat de immuunstimulerende effecten van kationische lipiden niet alleen afhangen van hun netto lading, maar ook

afhangen van structurele determinanten die de membraanrigiditeit en interactie met immuuncellen beïnvloeden. Het onderzoek beschreven in dit hoofdstuk benadrukt het belang van zorgvuldige keuze voor lipiden bij het ontwerpen van effectieve vaccindragers en identificeerde op DOTAP- en EPC-gebaseerde formuleringen als veelbelovende kandidaten.

In het onderzoek gepresenteerd in **Hoofdstuk 3** werden pH-gevoelige liposomen onderzocht voor cytosolische antigeen afgifte, een mechanisme dat cruciaal wordt geacht voor het induceren van $CD8^+$ T-cel activatie . Door de lipide samenstelling systematisch te wijzigen, werd een geoptimaliseerde formulering met EPC, 1,2-dioleoyl-sn-glycero-3-phosphoethanolamine (DOPE), N-(4-carboxybenzyl)-N,N-dimethyl-2,3-bis(oleoyloxy)propan-1-aminium (DOBAQ) en 1,2-dioleoyl-sn-glycero-3-phosphocholine (DOPC) bepaald. Deze formulering toonde efficiënte opname door humane monocyten-afgeleide dendritische cellen, induceerde cytokine productie en bevorderde antigeen-specifieke T-cel activatie. Dit onderzoek breidde het gebruik van pH-gevoelige afgiftesystemen uit buiten oncologie en introduceerde de relevantie ervan voor subunitvaccinatie tegen TB.

In **Hoofdstuk 4** wordt onderzoek beschreven waarin de geoptimaliseerde pH-gevoelige liposomale formulering met een preklinisch muismodel onderzocht. Dit toonde aan dat het deze liposomen de bacteriële last konden verminderen na infectie met *Mycobacterium tuberculosis* (Mtb). Het in liposoom-geïncorporeerde AER-vaccin presteerde beter dan mengsels van antigeen-adjuvans voor zowel $CD4^+$ als $CD8^+$ T-cel activatie, inclusief polyfunctionele en centrale geheugenachtige T-cellen. Opmerkelijk genoeg werd bescherming bereikt met aanzienlijk lagere doses antigeen en adjuvantia, wat de werkzaamheid en dosisbesparende voordelen van dit afgifteplatform onderstreept.

In **Hoofdstuk 5** wordt onderzoek gepresenteerd waarin drie typen formuleringen van nanodeeltjes, PLGA-nanodeeltjes, lipid-PLGA hybride nanodeeltjes en kationische pH-gevoelige liposomen, met elkaar vergeleken werden in een intranasaal Mtb-infectiemodel. Alle NP-gebaseerde vaccins verminderden significant de hoeveelheid Mtb bacteriën in long en milt, terwijl het antigeen-adjuvansmengsel geen bescherming bood. PLGA-nanodeeltjes toonden de grootste reductie, een volledige log lager dan BCG. Hybride NPs en liposomen boden ook bescherming, zij het in mindere mate. Hoewel statistisch geen significante verschillen werden

waargenomen tussen de NP-groepen, suggereerde een trend een volgorde in effectiviteit: PLGA > hybride > liposoom. Opmerkelijk is dat liposomen de hoogste antigeenspecifieke T-cel activatie induceerden maar de minste bescherming boden, terwijl het antigeen-adjuvansmengsel T-cellen induceerde die vergelijkbaar waren met de meest beschermende PLGA-formulering. Deze bevindingen tonen een discrepantie tussen immunogeniciteit en bescherming en dagen daarmee conventionele vaccinbeoordelingscriteria uit. Vergelijkbare patronen werden gezien bij B-cel activatie en antilichaamtiters.

In **Hoofdstuk 6** wordt het effect van toedieningsroute op immuunuitkomsten beschreven. Dit werd onderzocht met \ een lipid-PLGA hybride NP-vaccin toegediend via intradermale of subcutane injectie. Intradermale vaccinatie induceerde sterkere polyfunctionele T-celreacties en hogere AER-specifieke IgG2a antilichaamtiters, wijzend op verbeterde Th1-type immuniteit. Belangrijk is dat deze route ook meer B-cel-subsets activeerde en betere immunogeniciteit opleverde, wat de waarde van intradermale toediening onderstreept voor dosisbesparing en verbeterde immuunkwaliteit.

Samengevat tonen de bevindingen van dit proefschrift de kracht van rationeel ontwerp van nanodeeltjes om vaccin-geïnduceerde immuunresponsen nauwkeurig af te stemmen. Kationische en pH-gevoelige lipiden bieden structurele controle over antigeenpresentatie routes, terwijl polymere en hybride platforms langdurige antigeen afgifte en depotvorming mogelijk maken. Intradermale toediening versterkt bovendien de immunogeniciteit en ondersteunt dosis reductie, wat het aantrekkelijk maakt voor gebruik in situaties waarbij beperkte middelen beschikbaar zijn. Deze innovaties dragen niet alleen bij aan de ontwikkeling van TB-vaccins, maar hebben ook potentieel voor bredere toepassingen in infectieziekten en immunotherapie van kanker. Toekomstig onderzoek op basis van deze platforms zou zich moeten richten op geavanceerdere modellen en klinische settings, de immuun-correlaten van bescherming verfijnen en blijven innoveren in afgiftesystemen die ons dichter bij effectieve en opschaalbare vaccins van de volgende generatie brengen.

LITERATUURLIJST

1. World Health Organization. *Global Tuberculosis Report 2024*. (2024).
2. World Health Organization. *The End TB Strategy*. (2015).
3. Brewer, T. F. Preventing Tuberculosis with Bacillus Calmette-Guérin Vaccine: A Meta-Analysis of the Literature. *Clinical Infectious Diseases* 31, S64–S67 (2000).

CURRICULUM VITAE

Mikołaj Mieczysław Szachniewicz was born on January 9, 1992, in Łódź, Poland. His passion for science began at the age of five, sparked by a fascination with astronomy – an interest that continues to this day. Over time, his scientific curiosity expanded into other disciplines and was nurtured during his education at the General Education High School of the Lodz University of Technology, where he developed a particular interest in chemistry.

In 2011, he enrolled in the Nanotechnology Engineering Program at the Faculty of Chemistry, Lodz University of Technology, drawn by the promise and interdisciplinary nature of the emerging field of nanotechnology. During his first year, he began his research journey as a volunteer at the Division of Applied Radiation Chemistry under the supervision of Dr. Radosław Wach, contributing to an international IAEA research project focused on the synthesis and characterization of biomaterials.

His academic interests gradually shifted toward the biomedical applications of nanotechnology. For his BSc/Eng. thesis, he worked on the chemical modification of surgical implants in collaboration with a local medical device manufacturer. He completed his undergraduate studies in the top 5 % of students of the university.

Continuing in the Nanotechnology MSc program at Lodz University of Technology, Mikołaj was selected for a double diploma degree program with the University of Twente (Netherlands). His research focused increasingly on biomedical applications. Under the supervision of Prof. Ruchi Bansal, he completed his master's thesis on "Nanotechnology-based targeted drug delivery systems for the treatment of liver fibrosis" at the Biomaterials Science and Technology Group, Faculty of Science and Technology.

To further expand his expertise, he completed an internship at RWTH Aachen University Hospital (Germany) in the Department of Medicine III, where he conducted *in vitro* studies on nanoparticle-based drug delivery systems. He earned dual MSc degrees in Nanotechnology, graduating in the top 1 % of students at Lodz University of Technology.

In 2017, Mikołaj began his PhD at Leiden University Medical Center in the Department of Infectious Diseases (now Leiden University Center for Infectious Diseases, LUCID), under the supervision of Prof. Tom Ottenhoff (LUCID) and Prof. Joke Bouwstra (Leiden Academic Centre for Drug Research, LACDR). In this research, he was also guided by Prof. Annemieke Geluk (LUCID) and Prof. Wim Jiskoot (LACDR). The results of his doctoral studies are presented in this thesis.

LIST OF PUBLICATIONS

1. **M.M. Szachniewicz**, M.A. Neustrup, K.E. van Meijgaarden, W. Jiskoot, J.A. Bouwstra, M.C. Haks, A. Geluk, T.H.M. Ottenhoff, Intrinsic immunogenicity of liposomes for tuberculosis vaccines: Effect of cationic lipid and cholesterol, *European Journal of Pharmaceutical Sciences* 195 (2024) 106730.

2. **M.M. Szachniewicz**, K.E. van Meijgaarden, E. Kavrik, W. Jiskoot, J.A. Bouwstra, M.C. Haks, A. Geluk, T.H.M. Ottenhoff, Cationic pH-sensitive liposomes as tuberculosis subunit vaccine delivery systems: Effect of liposome composition on cellular innate immune responses, *International Immunopharmacology* 145 (2025) 113782.

3. **M.M. Szachniewicz**, S.J.F. van den Eeden, K.E. van Meijgaarden, K.L.M.C. Franken, S. van Veen, A. Geluk, J.A. Bouwstra, T.H.M. Ottenhoff, Cationic pH-sensitive liposome-based subunit tuberculosis vaccine induces protection in mice challenged with Mycobacterium tuberculosis, *European Journal of Pharmaceutics and Biopharmaceutics* 203 (2024) 114437.

4. **M.M. Szachniewicz**, S.J.F. van den Eeden, K.E. van Meijgaarden, K.L.M.C. Franken, S. van Veen, A. Geluk, J.A. Bouwstra, T.H.M. Ottenhoff, Intradermal versus subcutaneous immunization: Effects of administration route using a lipid-PLGA hybrid nanoparticle tuberculosis vaccine, *European Journal of Pharmaceutical Sciences* 205 (2025) 106995.

5. **M.M. Szachniewicz**, M.A. Neustrup, S.J.F. van den Eeden, K.E. van Meijgaarden, K.L.M.C. Franken, S. van Veen, R.I. Koning, R.W.A.L. Limpens, A. Geluk, J.A. Bouwstra, T.H.M. Ottenhoff, Evaluation of PLGA, lipid-PLGA hybrid nanoparticles, and cationic pH-sensitive liposomes as tuberculosis vaccine delivery systems in a Mycobacterium tuberculosis challenge mouse model – A comparison, *International Journal of Pharmaceutics* 666 (2024) 124842.

ACKNOWLEDGMENTS (PODZIĘKOWANIA)

This journey would not have been possible without the support, guidance, and kindness of many people, to whom I owe my deepest thanks.

First and foremost, I want to thank my supervisor, prof. Tom Ottenhoff. Tom, you have been an incredible mentor, not only scientifically but also on a personal level. Your support during my health struggles meant more to me than I can ever express.

I am also deeply grateful to my other supervisor, prof. Joke Bouwstra. Your scientific guidance and support in areas beyond Tom's expertise were essential for this thesis.

To prof. Annemieke Geluk, my unofficial promotor, thank you for your invaluable help, especially with the mouse studies and for your meticulous revisions of all publications and this thesis.

A special mention goes to Wim Jiskoot, who guided me in the early years of my PhD. I am saddened by his passing and thankful for the mentorship he offered me.

To Krista, my daily supervisor, colleague, friend, and almost a mother-figure, thank you for being the constant in my PhD life. You solved problems, lifted me up, and always took care of me.

Susan, thank you for your tremendous work on the mouse experiments and for always being there, for science, for chats, and for emotional support. You checked on me when I was struggling, and I'll never forget your kindness and friendship.

I would also like to extend my heartfelt gratitude to all those who were pivotal in the realization of this dissertation, and without whose friendship, guidance, patience, and support this journey would not have been possible:

- My deepest thanks go to my lab mates, Malene and Jihui, with whom I worked closely on this project; my student Eşe, who contributed to Chapter 3; and my colleagues Gül, Suus, Amy, Paula, Lisa, Robin, Anno, Anouk, Ellen, Sven, Michella, Bep, Kees, and Kimberley, for creating a supportive environment and for their invaluable advice and assistance with many experiments and techniques.
- I am especially grateful to my mentors, dr. Radoslaw Wach, prof. Piotr Ulanski, prof. Ruchi Bansal, and dr. Matthias Bartneck, whose lessons guided me in the realization of this work. My heartfelt thanks also go to my LIFI friends—Annieck, Kyra, Mikhail, and Douwe—for sharing their knowledge of immunology and helping me maintain perspective throughout this journey.
- Finally, I am deeply grateful to my Mom and Dad, my partner Iván, my aunt Teresa, my family Michał, Kasia, Ola, Ania, and Darek, and my closest friends Maxim, Dilovan, Radek, Zuza, and Agnieszka. Without you this dissertation would not be finished. Thank you all. Dziękuję Wam wszystkim.